Multi-organ dysfunction and therapeutical potentials in COPD
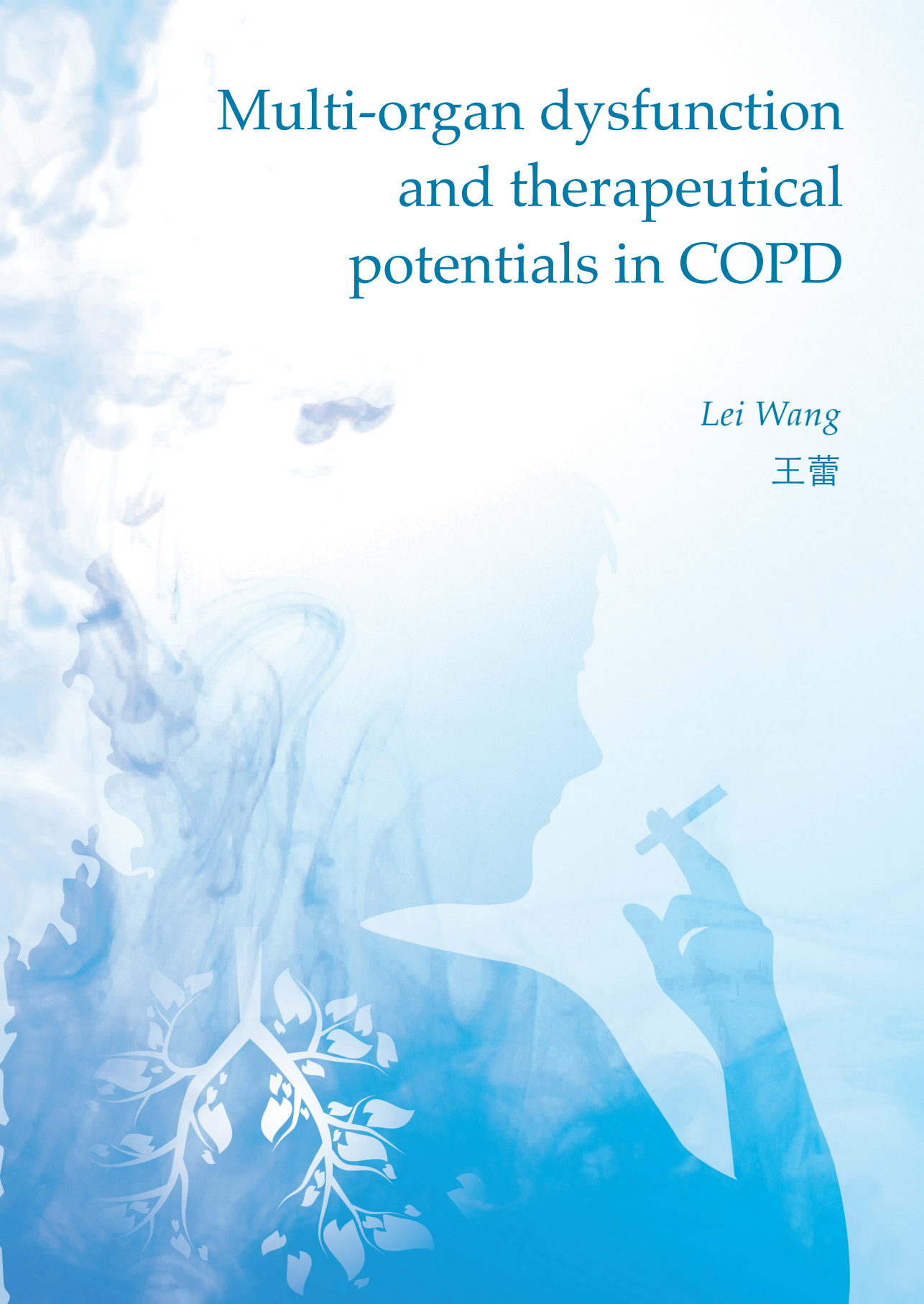
Lei Wang

王蕾

Multi-organ dysfunction and therapeutical potentials in COPD

Lei Wang

Multi-organ dysfunction and therapeutical potentials in COPD

Multi-orgaandisfunctie en therapeutische mogelijkheden bij COPD
(met een samenvatting in het Nederlands)

Proefschrift

ter verkrijging van de graad van doctor aan de Universiteit Utrecht
op gezag van de rector magnificus, prof. dr. H.R.B.M. Kummeling,
ingevolge het besluit van het college voor promoties
in het openbaar te verdedigen op

dinsdag 13 december 2022 des ochtends te 10.15 uur

door

Lei Wang
geboren op 09 oktober 1992
te Mudanjiang stad, provincie Heilongjiang, China

Contents

Chapter 1

General Introduction and
Thesis Outline

What is COPD?

Chronic obstructive pulmonary disease (COPD) is a progressive lung disease characterized by irreversible alterations in the structure of the lungs and chronic inflammation in the pulmonary tissues [1]. COPD is a serious public health problem and the third leading cause of death worldwide [2-4]. The main phenotypes of COPD are chronic bronchitis and emphysema. Bronchitis is defined by the presence of chronic and recurrent increases in bronchial secretions, leading to expectoration and airflow limitation. Emphysema is defined by permanent and destructive enlargement of airspaces [5]. COPD can include a range of symptoms, sputum production, difficulty in breathing, chest tightness and/or cough [6]. Pulmonary chronic inflammation, oxidative stress and protease-antiprotease imbalance play dominant roles in the pathogenesis of COPD [7].

Risk factors and COPD exacerbations

There are many risk factors for COPD, such as genetic factors, infections, occupational exposures, different environmental exposures, including indoor and outdoor pollutants, but cigarette smoke remains the most important cause of COPD. These factors could also be influenced by comorbid diseases [8].

A large number of COPD patients suffer from exacerbations [9]. COPD exacerbations are characterized by acute worsening of symptoms and have a negative impact on comorbidities, disease progression and survival outcome. These exacerbations always require additional therapy and often hospitalization is needed [9, 10]. Exacerbations do not only represent periods of increased complaints but lead to loss of quality of life, and especially lung function [11]. In most cases, COPD exacerbations are triggered by respiratory viral and/or bacterial infections, but exposure to environmental factors, such as pollutants, also trigger or worsen these events [12].

Systemic manifestations of COPD

Increasing evidence indicates that COPD is a complex disease with systemic consequences [13]. This might be partly due to the airflow obstruction, which can affect pulmonary gas exchange and cardiac function [14]. In addition, COPD is associated with increased pulmonary inflammation and the "spill-over" of inflammatory mediators into the circulation may induce systemic manifestations, such as cardiovascular diseases, skeletal muscle wasting, cachexia, metabolic diseases as well as depression and gastrointestinal complaints [15]. Comorbid diseases enhance the morbidity of COPD, leading to increased hospitality

and mortality [13]. Therefore, a better understanding of COPD comorbidities is very essential for the management of COPD.

COPD and the gut-lung axis

COPD patients often have a high prevalence and incidence of intestinal manifestations such as inflammatory cell infiltration, increased intestinal permeability and absorptive impairment [16-18]. There is growing evidence that patients with COPD have an increased risk of developing inflammatory bowel disease (IBD) and this risk increases with the severity of COPD [19-21].

The intestine contains the largest collection of microbes in the body. Dynamic interactions between the intestinal microbiota and a host's immune system are crucial in maintaining intestinal homeostasis and regulating intestinal inflammation [22]. The host-microbe interactions not only affect the local intestinal environment but also show the ability to influence other peripheral tissues, such as the lungs [23]. The crosstalk between gut and lung, as two mucosal tissues in our body, can be noticed by intestinal disease manifestations during respiratory diseases and vice versa [23, 24].

Cachexia and COPD

Metabolic syndrome is another comorbidity of COPD and is associated with skeletal muscle dysfunction and alterations in adipose tissue, eventually leading to cachexia [25]. Cachexia is a wasting syndrome, which is characterized by continuous unintended weight loss, affecting both fat mass and skeletal muscle mass, causing further detrimental effects on disease progression [26, 27]. Approximately 25% of the patients with COPD will develop cachexia, which is associated with around 50% reduction in median survival [28]. Adipose tissue plays an important role in the regulation of local and systemic metabolic and inflammatory pathways by the release of different biologically active factors, including adipokines, cytokines and hormones [29], which may contribute to the progression of respiratory diseases [30].

Modeling of COPD

Understanding the pathophysiological mechanisms of COPD and COPD-related comorbidities could lead to new therapeutic strategies. The development and use of experimental models will help to dissect these mechanisms at the cellular and molecular level

[31]. Different *in vivo* models of COPD have been developed but considering the complexity of human COPD, researchers should be aware of the limitations of these models as only a limited number of major features of COPD can be mimicked [32]. Exposure to noxious substances such as cigarette smoke or nitrogen dioxide, varying in duration and intensity, are commonly used to induce airway inflammation and remodeling. Exposure to tissue degrading enzymes, such as elastase that disrupts the protease-antiprotease balance, can also be used to induce an inflammatory response and emphysema-like changes *in vivo* [33, 34]. Cigarette smoke (or elastase) exposure combining with bacterial and viral triggers by using, for example, lipopolysaccharide (LPS) or Polyinosinic:polycytidylic acid (Poly I:C), respectively, may reproduce the features of COPD exacerbations [35-37].

Treatment of COPD

Nowadays, long-acting antimuscarinics or long-acting β-adrenergic receptor agonists, with or without inhaled glucocorticoids, are indicated therapies by COPD guidelines [38]. These strategies reduce respiratory symptoms and exacerbations but do not affect the disease progression. In addition, most COPD patients respond poorly to high doses of inhaled or oral glucocorticoids. Therefore, there is an urgent need for the development of safe and effective new drugs for patients with COPD.

Oxidative stress resulting from an imbalance between oxidants and antioxidants is an important feature in the pathogenesis of COPD and may play a role in the poor clinical efficacy of corticosteroids in the treatment of COPD [39]. Markers of oxidative stress are increased in COPD, for example, the reactive oxygen species (ROS), which are a major cause of the lung tissue and cell damage observed in COPD patients [40]. The imbalance between oxidants and antioxidants is even more pronounced during exacerbations [41]. Various approaches described in literature, such as antioxidant vitamins, thiol compounds, diet-derived polyphenols, suggest the effectiveness of using antioxidants in the treatment of COPD [42].

Recently, a novel class of pharmacological compounds, called SUL compounds, was developed exhibiting promising mitoprotective and antioxidant effects. These compounds emerged from the principles acquired in hibernation research as hibernating species are protected from oxidative stress damage [43]. A specific SUL compound (SUL-121) has been shown to decrease neutrophilia, hyperresponsiveness and oxidative stress in the airways caused by LPS in a guinea pig model. In addition, this SUL compound has the capacity to inhibit the release of cigarette smoke-induced IL-8 associated with decreased cellular ROS in cultured human airway smooth muscle cells [44]. This novel class of compounds with antioxidative properties appears as a promising candidate for the treatment of COPD in the future.

Aims and outline of the thesis

In this thesis, we would like to shed light on the effect of cigarette smoking on other organs besides the lungs, with a special focus on the intestine and adipose tissue. For this purpose, a cigarette smoke-induced murine COPD model with and without LPS exposure has been used and effects on lung inflammation and damage, intestinal homeostasis and immunity, alterations in adipose tissue and skeletal muscle function have been investigated. Furthermore, due to the urgent need for the development of safe and effective new drugs for patients with COPD, the efficacy of a novel compound (SUL-151) with promising mitoprotective and antioxidant properties was investigated in a murine cigarette smoke-induced inflammation model.

The following specific major aims were explored:

1. What is the effect of cigarette smoke exposure on intestinal homeostasis and immunity and what is the importance of the gut-lung axis in COPD (Chapter 2, Chapter 3, Chapter 4)?
2. What is the effect of cigarette smoke exposure on adipose and skeletal muscle tissue (Chapter 5)?
3. Is the SUL compound (SUL-151) as a prophylactic and therapeutic treatment capable of decreasing cigarette smoke-induced airway inflammation in mice (Chapter 6)?

In line with the aims, the following content of each chapter is described:
Chapter 2 provides a general overview of the gut-lung axis in COPD. In this review we explore the possible links between intestinal complaints and lung disorders, mainly focusing on COPD. This chapter has been written in a translational approach and the interactions between gut and lung in *in vivo*, *in vitro* and clinical settings have been described and possible mechanisms have been discussed.

Chapter 3 investigates the effects of cigarette smoke exposure with or without LPS treatment on intestinal health by focusing on intestinal histomorphology and intestinal immune responses. Moreover, the role of systemic inflammation is investigated related to the gut-lung crosstalk. These findings might contribute to a better understanding of the development of intestinal disorders related to COPD.

Chapter 4 presents an overview of the transcriptomic insights of the lung and distal small intestine (ileum) in a cigarette smoke-induced model for COPD. In addition, highly expressed genes in the murine lung are compared with genes in the lung of COPD patients, while highly expressed genes in the murine intestine are compared with genes in the intestine of

Crohn's disease patients. This transcriptomic analysis can provide essential components to a better understanding of disease progression and pave the way for future research.

Chapter 5 explores the alterations in adipose and skeletal muscle tissue in a cigarette smoke-induced COPD model by evaluating the body composition, adipose tissue atrophy and inflammatory infiltration, as well as investigating the skeletal muscle function, mitochondrial and protein turnover in muscle tissue. In addition, 3T3-L1 cells are exposed to cigarette smoke total particulate matter (TPM) to further understand the effect of cigarette smoke exposure on lipid metabolism.

Chapter 6 investigates the anti-inflammatory properties of a mitoprotective compound (SUL-151) in a prophylactic and therapeutic setting in mice triggered by cigarette smoke exposure to provoke oxidative stress and airway neutrophilia.

Chapter 7 summarizes and discusses the most relevant findings of all studies and provides suggestions for future research.

References

1. Saetta, M., et al., Cellular and structural bases of chronic obstructive pulmonary disease. Am J Respir Crit Care Med, 2001. 163(6): p. 1304-9.
2. Faner, R., et al., Distribution, temporal stability and association with all-cause mortality of the 2017 GOLD groups in the ECLIPSE cohort. Respir Med, 2018. 141: p. 14-19.
3. Raherison, C. and P.O. Girodet, Epidemiology of COPD. Eur Respir Rev, 2009. 18(114): p. 213-21.
4. WHO. The top 10 causes of death. 2020 9 December 2020]; Available from: https://mdanderson.libanswers.com/faq/26219.
5. Viegi, G., et al., Definition, epidemiology and natural history of COPD. Eur Respir J, 2007. 30(5): p. 993-1013.
6. Leidy, N.K., et al., Development of the EXAcerbations of Chronic Obstructive Pulmonary Disease Tool (EXACT): a patient-reported outcome (PRO) measure. Value Health, 2010. 13(8): p. 965-75.
7. Stanojkovic, I., et al., Relationship between bone resorption, oxidative stress and inflammation in severe COPD exacerbation. Clin Biochem, 2013. 46(16-17): p. 1678-82.
8. Mannino, D.M. and A.S. Buist, Global burden of COPD: risk factors, prevalence, and future trends. Lancet, 2007. 370(9589): p. 765-73.
9. Viniol, C. and C.F. Vogelmeier, Exacerbations of COPD. Eur Respir Rev, 2018. 27(147).
10. Perera, W.R., et al., Inflammatory changes, recovery and recurrence at COPD exacerbation. Eur Respir J, 2007. 29(3): p. 527-34.
11. Niewoehner, D.E., The impact of severe exacerbations on quality of life and the clinical course of chronic obstructive pulmonary disease. Am J Med, 2006. 119(10 Suppl 1): p. 38-45.
12. MacLeod, M., et al., Chronic obstructive pulmonary disease exacerbation fundamentals: Diagnosis, treatment, prevention and disease impact. Respirology, 2021. 26(6): p. 532-551.
13. Barnes, P.J. and B.R. Celli, Systemic manifestations and comorbidities of COPD. Eur Respir J, 2009. 33(5): p. 1165-85.
14. Cukic, V., The changes of arterial blood gases in COPD during four-year period. Med Arch, 2014. 68(1): p. 14-8.
15. Cavailles, A., et al., Comorbidities of COPD. Eur Respir Rev, 2013. 22(130): p. 454-75.
16. Niklasson, A., et al., Prevalence of gastrointestinal symptoms in patients with chronic obstructive pulmonary disease. Eur J Gastroenterol Hepatol, 2008. 20(4): p. 335-41.
17. Sprooten, R.T.M., et al., Increased Small Intestinal Permeability during Severe Acute Exacerbations of COPD. Respiration, 2018. 95(5): p. 334-342.
18. Beloborodova, E.I., et al., [Trophologic insufficiency and absorptive function of small intestine in patients with chronic obstructive pulmonary disease]. Klin Med (Mosk), 2009. 87(3): p. 59-63.
19. Labarca, G., et al., Association between inflammatory bowel disease and chronic obstructive pulmonary disease: a systematic review and meta-analysis. BMC Pulm Med, 2019. 19(1): p. 186.
20. Raftery, A.L., et al., Links Between Inflammatory Bowel Disease and Chronic Obstructive Pulmonary Disease. Front Immunol, 2020. 11: p. 2144.
21. Lee, J., et al., Risk of inflammatory bowel disease in patients with chronic obstructive pulmonary disease: A nationwide, population-based study. World J Gastroenterol, 2019. 25(42): p. 6354-6364.
22. Garrett, W.S., J.I. Gordon, and L.H. Glimcher, Homeostasis and inflammation in the intestine. Cell, 2010. 140(6): p. 859-70.
23. Marsland, B.J., A. Trompette, and E.S. Gollwitzer, The Gut-Lung Axis in Respiratory Disease. Ann Am Thorac Soc, 2015. 12 Suppl 2: p. S150-6.
24. Zhang, D., et al., The Cross-Talk Between Gut Microbiota and Lungs in Common Lung Diseases. Front Microbiol, 2020. 11: p. 301.
25. Naik, D., et al., Chronic obstructive pulmonary disease and the metabolic syndrome: Consequences of a dual threat. Indian J Endocrinol Metab, 2014. 18(5): p. 608-16.
26. Evans, W.J., et al., Cachexia: a new definition. Clin Nutr, 2008. 27(6): p. 793-9.
27. Remels, A.H., et al., The mechanisms of cachexia underlying muscle dysfunction in COPD. J Appl Physiol (1985), 2013. 114(9): p. 1253-62.
28. Wagner, P.D., Possible mechanisms underlying the development of cachexia in COPD. Eur Respir J, 2008. 31(3): p. 492-501.
29. Richard, A.J., et al., Adipose Tissue: Physiology to Metabolic Dysfunction, in Endotext, K.R. Feingold, et al., Editors. 2000: South Dartmouth (MA).
30. Plihalova, A., et al., The effect of hypoxia and re-oxygenation on adipose tissue lipolysis in COPD patients. Eur Respir J, 2016. 48(4): p. 1218-1220.
31. Groneberg, D.A. and K.F. Chung, Models of chronic obstructive pulmonary disease. Respir Res, 2004. 5: p. 18.
32. Mortaz, E. and I.A. Adcock, Limitation of COPD Studies in Animal Modeling. Tanaffos, 2012. 11(3): p. 7-8.
33. Liang, G.B. and Z.H. He, Animal models of emphysema. Chin Med J (Engl), 2019. 132(20): p. 2465-2475.
34. Antunes, M.A. and P.R. Rocco, Elastase-induced pulmonary emphysema: insights from experimental models. An Acad Bras Cienc, 2011. 83(4): p. 1385-96.
35. Hardaker, E.L., et al., Exposing rodents to a combination of tobacco smoke and lipopolysaccharide results in an exaggerated

inflammatory response in the lung. Br J Pharmacol, 2010. 160(8): p. 1985-96.

36. Mebratu, Y.A., et al., Inflammation and emphysema in cigarette smoke-exposed mice when instilled with poly (I:C) or infected with influenza A or respiratory syncytial viruses. Respir Res, 2016. 17(1): p. 75.

37. Mebratu, Y.A. and Y. Tesfaigzi, IL-17 Plays a Role in Respiratory Syncytial Virus-induced Lung Inflammation and Emphysema in Elastase and LPS-injured Mice. Am J Respir Cell Mol Biol, 2018. 58(6): p. 717-726.

38. Hanania, N.A., S.C. Lareau, and B.P. Yawn, Safety of inhaled long-acting anti-muscarinic agents in COPD. Postgrad Med, 2017. 129(5): p. 500-512.

39. Rahman, I., The role of oxidative stress in the pathogenesis of COPD: implications for therapy. Treat Respir Med, 2005. 4(3): p. 175-200.

40. McGuinness, A.J. and E. Sapey, Oxidative Stress in COPD: Sources, Markers, and Potential Mechanisms. J Clin Med, 2017. 6(2).

41. Fischer, B.M., J.A. Voynow, and A.J. Ghio, COPD: balancing oxidants and antioxidants. Int J Chron Obstruct Pulmon Dis, 2015. 10: p. 261-76.

42. Rahman, I., Antioxidant therapies in COPD. Int J Chron Obstruct Pulmon Dis, 2006. 1(1): p. 15-29.

43. Orr, A.L., et al., Physiological oxidative stress after arousal from hibernation in Arctic ground squirrel. Comp Biochem Physiol A Mol Integr Physiol, 2009. 153(2): p. 213-21.

44. Han, B., et al., The novel compound Sul-121 inhibits airway inflammation and hyperresponsiveness in experimental models of chronic obstructive pulmonary disease. Sci Rep, 2016. 6: p. 26928.

Chapter 2

The Bidirectional
Gut-Lung Axis in COPD

Lei Wang[1,2], Yang Cai[1], Johan Garssen[1,2], Paul. A.J. Henricks[1],
Gert Folkerts[1], Saskia Braber[1*]

[1] Division of Pharmacology, Utrecht Institute for Pharmaceutical Sciences,
Faculty of Science, Utrecht University, Utrecht, The Netherlands
[2] Danone Nutricia Research, Utrecht, The Netherlands

Abstract

Epidemiological studies indicate that the incidence of chronic obstructive pulmonary disease (COPD) is associated with changes in intestinal health. Cigarette smoking, as one of the major causes of COPD, can impact the gastrointestinal system and promotes intestinal diseases. This may indicate the existence of gut-lung interactions, however, an overview of the underlying mechanisms of the bidirectional connection between the lungs and the gut in COPD is lacking.

The interaction between the lungs and the gut can occur through circulating inflammatory cells and mediators. Moreover, gut microbiota dysbiosis, observed in both COPD and intestinal disorders, can lead to an altered mucosal environment, including the intestinal barrier and immune system, and hence, may negatively affect both the gut and the lungs. Last but not least, systemic hypoxia and oxidative stress that occurs in COPD may also be involved in intestinal injury and play a role in the gut-lung axis.

In this review, we summarize the evidence from clinical research, animal models and *in vitro* studies to explain the potential mechanisms of gut-lung interactions related to COPD. Interesting observations on mechanisms driving the gut-lung axis in other respiratory diseases will be discussed and the possibility of promising future add-on therapies for intestinal dysfunction in COPD patients will be highlighted.

Keywords
Gut-lung axis; lung diseases; systemic inflammation; hypoxia; microbiota

Introduction

Chronic obstructive pulmonary disease (COPD) is characterized by chronic inflammation and chronic airway obstruction, leading to a progressive and irreversible decline in lung function [1]. COPD is associated with exacerbations and comorbidities resulting in a significant social and economic burden [2]. There are several risk factors for COPD, including cigarette smoking, genetic factors, environmental pollution and infections [3].

Intestinal diseases, such as inflammatory bowel disease (IBD) and irritable bowel syndrome (IBS), are commonly observed in COPD [4]. The incidence of IBD is higher in COPD patients compared to healthy subjects [5]. Patients with COPD suffer from intestinal microbiome dysbiosis and have an increased intestinal permeability, which is associated with inflammatory cell infiltration [6].

Although the gut and lungs are separate organs with different functions and environment, they have structural similarities and interact in health and disease. There is growing interest in how lung health impacts the function of the intestinal system, and vice versa [7]. Cigarette smoke as one of the leading causes of COPD has detrimental effects on the respiratory and gastrointestinal mucosal health. Cigarette smoke can induce inflammatory responses in the lung, which "spills" into the systemic circulation causing systemic inflammation and leading to inflammatory responses in the intestine [8]. Cigarette smoke can also cause oxidative stress and hypoxia in airway epithelium [9], while the impaired gas exchange induced by cigarette smoke in COPD patients also leads to intestinal hypoxia and enterocyte damage, and can result in an enhancement of intestinal permeability, altered immune responses and microbiome dysbiosis [6, 10]. In addition, due to mucocilliary clearance of the respiratory tract, tobacco products will end up in the intestine, which may directly affect the gastrointestinal tract [11] and hence affect lung health.

Here, we will focus on recent advances in the understanding of these interactions between the lungs and the gut in COPD. Systemic inflammation, epithelial barrier dysfunction, oxidative stress, hypoxia and gut microbiome dysbiosis are considered to play a major role in gut-lung interactions. Clinical studies and pre-clinical *in vivo* and *in vitro* experiments related to the gut-lung axis in COPD will be discussed, as well as potential interventions and their modulation via the gut-lung axis aimed at treating or preventing the progression of COPD and its intestinal comorbidities.

Clinical trials: gut-lung axis in COPD patients

Intestinal disorders as a component of COPD

There is an association between intestinal disorders and COPD. Intestinal diseases are more prevalent in COPD patients than in healthy subjects. A population-based retrospective cohort study showed that the incidence of inflammatory bowel diseases (IBD), i.e., Crohn's disease (CD) and ulcerative colitis (UC), was 55% and 30% higher in COPD patients than in the general population, respectively [5]. In addition, both CD and UC were associated with an increased mortality in asthma-related COPD patients, while UC also increased the mortality in COPD patients [12]. Shared environmental risks (i.e., smoking and air pollution) are unlikely to fully explain this association because cigarette smoke may have a protective role in UC [13]. In the next section, the interaction between the respiratory and gastrointestinal system will be discussed and its possible involvement in COPD, including changes in immunological and systemic inflammation, epithelial barrier function, hypoxia-related and oxidative stress processes and alterations in microbiota composition. In addition, clinical evidence for the existence of the gut-lung axis in COPD is summarized in Table 1 (clinical part).

Systemic inflammation

Keely et al. reviewed that exaggerated innate immune responses, characterized by an increase of systemic pro-inflammatory mediators such as IL-6 and TNF-α, can contribute to the development of COPD [10]. There is clear evidence that immune dysfunction precedes symptoms of intestinal disorders [14]. The circulating pro-inflammatory mediators in COPD patients may drive cross-organ inflammation, for example, systemic IL-6 together with pulmonary TGF-β can trigger Th17-polarized inflammatory responses in the intestine [10]. A prospective case-control study showed that circulating levels of IL-6 and C-reactive protein (CRP) before diagnosis were associated with the risk of CD and UC [14]. In addition, raised plasma levels of CRP and IL-6 are present in COPD patients [15]. TNF-α is believed to play a central role in the pathophysiology of COPD and IBD [10, 16]. There are elevated levels of TNF-α in peripheral blood, bronchial biopsies, induced sputum and broncho-alveolar lavage fluid of COPD patients [16]. The anti-TNF-α antibody etanercept, but not infliximab, reduced the rate of COPD hospitalization [17]. Moreover, the anti-TNF-α antibodies infliximab, adalimumab, certolizumab pegol, and etanercept are currently in use for the remission of IBD patients [18]. Therefore, it can be hypothesized that excessive pro-inflammatory mediators produced in the lungs of COPD patients affect the intestine through systemic circulation contributing to intestinal disease. Vice versa, continuous intestinal inflammation can also exacerbate lung diseases by the presence of inflammatory mediators in the systemic circulation.

Epithelial barrier dysfunction, oxidative stress and hypoxia

The integrity of the epithelial barrier is essential for maintaining respiratory and intestinal mucosal health. Cigarette smoke impairs the airway epithelial barrier function and induces an increased permeability, which was more common in smokers with COPD compared to smokers with normal lung function [9, 19]. Further downregulation of apical junctional complex gene expression in airway epithelium was observed in COPD smokers compared to healthy smokers [19]. Cigarette smoke can promote the production of endogenous reactive oxygen species (ROS) by airway epithelial cells and pulmonary immune cells, while the presence of exogenous ROS in cigarette smoke can induce the fragmentation of hyaluronic acid in airway epithelial cells, which can impair the airway barrier integrity [9]. The ongoing production of ROS during cigarette smoke exposure and exacerbations will result in a substantial reduction in the general antioxidant capacity in COPD patients [20], which may affect intestinal disorders.

The unavailable metabolic demands (hypoxia) in COPD patients during daily activities results in an increase in intestinal permeability and cause enterocyte damage [21]. In addition, impaired gas exchange in COPD patients is associated with systemic hypoxia, which can drive intestinal epithelial integrity damage [22]. Systemic hypoxia markers also can be found elevated in CD patients [22]. Overall, the toxic effects of cigarette smoke, inhaled ROS and/or systemic hypoxia may extend systemically to the intestinal epithelium, resulting in intestinal epithelial dysfunction.

Changes in microbiota composition

COPD patients have an altered gut microbiota compared with healthy individuals. Li et al. observed a *Prevotella*-dominated gut enterotype and lower levels of short-chain fatty acids (SCFAs) in COPD patients [23]. In addition, mice receiving fecal transplantation from these COPD patients developed lung inflammation and cigarette smoke aggravated the deterioration of lung function in those transplanted mice [23].

Recently, a large multicenter study showed that the severity of COPD is associated with a decreased abundance of *Prevotella* and increased abundance of *Moraxella* in the airways and in concert with the downregulation of genes promoting epithelial defense and upregulation of pro-inflammatory pathway responses [24]. In addition, the abundance of *Streptococcus* in the airways was higher in patients with mild-to-moderate COPD than in healthy individuals [24]. The increased abundance of several *Streptococcus* species, including *S. parasanguinis_B* and *S. salivarius*, was also found in the intestine of COPD patients [25]. However, there were no differences between the microbiome composition of non-smokers with COPD and smokers with COPD, supporting this is a disease-associated phenotype rather than a phenotype driven by the influence of cigarette smoking on the gut microbiome [25]. The coordination of ventilation and swallowing may be subverted in COPD patients [26] resulting in the simultaneous micro-aspiration of the pharyngeal or oral microbiota into the respiratory and gastrointestinal tract. Another possible explanation is that the same embryonic origin and structural similarities of the gastrointestinal and

respiratory tract lead to similar responses and changes of the microbiota in these organs to the systemic inflammation and immune responses caused by COPD [4].

Translocation of gut microbiota may also play a role in the gut-lung crosstalk in COPD patients. Dysbiosis of the intestinal microbiota has been shown to influence the composition of the respiratory microbiota through changes in circulating inflammatory cytokines and via translocation of intestinal microbiota to the airways [27]. Translocation of gut microbiota to the airways might be related to the leaky gut induced by cigarette smoke, although this has not yet been confirmed in COPD patients yet [27]. Pathogens frequently colonize the airways, which is associated with exacerbations in COPD patients, promoting COPD development by amplifying lung and systemic inflammation. We speculate that the disruption of the lung epithelial barrier function may lead to the translocation of pathogenic bacteria. Translocated pathogens and pathogen-associated virulence factors may also enter the gastrointestinal tract, causing intestinal inflammation and related diseases.

Animal studies: gut-lung axis in COPD models

Immunological changes and systemic inflammation in cigarette smoke-exposed mice
The gut-lung axis might be involved in systemic inflammation and immune dysfunction in COPD [28]. Cigarette smoke-exposed mice challenged with dextran sodium sulfate (DSS) showed exaggerated intestinal inflammation with elevated Th17 cell, ILC3, and neutrophil responses in the intestine. This might be due to the increased systemic susceptibility to inflammation by a higher number of Th17 cells and neutrophils in circulation after cigarette smoke exposure [29]. There is an accumulation in the number of CD11b+ DCs in the intestinal Peyer's patches of mice after cigarette smoke exposure [30]. Interestingly, lung DCs, like CD103+ MLN DCs, can stimulate the translocation of T cells into the gastrointestinal tract probably via up-regulating the gut-homing integrin α4β7 *in vivo* [31].

Remarkably, CCR6 (chemokine CCL20 receptor) might be involved in regulating gut-lung crosstalk. In CCR6-deficient mice exposed to cigarette smoke, a deceased accumulation of several immune cell types, including DCs, neutrophils and T cells, in the lungs was observed [32]. CCR6 can also modulate harmful inflammatory processes in the gut, for example, DSS–induced colitis was less severe in CCR6-deficient mice [33]. In addition to the CCL20-CCR6 pathway, the CCL9-CCR1 pathway may also play a role in the gut-lung connection [30]. Increased numbers of CD11b+ DCs were still observed in cigarette smoke-exposed CCR6 knock-out mice, which might be related to the increased CCL9 expression in the small intestinal Peyer's patches after cigarette smoke exposure. The upregulation of CCL9 and CCL20 induced by cigarette smoke may contribute to increased epithelial apoptosis in the intestinal follicle-associated epithelium and to the accumulation of CD11b+ DC, CD4+ T cells, and CD8+ T cells in the small intestine [30].

Epithelial barrier dysfunction, oxidative stress, and hypoxia
Animal studies have demonstrated that cigarette smoke-induced intestinal barrier dysfunction and subsequent inflammation of the intestinal mucosa may be one of the mechanisms of intestinal damage in COPD [34, 35], although this cannot explain the protective effect of smoking observed in UC. In a rat model of COPD, dysfunctional and structural changes in the intestinal mucosal barrier was observed, including neutrophil infiltration, epithelial shedding, reduced tight junction protein expression (occludin and ZO-1) and increased secretion of TNF-α, IFN-γ and IL-8 [34]. Mice exhibited elevated intestinal inflammation and reduced intestinal Paneth cell integrity after intragastric administration of cigarette smoke condensate, resulting in reduced antimicrobial peptide production and bactericidal capacity [36]. Instead of changes in tight junction gene expression, it was demonstrated that cigarette smoke-induced intestinal inflammation in mice was related to altered epithelial mucus profiles, including increased mRNA expression of Muc2 and Muc3 in the ileum and Muc4 in the distal colon [37]. Impaired gas exchange induced by chronic cigarette smoke exposure caused systemic and intestinal hypoxia in mice, which drive angiogenesis and intestinal epithelial barrier dysfunction, resulting in increased risk and severity of CD [22]. Systemic and local ischemia might be caused by oxygen free radicals present in inhaled smoke, as described in the previous part: "clinical trials". In addition, cigarette smoke exposure elevated HIF-1α expression in the rat small intestine, which was associated with increased oxidative stress and apoptosis, leading to the destruction of intestinal tight junctions [38]. Although, nicotine in cigarette smoke may ameliorate the severity of UC by regulating the immune system and gut permeability [39], nicotine causes an increased frequency of colonic contractions and decreased colonic diameter in mice, possibly by acting on enteric neurons expressing nicotinic Acetylcholine receptors (nAChR). [40]. The antioxidant Ebselen prevents the reduction in colonic diameter in cigarette smoke-exposed mice [41].

Changes in microbiota composition
Papoutsopoulou et al. have reviewed the influence of smoking on the human gut microbiota [42], while information is scarce in animal species. Cigarette smoke reduces the relative abundance of *Bacteroidales* but increases the presence of *Firmicutes* in the feces in a murine model of COPD, while a high-fat diet can exacerbate the cigarette smoke-induced reduction in gut microbiota diversity [43, 44]. Interestingly, fecal microbiota transplantation reduces COPD pathogenesis, where the commensal bacterium *Parabacteroides goldsteinii* plays a key role. The LPS derived from *P. goldsteinii* exhibits anti-inflammatory properties, which can ameliorate COPD by acting as an antagonist of the Toll-like receptor 4 signaling pathway [44]. An increased abundance of gut *Lachnospiraceae sp.* was found in cigarette smoke-exposed mice, which might be one of the contributing factors leading to aberrant inflammation and

reduction of cellular physiological activities in the colon [37, 44]. Consistently, an increased abundance of *Lachnospiriaceae sp.* was also reported in other chronic inflammatory diseases such as IBD, IBS with diarrhea, and obesity [25, 44]. Cigarette smoke reduces the abundance of potentially beneficial bacteria (i.e., *Clostridium, Turicibacter*) and increased abundance of potentially harmful bacteria (i.e., *Desulfovibrio, Bilophila*) in a rat model of active cigarette smoking. *Clostridium* and *Turicibacter* are important commensal bacteria, which have the ability to regulate the gut barrier and inflammatory/immune responses related to intestinal diseases [45-47]. The genera *Desulfovibrio* and *Bilophila* can participate in the development of colorectal cancer by producing hydrogen sulfide and promoting chronic inflammation [45]. In addition, active smoking also reduced propionate (one of the SCFAs) metabolism in the cecal and colonic contents [45]. All pre-clinical evidence for the connection between the lungs and the gut in COPD is summarized in Table 1 (pre-clinical part).

Lessons learned from *in vitro* studies

In vitro studies can contribute to the knowledge of the underlying mechanisms of intestinal complications in COPD, although there are many limitations to investigating the link between gut and lung using *in vitro* studies. Cigarette smoke extract-exposed human colorectal cancer (Caco-2) cells showed a reduction of cell necrosis, claudin-1 and E-cadherin expression, and an increase in miR-21 (a diagnostic marker for colorectal carcinoma), cytoskeleton rearrangement, cell motility and invasiveness [48]. Cigarette smoke-induced cellular toxicity in Caco-2 cells might be caused by ROS in cigarettes and was suppressed by ROS scavenging [49]. Increased oxidative stress contributes to reduced gene and protein expression of tight and adherens junctions [9]. Papoutsopoulou et al. have summarized the effects of cigarette smoke components (e.g., nicotine, acrolein, ROS) on intestinal mucosal epithelial cells and/or immune cells [42]. Among all the components described, nicotine has gained the greatest interest due to its controversial effects as highlighted in several studies. Nicotine-derived nitrosamine ketone (NNK), a highly carcinogenic tobacco-specific nitrosamine, stimulates colon cancer HT-29 cell proliferation, and the effect was abolished by β1- or β2-receptor antagonists [50]. Nicotine was found to reduce TNF-α release from human leukemia (THP-1) cells *in vitro* [51] and inhibit the *ex vivo* production of IL-2 and TNF-α by mononuclear cells isolated from healthy volunteers [52]. An *in vitro* experiment using HT29 cells showed that nicotine can inhibit TNF-α-induced IL-8 release in a concentration-related manner via binding to the nAChR subunits alpha7 [53]. Nicotine may bind to nAChR and prevents nuclear factor (NF)-κB signaling, thereby preventing the release of high-mobility group box 1 (HMGB1) and inhibiting the release of proinflammatory cytokines, such as TNF-α [40]. The protective effect of nicotine on epithelium may explain the findings of the protective effect of cigarette smoking on UC as observed in clinical studies [39]. More *in vivo* studies are essential for understanding this underlying mechanism. On the

contrary, clinical trials do not support the positive effects of nicotine-based treatments for UCs [54]. All *in vitro* evidence regarding cigarette smoke-related effects on the intestine is summarized in Table 1 (*in vitro* part).

Table 1. Clinical, pre-clinical, and *in vitro* evidences for gut-lung axis in COPD.

	Experimental details	Effects on intestine	Reference
Clinical evidence for gut-lung axis in COPD			
COPD patients		Intestinal permeability ↑ Enterocyte damage	[21]
CD patients	Smoker	Systemic hypoxia ↑ Mucosal vasculature in ileum ↑	[22]
COPD patients	-	SCFAs ↓ *Prevotella* ↑	[23]
COPD patients	-	*Streptococcus* sp.↑	[25]
Pre-clinical evidence for gut-lung axis in COPD			
Male Sprague Dawley rats	CS exposure 6 months	Occludin and ZO-1 protein ↓ TNF-α, IFN-γ and IL-8 ↑ Neutrophil infiltration Epithelial shedding	[34]
Male C57BL/6 mice	Intragastric CS condensate	Intestinal inflammation ↑ Intestinal Paneth cell integrity ↓ Antimicrobial peptide production ↓ Bactericidal capacity ↓	[36]
Male C57BL/6 mice	CS exposure 24 weeks	Intestinal inflammation ↑ Muc2 and Muc3 in ileum ↑ Muc4 in distal colon ↑ *Lachnospiraceae* ↑	[37]
Female C57BL/6 mice	CS exposure	Systemic and intestinal hypoxia ↑ Epithelial barrier dysfunction ↑	[22]
Male Wistar rats	CS exposure 14 weeks	HIF-1α expression in small intestine ↑ Intestinal tight junctions ↓ Oxidative stress ↑ Apoptosis ↑	[38]
Female C57BL/6J mice	CS exposure 2 months + DSS challenge	Intestinal inflammation ↑ Th17 cells, ILC3, and neutrophils in intestine ↑	[29]
Male C57BL/6 mice	CS exposure 24 weeks	CD11b⁺ DCs in small intestine ↑ Epithelial apoptosis ↑ CD4+ and CD8+ T cells in small intestine ↑ mRNA expression of CCL9 and CCL20 ↑	[30]
Male C57BL/6 mice	CS exposure 4 weeks	*Bacteroidales* ↓ *Firmicutes* ↑	[43]
C57BL/6 mice	CS exposure 12 weeks	*Lachnospiraceae* ↑ *Erysipelotrichaceae* ↓ *Bacteroidales* ↓ *Ruminococcaceae* ↓	[75]
Female and male Wistar rats	CS exposure 3 months	*Clostridium* and *Turicibacter* ↓ *Desulfovibrio* and *Bilophila* ↑	[45]
***In vitro* studies**			
Caco-2 cells	CSE	Cell necrosis ↑ Claudin-1 and E-cadherin expression ↓ Cell permeability ↑	[48]
HT29 cells	Nicotine	TNF-α-induced IL-8 release ↓	[53]

CS, cigarette smoke; **CSE**, cigarette smoke exact; **GI**, Gastrointestinal.

The gut-lung axis in other respiratory diseases

Asthma

The importance of the gut-lung axis in COPD has been less well defined as compared to asthma. An increased risk of asthma has been connected to the disturbance of the gut microbiota during early life [4]. Study found that Vancomycin-treated mice have an altered microbiome profile and are more susceptible to allergic lung inflammation [55]. Furthermore, the systemic effects of the gut microbiota are partially attributed to the metabolites, such as SCFAs, which suppress lung inflammation through the activation of G protein-coupled receptors [56]. Supplementation with SCFAs ameliorated this enhanced susceptibility to asthma by lowering IL-4-producing T cells and decreasing the circulating IgE levels [55]. Our group previously showed that a diet containing non-digestible galacto-oligosaccharides has a beneficial effect on the prevention of house dust mite-induced allergic asthma by supporting pulmonary Treg function [57].

Infectious respiratory diseases

Similar to other chronic lung disorders, respiratory infections are often accompanied by intestinal symptoms [58]. For example, respiratory influenza infection causes lung injury accompanied by intestinal injury, however, this was not directly related to an intestinal viral infection. Influenza infection modified the microbiota composition in the intestine, which was associated with IFN-γ produced by lung-derived CCR9+CD4+ T cells that recruit into the small intestine [59, 60]. In addition, inflammasome activation during influenza virus infection caused the migration of DCs from the lungs into the lymph nodes and T-cell priming [61]. Similar evidence of a gut-lung interaction can be noticed in bacterial pneumonia. The gut microbiota protects the host during pneumococcal pneumonia, as in microbiota-depleted mice increased bacterial dissemination, inflammation, and mortality were observed. Moreover, alveolar macrophages from gut microbiota-depleted mice showed a decreased capacity to phagocytose S. pneumoniae [62]. Dietary pectin–derived acidic oligosaccharides were found to improve the pulmonary bacterial clearance of Pseudomonas aeruginosa-induced lung infection in mice by modulating intestinal microbiota and immunity [63].

Gastrointestinal symptoms are also commonly found in COVID-19 (SARS-CoV-2) patients and sometimes the gastrointestinal symptoms appeared even before the development of respiratory symptoms, which indicates that the gut-lung axis might be involved in COVID-19 [64]. The fecal microbiome of patients with COVID-19 showed persistent alterations, which were associated with COVID-19 severity [65]. SARS-CoV-2 could enter the intestine via the oral-intestinal route (from the trachea to the esophagus and intestine) [66]. However, the virus could also be translocated to the systemic circulation after damaging the lung tissue and subsequently, migration to the intestine via the circulatory and lymphatic system might occur [67]. The disruption of the gut barrier integrity due to gut microbiome dysbiosis might also contribute to SARS-CoV-2 translocation [68]. Modulating and restoring the gut microbiome of individuals infected with SARS-CoV-2 via therapeutic dietary interventions might mitigate systemic inflammation, and intestinal damage and decrease respiratory symptoms [69].

Conclusion and summary

COPD is a complex disease and is often associated with comorbidities like intestinal diseases. The concept of "gut-lung axis" has gained attention with the discovery of the influence of gut health on lung immunity [70]. Advances in understanding the potential mechanisms of gut-lung crosstalk have highlighted the bi-directional crosstalk between the gut and the lungs, showing the impact of the lungs on intestinal health and the importance of the intestine in maintaining immune homeostasis. In this translational review, this bidirectional crosstalk between the gut and the lungs in COPD is verified based on clinical, in vivo, and in vitro studies. Overall, the findings of these studies support each other and demonstrate that COPD and/or cigarette smoking can cause intestinal inflammation, barrier disruption, hypoxia and oxidative stress, as well as microbiota dysbiosis. The possible connections between the gut and the lungs and postulated mechanisms of how the gut-lung axis impacts COPD are described in Figure 1. Systemic inflammation is considered one of the major causes of gut-lung crosstalk in COPD. Excessive inflammatory mediators generated from the lung can affect intestinal health through the systemic and lymphatic systems. Vice versa, inflammation in the intestine can also potentiate the development of lung diseases. Moreover, impaired gas exchange capacity in the lung and systemic hypoxia in COPD can lead to intestinal epithelial integrity damage. In addition, gut microbiota dysbiosis in COPD can lead to disruption of the intestinal barrier integrity and can activate local and systemic immune responses, thereby aggravating the immunity and pathology in the lung. Although the function of intestinal microbiota in modulating local and systemic immune responses has been extensively studied, the impact of the lung microbiota and its products in regulating immunity has just begun and further research is needed to better understand host immune-lung microbiome interactions.

The current management of COPD is mainly focused on suppressing airway inflammation and decreasing symptoms. The purpose of this translational review is not only to emphasize the interaction between the gut and the lung in COPD, but also to highlight the possibility to target the intestine to improve the clinical outcome in COPD. There is an urgent need for research into the primary prevention of COPD and the deceleration of disease progression. The intestine might be a promising target, through bi-directional gut and lung crosstalk, to improve lung health and minimize COPD and related comorbidities. An understudied area of COPD management might be nutritional interventions. Based on the literature presented in

this review, understanding the importance of the gut-lung axis in COPD, it can be suggested that anti-inflammatory and/or nutritional intervention targeting the intestine might be used as a new add-on therapy to suppress the development of COPD and its co-morbidities.
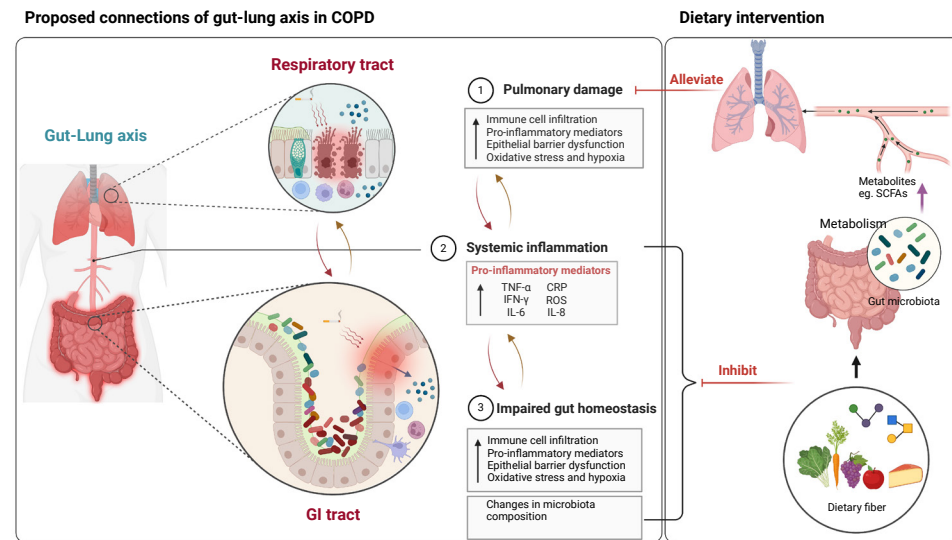

Figure 1. Proposed connections in the gut–lung axis and its mechanistic role in COPD. COPD is characterized by immune cell infiltration, pro-inflammatory mediators in the lungs, impaired epithelial barrier function, and oxidative stress and hypoxia in the lungs (1). Damaged and activated lung cells further stimulate the innate immune response through elevated pro-inflammatory mediators (e.g., TNF-α, IFN-γ, IL-6, IL-8, CRP, ROS) (2). Those pro-inflammatory mediators (and cigarette smoke particles) can migrate to the gastrointestinal tract, (partly) via systemic circulation, exacerbating intestinal impairments, including increased inflammatory immune infiltration, epithelial barrier damage, oxidative stress, and hypoxia in the intestine. Moreover, (long-term) cigarette smoking and inflammatory immune cell infiltration in the gut can change the microbiota composition, including the decreased abundance of health-promoting commensal bacteria (3). Impaired gut function not only increases the production and entry of pro-inflammatory mediators into the systemic circulation but also attenuates nutrient absorption, antioxidant capacity, and protection from pathogens and other environmental stimuli, further exacerbating COPD.
Dietary intervention, such as fibers can modulate gut microbiota composition, increasing the abundance of health-promoting commensal bacteria, decreasing the permeability of intestinal mucosa, and enhancing the bacterial synthesis of immune-modulating compounds (e.g. SCFA). All of these may decrease pro-inflammatory mediators and alleviate the symptoms in the lung.
COPD, chronic obstructive pulmonary disease; **CRP**, C-reactive protein; **TNF-α**, tumor necrosis factor alpha; **IFN-γ**, Interferon gamma; **IL-6**, Interleukin 6; **IL-8**, Interleukin 8; **ROS**, reactive oxygen species; **SCFAs**, short-chain fatty acids.

Future perspectives

The gut-lung axis exists in many respiratory diseases, and the gut microbiome plays an important role in profiling the intestinal immune system, thus regulating lung health. Therapies focusing on gut microbiota modification can also be considered in COPD treatment. Firstly, diet fibers are known to increase SCFA-producing bacteria [71] and exert anti-inflammatory effects on respiratory diseases, such as asthma [46]. SCFA themselves are also potent anti-inflammatory molecules, which may reach the airways via systemic circulation [72]. Interestingly, evidence showed that a mixture of non-digestible oligosaccharides decreased the LPS-induced neutrophil influx by >60% in broncho-alveolar lavage fluid and prevented the development of lung emphysema [73], which confirms that shaping the gut microbiota composition with dietary supplementation might be a potential treatment for COPD. Dietary interventions may also be a potential niche to decrease inflammation and thereby prevent the progression of airway diseases and their co-morbidities. Secondly, a murine study showed that fecal microbiota transplantation attenuates emphysema development via local and systemic inhibition of inflammation and changes in gut microbiota composition [74]. This might provide a new paradigm for the treatment of COPD and further research in this area is certainly needed.

References

1. Wang, Y., et al., Role of inflammatory cells in airway remodeling in COPD. Int J Chron Obstruct Pulmon Dis, 2018. 13: p. 3341-3348.

2. Vaughan, A., et al., COPD and the gut-lung axis: the therapeutic potential of fibre. J Thorac Dis, 2019. 11(Suppl 17): p. S2173-S2180.

3. Decramer, M., W. Janssens, and M. Miravitlles, Chronic obstructive pulmonary disease. Lancet, 2012. 379(9823): p. 1341-51.

4. Budden, K.F., et al., Emerging pathogenic links between microbiota and the gut-lung axis. Nat Rev Microbiol, 2017. 15(1): p. 55-63.

5. Brassard, P., et al., Increased incidence of inflammatory bowel disease in Quebec residents with airway diseases. Eur Respir J, 2015. 45(4): p. 962-8.

6. Keely, S. and P.M. Hansbro, Lung-gut cross talk: a potential mechanism for intestinal dysfunction in patients with COPD. Chest, 2014. 145(2): p. 199-200.

7. Willis, K.A., J.D. Stewart, and N. Ambalavanan, Recent advances in understanding the ecology of the lung microbiota and deciphering the gut-lung axis. Am J Physiol Lung Cell Mol Physiol, 2020. 319(4): p. L710-L716.

8. Beloborodova, E.I., et al., [Activity of systemic inflammatory reaction in patients with chronic obstructive pulmonary disease in regard to small intestinal absorption function]. Ter Arkh, 2009. 81(3): p. 19-23.

9. Aghapour, M., et al., Airway Epithelial Barrier Dysfunction in Chronic Obstructive Pulmonary Disease: Role of Cigarette Smoke Exposure. Am J Respir Cell Mol Biol, 2018. 58(2): p. 157-169.

10. Keely, S., N.J. Talley, and P.M. Hansbro, Pulmonary-intestinal cross-talk in mucosal inflammatory disease. Mucosal Immunol, 2012. 5(1): p. 7-18.

11. Cai, Z., et al., Hyaluronan-Inorganic Nanohybrid Materials for Biomedical Applications. Biomacromolecules, 2017. 18(6): p. 1677-1696.

12. Vutcovici, M., et al., Inflammatory bowel disease and risk of mortality in COPD. Eur Respir J, 2016. 47(5): p. 1357-64.

13. Birrenbach, T. and U. Bocker, Inflammatory bowel disease and smoking: a review of epidemiology, pathophysiology, and therapeutic implications. Inflamm Bowel Dis, 2004. 10(6): p. 848-59.

14. Lochhead, P., et al., Association Between Circulating Levels of C-Reactive Protein and Interleukin-6 and Risk of Inflammatory Bowel Disease. Clin Gastroenterol Hepatol, 2016. 14(6): p. 818-824 e6.

15. Yanbaeva, D.G., et al., IL6 and CRP haplotypes are associated with COPD risk and systemic inflammation: a case-control study. BMC Med Genet, 2009. 10: p. 23.

16. Matera, M.G., L. Calzetta, and M. Cazzola, TNF-alpha inhibitors in asthma and COPD: we must not throw the baby out with the bath water. Pulm Pharmacol Ther, 2010. 23(2): p. 121-8.

17. Suissa, S., P. Ernst, and M. Hudson, TNF-alpha antagonists and the prevention of hospitalisation for chronic obstructive pulmonary disease. Pulm Pharmacol Ther, 2008. 21(1): p. 234-8.

18. Ringerike, T., et al., in TNFalpha-Inhibitors in Inflammatory Bowel Disease. 2008: Oslo, Norway.

19. Shaykhiev, R., et al., Cigarette smoking reprograms apical junctional complex molecular architecture in the human airway epithelium in vivo. Cell Mol Life Sci, 2011. 68(5): p. 877-92.

20. Kirkham, P.A. and P.J. Barnes, Oxidative stress in COPD. Chest, 2013. 144(1): p. 266-273.

21. Rutten, E.P.A., et al., Disturbed intestinal integrity in patients with COPD: effects of activities of daily living. Chest, 2014. 145(2): p. 245-252.

22. Fricker, M., et al., Chronic cigarette smoke exposure induces systemic hypoxia that drives intestinal dysfunction. JCI Insight, 2018. 3(3).

23. Li, N., et al., Gut microbiota dysbiosis contributes to the development of chronic obstructive pulmonary disease. Respir Res, 2021. 22(1): p. 274.

24. Ramsheh, M.Y., et al., Lung microbiome composition and bronchial epithelial gene expression in patients with COPD versus healthy individuals: a bacterial 16S rRNA gene sequencing and host transcriptomic analysis. The Lancet Microbe, 2021.

25. Bowerman, K.L., et al., Disease-associated gut microbiome and metabolome changes in patients with chronic obstructive pulmonary disease. Nat Commun, 2020. 11(1): p. 5886.

26. Cvejic, L., et al., Laryngeal penetration and aspiration in individuals with stable COPD. Respirology, 2011. 16(2): p. 269-75.

27. Raftery, A.L., et al., Links Between Inflammatory Bowel Disease and Chronic Obstructive Pulmonary Disease. Front Immunol, 2020. 11: p. 2144.

28. Bhat, T.A., et al., Immune Dysfunction in Patients with Chronic Obstructive Pulmonary Disease. Ann Am Thorac Soc, 2015. 12 Suppl 2: p. S169-75.

29. Kim, M., et al., Cigarette Smoke Induces Intestinal Inflammation via a Th17 Cell-Neutrophil Axis. Front Immunol, 2019. 10: p. 75.

30. Verschuere, S., et al., Cigarette smoking alters epithelial apoptosis and immune composition in murine GALT. Lab Invest, 2011. 91(7): p. 1056-67.

31. Ruane, D., et al., Lung dendritic cells induce migration of protective T cells to the gastrointestinal tract. J Exp Med, 2013. 210(9): p. 1871-88.

32. Bracke, K.R., et al., Cigarette smoke-induced pulmonary inflammation and emphysema are attenuated in CCR6-deficient mice. J Immunol, 2006. 177(7): p. 4350-9.

33. Varona, R., et al., CCR6 has a non-redundant role in the development of inflammatory bowel disease. Eur J Immunol, 2003. 33(10): p. 2937-46.

34. Xin, X., et al., Mechanism of intestinal mucosal barrier dysfunction in a rat model of chronic obstructive pulmonary disease: An observational study. Exp Ther Med, 2016. 12(3): p. 1331-1336.

35. Zuo, L., et al., Cigarette smoking is associated with intestinal barrier dysfunction in the small intestine but not in the large intestine of mice. J Crohns Colitis, 2014. 8(12): p. 1710-22.

36. Berkowitz, L., et al., Mucosal Exposure to Cigarette Components Induces Intestinal Inflammation and Alters Antimicrobial Response in Mice. Front Immunol, 2019. 10: p. 2289.

37. Allais, L., et al., Chronic cigarette smoke exposure induces microbial and inflammatory shifts and mucin changes in the murine gut. Environ Microbiol, 2016. 18(5): p. 1352-63.

38. Li, H., et al., Increased oxidative stress and disrupted small intestinal tight junctions in cigarette smoke-exposed rats. Mol Med Rep, 2015. 11(6): p. 4639-44.

39. Berkowitz, L., et al., Impact of Cigarette Smoking on the Gastrointestinal Tract Inflammation: Opposing Effects in Crohn's Disease and Ulcerative Colitis. Front Immunol, 2018. 9: p. 74.

40. McGilligan, V.E., et al., Hypothesis about mechanisms through which nicotine might exert its effect on the interdependence of inflammation and gut barrier function in ulcerative colitis. Inflamm Bowel Dis, 2007. 13(1): p. 108-15.

41. Balasuriya, G.K., et al., Ebselen prevents cigarette smoke-induced gastrointestinal dysfunction in mice. Clin Sci (Lond), 2020. 134(22): p. 2943-2957.

42. Papoutsopoulou, S., et al., Review article: impact of cigarette smoking on intestinal inflammation-direct and indirect mechanisms. Aliment Pharmacol Ther, 2020. 51(12): p. 1268-1285.

43. Yang, Y., et al., Cigarette smoking exposure breaks the homeostasis of cholesterol and bile acid metabolism and induces gut microbiota dysbiosis in mice with different diets. Toxicology, 2021. 450: p. 152678.

44. Lai, H.C., et al., Gut microbiota modulates COPD pathogenesis: role of anti-inflammatory Parabacteroides goldsteinii lipopolysaccharide. Gut, 2022. 71(2): p. 309-321.

45. Wang, X., et al., Active Smoking Induces Aberrations in Digestive Tract Microbiota of Rats. Front Cell Infect Microbiol, 2021. 11: p. 737204.

46. Cai, Y., et al., Microbiota-dependent and -independent effects of dietary fibre on human health. Br J Pharmacol, 2020. 177(6): p. 1363-1381.

47. Zhong, Y., M. Nyman, and F. Fak, Modulation of gut microbiota in rats fed high-fat diets by processing whole-grain barley to barley malt. Mol Nutr Food Res, 2015. 59(10): p. 2066-76.

48. Dino, P., et al., Cigarette smoke extract modulates E-Cadherin, Claudin-1 and miR-21 and promotes cancer invasiveness in human colorectal adenocarcinoma cells. Toxicol Lett, 2019. 317: p. 102-109.

49. Yoshitomi, T., et al., Development of nitroxide radicals-containing polymer for scavenging reactive oxygen species from cigarette smoke. Sci Technol Adv Mater, 2014. 15(3): p. 035002.

50. Wu, W.K., et al., 4-(Methylnitrosamino)-1-(3-pyridyl)-1-butanone from cigarette smoke stimulates colon cancer growth via beta-adrenoceptors. Cancer Res, 2005. 65(12): p. 5272-7.

51. Sykes, A.P., et al., An investigation into the effect and mechanisms of action of nicotine in inflammatory bowel disease. Inflamm Res, 2000. 49(7): p. 311-9.

52. Madretsma, G.S., et al., Nicotine inhibits the in vitro production of interleukin 2 and tumour necrosis factor-alpha by human mononuclear cells. Immunopharmacology, 1996. 35(1): p. 47-51.

53. Summers, A.E., C.J. Whelan, and M.E. Parsons, Nicotinic acetylcholine receptor subunits and receptor activity in the epithelial cell line HT29. Life Sci, 2003. 72(18-19): p. 2091-4.

54. Lunney, P.C. and R.W. Leong, Review article: Ulcerative colitis, smoking and nicotine therapy. Aliment Pharmacol Ther, 2012. 36(11-12): p. 997-1008.

55. Cait, A., et al., Microbiome-driven allergic lung inflammation is ameliorated by short-chain fatty acids. Mucosal Immunol, 2018. 11(3): p. 785-795.

56. McAleer, J.P. and J.K. Kolls, Contributions of the intestinal microbiome in lung immunity. Eur J Immunol, 2018. 48(1): p. 39-49.

57. Verheijden, K.A., et al., Regulatory T Cell Depletion Abolishes the Protective Effect of Dietary Galacto-Oligosaccharides on Eosinophilic Airway Inflammation in House Dust Mite-Induced Asthma in Mice. J Nutr, 2015. 146(4): p. 831-837.

58. Dilantika, C., et al., Influenza virus infection among pediatric patients reporting diarrhea and influenza-like illness. BMC Infect Dis, 2010. 10: p. 3.

59. Wang, J., et al., Respiratory influenza virus infection induces intestinal immune injury via microbiota-mediated Th17 cell-dependent inflammation. J Exp Med, 2014. 211(12): p. 2397-410.

60. Deriu, E., et al., Influenza Virus Affects Intestinal Microbiota and Secondary Salmonella Infection in the Gut through Type I Interferons. PLoS Pathog, 2016. 12(5): p. e1005572.

61. Ichinohe, T., et al., Microbiota regulates immune defense against respiratory tract influenza A virus infection. Proc Natl Acad Sci U S A, 2011. 108(13): p. 5354-9.

62. Schuijt, T.J., et al., The gut microbiota plays a protective role in the host defence against pneumococcal pneumonia. Gut, 2016. 65(4): p. 575-83.

63. Bernard, H., et al., Dietary pectin-derived acidic oligosaccharides improve the pulmonary bacterial clearance of Pseudomonas aeruginosa lung infection in mice by modulating intestinal microbiota and immunity. J Infect Dis, 2015. 211(1): p. 156-65.

64. Nobel, Y.R., et al., Gastrointestinal Symptoms and Coronavirus Disease 2019: A Case-Control Study From the United States. Gastroenterology, 2020. 159(1): p. 373-375 e2.

65. Zuo, T., et al., Alterations in gut microbiota of patients with COVID-19 during time of hospitalization. Gastroenterology, 2020. 159(3): p. 944-955. e8.

66. Devaux, C.A., J.C. Lagier, and D. Raoult, New Insights into the Physiopathology of COVID-19: SARS-CoV-2-Associated Gastrointestinal Illness. Front Med (Lausanne), 2021. 8: p. 640073.

67. Aktas, B. and B. Aslim, Gut-lung axis and dysbiosis in COVID-19. Turk J Biol, 2020. 44(3): p. 265-272.

68. Monkemuller, K., L. Fry, and S. Rickes, COVID-19, coronavirus, SARS-CoV-2 and the small bowel. Rev Esp Enferm Dig, 2020. 112(5): p. 383-388.

69. Lau, H.C., S.C. Ng, and J. Yu, Targeting the Gut Microbiota in Coronavirus Disease 2019: Hype or Hope? Gastroenterology, 2022. 162(1): p. 9-16.

70. Bulanda, E. and T.P. Wypych, Bypassing the Gut-Lung Axis via Microbial Metabolites: Implications for Chronic Respiratory Diseases. Front Microbiol, 2022. 13: p. 857418.

71. Fu, Y., et al., Relationship Between Dietary Fiber Intake and Short-Chain Fatty Acid-Producing Bacteria During Critical Illness: A Prospective Cohort Study. JPEN J Parenter Enteral Nutr, 2020. 44(3): p. 463-471.

72. Correa-Oliveira, R., et al., Regulation of immune cell function by short-chain fatty acids. Clin Transl Immunology, 2016. 5(4): p. e73.

73. Janbazacyabar, H., et al., Non-digestible oligosaccharides partially prevent the development of LPS-induced lung emphysema in mice. PharmaNutrition, 2019. 10: p. 100163.

74. Jang, Y.O., et al., Fecal microbial transplantation and a high fiber diet attenuates emphysema development by suppressing inflammation and apoptosis. Exp Mol Med, 2020. 52(7): p. 1128-1139.

75. Lai, H.C., et al., Gut microbiota modulates COPD pathogenesis: role of anti-inflammatory Parabacteroides goldsteinii lipopolysaccharide. Gut, 2021.

Chapter 3

Changes in Intestinal Homeostasis and Immunity in a Cigarette Smoke- and LPS-induced Murine Model for COPD: the Gut-Lung Axis

Lei Wang[1], Charlotte E. Pelgrim[1], Lucía N. Peralta Marzal[1], Stephanie Korver[1], Ingrid van Ark[1], Thea Leusink-Muis[1], Ardy van Helvoort[2,3], Ali Keshavarzian[4], Aletta D. Kraneveld[1], Johan Garssen[1,2], Paul A.J. Henricks[1], Gert Folkerts[1], Saskia Braber[1*]

[1] Division of Pharmacology, Utrecht Institute for Pharmaceutical Sciences, Faculty of Science, Utrecht University, Utrecht, The Netherlands
[2] Danone Nutricia Research, Utrecht, The Netherlands
[3] NUTRIM School of Nutrition and Translational Research in Metabolism, Maastricht University, Maastricht, The Netherlands
[4] Department of Internal Medicine, Division of Digestive Diseases and Nutrition, Rush Medical College, Chicago, USA

Abstract

Chronic obstructive pulmonary disease (COPD) is often associated with intestinal comorbidities. In this study, changes in intestinal homeostasis and immunity in a cigarette smoke and lipopolysaccharide (LPS)-induced COPD model were investigated. Mice were exposed to cigarette smoke or air for 72 days, except days 42, 52 and 62 on which the mice were treated with saline or LPS via intratracheal instillation.

Cigarette smoke-exposed mice showed increased alveolar enlargement and numbers of total cells, macrophages, and neutrophils in bronchoalveolar lavage. Cigarette smoke exposure increased mucus production and different inflammatory mediators, including C-reactive protein (CRP) and keratinocyte-derived chemokine (KC), in bronchoalveolar lavage (BAL) fluid and serum. LPS did not further impact the mean linear intercept (Lm), total BAL cell numbers, and mucus production but increased macrophages, as well as decreased neutrophils and related inflammatory mediators levels in BAL fluid. T helper (Th) 1 cells were enhanced in the spleen after cigarette smoke exposure, however, in combination with LPS caused an increase in Th1 and Th2 cells. Histomorphological changes were observed in the proximal small intestine after cigarette smoke exposure and the addition of LPS had no effect. Cigarette smoke activated the intestinal immune network for IgA production in the distal small intestine which was associated with increased fecal sIgA levels and enlargement of Peyer's patches. Cigarette smoke plus LPS decreased fecal sIgA levels and the size of Peyer's patches.

In conclusion, cigarette smoke with or without LPS affects intestinal health as observed by changes in intestinal histomorphology and immune network for IgA production. Elevated systemic mediators might play a role in the gut-lung crosstalk. These findings contribute to a better understanding of intestinal disorders related to COPD.

Keywords
COPD; Gut-lung axis; Intestinal immunity; Systemic inflammation; Cigarette smoke exposure.

Introduction

Chronic obstructive pulmonary disease (COPD) is one of the leading causes of morbidity and mortality worldwide and is characterized by irreversible alterations to the structure of the lungs and chronic inflammation in pulmonary tissues [1]. COPD is also a multifactorial systemic disease and the chronic inflammation observed in the lungs of COPD patients is associated with systemic effects, such as mental [2], cardiovascular, metabolic, musculoskeletal, and gastrointestinal comorbidities [3]. COPD patients often have a high prevalence and incidence of intestinal symptoms such as inflammatory infiltration, increased intestinal permeability and absorptive impairment [4-6]. For example, patients with COPD have an increased risk of developing inflammatory bowel disease (IBD) [7, 8], and this risk increases with the severity of COPD [9]. COPD and IBD share many similarities in epidemiological and clinical features, as well as in inflammatory responses. Dysregulation of immunity at mucosal surfaces is thought to be responsible for the development and progression of COPD and IBD [10]. It has been hypothesized that the airway inflammation observed in COPD results in enhanced systemic inflammation [11]. Systemic inflammation may be a central pathogenic link between the pulmonary and extrapulmonary components, like the gastrointestinal tract [12]. The systemic impact of COPD further increases the risk of morbidities and mortality [13, 14].

The bi-directional crosstalk between the gut and the lungs with their shared mucosal immune system has been called the gut-lung axis [15]. During inflammation the bronchus-associated lymphoid tissue (BALT) controls immune cell trafficking from the lung tissue into the systemic circulation, which reflects the role of the gut-associated lymphoid tissue (GALT). These immune cells from lung and intestinal tissue exhibit the ability to migrate to the other mucosal sites [16, 17]. Immunoglobulin A (IgA) is one of the key antibodies in mucosal tissues and seems to be essential to establish a balanced and healthy intestinal mucosal immune response in order to protect against invading pathogens, but also to influence mucosal tolerance towards safe food proteins/antigens [18, 19]. Additionally, systemic mediators, dysregulation of protease activity, and interaction of the lung and intestinal microbiome might play an important role in the gut-lung crosstalk [17].

Cigarette smoke is one of the most prominent risk factors for developing COPD [20]. Epidemiologic studies indicated that there are shared risk factors, such as cigarette smoking and an unhealthy lifestyle (e.g. diet) for the development of respiratory diseases, such as COPD and gastrointestinal complaints [21]. Besides the effects of cigarette smoke on the development of COPD, respiratory bacterial, viral and/or fungi infections are also major risk factors potentially exacerbating symptoms of COPD and resulting in hospitalization and additional treatment [22, 23]. It is well established that additional exposure to the bacterial endotoxin lipopolysaccharide (LPS) in cigarette smoke- or elastase- induced animal models for COPD can cause an exaggerated inflammatory response in the lungs [24, 25]. Intestinal

changes in cigarette smoke-exposed mice following repetitive exacerbations have not yet been studied so far. Therefore, a murine model of long-term cigarette smoke exposure with or without LPS co-stimulation was used to better understand the effects of pulmonary inflammation and emphysema on systemic inflammation and intestinal homeostasis and immunity. In this perspective, inflammatory mediators in bronchoalveolar lavage (BAL) fluid and lung histology were investigated to confirm that cigarette smoke with or without LPS exposure induced lung injury. Systemic inflammation was confirmed by measuring inflammatory mediators in serum and T cell subsets in spleen. The impact of cigarette smoke with or without LPS exposure on intestinal homeostasis was studied by exploring intestinal histomorphology, the short chain fatty acids (SCFAs) production in the gut and the intestinal immune network for IgA production. We hypothesize that cigarette smoke exposure might affect the immunity of the gut and induce intestinal damage besides the observed lung injury, and the additional LPS triggers may influence the cigarette smoke-induced immune modulation within the gut-lung axis.

Results

Evaluation of lung damage

Lung emphysema, BAL fluid cells

Mean linear intercept (Lm) is a measure of alveolar size in the lungs and was used to determine the presence and severity of emphysema in histological lung sections [26]. Histological sections show increased airspaces in cigarette smoke-exposed mice (Figure 1A). There was a significant effect of cigarette smoke on Lm values (Figure 1B). No significant additional effects of LPS exposure on Lm were observed (Figure 1B).

Ten days after the final LPS exposure, the number of inflammatory cells in BAL fluid was determined to assess the presence and degree of lung inflammation. There was a significant effect of cigarette smoke on total cell numbers in the BAL fluid (Figure 1C). LPS administration in cigarette smoke-exposed mice have no additionally effects on the total cell numbers (Figure 1C). In addition, air-exposed mice treated with LPS showed significantly higher total inflammatory cell numbers as compared to vehicle-treated mice (Figure 1C).

Total BAL cells were differentiated to determine macrophage, neutrophil and lymphocyte cell numbers. There was an effect of cigarette smoke exposure on macrophage numbers (Figure 1D; P= 0.0547). In both air- and cigarette smoke-exposed animals, LPS significantly increased macrophage numbers (Figure 1D). Cigarette smoke exposure significantly increased neutrophil numbers whereas additional exposure to the LPS resulted in a significant decrease in neutrophil numbers (Figure 1E). Finally, Cigarette smoke exposure showed a tendency to increase the numbers of lymphocyte in the BAL fluid (Figure 1F; P= 0.0767).
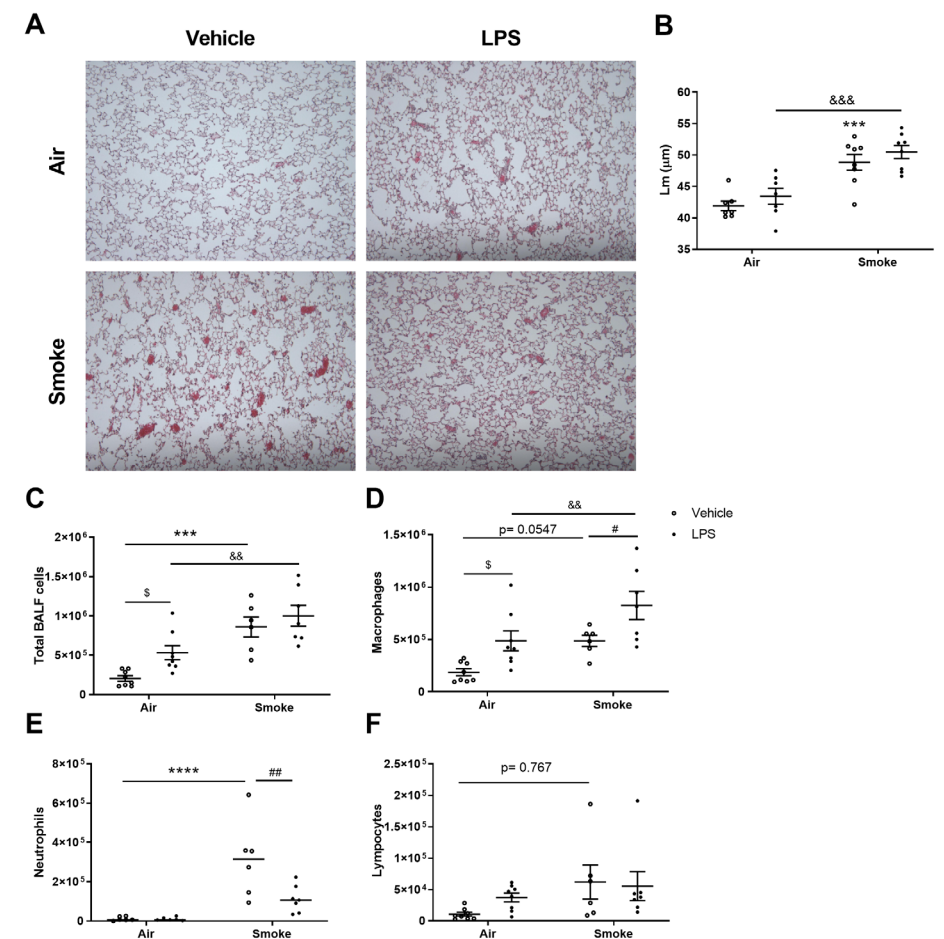

Figure 1. Photomicrographs of H&E stained lung sections and inflammatory cell numbers in BAL fluid. Mean linear intercept (Lm) was determined in H&E stained lung slices in the experimental groups (A; ×100 magnification), Lm were quantified (B). Data are presented as mean ± SEM. ***$p<0.001$; CS group compared with air group; &&&$p <0.001$; CS + LPS group compared with LPS group; Air + vehicle: n=7; air + LPS: n=7; CS + vehicle: n=8; CS + LPS: n=8. Inflammatory cell numbers in BAL fluid are increased after cigarette smoke and/or LPS exposure. Total number of cells (C) was determined from BAL fluid samples and cells were differentiated into macrophages (D), neutrophils (E) and lymphocytes (F). Data are presented as mean ± SEM. ***$p<0.001$; ****$p<0.0001$; CS group compared with air group; $$p<0.05$; LPS group compare with air group; &&$p <0.01$; CS + LPS group compared with LPS group; #$p<0.05$, ##$p<0.01$; CS + LPS group compared with CS group. Air + vehicle: n=8; air + LPS: n=8; CS + vehicle: n=6; CS + LPS: n=7. CS=cigarette smoke.

Lung inflammation, and mucus production

Inflammatory cell infiltration and mucus producing cells were quantified in H&E- and PAS-stained lung tissue after air or cigarette smoke exposure with or without LPS treatment. Representative histological pictures are depicted in Figure 2A. Exposure to only LPS slightly

increased the number of inflammatory cells (Figure 2B) and mucus producing cells in the lungs (Figure 2C), although this was not significantly different compared to air-exposed mice. Exposure to cigarette smoke significantly increased the number of inflammatory (Figure 2A, red arrows in H&E-stained lung tissue) and mucus producing cells (Figure 2A, red arrows in PAS-stained lung tissue) ($p< 0.05$ and $p< 0.0001$; Figure 2B-C) compared to air-exposed mice. LPS administration in cigarette smoke-exposed mice did not additionally affect the inflammatory and mucus producing cell numbers in the lungs (Figure 2B-C). The Lm was positively correlated with the inflammatory cell infiltration ($r= 0.5689$, $p= 0.0013$; Figure 2D) and the number of mucus producing cells in the lungs ($r= 0.5276$, $p= 0.0033$; Figure 2E).
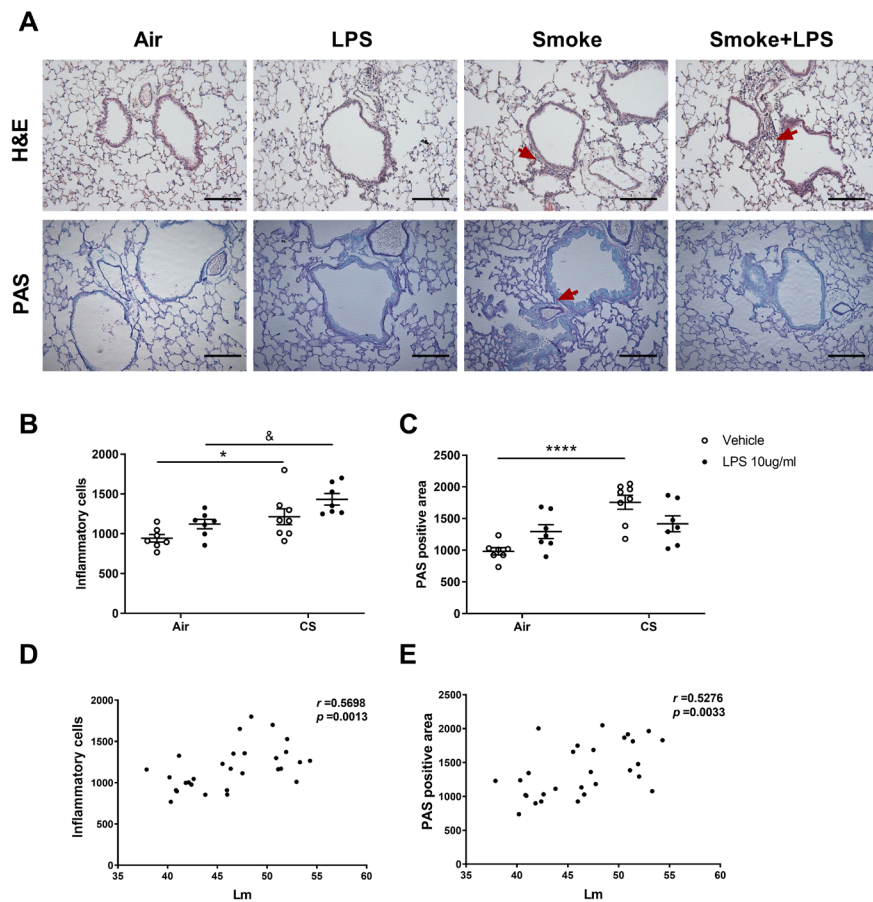

Figure 2. Lung emphysema, inflammation, and mucus production. Mice were exposed to air or cigarette smoke for 72 days, except on day 42, 52 and 62. On these days mice were treated with saline or LPS via intratracheal (i.t.) instillation. Lung tissue was collected and stained with H&E (A, upper pictures) and PAS (A, lower pictures) (800 μm depth) for each treatment group (magnification, x200, scale bar = 200 μm). Inflammatory cells (B) and PAS positive cells (C) were analyzed by ImageJ. Correlations between inflammatory cells and Lm (D) and correlations between PAS positive cells and Lm (E) were analyzed using spearman correlation. Values are expressed as mean±SEM. *$p < 0.05$, ****$p<0.0001$, CS group compared with air group; &$p<0.05$, CS + LPS group compared with LPS group; Air + vehicle: n=7; air + LPS: n=7; CS + vehicle: n=8; CS + LPS: n=7. CS=cigarette smoke.

Inflammatory markers in BAL fluid

Inflammatory markers were measured in BAL fluid to further confirm lung inflammation after air or cigarette smoke exposure with or without LPS administration. Administration of LPS alone increased IL-10 levels in the BAL fluid compared to air-exposed mice ($p< 0.05$; Figure 3E). However, exposure to cigarette smoke significantly increased the levels of CRP, KC, VEGF-A and IL-12 in the BAL fluid compared to air-exposed mice ($p< 0.05$ or $p< 0.001$; Figure 3A-D). Cigarette smoke exposure plus LPS treatment decreased the KC, VEGF-A and IL-12 levels in BAL fluid compared to cigarette smoke treatment alone ($p< 0.05$ or $p< 0.01$; Figure 3B-D). IL-6 levels in BAL fluid were not altered by any treatment (Figure 3F). Significant positive correlations between neutrophil numbers and KC, VEGF-A and IL-12 levels were demonstrated in the BAL fluid ($r= 0.8015$, $p= 0.0001$; $r= 0.7824$, $p= 0.0001$; $r= 0.5956$, $p= 0.0021$; Figure 3G-I).
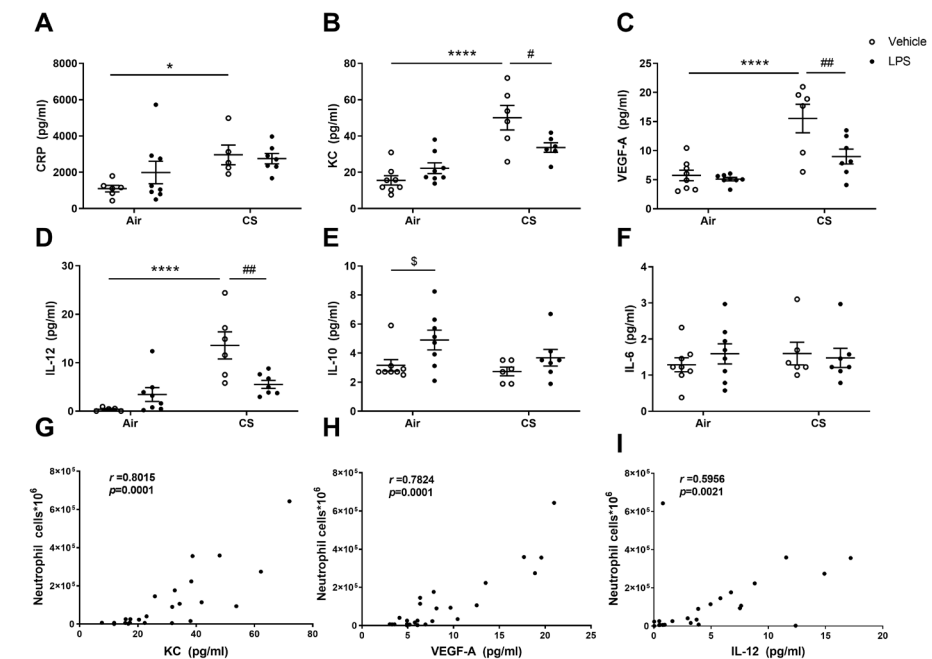

Figure 3. Inflammatory markers in BAL fluid. Mice were exposed to air or cigarette smoke for 72 days, except on day 42, 52 and 62. On these days mice were treated with saline or LPS via i.t. instillation. BAL fluid was collected, and the concentration of inflammatory mediators was determined. The levels of CRP (A), KC (B), VEGF-A (C), IL-12 (D), IL-10 (E) and IL-6 (F) were determined by using an ELISA and Milliplex Luminex assay kit as described in material and methods. Values are expressed as mean±SEM. *$p < 0.05$, ****$p <0.0001$, CS group compared with air group; $p <0.05$, LPS group compared with vehicle group; #$p < 0.05$, ##$p < 0.01$, CS + LPS group compared with CS group; the correlation between KC, VEGF-A, IL-12 and the number of neutrophils in BAL fluid (G, H, I) were analyzed by using spearman correlation. Air + vehicle: n=8; air + LPS: n=8; CS + vehicle: n=6; CS + LPS: n=7. CS=cigarette smoke.

Intestinal responses

Morphology of the small intestines

The effect of air or cigarette smoke exposure with or without LPS administration on histopathological characteristics of the small intestine was examined as well. Representative histological pictures of the proximal and distal small intestines are depicted in Figure 4A and 4B, respectively. LPS alone showed no effect on the histomorphology of the small intestines when compared to air-exposed mice (Figure 4C-H). Cigarette smoke exposure increased the villus length ($p < 0.01$; Figure 4C) and decreased the crypt depth ($p < 0.05$; Figure 4D) of the proximal small intestine compared to the air-exposed mice (Figure 4A, red arrows in H&E-stained intestinal tissue). The morphological change is represented in the significantly increased villus length to crypt depth ratio in cigarette smoke-exposed mice ($p < 0.0001$; Figure 4E). LPS administration did not induce any additional effect in cigarette smoke-exposed mice, since no significant changes were observed between cigarette smoke-exposed mice and cigarette smoke-exposed mice with the additional LPS treatment (Figure 4E). No significant changes in the villus length, crypt depth and villus length to crypt depth ratio in the distal small intestine after cigarette smoke exposure and/or LPS treatment have been demonstrated (Figure 4F-H).

SCFAs in cecum content

The concentrations of SCFAs in the cecum were measured to determine the metabolic activity of the intestinal microbiota. Administration of LPS alone had no significant effect on SCFAs levels in cecum content. The levels of total (iso-) SCFAs, acetic acid, propionic acid, butyric acid, iso-butyric acid, valeric acid and iso-valeric acid were also not significantly changed after CS exposure (Supplementary Figure 1A-H). Statistically significant effects were only visible for valeric acid and iso-valeric acid when cigarette smoke exposure combined with LPS was compared to the LPS alone group ($p < 0.01$; Supplementary Figure 1C and $p < 0.05$; Supplementary Figure 1D respectively). In addition, the total iso-SCFAs were tended to be decreased by CS exposure combined with LPS when compared to the LPS only group ($p = 0.0529$; Supplementary Figure 1B)

RNA-sequence, fecal sIgA and IgA expression

RNA-sequence analysis was performed to detect transcriptome changes in the proximal and distal small intestines in the different treatment groups. KEGG analysis (settings: Padj<0.05 and fold change >1) indicates that differentially expressed genes were highly enriched in signaling pathways related to the intestinal immune network for IgA production in the distal small intestine of cigarette smoke-exposed mice (Supplementary Figure 4). A heat map visualization of the gene expression in intestinal samples from different treatment groups was displayed in Figure 5A-B. After cigarette smoke exposure, alterations were observed in the genes associated with the immune network involved in IgA production signaling pathways in the distal small intestine (genes fold change >1) (Figure 5B), while

these alterations were less obvious (more variation within groups) in the proximal small intestine (Figure 5A). The changes in genes related to the intestinal immune network for IgA production were supported by increased sIgA levels in fecal samples of cigarette smoke-exposed mice ($p<0.01$; Figure 5C). Conversely, cigarette smoke exposure plus LPS treatment decreased the fecal sIgA levels ($p< 0.001$; Figure 5C) compared to cigarette smoke only. In addition, immunofluorescent staining for IgA in the distal small intestine confirmed this IgA expression pattern (Figure 5E, white arrow). The negative control showed no staining in the absence of the primary antibodies (Supplementary Figure 5). IgA induction primarily occurs in the intestinal Peyer's patches, the immune sensors of the intestine, and the enlargement of Peyer's patches indicates the induction of adaptive immune responses [27]. For this reason, the size of the Peyer's patches was determined as well. Similarly, cigarette smoke exposure tended to enlarge the size of the Peyer's patches in the distal small intestine ($p= 0.077$; Figure 5D) whereas cigarette smoke exposure plus LPS treatment decreased the size of the Peyer's patches ($p< 0.05$; Figure 5D).

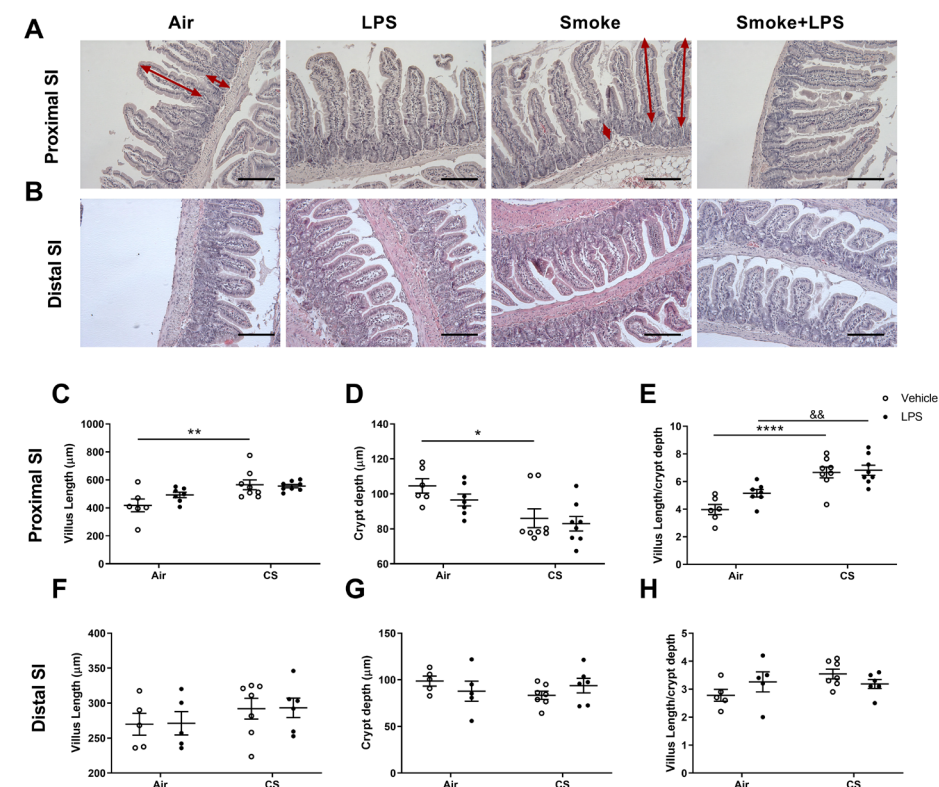Figure 4. **Morphology of the small intestines.** Mice were exposed to air or cigarette smoke for 72 days, except on day 42, 52 and 62. On these days mice were treated with saline or LPS via i.t. instillation. Intestinal samples were collected, fixed in formalin and embedded in paraffin. Proximal (A) and distal (B) small intestinal samples from different treatment groups were stained with H&E. Villus

length (C, F) and crypt depth (D, G) were quantified in the proximal and distal small intestine and villus length/crypt depth ratio was calculated (E, H), (Magnification 200x, scale bar = 200 μm). Values are expressed as mean±SEM. *$p < 0.05$, **$p < 0.01$, ****$p < 0.0001$, CS group compared with air group; &&$p < 0.01$, CS + LPS group compared with LPS group; Air + vehicle: n=6; air + LPS: n=7; CS + vehicle: n=8; CS + LPS: n=8. CS=cigarette smoke.
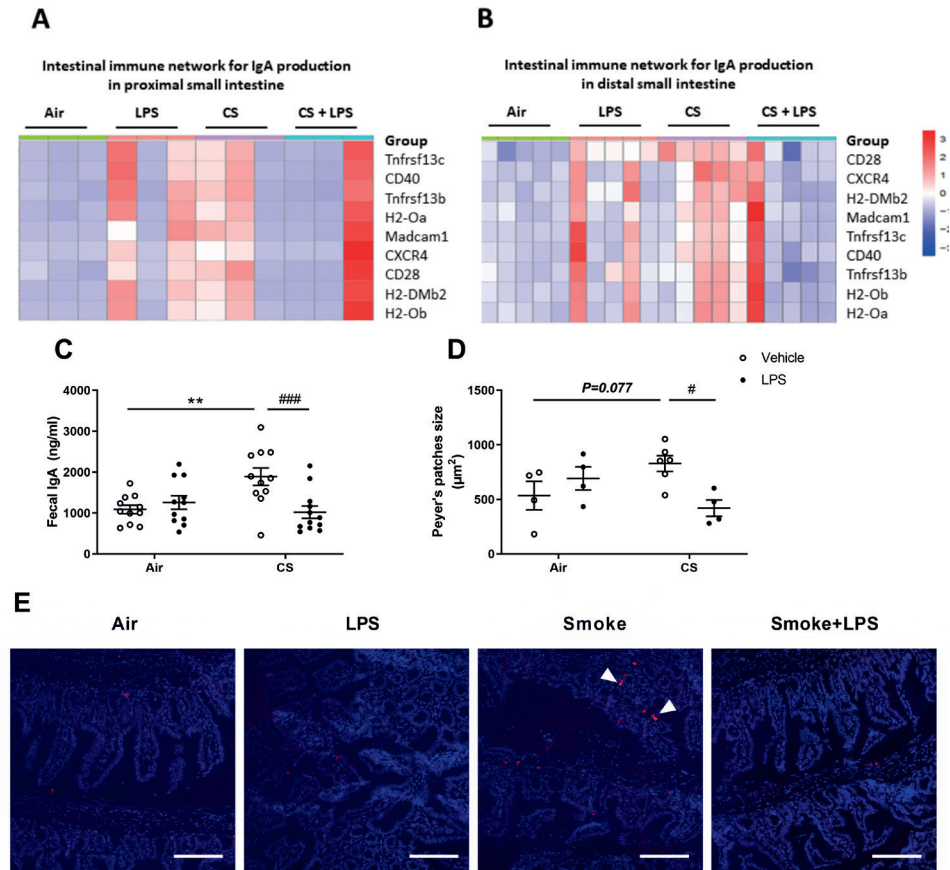

Figure 5. RNA-sequence, fecal sIgA and IgA expression. Mice were exposed to air or cigarette smoke for 72 days, except on day 42, 52 and 62, on these days mice were treated with saline or LPS via i.t. instillation. Total RNA was isolated and extracted from proximal and distal small intestine tissue. Heat map depicting the scaled gene expression changes in the intestinal immune network for IgA production signaling pathways in the proximal (A) and distal (B) small intestine. Expression levels of biological replicates were compared (n=3 for proximal small intestine or n=5 for distal small intestine per group). Color scale of heatmaps represents Z-score. Fecal samples were collected and SIgA levels were measured (C). Distal small intestinal samples from different treatment groups were collected, fixed in formalin and embedded in paraffin. The size of the Peyer's patches was determined in H&E-stained slides from the distal small intestine (D). Values are expressed as mean±SEM. **$p < 0.01$, CS group compared with air group; #$p < 0.05$, ###$p < 0.001$, CS + LPS group compared with CS group; Air + vehicle: n=11; air + LPS: n=11; CS + vehicle: n=11; CS + LPS: n=12. Representative images of an immunofluorescent staining with anti-IgA (red) and DAPI (blue) in the distal small intestine are depicted (E) (Magnification 250x, scale bar = 100 μm). CS=cigarette smoke. H2-DMb2: Histocompatibility 2, CD40: Cluster of differentiation 40, CD28: Cluster of differentiation 28, Tnfrsf13b: Tumor necrosis factor receptor superfamily 13b, Tnfrsf13c: Tumor necrosis factor receptor superfamily 13c, H2-Oa: Histocompatibility 2, O region alpha locus, H2-Ob: Histocompatibility 2, O region beta locus, CXCR4: C-X-C chemokine receptor type 4, Madcam1: Mucosal vascular addressin cell adhesion molecule 1.

Systemic inflammation
Inflammatory markers in serum

Inflammatory markers were measured in the serum to investigate systemic inflammation after air or cigarette smoke exposure with or without LPS administration. Administration of LPS alone did not change CRP or KC levels in serum (Figure 6A-B), while exposure to cigarette smoke significantly enhanced the levels of both CRP ($p< 0.05$; Figure 6A) and KC in serum ($p< 0.05$; Figure 6B) when compared to air-exposed mice. Although LPS treatment reduced the cigarette smoke-induced KC and CRP levels in the blood, the effect was not statistically significant. The serum level of VEGF-A was not significantly changed in any treatment group (Figure 6C). There was a significant positive correlation between the level of KC in BAL fluid and the amount of KC in serum ($r= 0.5539$, $p< 0.0022$; Figure 6D). Other cytokines in serum, including IL-12, IL-10 and IL-6, were below the detection limit (data not shown).

Figure 6. Inflammatory markers in serum. Mice were exposed to air or cigarette smoke for 72 days, except on day 42, 52 and 62. On these days mice were treated with saline or LPS via i.t. instillation. Serum was collected and the concentration of inflammatory mediators was determined. CRP (A), KC (B) and VEGF-A (C) levels were detected by using an ELISA and Milliplex Luminex assay kit, respectively. Values are expressed as mean±SEM. *$p < 0.05$; CS group compared with air group. Correlations between KC levels in BAL fluid and KC levels in serum (D) were analyzed by using spearman correlation. Air + vehicle: n=12; air + LPS: n=13; CS + vehicle: n=12; CS + LPS: n=13. CS=cigarette smoke.

T-cell subsets in the spleen

Flow cytometric analysis of Th1, Th2, Th17 and Treg cells in the spleen was performed to investigate the effect of air or cigarette smoke exposure with or without LPS administration on T cell subsets in the spleen. Administration of LPS alone had no effect on the different T cell subsets in the spleen when compared to air-exposed mice (Figure 7A-D). Exposure to cigarette smoke enhanced the number of activated Th1 cells compared to the air-exposed control mice ($p < 0.05$; Figure 7A). Cigarette smoke exposure plus LPS treatment significantly increased the percentage of activated Th1 and Th2 cells in the spleen compared to the LPS only and cigarette smoke only treatment groups ($p < 0.05$, $p < 0.001$ or $p < 0.0001$; Figure 7A-B). The percentage of activated Th17 (Figure 7C) and Treg cells (Figure 7D) in the spleen was not affected by any treatments.
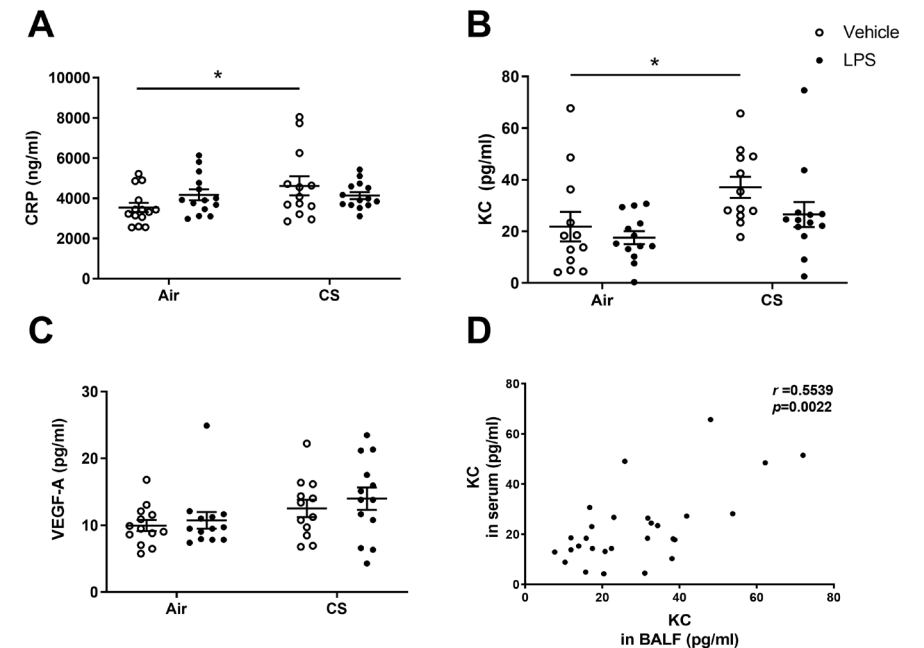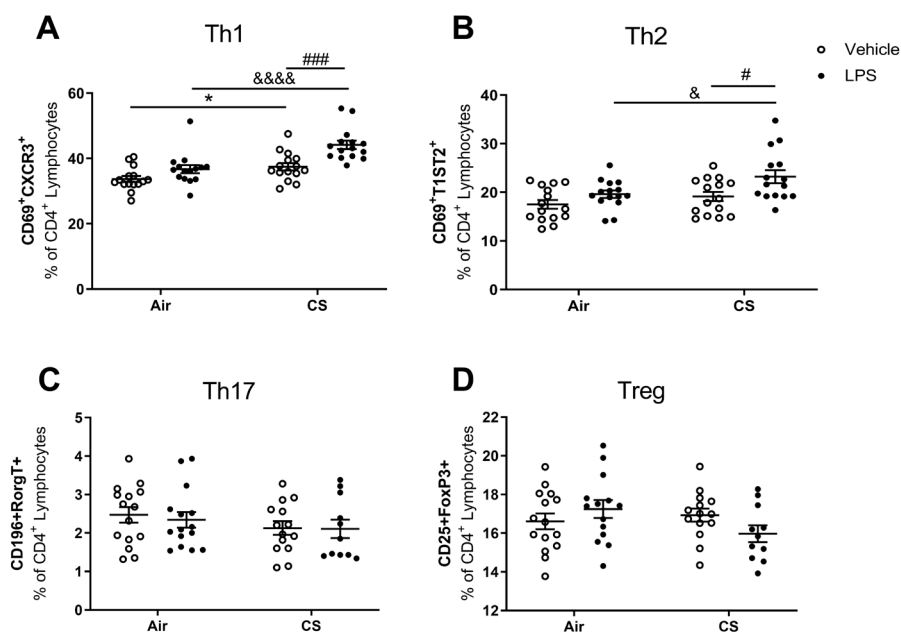

Figure 7. T-cell subsets in the spleen. Mice were exposed to air or cigarette smoke for 72 days, except on day 42, 52 and 62. On these days mice were treated with saline or LPS via i.t. instillation. Spleens were collected and lymphocytes were isolated and analyzed by flow cytometry for activated Th1 (A), Th2 (B), Th17 (C) and Treg (D) cell phenotypes. Values are expressed as mean±SEM. *$p < 0.05$, CS group compared with air control group; $^{\&}p < 0.05$, $^{\&\&\&\&}p < 0.0001$; CS + LPS group compared with LPS group; $^{\#}p < 0.05$, $^{\#\#\#}p < 0.001$, CS + LPS group compared with CS group; Air + vehicle: n=15; air + LPS: n=15; CS + vehicle: n=15; CS + LPS: n=15. CS=cigarette smoke.

Discussion

Intestinal symptoms are highly prevalent among COPD patients, and it is becoming clearer that the severity of these intestinal symptoms coincides with the severity of the respiratory symptoms [28]. However, the connections and relevance of the connections between the lung and gut are still poorly understood in COPD. The intestines contain many important immune cells and tissues, such as GALT. It has been described that BALT and GALT are both solitary organized mucosa-associated lymphoid follicles and these follicle aggregates have common features and are the origin of B-cell trafficking to mucosal effector sites [29]. A better understanding of the links between the immune system in the intestine, the systemic immune system and the lungs might provide insight in COPD but additionally might help the development of new concepts for the treatment of COPD and its co-morbidities. To date, experimental research with preclinical COPD exacerbation models (CS + LPS or elastase + LPS) has mainly focused on measuring lung inflammation and lung damage [30], while research on intestinal immunity is an unexplored area yet. In this study, cigarette smoke exposure with or without intratracheal LPS treatment was used as a novel model for COPD to investigate the effects on systemic inflammation, and intestinal homeostasis by exploring intestinal histomorphology, the SCFA production in the cecal content and the intestinal immune network for IgA production in the gut.

To confirm a cigarette smoke-induced lung inflammation and lung damage in our COPD model, airway inflammation, mucus hypersecretion and mean linear intercept were determined. Airway inflammation and mucus hypersecretion are known to be one of the underlying pathophysiological processes in COPD [31]. In the current study, histological analysis showed that cigarette smoke exposure induced inflammatory cell infiltration and increased number of mucus-producing cells in the lung compared to the air exposed control. These findings were supported by damaged alveoli (Lm). Additional LPS triggers (to mimic bacterial (opportunistic) infections) did not modify the inflammatory cell infiltration, mucus-producing cells in the lung and Lm values, which was in agreement with the effect on the number of total BAL fluid cells.

The number of neutrophils and macrophages were both increased after smoke exposure, however, additional LPS exposure on top increased the number of macrophages, but in contrast decreased the number of neutrophils in BAL fluid. The decreased number of neutrophils after additional LPS exposure conflicts with the results of previous research in rats, where the BAL neutrophils were elevated in response to a combination of LPS and CS exposure [24]. An in vitro study showed decreased neutrophil numbers after combined CS and LPS exposure, where it was suggested that CS decreased the bacterial pathogen-induced production of neutrophil-mobilizing cytokines by inhibiting activator protein-1 activation in bronchial epithelial cells [32]. This decrease in neutrophil numbers in BAL fluid

caused by the additional LPS trigger in CS-exposed mice might also be related to the protective role of the immune system after repeated stressors, thereby promoting resilience (and thereby preventing tissue damage [33]. In addition, future research should demonstrate whether LPS of any other serotype will cause comparable results.

In general, the degree of damaged lung tissue (Lm) was positively correlated with the inflammatory cell infiltration and the number of mucus producing cells in the lungs, which indicated progressive and irreversible tissue destruction after cigarette smoke exposure. In agreement with the observations of changed neutrophil numbers in BAL fluid, the levels of CRP, KC, VEGF-A and IL-12 in BAL fluid were significantly increased after cigarette smoke exposure compared to air-exposed mice, while additional LPS decreased the level of KC, VEGF-A and IL-12 in cigarette smoke -exposed mice. Since KC is a neutrophil chemoattractant [34], VEGF-A is expressed by neutrophils and regulates angiogenesis [35] and IL-12 is produced by neutrophils and stimulate growth and function of T cells [36], which explains the correlation of the number of neutrophils and KC, VEGF-A and IL-12 levels in BAL fluid. This decrease in neutrophil numbers and neutrophil-related cytokines in BAL fluid caused by the additional LPS trigger in cigarette smoke-exposed mice might also be related to the protective role of the immune system after repeated stressors, thereby promoting resilience (and thereby preventing tissue damage) [33].

The next step in this study was to investigate the effect of cigarette smoke with or without LPS on intestinal homeostasis, including small intestinal morphology, cecal SCFA levels and the small intestinal immune network involved in IgA production have been examined.

In the current study, we focused on the effects of the small intestine, which is an important organ in supporting the body's immune system. Especially, the Peyer's patches, located within the small intestine, are an important part of the intestinal local immune system [37]. In addition, trophologic insufficiency and absorptive dysfunction of small intestine were often found in patients with COPD [38]. In our study, mice treated with cigarette smoke showed an increased villus length and a decreased crypt depth (increased villus length to crypt depth ratio) in the proximal small intestines. LPS treatment did not have any additional effect on the villus length and crypt depth. No differences were demonstrated in the distal small intestines. The increased villus length in the proximal small intestine may indicate mucosal adaptation, as this is regularly seen in patients suffering intestinal failure [39]. In addition, the increased villus length in the proximal small intestine also correlated with decreased body weight as observed in patients with intestinal failure [39]. In the current study, a decrease in body weight was noticed in cigarette smoke-exposed mice compared to control mice (see Chapter 5). A decreased body weight is also observed in COPD patients, especially in those characterized as lean "pink puffers" (the emphysematous patients) [40].

The results related to the observed changes in small intestinal morphology caused by cigarette smoke with and without LPS, raised further interest to investigate the microbial production of SCFAs, to get a first indication of relevant changes in the microbiota composition and activity. Gut microbiota interacts with the immune system and plays a crucial role in health and disease [41]. SCFAs, produced by intestinal bacteria after fermentation of fibers, are important metabolites for maintaining intestinal homeostasis and regulating immune cell function [42]. Although no obvious changes in cecal SCFAs production were observed induced by cigarette smoke or LPS only treatment, total iso-SCFAs, valeric acid and iso-valeric acid levels were significantly decreased in mice after cigarette smoke exposure plus LPS treatment compared to the LPS treatment only group. However, this effect might be due to the slight increase of total iso-SCFAs, valeric acid and iso-valeric acid levels induced by LPS treatment. Although we did not find a change in total SCFAs concentrations, in another COPD model, ambient particulate matter exposure induces gut microbial dysbiosis and as a consequence a decrease in total SCFA levels was observed [43]. Cecal levels of valeric acid were also significantly decreased in cigarette smoke-exposed rats, which was associated with a decreased population of *Bifidobacterium* and an increase in cecum pH [44]. A limitation of this study is the lack of information regarding the gut microbiome. Future studies based on the analyses of the gut microbiota are required to better understand the effect of cigarette smoke with and without LPS on the intestinal microbiota composition and activity.

IgA (also referred to as sIgA in its secretory form) is known to be a key factor in controlling gut bacterial translocation and development of the mucosal immune system [45, 46]. IgA is a hallmark feature of mucosal tissues, of which Peyer's patches serve as the prototypical model, in which mainly B cells contribute to this mucosal IgA response [47]. In the current study, sIgA levels in fecal samples were significantly increased after cigarette smoke exposure, which was confirmed by increased expression of IgA in the distal small intestine of cigarette smoke-exposed mice as observed by an immunofluorescent staining. Interestingly, RNA-sequence analysis revealed that the most altered genes in the distal small intestine are involved in the intestinal immune network for IgA production signaling pathways. The changed gene expression may be the result of changes in the differentiation process of the B cells and interactions between B cells, T cells and dendritic cells after cigarette smoke exposure (or due to changes in the microbiota composition caused by cigarette smoke exposure) [45, 48], possibly leading to higher IgA production. Striking is the finding that changes were observed in the distal small intestine, but not in the proximal small intestine. This might be partly due to the higher density of bacteria in the distal small intestine [18] and the role of gut microbiota in regulating the immune homeostasis in the intestine [49]. IgA induction primarily occurs in Peyer's patches, and the size of Peyer's patches were tended to be enlarged after cigarette smoke exposure in this study. We hypothesize that the changed composition of the microbiota (and related SCFAs) and/or chronic systemic inflammation observed after cigarette smoke exposure can stimulate the IgA production

pathway (Figure 8). Different findings highlight the increased risk of IBD in patients suffering from COPD [7, 9]. Interestingly, patients with Crohn's disease also typically display elevated systemic inflammation and increased systemic anti-microbial IgA responses [50, 51].

An additional effect of LPS was not observed on the intestinal host immunity in the current study. In fact, cigarette smoke exposure plus LPS administration decreased fecal sIgA levels and IgA expression, and reduced the size of the Peyer's patches in the distal small intestine compared to the cigarette smoke-exposed only group. More research is needed to unravel the mechanism behind the immunosuppressive effect of LPS when combined with cigarette smoke.

One explanation for the gut-lung interaction observed in this study following cigarette smoke exposure can be caused by the initial, localized pulmonary inflammatory response "spill over" and triggering the observed systemic inflammation. The systemic inflammation may affect other immune-related organs, like the spleen and intestine, and hence may disturb intestinal homeostasis and immunity.

The systemic inflammation present in many COPD patients is correlating with the regulation of inflammation in other tissues and organs, including the intestine, adipose tissue, and spleen [52-54]. Blood serum CRP is mostly used as a clinical marker of (acute) systemic inflammation [55]. Increased CRP levels in the circulation are associated with poor lung function, systemic comorbidities, worse quality of life and a higher late mortality in patients with COPD [56, 57]. Previous clinical studies showed that systemic inflammation in COPD patients was associated with increased blood CRP levels and neutrophil cell counts [58, 59]. In the current study, cigarette smoke exposure increased serum CRP levels and KC levels and the serum KC levels positively correlated with the KC concentration in BAL fluid. It might be possible that inflammatory mediators leak from the pulmonary to the systemic compartments. Additional LPS treatment did not significantly change the cigarette smoke -induced increase in serum CRP, which was in agreement with the observation in BAL fluid. The decrease in KC serum levels observed by the additional LPS treatment was not significantly different compared to cigarette smoke exposure only group, but a significant LPS-induced decrease in KC levels in BAL fluid was observed.

Systemic inflammation was also examined by T cells in the spleen. The present results showed that cigarette smoke exposure increased the percentage of Th1 cells in the spleen, while additional LPS treatment further increased the percentage of activated Th1 cells, which might be related to poor prognosis in COPD patients due to the role of systemic Th1 cells in promoting the inflammatory response [60]. Different studies pointed out that increased expression of Th1 cytokines during exacerbations are related to poor prognosis in COPD patients [60, 61]. This was not in agreement with the findings in the current study where the additional LPS treatment did not (yet) affect the Lm values and decreased the neutrophil influx in the lungs. However,

an increased number of macrophages in BAL fluid was observed after the additional trigger with LPS in cigarette smoke-exposed mice as compared to cigarette smoke-exposed mice. Interestingly, cigarette smoke exposure in combination with LPS increased the percentage of activated Th2 cells compared with cigarette smoke-exposed only mice. This result aligns with reports of COPD patients with acute exacerbations due to bacterial infections that have more Th2 cells in their peripheral blood than those without infection [61, 62]. LPS-only treatment also caused an increase in IL-10 in BAL fluid, which is mainly produced by macrophages, Th2 and Treg cells. This is in line with the increased number of macrophages in the BAL fluid after LPS exposure in air-exposed mice.

Besides our findings related to systemic inflammation, which may explain the gut-lung interaction, we cannot exclude a direct effect of soluble compounds from cigarette smoke that enter the blood stream and affect the intestine [63]. Alternatively, due to the muco-ciliary clearance of the lungs or direct swallowing of cigarette smoke [64], the cigarette smoke particles may end up in the esophagus and enter the gastro-intestinal tract, and possibly having local effects on the immune system along the way (Figure 8).

In summary, this murine COPD model clearly demonstrated gastro-intestinal changes after cigarette smoke exposure, including changes in: histomorphology, small fluctuations in cecal SCFA levels, the intestinal immune network related to mucosal IgA production and size of Peyer's patches one of the most relevant mucosal immune organs. Hence, future COPD research should not only focus on the lung as the target organ, but a broader perspective related to other organs, such as the intestines, should be considered. In future, therapeutical strategies for COPD patients might therefore not only directed to the lung, but also the intestine (gut-lung axis), to decrease systemic disease progression and related co-morbidities, like mental diseases as indicated by Pelgrim et al. (lung-gut-brain axis) [2].
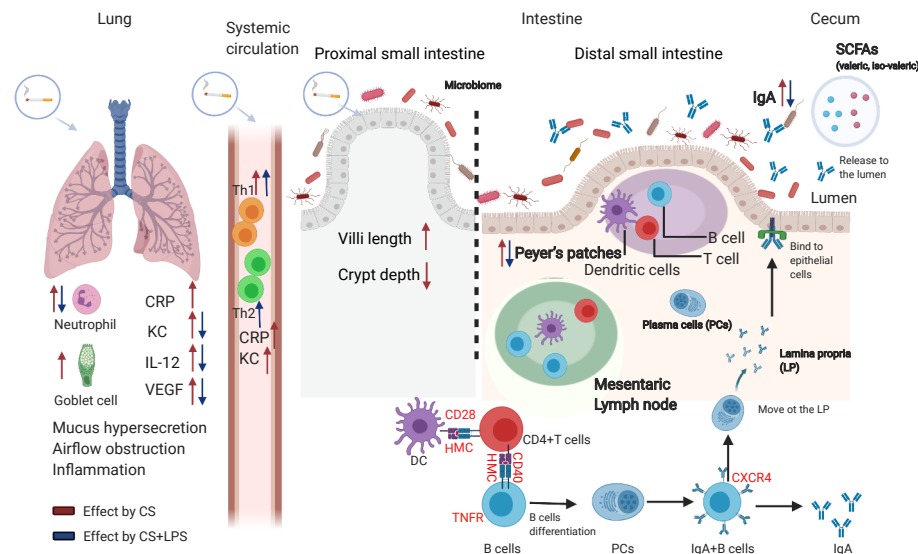
Figure 8. Cigarette smoke exposure leads to lung injury and/or intestinal changes possibly via systemic immune responses. Lung inflammation was induced by cigarette smoke exposure as observed by increased inflammatory cell numbers and PAS-positive cells in lung tissue as well as enhanced mediator release in BAL fluid (CRP, KC, IL-12 and VEGF-A). LPS treatment of cigarette smoke exposed mice decreased the number of neutrophils and neutrophils related cytokines (KC, IL-12 and VEGF-A). The interaction between the lung and gut mucosal parts might take place via blood and lymphatic circulation, as observed by increased inflammatory mediators in serum (CRP, KC) and increased Th1 and Th2 cell subsets in the spleen following cigarette smoke exposure. Cigarette smoke exposure plus LPS treatment increased the Th1 and Th2 cell subsets in cigarette smoke-exposed mice. Several intestinal changes were found after cigarette smoke exposure: histomorphological changes in the proximal small intestine, increased cecal SCFAs (possibly microbiota-related changes), stimulation of the intestinal immune network for IgA production, increased fecal IgA levels and increased size of Peyer's patches in the distal small intestine. Cigarette smoke exposure plus LPS treatment decreased the fecal IgA levels and size of Peyer's patches. The possibility that soluble compounds from cigarettes enter the blood stream and impact the intestine cannot be excluded, or cigarette smoke may directly enter the gastro-intestinal tract and may (in addition) have local effects on the (intestinal) immune system.
The red arrows represent "effects caused by CS" CS=cigarette smoke
The blue arrows represent "effects caused by CS+LPS"

Materials and Methods

Animals

Specific-pathogen free female Balb/c mice, 11-13 weeks old, were obtained from Charles River Laboratories [65, 66]. Balb/c mice show a high neutrophil influx in the lungs after exposure to cigarette smoke as compared to other mouse strains [67]. Mice were housed in groups (3 or 4 animals/cage) in filter-topped makrolon cages (22 cm×16 cm×14 cm, floor area 350 cm², Tecnilab- BMI, Someren, the Netherlands) with wood-chip bedding (Tecnilab-

BMI, Someren in the Netherlands) and tissues (VWR, the Netherlands) were available as cage enrichment. Mice were kept under standard conditions on a 12 h light/dark cycle (lights on from 7.00 am – 7.00 pm) at controlled relative humidity (relative humidity of 50 – 55 %) and temperature (21 ± 2 °C) at the animal facility of Utrecht University.

Food (AIN-93M, SNIFF Spezialdiäten GmbH, Soest, Germany) and water were refreshed once a week. Based on average body weight, mice were divided into four experimental groups (N = 15/16 per group): air exposure group, LPS treatment group, cigarette smoke exposure group and cigarette smoke exposure plus LPS treatment group. All animal procedures described in this study were approved by the Ethics Committee of Animal Research of Utrecht University, Utrecht, The Netherlands (AVD1080020184785) and were conducted in accordance with the governmental guidelines.

Murine COPD model

Mice were exposed in whole-body chambers to mainstream cigarette smoke or air using a peristaltic pump (SCIQ 232, Watson-Marlow 323, USA). A Plexiglas box containing four metal cages each with four compartments was used to expose the mice to either cigarette smoke or air. Two mice from the same home cage were placed in each compartment. Research cigarettes (3R4F) were obtained from the Tobacco Research Institute (University of Kentucky, Lexington, Kentucky) [68] and filters were removed before use [65]. Mice were exposed to cigarette smoke once a day for 72 consecutive days (except on day 42, 52 and 62). Mice were acclimatized to cigarette smoke exposure by gradually increasing the number of cigarettes during the first days of the experiment using 4 cigarettes at day 1; 6 cigarettes at day 2; 8 cigarettes at day 3; 10 cigarettes at day 4; 12 cigarettes at day 5; and 14 cigarettes from day 6 until the end of the study. 50 µl of 10 µg/mL LPS (Escherichia coli O55:B5, Sigma-Aldrich, Missouri, USA) [69] or vehicle (saline) was administrated via intratracheal instillation (i.t.) under isoflurane anesthesia [67] on days 42, 52 and 62 instead of being exposed to air or cigarette smoke (Figure 9) [70]. For practical reasons, one dose of LPS, 10 µg/mL, was selected based on the pilot study results. The smoke chamber was connected to a peristaltic pump and vacuum to produce smoke and control the air circulation. The speed of the pump was kept at 35 rpm and the CO levels ranged between 200 and 400 ppm. The mass concentration of cigarette smoke total particulate matter (TPM) was determined by gravimetric analysis of type A/E glass fiber filter (PALL life sciences, Mexico). The TPM concentration in the smoke exposure box generated by 14 cigarettes reached approximately 828 µg/L (828 ± 4.5 µg/L) [65].

Mice were anesthetized by an intraperitoneal injection of ketamine/medetomidine (196.8 mg/kg and 1.32 mg/kg respectively) ± 18 h after the last air or smoke exposure. Blood was obtained and collected in Mini collect tubes (Greiner bio-one, Alphen aan den Rijn, the Netherlands). Blood samples were centrifuged (14000 g for 10 min) and serum was stored

at −20 °C. Feces and cecum content were collected, snap-frozen in liquid nitrogen and kept at −80 °C until further analysis. Lungs, proximal and distal small intestine from half of the animals in each group (n = 7/8 per group) were collected and used for histology. (The proximal and distal small intestine from the other half of the animals in each group (n = 7/8 per group) were snap-frozen in liquid nitrogen and kept at −80 °C until RNA-sequence analysis (n =3 or 5 per group). Spleens were used for the FACS analysis (n=15 per group).
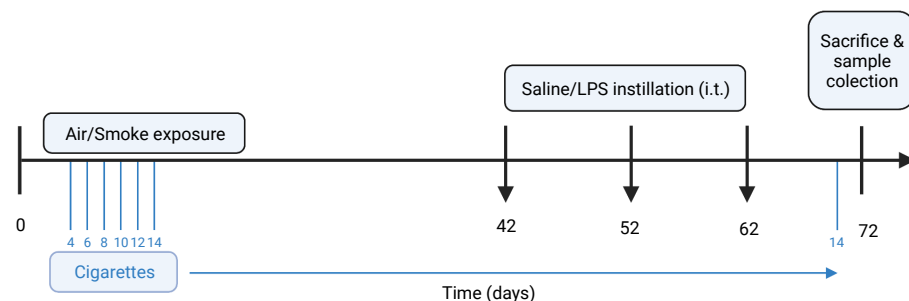

Figure 9. Experimental design. Mice were exposed to air or smoke for 72 days by using 4 cigarettes at day 1; 6 cigarettes at day 2; 8 cigarettes at day 3; 10 cigarettes at day 4; 12 cigarettes at day 5; and 14 cigarettes from day 6 until the end of the study. Mice were not exposed to air or smoke on day 42, 52 and 62, but were treated with saline or LPS via intratracheal (i.t.) instillation on these days. On day 72, mice were sacrificed, and samples were collected for future analysis.

Tissue preparation for histological analysis

Lungs were perfused and fixed with 10% formalin at a constant pressure of 25 cm H_2O for at least five minutes. Afterwards, left lungs were stored in 10% formalin for a minimum of 24 h followed by paraffin embedding. The proximal small intestine (duodenum) and distal small intestine (Ileum) were dissected. Fecal matter was removed by gentle flushing with phosphate-buffered saline (PBS), then 'swiss rolls' were obtained and fixed in 10% formalin for a minimum of 24 h followed by paraffin embedding. Tissues were embedded in paraffin (Tissue processor, Leica), 5 μm sections for the lung and intestinal tissue were cut using a microtome (Leica RM 2165) and mounted on glass slides (StarFrost adhensive slides, Knittelgläser, Gernamy). Slides were deparaffinized and used for hematoxylin and eosin (H&E) and Alcian blue-periodic acid-Schiff (AB-PAS) staining according to the standard protocols. Microscopic images were taken using an Olympus BX50 microscope (Olympus, Tokyo, Japan). The inflammatory cells and mucin-containing cells were evaluated around the airways at 800 μm depth (2-3 images per animal). The Lm was quantified with the lung tissue slides at 200 μm depth (6 images per animal) using a reference grid as previously described [26]. The villus length and crypt depth were measured in the proximal and distal small intestine (7-9 villi and crypts per animal) and the size of the Peyer's patches (2-3 Peyer's

patches per animal) was quantified in the distal small intestine. 7-8 animals per group for both lung and intestine were evaluated. Histological slides of the lungs and intestines were examined blind in treatment group using Image J.

BAL fluid collection and analysis

The trachea was exposed and a cannula was inserted in the trachea after making a small incision. BAL fluid was collected by lung lavage with 1 mL pyrogen-free saline (0.9% NaCl, 37 °C) supplemented with protease inhibitors (Complete Mini, EDTA-free Protease Inhibitor Cocktail, Sigma-Aldrich, Germany). This step was repeated for 3 times with 1 mL pyrogen-free saline. The BAL fluid was centrifuged (400 × g at 4°C for 5 min) and the supernatant of the first 1 mL was stored at −20 °C for ELISA measurement and a Luminex assay. Subsequently, lungs were lavaged three times with 1 mL non-supplemented 0.9% NaCl (37 °C). To isolate the BAL fluid cells, all lavages were centrifuged (400 × g, 5 min) and pellets were pooled and resuspended in Türk solution. A Bürker-Türker chamber was used to determine the total BAL cell counts. For the differentiation of BAL cells, cytospins were prepared and stained with DiffQuick™ (Merz and Dade A.G., Switzerland). Using standard morphology, an observer differentiated the cells into macrophages, neutrophils and lymphocytes in each sample. Around 200 cells were counted in each sample and the absolute number for each cell type was calculated using the total BAL cell counts of the corresponding sample [26].

Inflammatory mediators measurement in serum and BAL fluid

Concentrations of inflammatory mediators, KC, IL-12, VEGF-A, IL-10, and IL-6 in the BAL fluid, and KC in serum were determined by a quantitative Milliplex Luminex assay kit (ProcartaPlex, Thermo Fisher Scientific, Austria) according to manufacturer's instructions and using Luminex 200TM with Xponent software. CRP levels in the BAL fluid and serum were measured by ELISA (Mouse CRP ELISA kit, R&D Systems, USA) according to manufacturer's instructions and using a microplate reader (Glomax Discover, Promega).

SCFAs concentrations

Levels of the SCFAs: acetic acid, propionic acid, butyric acid, iso-butyric acid, valeric acid and iso-valeric acid in the cecum were quantified using direct-injection gas chromatography as described before [71, 72].

Preparations of cecum samples

Cecal contents were snap-frozen in liquid nitrogen and stored at −80°C until measurement. SCFA samples were prepared based on Thiel and Blaut [73]. The cecum content was weighed (30-60 mg) and diluted by 10x cold PBS (w/v) in a new 1.5 mL Eppendorf tube, followed by adding 3 mm glass beads (Sigma-Aldrich, USA). Samples were homogenized by vortexing for five minutes. To remove glass beads and large particles, the samples were

centrifuged at 300 g for one minute and the supernatant was transferred to a 1.5 mL Eppendorf tube. This was followed by centrifugation for 10 minutes at 15000 g (4 °C). 200 µl of the created supernatant was loaded into a 96-wells plate and stored at -80 °C for downstream analysis.

SCFA analysis

The SCFAs acetic, propionic, butyric, isobutyric, valeric and isovaleric acids were quantitatively determined using a Shimadzu GC2025 gas chromatograph (Shimadzu Corporation, Kyoto, Japan) equipped with a flame ionisation detector. The sample (0.5 µl) was injected at 80 °C into the column (Stabilwax, 15 m x 0.53 mm, film thickness 1.00 µm; Restek Co., Bellafonte, PA, USA) using H_2 as carrier gas (20.7 kPa). New columns were conditioned overnight at 200 °C. After injection of the sample, the oven was heated to 160 °C at a rate of 16 °C/min, followed by heating to 220 °C at 20 °C/min and finally maintained at a temperature of 220 °C for 1.5 min. The temperature of the injector and the detector was 200 °C. After every ten samples the column was cleared by injection of 0.5 µl formic acid (1 %, by vol.) to avoid memory effects of the column, followed by injection of 0.5 ml standard SCFA mix (1.77 mM acetic acid, 1.15 mM propionic acid, 0.72 mM butyric acid, 0.72 mM isobutyric acid, 0.62 mM valeric acid and 0.62 mM isovaleric acid; Sigma-Aldrich) to monitor the occurrence of memory effects. SCFA concentrations were determined using 2-ethylbutyric acid as an internal standard.

RNA isolation and RNA-sequence

RNA preparation

Total RNA was isolated and extracted from proximal and distal small intestine tissue using the RNeasy Mini Kit according to the manufacturer's protocol (Qiagen, Germany). RNA integrity and quantitation were assessed using the RNA Nano 6000 Assay Kit of the Bioanalyzer 2100 system (Agilent Technologies, CA, USA). RNA degradation and contamination were monitored on 1% agarose gels.

mRNA non-directional (polyA)

RNA sample was used for library preparation using NEB Next® Ultra RNA Library Prep Kit for Illumina ® Indices were included to multiplex multiple samples. Briefly, mRNA was purified from total RNA using poly-T oligo-attached magnetic beads. After fragmentation, the first strand cDNA was synthesized using random hexamer primers followed by the second strand cDNA synthesis. The library was ready after end repair, A-tailing, adapter ligation, and size selection. After amplification and purification, insert size of the library was validated on an Agilent 2100 and quantified using quantitative PCR (Q-PCR). Libraries were then sequenced on Illumina NovaSeq 6000 S4 flowcell with PE150 according to results from library quality control and expected data volume. Library preparation / sequencing / analysis are performed by Novogene (UK) Company Limited.

IgA measurement in feces

Fecal samples were collected by placing each mouse in a separate clean box for 3-5 minutes one day before sacrifice and freshly defecated fecal pellets, uncontaminated with urine, were sampled, snap-frozen in liquid nitrogen and stored at −80 °C till further analysis. The wet weight of feces samples ranged from 10 to 32 mg (median: 17.5 mg). Extraction buffer (PBS [pH=7.4], protease inhibitor cocktail (Sigma-Aldrich, Germany) and 0.01 % sodium azide) was added to each sample at a ratio of 1 mL buffer to 1 g feces. Samples were thoroughly homogenized by a homogenizer (Bertin Technologies, France) at 6000 g for 20 s. Fecal suspensions were centrifuged at 14000 g for 10 min at 4 °C and stored at −20 °C until further use. The optimum sample dilution was tested, and 200 times dilution was selected for the IgA measurement using an ELISA kit (Mouse IgA ELISA kit, Thermo Fisher Scientific, the Netherlands) according to manufacturer's instructions.

Immunofluorescent staining in distal small intestine

The 5 µm formalin-fixed, paraffin-embedded distal small intestinal sections on glass slides were deparaffinized, rehydrated in decreasing concentrations of ethanol and incubated with 0.3% H_2O_2/methanol for 30 min to quench endogenous peroxidase activity. Thereafter, the slides were incubated with rabbit-anti-IgA primary antibody (1:12000; Novus Biologicals) at room temperature for 2h after blocking with 5% goat serum in PBS containing 1% bovine serum albumin (BSA). After three washing steps with PBS containing 0.2% Tween-20 (PBST; pH 7.4), slides were incubated with Alexa fluorescently conjugated goat anti-rabbit secondary antibody (1:200; Invitrogen, The Netherlands) for 1h at room temperature. The nuclei were stained by Hoechst (1:2000; Invitrogen, USA), slides were rinsed after the Hoechst staining and mounted with FluorSave reagent (Merk Millipore, St. Louis, MO, USA). Images were captured by the confocal microscope (TCS SP8 X, Leica, Germany).

Fluorescence-activated cell sorting (FACS)

Cell isolation from tissues

Spleens were crushed through 70 µm cell strainers. The splenocyte suspension was incubated with lysis buffer (8.3 g NH_4Cl, 1 g $KHCO_3$, and 37.2 mg EDTA dissolved in 1 L demi water and filter sterilized) to remove red blood cells and then resuspended in RPMI 1640 (Lonza, Basel, Switzerland) supplemented with 10 % fetal bovine serum.

Flow cytometry of immune cells

Spleen cells were resuspended in PBS/1% bovine serum albumin and incubated with anti-mouse CD16/CD32 (1:100, BD Fc Block, USA) to block non-specific binding sites. For surface staining, cells were incubated with CD4-PerCp-Cy5.5, CD69-APC, CXCR3-PE, (1:400, 1:100 and 1:100, eBiosciences, USA), T1ST2-FITC, (1:200, MD Biosciences, USA), CD4-Brilliant, CD196 (CCR6)-PE (1:160, 1:640, Biolegend, USA), CD25-PerCp-Cy5.5 (1:1280, Thermo fisher, USA) and CD127-PE-Cy7 (1:320, Miltenyi Biotec, Germany). Viable

cells were distinguished by means of a fixable viability dye APC-Cy7 (1:2000, eBioscience, USA). For detecting transcription factors, cells were first fixed and permeabilized with Foxp3 Staining Buffer Set (eBioscience, USA) according to manufacturer's protocol and then stained with FoxP3-FITC (1:100, Thermo fisher, USA) and RorgT-APC (1:400, Biosciences, USA). The specificity of all antibodies was assessed and optimal working dilutions were determined in a previously published study from our group [74].

Results were collected with BD FACS Canto II flow cytometer (Becton Dickinson, USA) and analyzed with FlowLogic software (Inivai Technologies, Australia).

Statistical analysis

All results are presented as mean ± SEM. Differences between groups were statistically determined by two-way ANOVA followed by a Šidák's multiple comparisons test. Spearman tests were conducted for analyses of correlation. The difference was considered statistically significant at $p < 0.05$, and trends were considered when $0.05 < p < 0.1$. All statistical analyses were performed using GraphPad Prism (version 8.3.0).

Funding

Acknowledgments

References

1. Collaborators, G.B.D.C.R.D., *Prevalence and attributable health burden of chronic respiratory diseases, 1990-2017: a systematic analysis for the Global Burden of Disease Study 2017.* Lancet Respir Med, 2020. **8**(6): p. 585-596.
2. Pelgrim, C.E., et al., *Psychological co-morbidities in COPD: Targeting systemic inflammation, a benefit for both?* Eur J Pharmacol, 2019. **842**: p. 99-110.
3. Cavailles, A., et al., *Comorbidities of COPD.* Eur Respir Rev, 2013. **22**(130): p. 454-75.
4. Niklasson, A., et al., *Prevalence of gastrointestinal symptoms in patients with chronic obstructive pulmonary disease.* Eur J Gastroenterol Hepatol, 2008. **20**(4): p. 335-41.
5. Sprooten, R.T.M., et al., *Increased Small Intestinal Permeability during Severe Acute Exacerbations of COPD.* Respiration, 2018. **95**(5): p. 334-342.
6. Beloborodova, E.I., et al., *[Trophologic insufficiency and absorptive function of small intestine in patients with chronic obstructive pulmonary disease].* Klin Med (Mosk), 2009. **87**(3): p. 59-63.
7. Labarca, G., et al., *Association between inflammatory bowel disease and chronic obstructive pulmonary disease: a systematic review and meta-analysis.* BMC Pulm Med, 2019. **19**(1): p. 186.
8. Raftery, A.L., et al., *Links Between Inflammatory Bowel Disease and Chronic Obstructive Pulmonary Disease.* Front Immunol, 2020. **11**: p. 2144.
9. Lee, J., et al., *Risk of inflammatory bowel disease in patients with chronic obstructive pulmonary disease: A nationwide, population-based study.* World J Gastroenterol, 2019. **25**(42): p. 6354-6364.
10. Tulic, M.K., T. Piche, and V. Verhasselt, *Lung-gut cross-talk: evidence, mechanisms and implications for the mucosal inflammatory diseases.* Clin Exp Allergy, 2016. **46**(4): p. 519-28.
11. Oudijk, E.J., J.W. Lammers, and L. Koenderman, *Systemic inflammation in chronic obstructive pulmonary disease.* Eur Respir J Suppl, 2003. **46**: p. 5s-13s.
12. Fabbri, L.M. and K.F. Rabe, *From COPD to chronic systemic inflammatory syndrome?* Lancet, 2007. **370**(9589): p. 797-9.
13. Franssen, F.M. and C.L. Rochester, *Comorbidities in patients with COPD and pulmonary rehabilitation: do they matter?* Eur Respir Rev, 2014. **23**(131): p. 131-41.
14. Rutten, E.P.A., et al., *Disturbed intestinal integrity in patients with COPD: effects of activities of daily living.* Chest, 2014. **145**(2): p. 245-252.
15. Bingula, R., et al., *Desired Turbulence? Gut-Lung Axis, Immunity, and Lung Cancer.* J Oncol, 2017. **2017**: p. 5035371.
16. Bienenstock, J. and D. Befus, *Gut- and bronchus-associated lymphoid tissue.* Am J Anat, 1984. **170**(3): p. 437-45.
17. Keely, S., N.J. Talley, and P.M. Hansbro, *Pulmonary-intestinal cross-talk in mucosal inflammatory disease.* Mucosal Immunol, 2012. **5**(1): p. 7-18.
18. Santaolalla, R., M. Fukata, and M.T. Abreu, *Innate immunity in the small intestine.* Curr Opin Gastroenterol, 2011. **27**(2): p. 125-31.
19. Gutzeit, C., G. Magri, and A. Cerutti, *Intestinal IgA production and its role in host-microbe interaction.* Immunol Rev, 2014. **260**(1): p. 76-85.
20. Hikichi, M., et al., *Pathogenesis of chronic obstructive pulmonary disease (COPD) induced by cigarette smoke.* J Thorac Dis, 2019. **11**(Suppl 17): p. S2129-S2140.
21. Decramer, M. and W. Janssens, *Chronic obstructive pulmonary disease and comorbidities.* Lancet Respir Med, 2013. **1**(1): p. 73-83.
22. Papi, A., et al., *Infections and airway inflammation in chronic obstructive pulmonary disease severe exacerbations.* Am J Respir Crit Care Med, 2006. **173**(10): p. 1114-21.
23. Su, J., et al., *Sputum Bacterial and Fungal Dynamics during Exacerbations of Severe COPD.* PLoS One, 2015. **10**(7): p. e0130736.
24. Hardaker, E.L., et al., *Exposing rodents to a combination of tobacco smoke and lipopolysaccharide results in an exaggerated inflammatory response in the lung.* Br J Pharmacol, 2010. **160**(8): p. 1985-96.
25. Kobayashi, S., et al., *A single dose of lipopolysaccharide into mice with emphysema mimics human chronic obstructive pulmonary disease exacerbation as assessed by micro-computed tomography.* Am J Respir Cell Mol Biol, 2013. **49**(6): p. 971-7.
26. Braber, S., et al., *Inflammatory changes in the airways of mice caused by cigarette smoke exposure are only partially reversed after smoking cessation.* Respiratory research, 2010. **11**(1): p. 99.
27. Reboldi, A. and J.G. Cyster, *Peyer's patches: organizing B-cell responses at the intestinal frontier.* Immunol Rev, 2016. **271**(1): p. 230-45.
28. Ojha, U.C., et al., *Correlation of Severity of Functional Gastrointestinal Disease Symptoms with that of Asthma and Chronic Obstructive Pulmonary Disease: A Multicenter Study.* Int J Appl Basic Med Res, 2018. **8**(2): p. 83-88.
29. Brandtzaeg, P., *Function of mucosa-associated lymphoid tissue in antibody formation.* Immunol Invest, 2010. **39**(4-5): p. 303-55.
30. Ghorani, V., et al., *Experimental animal models for COPD: a methodological review.* Tob Induc Dis, 2017. **15**: p. 25.
31. Singanayagam, A., et al., *A short-term mouse model that reproduces the immunopathological*

features of rhinovirus-induced exacerbation of COPD. Clin Sci (Lond), 2015. **129**(3): p. 245-58.

32. Laan, M., S. Bozinovski, and G.P. Anderson, *Cigarette smoke inhibits lipopolysaccharide-induced production of inflammatory cytokines by suppressing the activation of activator protein-1 in bronchial epithelial cells.* J Immunol, 2004. **173**(6): p. 4164-70.

33. Dantzer, R., et al., *Resilience and immunity.* Brain Behav Immun, 2018. **74**: p. 28-42.

34. Gong, L., et al., *Promoting effect of neutrophils on lung tumorigenesis is mediated by CXCR2 and neutrophil elastase.* Mol Cancer, 2013. **12**(1): p. 154.

35. Valipour, A., et al., *Circulating vascular endothelial growth factor and systemic inflammatory markers in patients with stable and exacerbated chronic obstructive pulmonary disease.* Clin Sci (Lond), 2008. **115**(7): p. 225-32.

36. Powell, M.D., et al., *IL-12 signaling drives the differentiation and function of a TH1-derived TFH1-like cell population.* Sci Rep, 2019. **9**(1): p. 13991.

37. Canny, G.O. and B.A. McCormick, *Bacteria in the intestine, helpful residents or enemies from within?* Infect Immun, 2008. **76**(8): p. 3360-73.

38. Beloborodova, E.I., et al., *[Disturbed absorptive function of small intestines in patients with chronic obstructive pulmonary disease].* Klin Med (Mosk), 2012. **90**(1): p. 54-9.

39. Berlin, P., et al., *Villus Growth, Increased Intestinal Epithelial Sodium Selectivity, and Hyperaldosteronism Are Mechanisms of Adaptation in a Murine Model of Short Bowel Syndrome.* Dig Dis Sci, 2019. **64**(5): p. 1158-1170.

40. Ogawa, E., et al., *Body mass index in male patients with COPD: correlation with low attenuation areas on CT.* Thorax, 2009. **64**(1): p. 20-5.

41. He, Y., et al., *Gut-lung axis: The microbial contributions and clinical implications.* Crit Rev Microbiol, 2017. **43**(1): p. 81-95.

42. Lee, S.H., et al., *Association between Cigarette Smoking Status and Composition of Gut Microbiota: Population-Based Cross-Sectional Study.* J Clin Med, 2018. **7**(9).

43. Li, N., et al., *Chronic exposure to ambient particulate matter induces gut microbial dysbiosis in a rat COPD model.* Respir Res, 2020. **21**(1): p. 271.

44. Tomoda, K., et al., *Cigarette smoke decreases organic acids levels and population of bifidobacterium in the caecum of rats.* J Toxicol Sci, 2011. **36**(3): p. 261-6.

45. Tezuka, H. and T. Ohteki, *Regulation of IgA Production by Intestinal Dendritic Cells and Related Cells.* Front Immunol, 2019. **10**: p. 1891.

46. Bollinger, R.R., et al., *Human secretory immunoglobulin A may contribute to biofilm formation in the gut.* Immunology, 2003. **109**(4): p. 580-7.

47. Randall, T.D. and R.E. Mebius, *The development and function of mucosal lymphoid tissues: a balancing act with micro-organisms.* Mucosal Immunol, 2014. **7**(3): p. 455-66.

48. Lycke, N.Y. and M. Bemark, *The regulation of gut mucosal IgA B-cell responses: recent developments.* Mucosal Immunol, 2017. **10**(6): p. 1361-1374.

49. Wu, H.J. and E. Wu, *The role of gut microbiota in immune homeostasis and autoimmunity.* Gut Microbes, 2012. **3**(1): p. 4-14.

50. Castro-Dopico, T., J.F. Colombel, and S. Mehandru, *Targeting B cells for inflammatory bowel disease treatment: back to the future.* Curr Opin Pharmacol, 2020. **55**: p. 90-98.

51. Rivera, E.D., et al., *The Mesentery, Systemic Inflammation, and Crohn's Disease.* Inflamm Bowel Dis, 2019. **25**(2): p. 226-234.

52. Tkacova, R., *Systemic inflammation in chronic obstructive pulmonary disease: may adipose tissue play a role? Review of the literature and future perspectives.* Mediators Inflamm, 2010. **2010**: p. 585989.

53. Young, R.P., R.J. Hopkins, and B. Marsland, *The Gut-Liver-Lung Axis. Modulation of the Innate Immune Response and Its Possible Role in Chronic Obstructive Pulmonary Disease.* Am J Respir Cell Mol Biol, 2016. **54**(2): p. 161-9.

54. Tsantikos, E., et al., *Granulocyte-CSF links destructive inflammation and comorbidities in obstructive lung disease.* J Clin Invest, 2018. **128**(6): p. 2406-2418.

55. Broekhuizen, R., et al., *Raised CRP levels mark metabolic and functional impairment in advanced COPD.* Thorax, 2006. **61**(1): p. 17-22.

56. Man, S.F., et al., *C-reactive protein and mortality in mild to moderate chronic obstructive pulmonary disease.* Thorax, 2006. **61**(10): p. 849-53.

57. Aksu, F., et al., *C-reactive protein levels are raised in stable Chronic obstructive pulmonary disease patients independent of smoking behavior and biomass exposure.* J Thorac Dis, 2013. **5**(4): p. 414-21.

58. Lonergan, M., et al., *Blood neutrophil counts are associated with exacerbation frequency and mortality in COPD.* Respir Res, 2020. **21**(1): p. 166.

59. Leuzzi, G., et al., *C-reactive protein level predicts mortality in COPD: a systematic review and meta-analysis.* Eur Respir Rev, 2017. **26**(143).

60. Yu, Y., et al., *Th1/Th17 Cytokine Profiles are Associated with Disease Severity and Exacerbation Frequency in COPD Patients.* Int J Chron Obstruct Pulmon Dis, 2020. **15**: p. 1287-1299.

61. Wei, B. and C. Sheng Li, *Changes in Th1/Th2-producing cytokines during acute exacerbation chronic obstructive pulmonary disease.* J Int Med Res, 2018. **46**(9): p. 3890-3902.

62. Jiang, M., et al., *ILC2s Induce Adaptive Th2-Type Immunity in Acute Exacerbation of Chronic*

Obstructive Pulmonary Disease. Mediators Inflamm, 2019. **2019**: p. 3140183.

63. Berkowitz, L., et al., *Impact of Cigarette Smoking on the Gastrointestinal Tract Inflammation: Opposing Effects in Crohn's Disease and Ulcerative Colitis.* Front Immunol, 2018. **9**: p. 74.

64. Berkowitz, L., et al., *Mucosal Exposure to Cigarette Components Induces Intestinal Inflammation and Alters Antimicrobial Response in Mice.* Front Immunol, 2019. **10**: p. 2289.

65. Wang, L., et al., *SUL-151 Decreases Airway Neutrophilia as a Prophylactic and Therapeutic Treatment in Mice after Cigarette Smoke Exposure.* Int J Mol Sci, 2021. **22**(9), 4991.

66. Roda, M.A., et al., *Proline-Glycine-Proline Peptides Are Critical in the Development of Smoke-induced Emphysema.* Am J Respir Cell Mol Biol, 2019. **61**(5): p. 560-566.

67. Morris, A., et al., *Comparison of cigarette smoke-induced acute inflammation in multiple strains of mice and the effect of a matrix metalloproteinase inhibitor on these responses.* J Pharmacol Exp Ther, 2008. **327**(3): p. 851-62.

68. Eldridge, A., et al., *Variation in tobacco and mainstream smoke toxicant yields from selected commercial cigarette products.* Regul Toxicol Pharmacol, 2015. **71**(3): p. 409-27.

69. Vernooy, J.H., et al., *Long-term intratracheal lipopolysaccharide exposure in mice results in chronic lung inflammation and persistent pathology.* Am J Respir Cell Mol Biol, 2002. **26**(1): p. 152-9.

70. Ceelen, J.J.M., et al., *Altered protein turnover signaling and myogenesis during impaired recovery of inflammation-induced muscle atrophy in emphysematous mice.* Sci Rep, 2018. **8**(1): p. 10761.

71. Bakker-Zierikzee, A.M., et al., *Effects of infant formula containing a mixture of galacto- and fructo-oligosaccharides or viable Bifidobacterium animalis on the intestinal microflora during the first 4 months of life.* Br J Nutr, 2005. **94**(5): p. 783-90.

72. Zhao, G., M. Nyman, and J.A. Jonsson, *Rapid determination of short-chain fatty acids in colonic contents and faeces of humans and rats by acidified water-extraction and direct-injection gas chromatography.* Biomed Chromatogr, 2006. **20**(8): p. 674-82.

73. Thiel, R. and M. Blaut, *An improved method for the automated enumeration of fluorescently labelled bacteria in human faeces.* J Microbiol Methods, 2005. **61**(3): p. 369-79.

74. Verheijden, K.A.T., et al., *The Combination Therapy of Dietary Galacto-Oligosaccharides With Budesonide Reduces Pulmonary Th2 Driving Mediators and Mast Cell Degranulation in a Murine Model of House Dust Mite Induced Asthma.* Front Immunol, 2018. **9**: p. 2419.

Supplementary data
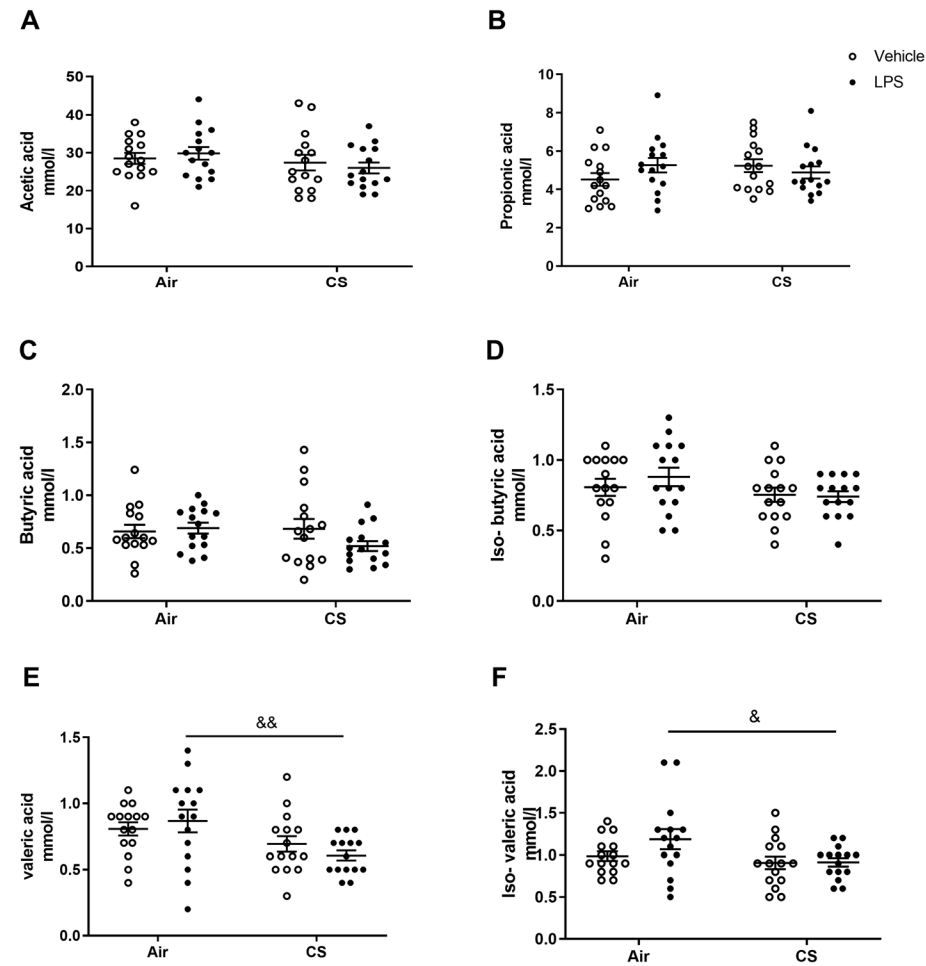
Supplementary Figure 1. SCFAs levels in cecum content.
Mice were exposed to air or cigarette smoke for 72 days, except on day 42, 52 and 62, on these days mice were treated with saline or LPS via i.t. instillation. Cecum content was collected and the absolute amounts of total SCFAs (A), total iso-SCFAs (B), valeric acid (C), iso-valeric acid (D), butyric acid (E), iso-butyric acid (F), acetic acid (G) and propionic acid (H) were measured. Values are expressed as mean±SEM. $^{\&}P < 0.05$, $^{\&\&}P < 0.01$, CS + LPS group compared with LPS group; Air + vehicle: n=15; air + LPS: n=15; CS + vehicle: n=15; CS + LPS: n=15. CS=cigarette smoke.
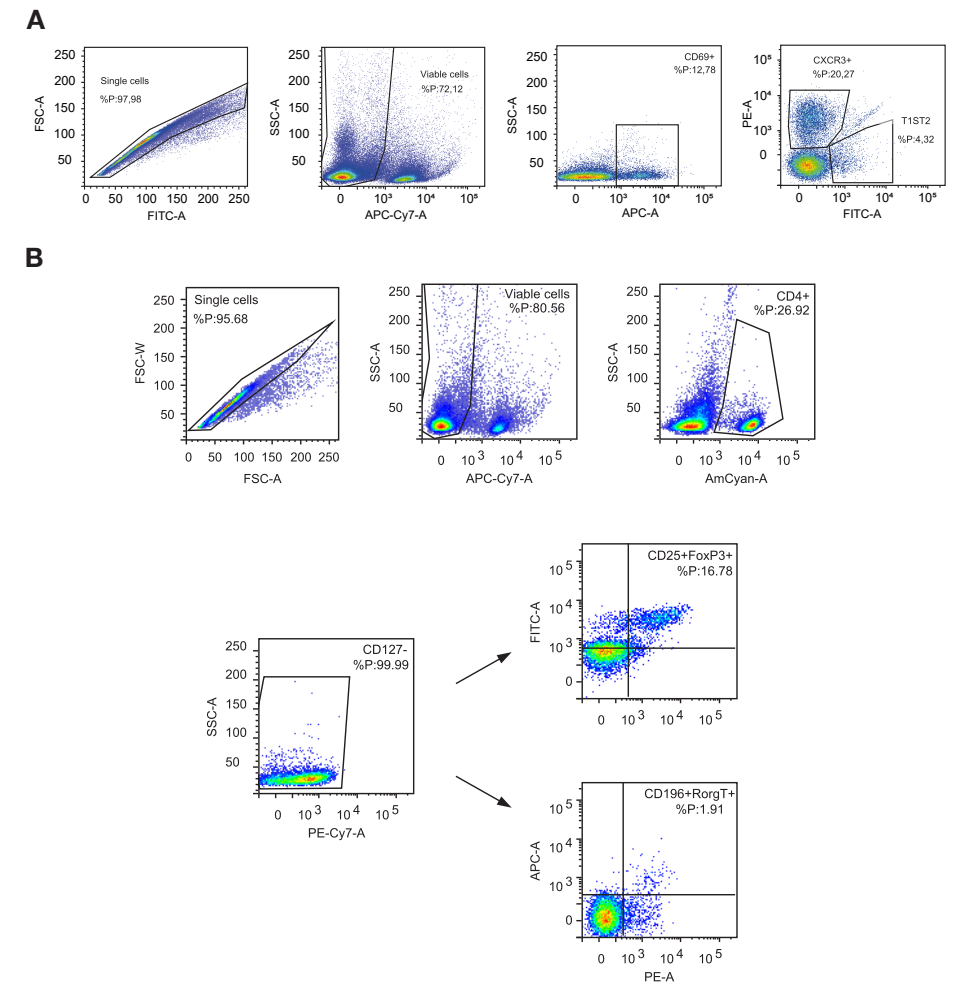
Supplementary Figure 2. Gating strategy for Th1 and Th2 cells (A), Th17 and Treg cells (B).

Supplementary Figure 3. An example of a villi picture measured via ImageJ. The measurement of the villus length and crypt depth is indicated. Magnification 200x.
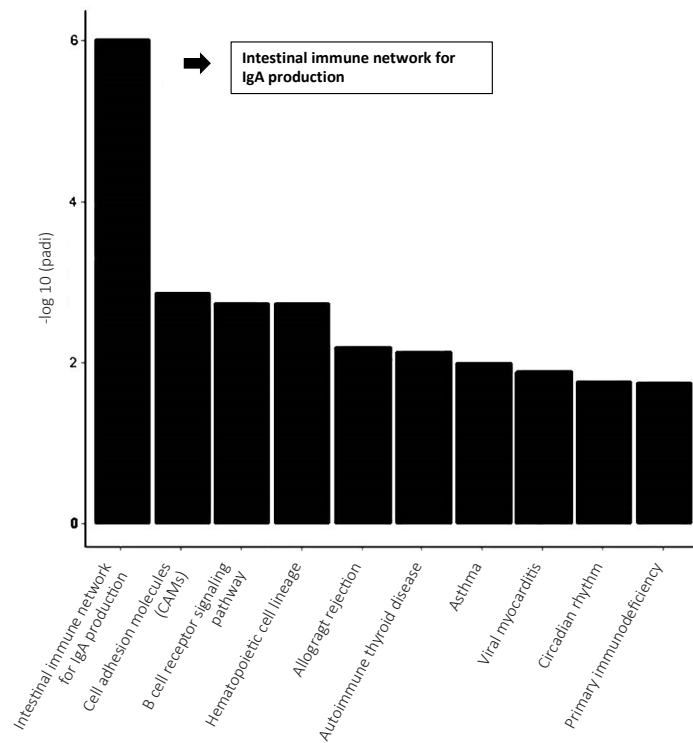
Supplementary Figure 4. KEGG pathway enrichment analysis in the distal small intestine of cigarette smoke-exposed mice.
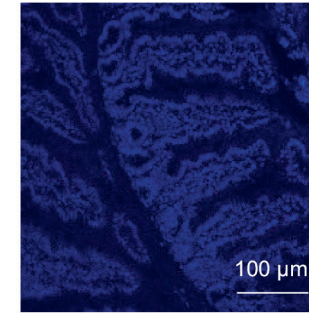
Supplementary Figure 5. Representative picture of the negative control related to the immunofluorescent staining for IgA in distal small intestine. No staining was observed in the negative control (primary antibody omitted) (DAPI; blue, scale bar = 100 μm).

Chapter 4

Transcriptomic Changes in Lung and
Intestinal Tissues of Cigarette
Smoke-exposed Mice Compared
to COPD and CD Patient Data Sets

Lei Wang[1], Pim J. Koelink[2], Johan Garssen[1,3], Gert Folkerts[1],
Paul A.J. Henricks[1], Saskia Braber[1*]

[1] Division of Pharmacology, Utrecht Institute for Pharmaceutical Sciences, Faculty of Science, Utrecht University,
The Netherlands
[2] Tytgat Institute for Liver and Intestinal Research, Amsterdam University Medical Centers; Amsterdam
Gastroenterology, Endocrinology, Metabolism (AGEM), Amsterdam, The Netherlands
[3] Nutricia Research, The Netherlands

Abstract

Background
Cigarette smoking is the major cause of chronic obstructive pulmonary disease (COPD). Both (healthy) smokers and COPD patients have a higher incidence of intestinal disorders. The aim of this study was to gain insight into the transcriptomic changes in the lung and intestine after cigarette smoke exposure.

Methods
Mice were exposed to cigarette smoke for 10 weeks and lung and ileum tissues were analyzed by RNA sequencing, followed by functional pathway analyses using the Kyoto Encyclopedia of Genes and Genomes (KEGG). The top 15 differentially expressed genes in the lung and ileum of cigarette smoke-exposed mice were investigated in publicly available gene expression datasets of lung tissue of COPD and ileum of Crohn's disease (CD) patients.

Results
Increased expression of MMP12, GPNMB, CTSK, CD68, SPP1, CCL22, and ITGAX was found in the lungs of both cigarette smoke-exposed mice and in COPD patients. Changes in the intestinal expression of CD79B, PAX5, and FCRLA were observed in the ileum of cigarette smoke-exposed mice and CD patients. Furthermore, inflammatory cytokine profiles and adhesion molecules in both the lung and intestine of cigarette smoke-exposed mice were profoundly changed compared to air-exposed mice. In both the lung and ileum, enrichment in the genes for the cytokine-cytokine receptor interaction pathways and pathways related to adhesion molecules were identified.

Conclusions
Altered gene expression in the murine lung tissue was detected after cigarette smoke exposure, which might simulate COPD-like alterations. However, the highly expressed genes in the ileum of cigarette smoke-exposed mice were less comparable to the gene expression pattern in the ileum of CD patients. This transcriptome dataset of the lung and ileum of smoke-exposed mice would be a valuable tool for future directions of research and potential clinical applications in COPD and related gastrointestinal comorbidities.

Introduction

Chronic obstructive pulmonary disease (COPD) was the third leading cause of death worldwide in 2019, and is caused by exposure to harmful gases and particles, while genetic factors may also contribute to the development of COPD [1]. COPD is associated with inflammatory bowel disease (IBD) [2], and COPD patients have a higher incidence and prevalence of IBD [3]. Cigarette smoke is considered as one of the most detrimental factors for COPD pathogenesis [4]. The impact of cigarette smoke exposure on the respiratory tract has been widely studied. Recently, attention has been drawn to cigarette smoke-induced changes within the gastrointestinal tract [5]. One explanation for the gut-lung interaction following cigarette smoke exposure, might be related to lung-induced systemic inflammation. In addition, cigarette smoke particles might enter the gastrointestinal tract due to mucociliary clearance of the lung or direct swallowing [6]. However, underlying mechanisms have not been fully clarified yet.

The importance of the gut–lung axis has been observed in the development of COPD, and changes in the gut may potentiate inflammation and progression of COPD [7]. The intestine is the largest immune organ in the body containing around 70% of the host's immune cells [8]. It also harbors various commensal microorganisms that are crucial for the functioning of the mucosal immune system [9]. Due to the vital role of the intestine in both health and disease conditions, it is essential to better understand the intestinal responses induced after exposure to cigarette smoke. The increased knowledge of the molecular mechanisms of immune responses in COPD patients could contribute to a better therapeutic management of COPD and COPD-related intestinal comorbidities.

Recent advances in genomics have enabled genome-wide mRNA profiling, a valuable tool in identifying host immune responses and associated gene regulatory networks [10]. To gain insight into the gut-lung axis in COPD, the molecular changes in the lung and ileum (distal small intestine) were investigated in a murine model of cigarette smoke-induced COPD through KEGG pathway analysis. The highly differentially expressed genes in the murine lung were compared with the altered gene expression in the lungs of COPD patients, and the highly differentially expressed genes in the Ileum of cigarette smoke-exposed mice were compared with gene expression changes in the ileum of Crohn's disease (CD) patients.

Results

Differential changes in lung tissue transcriptome of cigarette smoke-exposed mice

To investigate the influence of cigarette smoke exposure on gene expression in murine lung tissue, mice were exposed to air or cigarette smoke for 10 weeks, and RNA-sequence analysis was performed on whole lung tissue. We identified 908 differentially expressed genes in the lung (padj < 0.05, |log2 (Fold Change)|> 1) of which 694 genes were up-regulated and 214 genes were down-regulated in cigarette smoke-exposed animals (Figure 1A). The differentially expressed genes in response to cigarette smoke are shown in a volcano plot (Figure 1B), with red dots representing the up-regulated genes and green dots representing the down-regulated genes. The top 15 most significantly changed genes upon cigarette smoke exposure, were all up-regulated in cigarette smoke-exposed mice and are depicted in a table (Figure 1C).

Comparison of lung gene expression profiles of cigarette smoke exposed-mice and COPD patients

To gain insight into the translational potential of the murine model of cigarette smoke-induced COPD, the transcriptomic profiling of lung tissue from cigarette smoke-exposed mice was compared with the transcriptomic changes in the lungs of COPD patients. Therefore, lung tissue gene expression datasets were obtained from the Gene Expression Omnibus (GEO). Of the top 15 most significantly up-regulated genes upon cigarette smoke exposure in the murine model, 7 were also found to be significantly up-regulated in the lungs of COPD patients (*MMP12, SPP1, CCL22, ITGAX, GPNMB, CTSK* and *CD68*, Figure 1D-J), 5 genes were not significantly elevated (*CD177, LCN2, SLC6A20, CYP1A1* and *MSR1*, Supplementary Figure 2), while the 3 remaining genes (*Wfcd17, Clec4n, Ms4a7)* or their human orthologs, were not present in the database. This indicates that the murine model of cigarette smoke-induced COPD shows similarities with the development of COPD in humans.
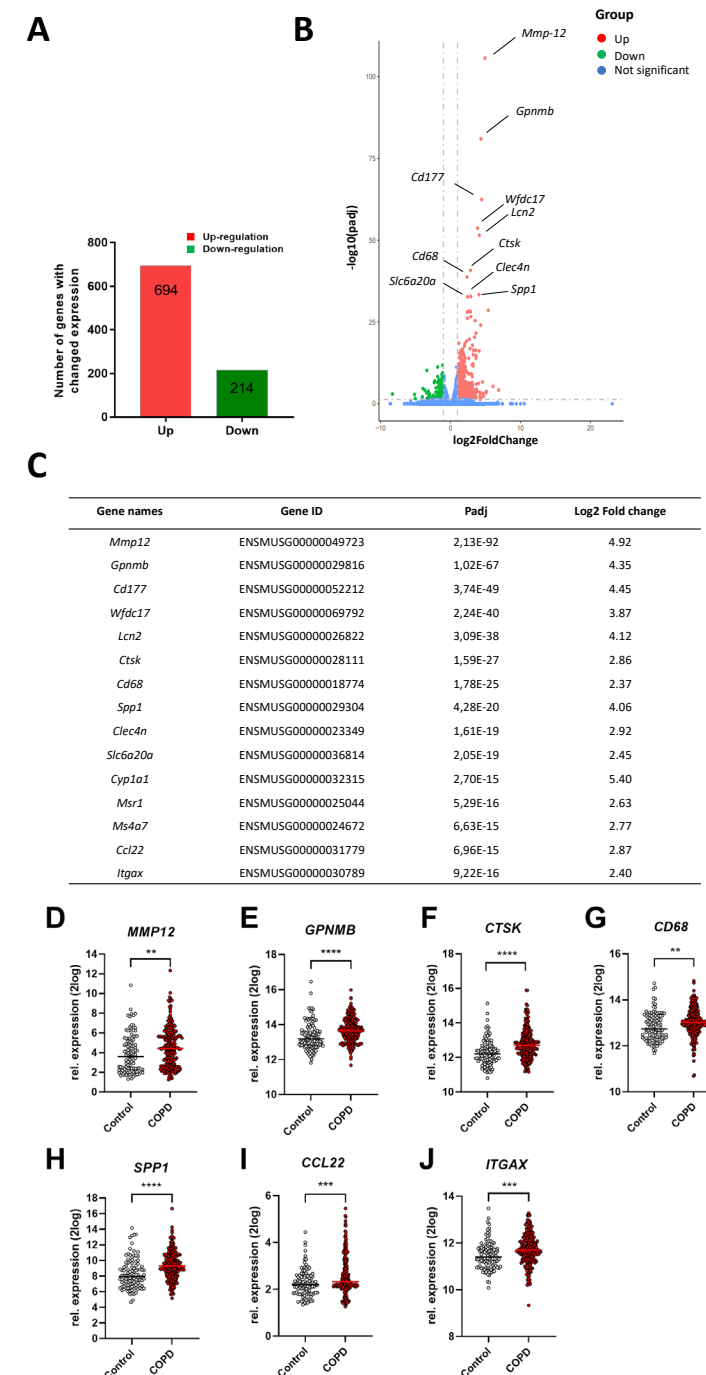

Gene names	Gene ID	Padj	Log2 Fold change
Mmp12	ENSMUSG00000049723	2,13E-92	4.92
Gpnmb	ENSMUSG00000029816	1,02E-67	4.35
Cd177	ENSMUSG00000052212	3,74E-49	4.45
Wfdc17	ENSMUSG00000069792	2,24E-40	3.87
Lcn2	ENSMUSG00000026822	3,09E-38	4.12
Ctsk	ENSMUSG00000028111	1,59E-27	2.86
Cd68	ENSMUSG00000018774	1,78E-25	2.37
Spp1	ENSMUSG00000029304	4,28E-20	4.06
Clec4n	ENSMUSG00000023349	1,61E-19	2.92
Slc6a20a	ENSMUSG00000036814	2,05E-19	2.45
Cyp1a1	ENSMUSG00000032315	2,70E-15	5.40
Msr1	ENSMUSG00000025044	5,29E-16	2.63
Ms4a7	ENSMUSG00000024672	6,63E-15	2.77
Ccl22	ENSMUSG00000031779	6,96E-15	2.87
Itgax	ENSMUSG00000030789	9,22E-16	2.40

Figure 1. Differential changes in lung tissue transcriptome of cigarette smoke-exposed mice and overlapping transcriptome changes in COPD patients. Mice were exposed to air or cigarette smoke for approximately 10 weeks and RNA-sequence analysis of lung tissues was performed. The

number of significantly up-regulated and down-regulated genes (A) and a volcano plot with these differentially expressed genes (B) are depicted. Red dots represent the up-regulated genes, green dots represent down-regulated genes, while blue dots indicate the non-significantly altered genes with a padj < 0.05 and ||log2(Fold Change)|>1. The top 15 up- or down-regulated genes (padj < 0.05 and |log2(Fold Change)|> 1) in lung tissue of cigarette smoke exposed mice are depicted in Table C. N=3 mice/group. The top 15 up- or down-regulated genes in murine lungs were also examined in COPD patients. MMP12 (D), GPNMB (E), CTSK (F), CD68 (G), SPP1 (H), CCL22 (I) and ITGAX (J) gene expression levels from COPD patients were compared to healthy individuals, N=220 for COPD patients, N=108 for healthy individuals.

Differential changes in ileum transcriptome of cigarette smoke-exposed mice

To investigate the effect of cigarette smoke exposure on gene expression in murine intestinal tissues, RNA-sequence analysis was performed on whole proximal (duodenum) and distal (ileum) small intestinal tissue. 223 genes were differentially expressed in the ileum of cigarette smoke-exposed mice compared to air-exposed mice (padj < 0.05, |log2 (Fold Change)|> 1), with 91 genes up-regulated and 132 genes down-regulated (Figure 2A). The differentially expressed genes in response to cigarette smoke are shown in a volcano plot (Figure 2B), with red dots representing the up-regulated genes and green dots representing the down-regulated genes. The top 15 differentially expressed genes are depicted as a table in Figure 2C.

In addition, 94 genes were differentially expressed (padj < 0.05, |log2 (Fold Change)|> 1) with 84 genes up-regulated and 10 genes down-regulated in the duodenum of cigarette smoke-exposed mice, as depicted in Supplementary Figure 1A. The differentially expressed genes in response to cigarette smoke are shown in a volcano plot (Supplementary Figure 1B). 18 common genes were differentially expressed in both duodenum and ileum of cigarette smoke-exposed mice.

Comparison of murine ileum gene expression profiles versus ileum gene expression levels of CD patients

To clarify whether transcriptomic changes in the intestine, observed in the murine model of cigarette smoke-induced COPD, are similar to IBD-like intestinal changes, the murine transcriptomic profiling was compared to the transcriptomic changes found in the ileum of CD patients. Of the top 15 differentially expressed genes in the murine ileum 3 genes (CD79B, FCRLA and PAX5) were differentially expressed in the ileum of patients with CD (Figure 2D-F), while 5 did not show an altered expression (CD79A, MEG3, CORO1A, TNFRSF13C, CCR7, Supplementary Figure 3). The 7 remaining genes (Gm13648, Snhg11, Fcrla, AC133488.1, Firre, Etohd2, AV026068 and Xist) or their human orthologs, were not present in the database. Surprisingly, CD79B, FCRLA and PAX5 were all up-regulated by cigarette smoke exposure in the murine model, while they are found down-regulated in CD, especially in actively inflamed tissue (Figure 2G-I).
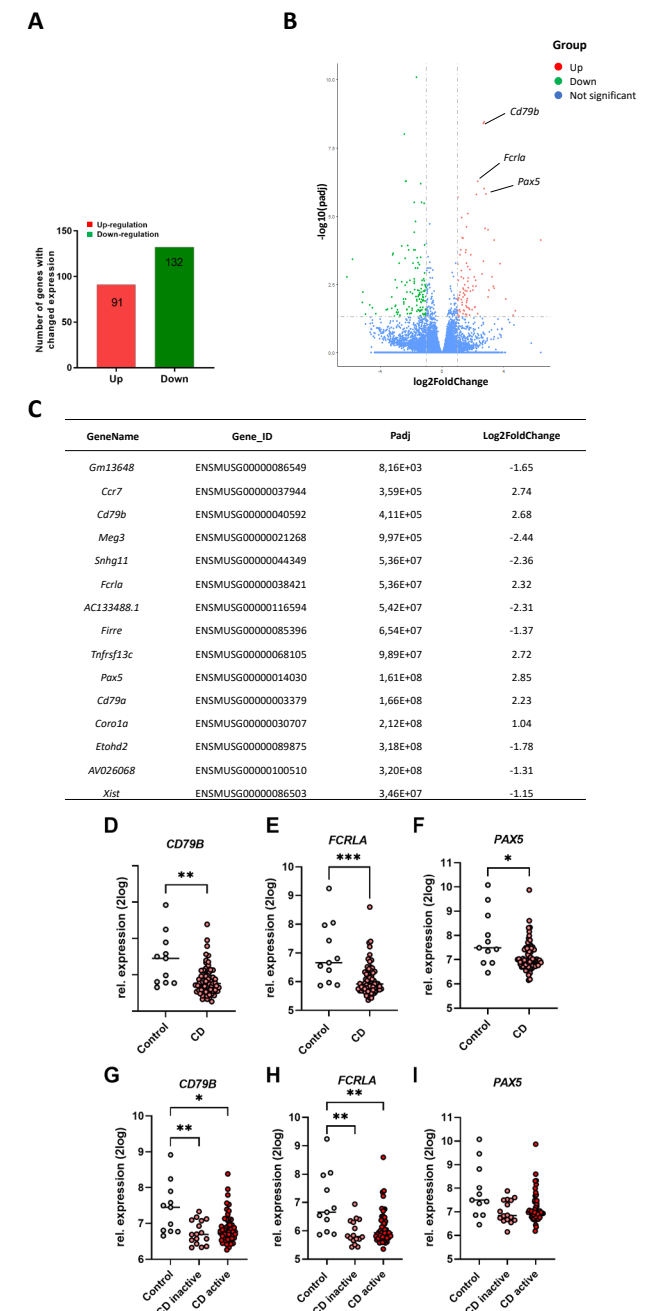

Figure 2: Differential changes in ileum transcriptome of cigarette smoke-exposed mice and overlapping transcriptome changes in CD patients. Mice were exposed to air or cigarette smoke for approximately 10 weeks and RNA-sequence analysis of ileum was performed. The number of significantly up-regulated and down-regulated genes (A) and a volcano plot with these differentially expressed genes (B) are depicted. Red dots represent the up-regulated genes, green dots represent down-regulated genes, while blue dots indicate the non-significantly altered genes with a padj < 0.05

and |log2(Fold Change)|> 1. The top 15 up- or down-regulated genes (padj < 0.05 and |log2(Fold Change)|> 1) in ileum of cigarette smoke-exposed murine lungs are depicted in Table C. N=5 mice/ group. The top 15 up- or down-regulated genes in murine ileum were also examined in the CD patients. *CD79B* (D), *FCRLA* (E) and *PAX5* (F) gene expression levels in ileum of CD patients were compared to healthy individuals; *CD79B* (G), *FCRLA* (H) and *PAX5* (I) gene expression levels in ileum of inactive and active CD patients were compared to healthy individuals. N=67 for CD patients (N=16 for inactive CD and N=51 for active CD patients), N=11 for healthy individuals.

Overlapping pathways in the lung and ileum of cigarette smoke-exposed mice

To identify potential signaling pathways that are associated in both lung and intestinal tissues upon cigarette smoke-exposure, a KEGG pathway enrichment analysis was performed. The top 20 pathways (padj< 0.05, |log2 (Fold Change)|> 1) in the lung and in the ileum are shown in Figure 3A-3B. The two signaling pathways that are highlighted by cigarette smoke exposure in both the lung and intestine are the Cytokine-Cytokine Receptor interaction and Cell Adhesion Molecule pathways. Heatmaps of the specific genes in the Cytokine-Cytokine Receptor interaction pathway that are significantly altered in the lung and intestine are depicted in Figure 3C and 3E. The upregulation of Il21r, Tnfrsf13c and Ltb by cigarette smoke (marked in red) from Cytokine-Cytokine Receptor interaction pathway was found in both organs. For the Cell Adhesion Molecule pathway, the heatmaps of the significantly altered genes in the lungs and intestines are shown in Figure 3D and 3F. Cd28, H2dmb2, Cd22, Cd2, H2ob and H2oa were up-regulated by cigarette smoke exposure (depicted in red).

In addition, the Cytokine-Cytokine Receptor interaction pathway was also the most enriched pathway in the duodenum (proximal small intestine) of cigarette smoke-exposed mice (Supplementary Figure 1C). The heatmap shows that *Il21r* are increased by cigarette smoke exposure in both intestinal parts and lung tissue (Figure 3E and Supplementary Figure 1D).
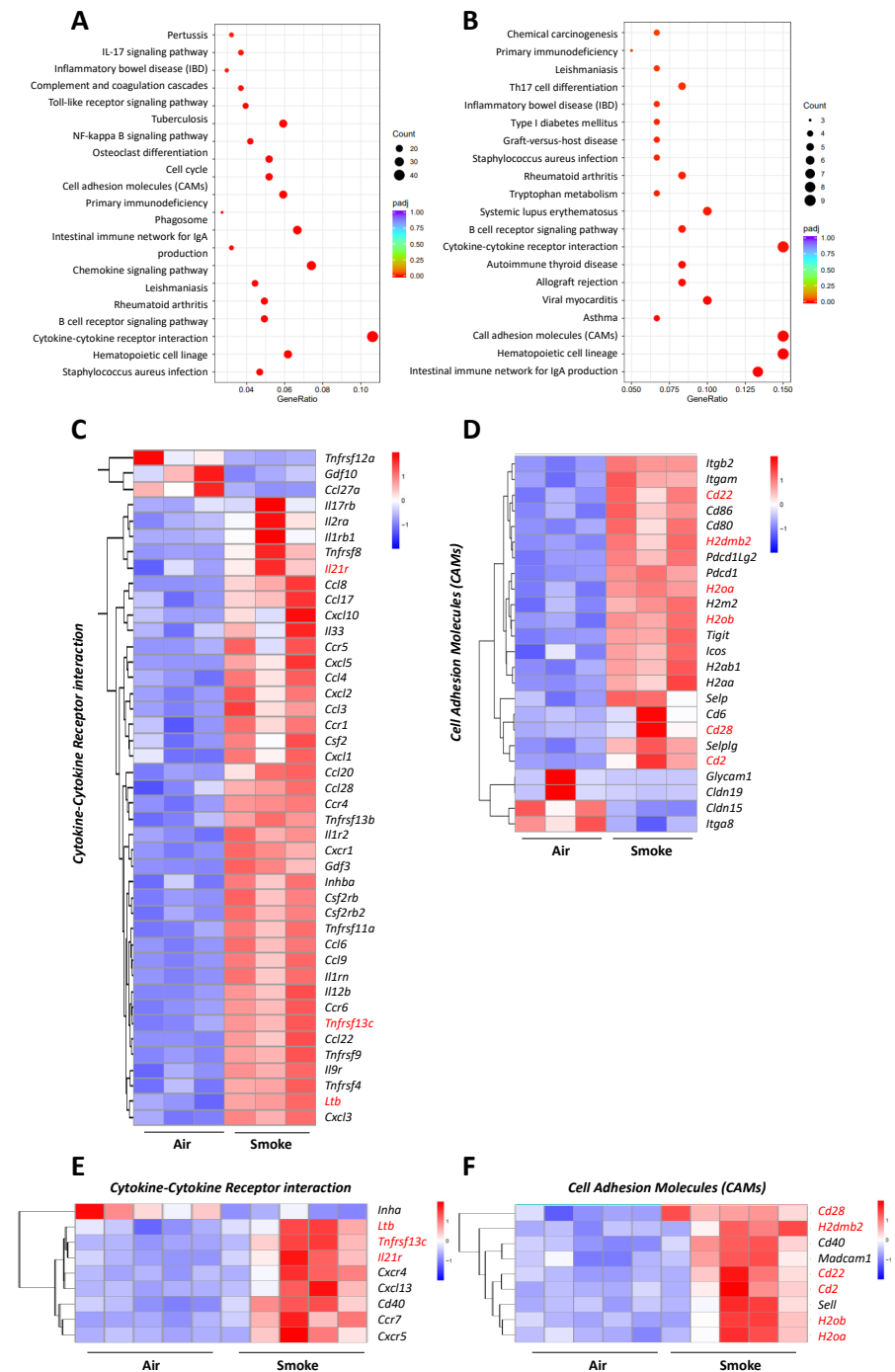

Figure 3. Overlapping pathways in the lung and ileum of cigarette smoke-exposed mice. KEGG pathway enrichment analysis of differentially expressed genes in lung tissue (A) and ileum (B) of cigarette smoke-exposed mice are depicted in dot plots. The size of the dots represents the number (counts) of

differentially expressed genes enriched in that particular pathway, while the color of the dots represents the padj values (based on the scale bar). Heatmaps depicting the expression levels of genes enriched in the cytokine-cytokine receptor interaction pathway in the lung (C) and ileum (E), or in the cell adhesion molecule pathways in the lung (D) and ileum (F) of air- and cigarette smoke-exposed mice. N=3 mice/group regarding the lung tissue, N=5 mice/group regarding the ileum samples.

Discussion

Cigarette smoke is one of the major triggers of lung inflammation and respiratory diseases, such as COPD [11]. Intestinal diseases are commonly observed in COPD patients [12] and the incidence of IBD is higher in COPD patients compared to healthy subjects [13]. Nowadays, intestinal immune responses induced by cigarette smoke are getting more and more attention [14]. In our previous study, we demonstrated changes in intestinal homeostasis and immunity in a cigarette smoke- and LPS-induced murine model for COPD [6]. The exact pathogenesis of these observations is not yet clear. Therefore, in the current study, we investigated the molecular changes and associated signaling pathways using RNA-sequence analysis in the lungs and intestines of mice exposed to cigarette smoke.

Pre-clinical animal models are a valuable tool for understanding the pathogenesis of COPD and related comorbidities. To gain insight into the translational potential of the murine model of cigarette smoke-induced COPD, we compared the transcriptional changes in mice with the transcriptomic profiles of the lungs of COPD patients. 10 weeks of cigarette smoke exposure induced the differential expression of 908 genes in the lungs compared with air-exposed mice. Among the top 15 differentially expressed (upregulated) genes in lungs of cigarette smoke-exposed mice, *MMP12, GPNMB, CTSK, CD68, SPP1, CCL22,* and *ITGAX* were also significantly up-regulated in the lung tissue of COPD patients. In another study, *Mmp12, GPNMB, CTSK* and *CD68* were identified as the top 20 genes that were up-regulated in murine lung tissue after 8-16 weeks and 24 weeks of cigarette smoke exposure [15].

Matrix metalloproteinase-12 (MMP-12) belongs to the matrix metalloproteinases family, which contributes to the remodeling of the small airways and to the proteolytic degradation of the alveolar wall matrix, leading to emphysema [16]. GPNMB, an endogenous glycoprotein, can influence the pathogenesis of COPD, for instance, by its contribution to tissue remodeling in COPD through promoting the secretion of MMP-9, another matrix metalloproteinase [17]. CTSK is a cysteine protease that is stimulated by inflammatory cytokines and released after tissue injury contributing to the destruction of connective tissues in the lung [18]. CTSK is up-regulated in alveolar macrophages of emphysema patients and in the lungs of cigarette smoke-exposed guinea pigs. CTSK is partially responsible for the loss of lung elasticity and recoil observed in the formation of emphysema [18, 19]. The expression of *SPP1,* Secreted Phosphoprotein 1, positively correlates with COPD severity as assessed by forced expiratory volume in 1 s (FEV1) [20]. In addition, *SPP1* was the only differential

expressed gene that was up-regulated in both patients with COPD and lung cancer. This indicates that the up-regulation of *SPP1* in COPD might be associated with the increased risk of lung cancer in these patients [21]. CCL22, chemokine (C-C motif) ligand 22, is a monocyte-derived chemokine and exerts functions in multiple lung-related diseases [22]. CCL22 is elevated in bronchial tissue from COPD patients and could potentially affect adaptive immune responses in COPD disease progression [23, 24]. *ITGAX,* the gene that encodes CD11c (a leukocyte integrin), mediates adherence of neutrophils and monocytes to activated endothelial cells [25]. *ITGAX* was identified as one of the top 7 genes with a > 2.5-fold increase observed in emphysema patients [26]. However, information regarding the role of *ITGAX* in the development of COPD is scarce.

The current study showed that 10 weeks of cigarette smoke exposure induced altered gene profiles in murine lungs comparable to changes observed in COPD patients, confirming the COPD-like features in our murine model. Besides the changes observed in the expression of *Mmp12, Gpnmb, Ctsk, Cd68, Spp1* and *Ccl22* in both murine lung tissue and lung tissue of COPD patients, other COPD characteristics, such as enlarged mean linear intercept (Lm), and increased number of neutrophils and macrophages in the bronchoalveolar lavage fluid were also observed in this murine model of cigarette smoke-induced COPD [27].

Having determined that the 10 weeks cigarette smoke-exposed mice show characteristics of COPD patients, we focused on the intestinal gene expression alterations upon cigarette smoke exposure. 10 weeks of cigarette smoke exposure induced more alterations in gene expression levels in the distal small intestine (223 altered genes; padj< 0.05, |log2 (Fold Change)|> 1)) compared to the proximal small intestine (94 altered genes). We compared the changes in the distal small intestine to the changes found in the ileum of patients with CD. CD, one of the major forms of IBD, can affect all segments of the gastrointestinal tract, most commonly the terminal ileum [28]. Smoking is known to be associated with the development of CD, and particularly impacts ileum homeostasis and inflammatory processes [29]. To clarify whether transcriptomic changes in the intestine observed in the murine model of cigarette smoke-induced COPD are comparable to IBD-like intestinal changes, the altered murine genes were evaluated in the ileum of CD patients. From the top 15 differentially expressed genes observed in the ileum of cigarette smoke-exposed mice, *CD79B, PAX5,* and *FCRLA* were up-regulated in the murine ileum, while down-regulated in CD patients. Although, more research is needed to explain these contradictory results, interestingly, all three genes are indicated in the functioning of B cells. B cells are a critical cell type in immune homeostasis at mucosal surfaces, including the gastrointestinal tract. B cell-related abnormalities, such as lympho-plasmacytic infiltrates and anti-microbial antibodies, are well reported in IBD patients [30]. *CD79B* is a B cell lineage-specific gene necessary for the expression and function of the B cell antigen receptor. The *PAX5* gene encodes the B cell lineage specific activator protein that is expressed at early stages of B

cell differentiation, and the *FCRLA* gene encodes a protein, which is selectively expressed in B cells and possibly involved in B cell development, but the exact role of these genes in IBD still needs to be determined. Targeting B-cell related genes and receptor pathways may hold promise as novel therapies for IBD or for intestinal symptoms observed in COPD patients [30].

In the current study, the changes observed in the ileum of cigarette smoke-exposed mice were not in agreement with changes observed in the ileum of CD patients, indicating that there were no obvious IBD-like abnormalities in this model. However, it cannot be excluded that long-term exposure to cigarette smoke might lead to more IBD-like changes.

Subsequently, the potential link between gut and lung in our cigarette smoke-induced COPD model was investigated by performing KEGG pathway enrichment analyses in both organs (padj< 0.05, |log2 (Fold change)|> 1). The genes in both lung and intestinal tissues that were affected by cigarette smoke exposure mainly belonged to the cytokine-cytokine receptor interaction pathway and pathways related to cell adhesion molecules. *Il21r*, *Tnfrsf13c* and *Ltb* were up-regulated by cigarette smoke exposure related to Cytokine-Cytokine Receptor interaction pathway, as well as *Cd28, H2dmb2, Cd22, Cd2, H2ob* and *H2oa* were up-regulated by cigarette smoke exposure associated with the Cell Adhesion Molecule pathway in both the lungs and intestines. COPD is strongly associated with systemic alterations including altered levels of circulating levels of cytokines and adhesion molecules [31]. There are several therapeutic approaches that target cytokine-mediated inflammation in COPD. However, inhibiting specific cytokines may not provide sufficient clinical benefit [32]. Considering the complex interactions between various cytokines involved in inflammatory diseases [33], broad-spectrum anti-inflammatory approaches or targeting multiple cytokines could be considered as an approach to COPD treatment. Cell adhesion molecules play a critical role in the recruitment and migration of cells to the sites of inflammation in patients with COPD [34]. Although the corresponding up-regulated genes observed in lung and ileum, including *Il21r, Tnfrsf13, Ltb, Cd28, H2dmb2, Cd22, Cd2, H2ob and H2oa,* related to the common pathways (Figure 3C-3F) have not been proven to play a role in the interactions between gut and lung, some of these genes, such as *Il21*, have been shown to play a critical role in chronic inflammatory diseases [35, 36].

Gene *Il21r* related to the cytokine-cytokine interaction pathway was the only significantly up-regulated in the lung as well as in the proximal and distal small intestine in cigarette smoke-exposed mice. IL21R transduces the growth-promoting signal of IL21, and is important for the proliferation and differentiation of T cells, B cells and natural killer cells. The IL21/IL21R interaction plays an important role in a variety of inflammatory diseases [35]. IL21R has been considered as the marker for Th17 cells, however, Th17 cells have not yet been specifically identified in the lungs of COPD patients, but Th17-related cytokines have been observed

in bronchial mucosa [37]. Duan et al., observed that levels of IL21 and the frequencies of Th1, Tc1, CD4+ IL21+, CD4+ IL21R+, and CD8+ IL21R+ T cells were much higher in CS-exposed mice as compared to control [38]. In addition, IL21 produced by CD4+ T cells could promote Th1/Tc1 response, leading to systemic inflammation in emphysema [38]. Recent studies indicated that the amount of IL21 was significantly increased in peripheral blood and intestinal tissue of patients with CD or UC, suggesting that *IL21/IL21R* signaling may be involved in the pathogenesis of IBD [36]. Therefore, *IL21/IL21R* might be an interesting target for future directions of research related to exploring the gut-lung crosstalk.

In conclusion, 10 weeks of cigarette smoke exposure altered the gene expression in the murine lung tissue. Some of these genes are also affected in COPD patients, which confirms COPD-like changes in this murine model of cigarette smoke-induced COPD. Cigarette smoke exposure highly altered the expression of genes in the murine ileum, however, these changes were less comparable to the altered genes observed in the ileum of CD patients. The cytokine-cytokine receptor interaction pathways and pathways related to cell adhesion molecules were the most enriched pathways observed in lungs as well as in the ileum, while the cytokine-cytokine receptor interaction pathways were also highly enriched in the duodenum. The common genes from both lung and intestine involved in these pathways might be considered as targets for the treatment of COPD and its gastrointestinal complains, as well as COPD-related inflammatory diseases, such as IBD.

Material & Methods

Animals

Specific-pathogen free female Balb/c mice [39, 40], 11-13 weeks old, were obtained from Charles River Laboratories. Mice were housed in filter-topped makrolon cages (Tecnilab-BMI, Someren, the Netherlands) with wood-chip bedding (Tecnilab- BMI, Someren in the Netherlands) and tissues (VWR, the Netherlands) were available as cage enrichment. Mice were kept under standard conditions on a 12 h light/dark cycle (lights on from 7.00 am – 7.00 pm) at controlled relative humidity (relative humidity of 50 – 55 %) and temperature (21 ± 2 °C) at the animal facility of Utrecht University. Food (AIN-93M, SNIFF Spezialdiäten GmbH, Soest, Germany) and water were provided ad libitum and were refreshed once a week. The study described in this article is part of a larger trial, including an air control group, cigarette smoke exposure group, and 6 other groups [6]. In accordance with the purpose of this study, investigating the effect of cigarette smoke exposure on transcriptomic sequencing of the RNAs isolated from the lung and intestine, air control and cigarette smoke exposure groups were explored. All animal procedures described in this study were approved by the Ethics Committee of Animal Research of Utrecht University, Utrecht, the Netherlands (AVD1080020184785) and were conducted in accordance with the governmental guidelines.

Cigarette smoke exposure

Mice were exposed in whole-body chambers to mainstream cigarette smoke or air by using a peristaltic pump (SCIQ 232, Watson-Marlow 323, USA). A Plexiglas box containing four metal cages each with four compartments was used to expose the mice to either cigarette smoke or air. Two mice from the same home cage were placed in each compartment. Research cigarettes (3R4F) were obtained from the Tobacco Research Institute (University of Kentucky, Lexington, Kentucky) [41] and filters were removed before use [39].

Mice were acclimatized to cigarette smoke exposure by gradually increasing the number of cigarettes during the first days of the experiment using 4 cigarettes at day 1; 6 cigarettes at day 2; 8 cigarettes at day 3; 10 cigarettes at day 4; 12 cigarettes at day 5; and 14 cigarettes from day 6 until the end of the study [6]. The smoke chamber was connected to a peristaltic pump and vacuum to produce smoke and control the air circulation. The speed of the pump was kept at 35 rpm and the CO levels ranged between 200 and 400 ppm. The mass concentration of cigarette smoke total particulate matter (TPM) was determined by gravimetric analysis of type A/E glass fiber filter (PALL life sciences, Mexico). The TPM concentration in the smoke exposure box generated by 14 cigarettes reached approximately 828 μg/L (828 ± 4.5 μg/L) [39]. Mice were anesthetized by an intraperitoneal injection of ketamine/medetomidine (196.8 mg/kg and 1.32 mg/kg respectively) approximately 18 h after the last air or smoke exposure, and lung and proximal and distal small intestinal tissues were isolated for the following measurements.

RNA isolation and gene sequence

RNA preparation

Total RNA was isolated and extracted from tissues using the RNeasy Mini Kit according to the manufacturer's protocol (Qiagen, Germany). RNA integrity and quantitation were assessed using the RNA Nano 6000 Assay Kit of the Bioanalyzer 2100 system (Agilent Technologies, CA, USA). RNA degradation and contamination were monitored on 1% agarose gels.

mRNA non-directional (polyA)

RNA samples were used for library preparation using NEB Next® Ultra RNA Library Prep Kit for Illumina ® Indices were included to multiplex multiple samples. Briefly, mRNA was purified from total RNA using poly-T oligo-attached magnetic beads. After fragmentation, the first strand cDNA was synthesized using random hexamer primers followed by the second strand cDNA synthesis. The library was ready after end repair, A-tailing, adapter ligation, and size selection. After amplification and purification, insert size of the library was validated on an Agilent 2100 and quantified using quantitative PCR (Q-PCR). Libraries were then sequenced on Illumina NovaSeq 6000 S4 flowcell with PE150 according to results from library quality control and expected data volume. Library preparation / sequencing / analysis are performed by Novogene (UK) Company Limited.

Clinical data

Whole-transcriptome data were derived from Gene Expression Omnibus (GEO) datasets: GSE47460 (LGR consortium, lung COPD (n=220) vs controls (n=108)) and GSE16879 (ileums CD patients (n=67) vs healthy controls(n=11)). Data sets were uploaded to and analyzed by the R2: Genomics Analysis and Visualization Platform (http://r2.amc.nl).

Statistics

Data from the *in vivo* study were analyzed using Novosmart software (Novosmart; Cambridge, UK). Differential expression analysis between two groups was performed using DESeq2 R package. The resulting P values were adjusted using the Benjamini and Hochberg's approach for controlling the False Discovery Rate (FDR). Genes with an adjusted P value < 0.05 found by DESeq2 were assigned as differentially expressed. KEGG pathway libraries were used to perform enrichment analysis. Clinical data were analyzed by Mann-Whitney test comparing two groups or Kruskal-Wallis test followed by Dunn's multiple comparisons test, and considered significant when p<0.05.

References

1. WHO. *The top 10 causes of death*. 2020 [cited 2021 14 Dec]; Available from: https://www.who.int/news-room/fact-sheets/detail/the-top-10-causes-of-death.

2. Vutcovici, M., et al., *Inflammatory bowel disease and risk of mortality in COPD.* Eur Respir J, 2016. **47**(5): p. 1357-64.

3. Raftery, A.L., et al., *Links Between Inflammatory Bowel Disease and Chronic Obstructive Pulmonary Disease.* Front Immunol, 2020. **11**: p. 2144.

4. Yoshida, M., et al., *Involvement of cigarette smoke-induced epithelial cell ferroptosis in COPD pathogenesis.* Nat Commun, 2019. **10**(1): p. 3145.

5. Berkowitz, L., et al., *Impact of Cigarette Smoking on the Gastrointestinal Tract Inflammation: Opposing Effects in Crohn's Disease and Ulcerative Colitis.* Front Immunol, 2018. **9**: p. 74.

6. Wang, L., et al., *Changes in intestinal homeostasis and immunity in a cigarette smoke- and LPS-induced murine model for COPD: the lung-gut axis.* Am J Physiol Lung Cell Mol Physiol, 2022. **323**(3): p. L266-L280.

7. Gokulan, K., et al., *Lung microbiome, gut-lung axis and chronic obstructive pulmonary disease.* Curr Opin Pulm Med, 2022. **28**(2): p. 134-138.

8. Wiertsema, S.P., et al., *The Interplay between the Gut Microbiome and the Immune System in the Context of Infectious Diseases throughout Life and the Role of Nutrition in Optimizing Treatment Strategies.* Nutrients, 2021. **13**(3).

9. Georgiou, N.A., J. Garssen, and R.F. Witkamp, *Pharma-nutrition interface: the gap is narrowing.* Eur J Pharmacol, 2011. **651**(1-3): p. 1-8.

10. Xiong, Y., et al., *Transcriptomic characteristics of bronchoalveolar lavage fluid and peripheral blood mononuclear cells in COVID-19 patients.* Emerg Microbes Infect, 2020. **9**(1): p. 761-770.

11. De Smet, E.G., et al., *The role of miR-155 in cigarette smoke-induced pulmonary inflammation and COPD.* Mucosal Immunol, 2020. **13**(3): p. 423-436.

12. Budden, K.F., et al., *Emerging pathogenic links between microbiota and the gut-lung axis.* Nat Rev Microbiol, 2017. **15**(1): p. 55-63.

13. Brassard, P., et al., *Increased incidence of inflammatory bowel disease in Quebec residents with airway diseases.* Eur Respir J, 2015. **45**(4): p. 962-8.

14. Papoutsopoulou, S., et al., *Review article: impact of cigarette smoking on intestinal inflammation-direct and indirect mechanisms.* Aliment Pharmacol Ther, 2020. **51**(12): p. 1268-1285.

15. Obeidat, M., et al., *The Overlap of Lung Tissue Transcriptome of Smoke Exposed Mice with Human Smoking and COPD.* Sci Rep, 2018. **8**(1): p. 11881.

16. Churg, A., S. Zhou, and J.L. Wright, *Series "matrix metalloproteinases in lung health and disease": Matrix metalloproteinases in COPD.* Eur Respir J, 2012. **39**(1): p. 197-209.

17. Zhang, X.J., et al., *GPNMB contributes to a vicious circle for chronic obstructive pulmonary disease.* Biosci Rep, 2020. **40**(6).

18. Golovatch, P., et al., *Role for cathepsin K in emphysema in smoke-exposed guinea pigs.* Exp Lung Res, 2009. **35**(8): p. 631-45.

19. Hu, G., et al., *Vitamin D3-vitamin D receptor axis suppresses pulmonary emphysema by maintaining alveolar macrophage homeostasis and function.* EBioMedicine, 2019. **45**: p. 563-577.

20. Shan, M., et al., *Cigarette smoke induction of osteopontin (SPP1) mediates T(H)17 inflammation in human and experimental emphysema.* Sci Transl Med, 2012. **4**(117): p. 117ra9.

21. Miao, T.W., et al., *High expression of SPP1 in patients with chronic obstructive pulmonary disease (COPD) is correlated with increased risk of lung cancer.* FEBS Open Bio, 2021. **11**(4): p. 1237-1249.

22. Gao, H.X., et al., *MiR-34c-5p plays a protective role in chronic obstructive pulmonary disease via targeting CCL22.* Exp Lung Res, 2019. **45**(1-2): p. 1-12.

23. Marjanovic, N., et al., *Macrolide antibiotics broadly and distinctively inhibit cytokine and chemokine production by COPD sputum cells in vitro.* Pharmacol Res, 2011. **63**(5): p. 389-97.

24. Frankenberger, M., et al., *Chemokine expression by small sputum macrophages in COPD.* Mol Med, 2011. **17**(7-8): p. 762-70.

25. Almansa, R., et al., *Critical COPD respiratory illness is linked to increased transcriptomic activity of neutrophil proteases genes.* BMC Res Notes, 2012. **5**: p. 401.

26. Esteve-Codina, A., et al., *Gender specific airway gene expression in COPD sub-phenotypes supports a role of mitochondria and of different types of leukocytes.* Sci Rep, 2021. **11**(1): p. 12848.

27. Pelgrim, C.E., et al., *Increased exploration and hyperlocomotion in a cigarette smoke and LPS induced murine model of COPD: linking pulmonary and systemic inflammation with the brain.* Am J Physiol Lung Cell Mol Physiol, 2022. **323**(3): p. L251-L265.

28. Ochsenkuhn, T., et al., *Crohn disease of the small bowel proximal to the terminal ileum: detection by MR-enteroclysis.* Scand J Gastroenterol, 2004. **39**(10): p. 953-60.

29. Berkowitz, L., et al., *Mucosal Exposure to Cigarette Components Induces Intestinal Inflammation and Alters Antimicrobial Response in Mice.* Front Immunol, 2019. **10**: p. 2289.

30. Castro-Dopico, T., J.F. Colombel, and S. Mehandru, *Targeting B cells for inflammatory bowel disease treatment: back to the future.* Curr Opin Pharmacol, 2020. **55**: p. 90-98.

31. Wouters, E.F., E.C. Creutzberg, and A.M. Schols, *Systemic effects in COPD.* Chest, 2002. **121**(5 Suppl): p. 127S-130S.

32. Barnes, P.J., *The cytokine network in chronic obstructive pulmonary disease.* Am J Respir Cell Mol Biol, 2009. **41**(6): p. 631-8.

33. Yamamoto-Furusho, J.K., *Inflammatory bowel disease therapy: blockade of cytokines and cytokine signaling pathways.* Curr Opin Gastroenterol, 2018. **34**(4): p. 187-193.

34. Vanderslice, P., et al., *Development of cell adhesion molecule antagonists as therapeutics for asthma and COPD.* Pulm Pharmacol Ther, 2004. **17**(1): p. 1-10.

35. Niu, W., et al., *IL-21/IL-21R Signaling Aggravated Respiratory Inflammation Induced by Intracellular Bacteria through Regulation of CD4(+) T Cell Subset Responses.* J Immunol, 2021. **206**(7): p. 1586-1596.

36. Wang, Y., et al., *IL-21/IL-21R signaling suppresses intestinal inflammation induced by DSS through regulation of Th responses in lamina propria in mice.* Sci Rep, 2016. **6**: p. 31881.

37. Cornwell, W.D., et al., *Pathogenesis of inflammation and repair in advanced COPD.* Semin Respir Crit Care Med, 2010. **31**(3): p. 257-66.

38. Duan, M., et al., *IL-21 is increased in peripheral blood of emphysema mice and promotes Th1/Tc1 cell generation in vitro.* Inflammation, 2014. **37**(3): p. 745-55.

39. Wang, L., et al., *SUL-151 Decreases Airway Neutrophilia as a Prophylactic and Therapeutic Treatment in Mice after Cigarette Smoke Exposure.* Int J Mol Sci, 2021. **22**(9).

40. Roda, M.A., et al., *Proline-Glycine-Proline Peptides Are Critical in the Development of Smoke-induced Emphysema.* Am J Respir Cell Mol Biol, 2019. **61**(5): p. 560-566.

41. Eldridge, A., et al., *Variation in tobacco and mainstream smoke toxicant yields from selected commercial cigarette products.* Regul Toxicol Pharmacol, 2015. **71**(3): p. 409-27.

4

Supplementary data

Supplementary Figure 1. Differential changes in transcriptome of proximal small intestinal tissue of cigarette smoke-exposed mice. Mice were exposed to the air or cigarette smoke for around 10 weeks and RNA-sequence analysis were performed for the proximal small tissue. Number of significantly up-regulated and down-regulated differentially expressed genes (A), volcano plots from differential expressed genes (B) were depicted. Red represents the up-regulated genes and green represents down-regulated genes. KEGG pathway analysis of differentially expressed genes enrichment in the cigarette smoke exposure treated proximal small tissue was shown in the dotplot (C). The counts represent the number of differentially expressed genes enriched in the particular pathway, the colors represent the padj values based on the scale bar. Heatmap depicting the expression levels of genes enriched in the cytokine-cytokine receptor interaction pathway (D) were demonstrated. N=3 mice/group.

The non-significantly altered top 15 genes from cigarette smoke-exposed murine lung observed in COPD patients

The transcriptomic profiling in murine lung tissue followed 10 weeks of cigarette smoke exposure was compared with the transcriptomic changes in human lungs of COPD patients. Gene expression levels of the top 15 most significantly regulated genes observed in murine lungs , which were not significantly changed in COPD patients compared to healthy individuals are depicted in Supplementary Figure 2. Genes, including *CD177, LCN2, SLC6A20, CYP1A1* and *MSR1* in COPD patients (Supplementary Figure 2A-2E).
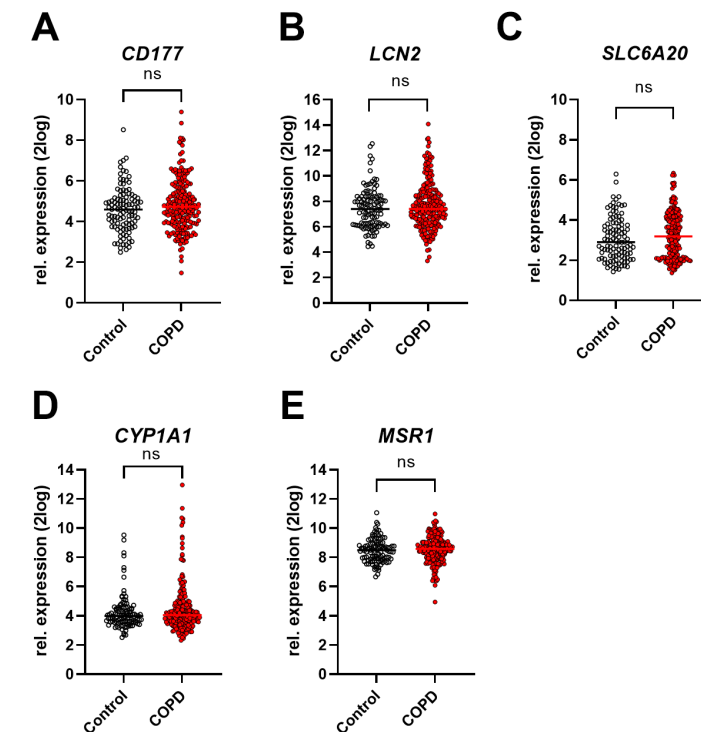
Supplementary Figure 2. The non-significantly altered top 15 genes from cigarette smoke-exposed murine lung observed in COPD patients. The top 15 most significantly up- or down-regulated genes in murine lungs, which were not significantly changed in COPD patients are depicted. *CD177* (A), *LCN2* (B), *SLC6A20* (C), *CYP1A1* (D), *MSR1* (E) gene expression levels from COPD patients were compared to healthy individuals, N=220 for COPD patients, N=108 for healthy individuals.

The non-significantly altered top 15 genes from ileum of cigarette smoke-exposed mice observed in CD patients

The transcriptomic profiling in ileum followed 10 weeks of cigarette smoke exposure was compared with the transcriptomic changes in ileum of CD patients. Gene expression levels of the top 15 most significantly altered genes observed in murine ileum, which were not significantly changed in CD patients were depicted in Supplementary Figure 3A-3E. Genes, including *CD79A, MEG3, CORO1A, TNFRSF13C* and *CCR7* did not show significant changes between CD patients and healthy individuals (Supplementary Figure 3A-3E). Genes, including *CD79A, MEG3, CORO1A* and *TNFRSF13C* did not show significant differences between CD active, CD inactive and healthy individuals (Supplementary Figure 3F-3I), however, *CCR7* was differently expressed between CD active and CD inactive patients.
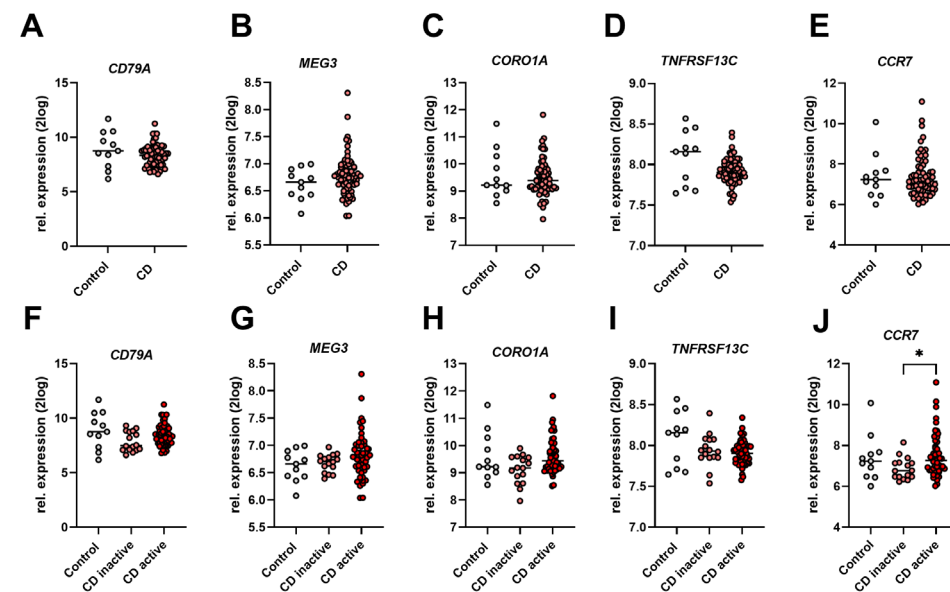
Supplementary Figure 3. The non-significantly altered top 15 genes from ileum of cigarette smoke-exposed mice observed in CD patients. The top 15 most significantly up- or down-regulated genes in murine ileum but were not significantly changed in CD patients are determined. *CD79A* (A), *MEG3* (B), *CORO1A* (C), *TNFRSF13C* (D) and *CCR7* (E) gene expression levels from CD patients were compared to healthy individuals. *CD79A* (F), *MEG3* (G), *CORO1A* (H) and *TNFRSF13C* (I) and *CCR7* (J) gene expression levels from CD active, CD inactive were compared with healthy individuals. N=67 for CD patients (N=16 for inactive CD and N=51 for active CD patients), N=11 for healthy individuals.

Chapter 5

Effects of Cigarette Smoke on Adipose
and Skeletal Muscle Tissue:
In Vivo and In Vitro Studies

Lei Wang [1], Lieke E. J. van Iersel [2], Charlotte E. Pelgrim [1], Jingyi Lu [1], Ingrid van Ark [1],
Thea Leusink-Muis [1], Harry R. Gosker [2], Ramon C. J. Langen [2], Annemie M. W. J. Schols [2],
Josep M. Argilés [4], Ardy van Helvoort [2,3], Aletta D. Kraneveld [1], Johan Garssen [1,3],
Paul A. J. Henricks [1], Gert Folkerts [1], and Saskia Braber [1,*]

[1] Division of Pharmacology, Utrecht Institute for Pharmaceutical Sciences, Faculty of Science, Utrecht University,
3584CG Utrecht, The Netherlands
[2] Department of Respiratory Medicine, NUTRIM School of Nutrition and Translational Research in Metabolism,
Maastricht University Medical Centre +, 6200 MD Maastricht, The Netherlands
[3] Danone Nutricia Research, 3584 CT Utrecht, The Netherlands
[4] Biochemistry and Molecular Biology of Cancer, Faculty of Biology, University of Barcelona, 08007 Barcelona, Spain

Abstract

Objective
Chronic obstructive pulmonary disease (COPD) is a chronic lung disease often caused by smoking with systemic manifestations, including metabolic comorbidities involving alterations in adipose and skeletal muscle tissue. This study investigates adaptive and pathological alterations in adipose and skeletal muscle following cigarette smoke exposure using *in vivo* and *in vitro* models.

Methods
Mice were exposed to cigarette smoke or air for 72 days. In adipose tissue, morphology and inflammation were determined and for skeletal muscle, muscle weight, muscle function (fore-limb grip strength), mitochondrial and protein turnover were measured. In addition, 3T3-L1 pre-adipocytes were exposed to cigarette smoke to further understand the direct effect on lipolysis.

Results
Cigarette smoke exposure decreased body weight, and the proportional loss in fat mass was more pronounced than the loss in lean mass. Fat mass correlated positively with serum leptin levels. Cigarette smoke exposure reduced adipocyte size and increased adipocyte numbers in adipose tissue. Adipose macrophage numbers and associated cytokine levels, including interleukin-1β, interleukine-6 and tumor necrosis factor-α were elevated in smoke-exposed mice. Muscle strength was decreased after cigarette smoke exposure, however, muscle mass was not different except for reduced muscle protein synthesis signaling, no significant changes in protein breakdown and mitochondrial turnover markers. *In vitro* studies demonstrated that lipolysis and fatty acid oxidation were upregulated in cigarette smoke-exposed pre-adipocytes.

Conclusions
Cigarette smoke exposure induces loss of whole-body fat mass and adipose atrophy which is likely due to enhanced lipolysis. It remains to be elucidated whether adipose tissue loss and parallel deterioration of skeletal muscle function precede muscle wasting.

Keywords
COPD; Cigarette smoke; Cachexia; Adipose tissue; Lipolysis, Skeletal muscle

Introduction

Chronic obstructive pulmonary disease (COPD) is a leading cause of death worldwide and smoking is by far its most important risk factor [1]. COPD is a chronic and complex systemic disease which can lead to manifestations beyond the lungs with systemic interactions over time [2]. Cachexia is a wasting syndrome commonly observed in a subgroup of COPD patients, which is characterized by progressive unintended weight loss (including both fat mass and skeletal muscle mass), causing further detrimental effects on disease progression and strongly associated with mortality [3, 4]. The extent of emphysema in COPD patients is correlated with weight loss and fat loss [5]. Generally, the loss of fat mass observed during cachexia is not related to a loss of fat cells, but a decrease in cellular lipid content [6]. Enhanced lipid metabolism and triglyceride hydrolysis are the major metabolic pathways involved in the initiation and progression of cancer cachexia [7]. Lipolysis is a metabolic process through which triacylglycerol (TAGs) breaks down via hydrolysis into glycerol and free fatty acids (FFAs). These fatty acids are utilized throughout the body for heat and energy supply [8]. Lipases participating in lipolysis can play an essential role in the development of cancer-associated cachexia by breaking down the stored fat during lipolysis [7]. These processes may also be affected in patients with COPD. Adipose tissue is an important systemic organ in modulating a range of local and systemic metabolic and inflammatory pathways by the release of different bioactive factors, including cytokines, adipokines and hormones [9], which may contribute to respiratory disease progression [10]. Adipose tissue undergoes tissue remodeling, leading to enhanced lipolysis and the secretion of certain inflammatory cytokines, contributing to systemic inflammation [11]. Skeletal muscle wasting is one of the core symptoms of cachexia [12]; however, it is suggested that adipose tissue wasting probably occurs before the appearance of the reduction in lean mass [6, 11]. The spill-over of systemic inflammation by the adipose tissue may be one of the underlying mechanisms involved in the depletion of skeletal muscle mass [13]. Reduced skeletal muscle mass is present in 4% up to 39% of patients with COPD [14], which is the consequence of an imbalance between processes of muscle protein synthesis and breakdown [15]. Moreover, it has been reported that mitochondrial quality control is dysregulated in cancer cachexia in tumor-bearing mice prior to skeletal muscle atrophy, showing an enhanced activity of the ubiquitin-proteasome pathway [16]. In patients with COPD, it is well-established that resting metabolic rate may be elevated, contributing to a disturbed whole body energy balance that ultimately causes weight loss [17], but abnormalities in adipose tissue and the effects of cigarette smoke on lipolysis are relatively unexplored. Furthermore, it is unclear whether disturbances in adipose tissue metabolism are intertwined with altered muscle maintenance regulation or could be a putative driver of skeletal muscle catabolism. Therefore, in this manuscript, the effect of cigarette smoke exposure on adipose and muscle tissue *in vivo* using a murine model of COPD was investigated. In addition, 3T3-L1 preadipocytes were exposed to cigarette smoke total particulate matter (TPM) to further understand the direct effects of cigarette smoke exposure on lipid metabolism in vitro.

Results

COPD-related characteristics, body composition, food Intake, leptin and cytokine levels in serum

The mean linear intercept (Lm), a measure of interalveolar wall distance representing lung tissue damage, and the BAL fluid cell numbers (macrophages, neutrophils and lymphocytes) and cytokines were significantly increased after cigarette smoke exposure as compared to the air-exposed group [18, 19]. These findings confirm that cigarette smoke exposure induced COPD-related characteristics.

The average body weight between the groups did not differ before starting the exposures. The body weight gain (from day 1 to day 72) in the cigarette smoke-exposed mice was significantly lower compared to the air-exposed animals (Figure 1A). At the endpoint (day 72), the echo MRI showed a lower body weight in cigarette smoke-exposed mice (Figure 1B). The difference in body weight between the groups could be explained by a proportional loss in lean mass of 4.9%, as well as fat mass of 43.8% (Figure 1B). Cigarette smoke exposure significantly decreased serum leptin levels [19], and the leptin levels were positively correlated with fat mass (Figure 1C). Food intake data were collected from day 7 and recorded weekly; smoke exposure clearly affected the appetite of the mice, as demonstrated by a lower food intake (Figure 1D). The area under the curve (AUC) for food intake in the cigarette smoke-exposed mice was decreased as compared to air-exposed mice (Figure 1E). KC levels were measured in the serum, which were increased after exposure to the cigarette smoke [18], and KC levels were negatively correlated with the fat mass (Figure 1F).

Histomorphological changes in adipose tissue

To investigate the morphological changes in adipose tissue, two different types of white adipose tissue (para-ovary and inguinal adipose tissue) were isolated and stained with H&E. Representative histological pictures of para-ovary adipose (Figure 2A,B) and inguinal adipose tissue (Figure 2C,D) of air- (Figure 2A,C) and cigarette smoke-exposed mice (Figure 2B,D) are depicted. Cigarette smoke exposure significantly increased the number (Figure 2E,G) and decreased the size of adipocytes (Figure 2F,H) in both para-ovary and inguinal adipose tissues.
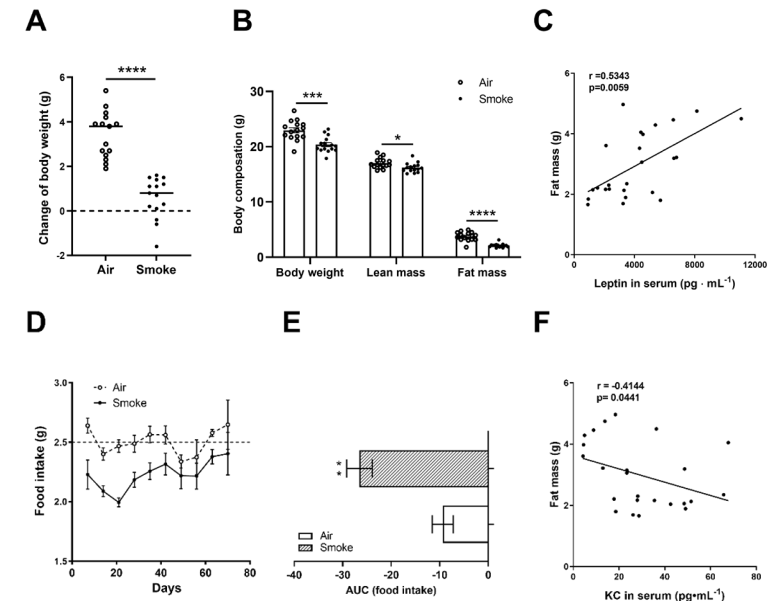

Figure 1. Body composition, food intake, leptin and cytokine levels in serum. Body weight changes (from day 1 to day 72) (A) and body composition at the endpoint (body weight, lean mass and fat mass) (B) were quantified. Correlations between fat mass and leptin levels in serum (C) were analyzed using Spearman correlation. Food intake was recorded every week (D) and the area under the curve of food intake (E) was analyzed. Correlation between fat mass and KC levels (F) were analyzed using Spearman's correlation. N = 12—16 mice/group. Values are represented as mean ± SEM. * $p < 0.05$, ** $p < 0.01$, *** $p < 0.001$, **** $p < 0.0001$; smoke group compared with air group.
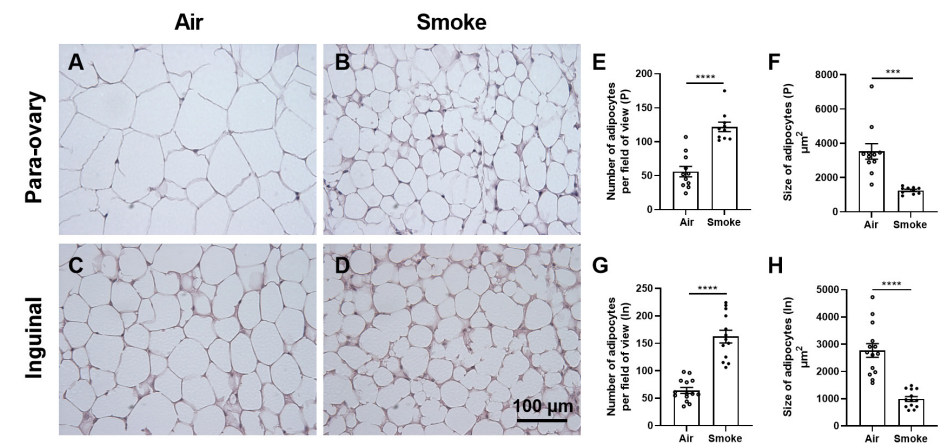
Figure 2. Histomorphological changes in adipose tissue. Para-ovary (A, B) and inguinal (C, D) white adipose tissues were collected and stained with H&E (scale bar = 100 μm). The number (E) and size (F) of adipocytes of para-ovary white adipose tissue, and the number (G) and size (H) of adipocytes of inguinal white adipose tissue were determined by ImageJ. Values are expressed as mean ± SEM. *** $p < 0.001$, **** $p < 0.0001$, smoke group compared with air group; N = 10—14 mice/group.

Macrophages and pro-inflammatory cytokines in adipose tissue

To investigate the inflammatory response induced by cigarette smoke exposure in adipose tissue, macrophage infiltration (staining with anti-CD68 antibodies) and pro-inflammatory cytokine (IL-1β, TNF-α and IL-6) concentrations were measured in both para-ovary and inguinal white adipose tissues. Representative pictures of CD68-positive macrophages are depicted in Figure 3A, while pictures of the isotype control and negative control are depicted in Supplementary Figure 4. The number of CD68-positive cells is significantly increased in cigarette smoke-exposed mice (Figure 3B,F). Cigarette smoke exposure significantly increased the level of IL-1β, TNF-α and IL-6 (Figure 3C,D,E) in para-ovary adipose tissue. No significant differences in IL-1β, TNF-α and IL-6 levels were observed in inguinal adipose tissue (Figure 3G,H,I).

Muscle function, muscle weight, mitochondrial and protein turnover markers in soleus muscle

Grip strength was measured after the last time of cigarette smoke exposure to determine the muscle function. Cigarette smoke exposure significantly decreased the average and maximum grip strength (Figure 4A, B). Smoke exposure tends to decrease the weight of the tibialis ($p = 0.0617$, Figure 4C). No significant differences were observed in the weight of EDL, soleus and gastrocnemius (Figure 4D,E,F). The effect of cigarette smoke exposure on protein turnover signaling in the soleus muscle was investigated, including the protein levels of total ribosomal protein S6 (S6), phosphorylated S6 (pS6), total initiation factor 4E binding protein 1 (4EBP1) and p4EBP1. 4EBP1 phosphorylation (Figure 4J—L) was significantly reduced in the cigarette smoke-exposed group. In addition, the trend of reduced S6 phosphorylation (Figure 4G—I) was also observed in the smoke-exposed group. This indicated an attenuated protein synthesis signaling in the muscle of cigarette smoke-exposed mice. Furthermore, smoke exposure did not result in consistent and significant alterations in the mRNA levels of molecular markers involved in protein degradation, including the mRNA levels of myostatin (Mstn), Atrogin-1, f-box protein 21 (SMART), forkhead box O1 (FoxO1), DNA-damage-inducible transcript 4 (REDD1), and Neural precursor cell expressed, developmentally down-regulated 4 (NEDD4) (Figure 4M-4O, 4Q-4S) and protein levels of the ratio LC3BII/LC3BI (Figure 4T). Only the mRNA levels of Muscle Ring Finger protein 1 (MuRF-1) showed a significant decrease after smoke exposure (Figure 4P). Original blots are depicted in Supplementary Figure 3. Furthermore, to investigate whether loss of muscle oxidative capacity was evident as it has been suggested to precede skeletal muscle atrophy, the molecular markers of mitochondrial biogenesis and content were measured in the soleus. Nuclear respiratory factor 1 (Nrf1) decreased significantly after smoke exposure compared to air control, and key regulator of biogenesis peroxisome proliferator-activated receptor-gamma coactivator 1-alpha (PGC-1α) tended to decrease after smoke exposure ($p = 0.056$). Further, no significant alterations were observed for mitochondrial biogenesis and oxidative phosphorylation complexes (Supplementary Figure 5).
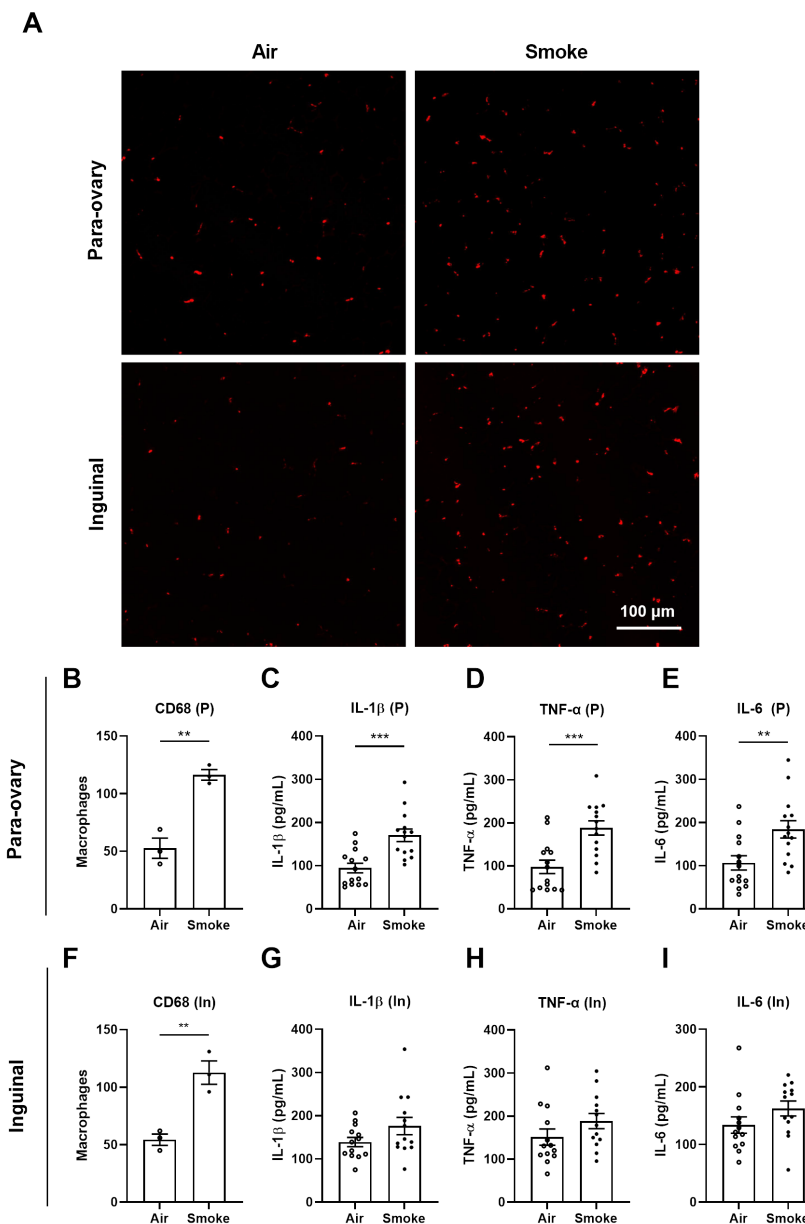

Figure 3. Macrophages and pro-inflammatory cytokines in adipose tissue. The presence of macrophages in para-ovary and inguinal adipose tissues was investigated by immunofluorescence microscopy using anti-CD68 antibodies (**A**) (scale bar = 100 μm). The macrophages numbers of CD68 staining for para-ovary (**B**) and inguinal (**F**) adipose tissue were counted. N = 3 for each group. The levels of IL-1β (**C**), TNF-α (**D**) and IL-6 (**E**) in para-ovary adipose tissue homogenates and the levels of IL-1β (**G**), TNF-α (**H**) and IL-6 (**I**) in inguinal adipose tissue homogenates were determined by ELISA. Values are expressed as mean ± SEM. ** $p < 0.01$, *** $p < 0.001$, smoke group compared with air group; N = 13-14 mice/group were used for ELISA.
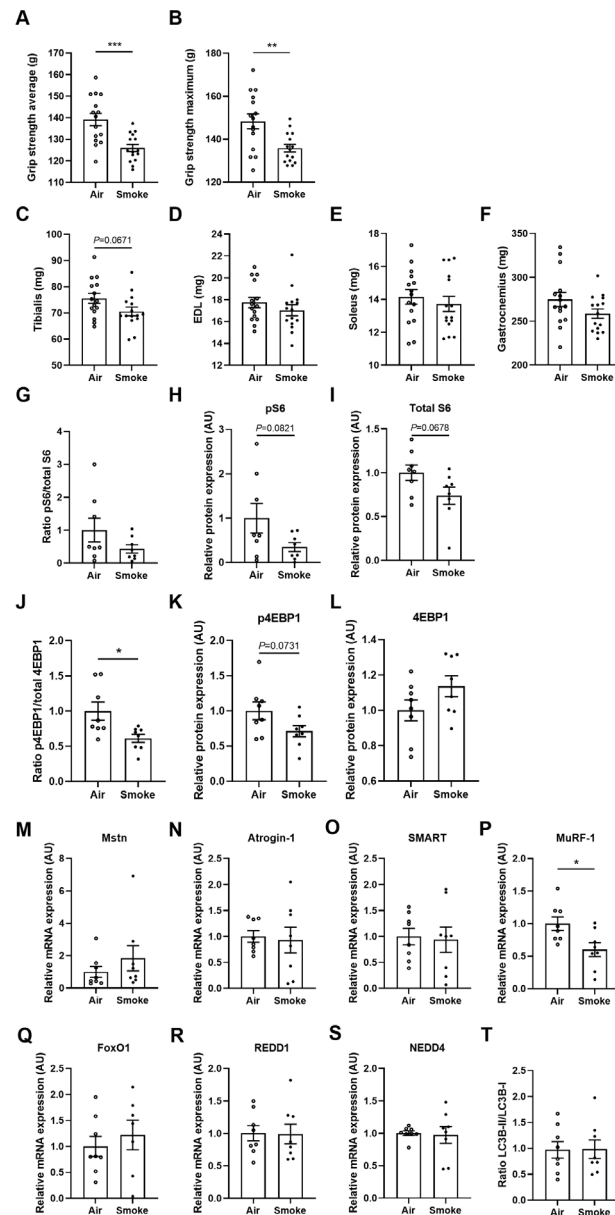
Figure 4. Muscle function, muscle weight, mitochondrial and protein turnover markers in soleus muscle. Grip strength was determined at day 72 and represented as the average values (**A**) and maximum values (**B**) of five measurements per mouse. Paired muscle weights of tibialis (**C**), EDL (**D**), soleus (**E**) and gastrocnemius (**F**) were determined. N = 15—16 mice/group. Protein expression of ratio pS6/total S6 (**G**), pS6 (**H**) S6 (**I**), ratio p4EBP1/total 4EBP1 (**J**), p4EBP1 (**K**), 4EBP1 (**L**) and ratio LC3BII/LC3BI was analyzed by Western blot (T). Gene expression levels of Mstn (**M**), Atrogin-1 (**N**), SMART (**O**), MuRF-1 (**P**), FoxO1 (**Q**) REDD1 (**R**) and NEDD4 (**S**) were assessed, normalized to GeNorm and expressed as fold change compared to control, N = 8 mice/group. Values are represented as mean ±SEM. * $p < 0.05$, ** $p < 0.01$, *** $p < 0.001$; smoke group compared with air group.

Lipid accumulation and leptin levels in 3T3-L1 pre-adipocytes

Based on the obvious fat mass decrease after cigarette smoke exposure in mice, 3T3-L1 pre-adipocytes were exposed to cigarette smoke TPM to further understand the effect of cigarette smoke exposure on lipid metabolism. Concentrations of TPM were determined by cell viability assay and used in the following experiment (Supplementary Figure 6).

The different TPM concentrations were administered to the 3T3-L1 pre-adipocytes during the differentiation process (day 0 until day 8) (see also Figures S1 and S7 for more details). The cells were stained with a mixture of Nile red (intracellular lipid droplets) and Hoechst (nuclei) at day 8. Representative images are depicted in Figure 5A, and the fluorescent intensity of the red dye was quantified (Figure 5B). The percentage of lipid droplets was increased after the addition of 12.5 μg/mL of TPM compared to 6.25 μg/mL of TPM, but not to the control. The higher concentration of 25 μg/mL of TPM did not induce a significant effect on the percentage of lipid droplets compared to the control (Figure 5B). Leptin mRNA expression levels were analyzed. Although 6.25 μg/mL of TPM did not significantly affect the leptin mRNA levels, TPM (12.5 μg/mL) significantly increased the mRNA expression of leptin compared to the control cells, and this increase was significantly decreased by increasing the TMP concentration to 25 μg/mL (Figure 5C).

Lipolysis and fatty acid oxidation in 3T3-L1 adipocyte

Lipolysis is an important step in lipid metabolism that regulates lipid mobilization. Glycerol as the final lipolysis product was determined. The concentrations of 12.5 and 25 μg/mL of TPM significantly increased the glycerol production compared to the control cells (Figure 6A). The increased glycerol release was supported by the mRNA expression of aquaporin 7 (Aqp7), the water-selective membrane channel responsible for glycerol efflux, which was also significantly increased by 12.5 and 25 μg/mL of TPM as compared to the control cells (Figure 6E). Furthermore, the mRNA expression of the enzymes involved in the lipolysis was increased by TPM exposure: 25 μg/mL of TPM tended to increase the mRNA expression of adipose triglyceride lipase (ATGL) (p = 0.0672, Figure 6B), and 12.5 and 25 μg/mL of TPM significantly upregulated the mRNA expression of hormone-sensitive lipase (HSL) (Figure 6C) and monoglyceride lipase (MGLL) compared to the control cells (Figure 6D). The mRNA expression level of perilipin 1 (Plin 1), a lipid droplet-associated protein that is required for the translocation of HSL from the cytosol to lipid droplets upon stimulation [20], was significantly upregulated by 12.5 and 25 μg/mL of TPM compared to the control cells (Figure 6F). Since HSL, a hormone-sensitive lipase, is crucial for the rate-limiting step in lipolysis, the protein level of HSL and the phosphorylation of HSL were also determined (Figure 6G and Supplementary Figure 8). TPM at 12.5 and 25 μg/mL significantly increased the HSL protein expression, and 25 μg/mL of TPM increased phosphorylated HSL compared to the control cells.
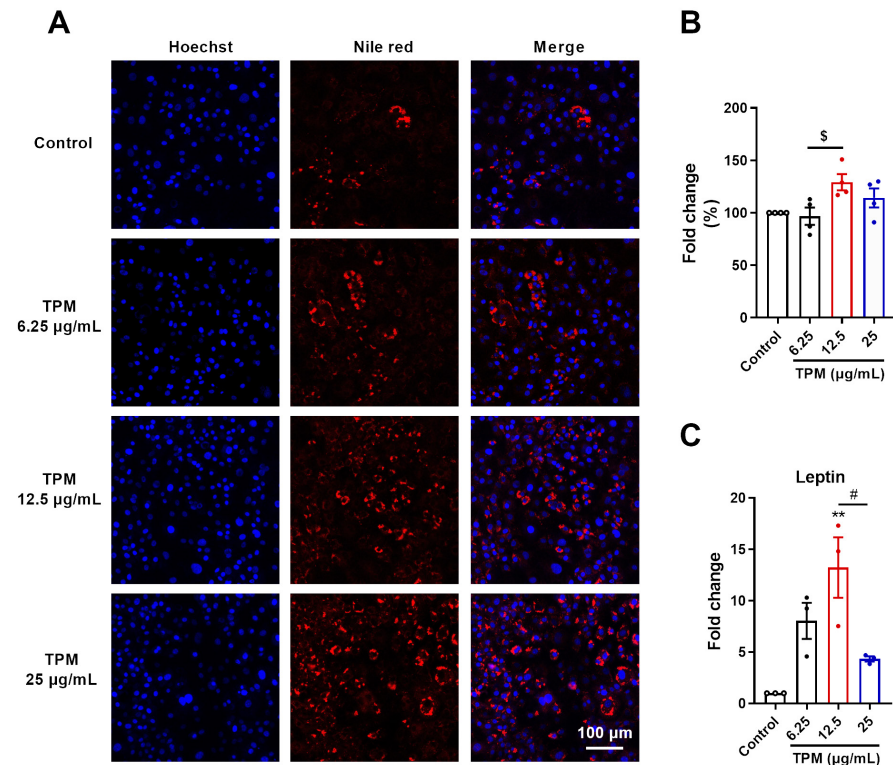
Figure 5. Lipid accumulation and leptin levels in 3T3-L1 pre-adipocytes. Different TPM concentrations (6.25, 12.5 and 25 μg/mL) were added to the 3T3-L1 pre-adipocytes during the differentiation process of 8 days. Nuclei and lipid droplets were stained with Hoechst and Nile red dye, respectively (**A**). Nile red fluorescent intensity was read and quantified (**B**), N = 4 replicates. mRNA expression levels of leptin were evaluated (**C**), N = 3 replicates. Values are expressed as mean ± SEM. ** $p < 0.01$, compared with control group; \$ $p < 0.05$, compared with 6.25 μg/mL of TPM group; # $p < 0.05$, compared with 12.5 μg/mL of TPM group.

To further understand the effects of TPM on lipid metabolism, FFAs, another product liberated from lipolysis, were measured in the supernatant. Interestingly, no significant changes were found in FFA release after exposure to increasing concentrations of TPM (Figure 6H). The utilization of FFAs in mitochondria (fatty acid oxidation) was also determined. Acyl-CoA synthetase long chain family member 1 (ACSL1) is known to convert free long-chain fatty acids into fatty acyl-CoA esters, and thereby play a key role in lipid biosynthesis, as well as in fatty acid transport and degradation [26]. The mRNA expression levels of ACSL1 were elevated in 12.5 μg/mL and 25 μg/mL of TPM-exposed groups (Figure 6I). PGC-1α is associated with mitochondrial oxidative capacity, and PGC-1α mRNA levels were elevated in the 25 μg/mL of TPM group (Figure 6J). ATP production as the result of FFAs utilization for energy production was measured in the cells. TPM concentration dependently increased the ATP production, and 25 μg/mL of TPM had the most obvious effect on ATP production

(Figure 6K). To further support these results, RNA-sequence analysis was performed, and the data showed that genes involved in mitochondrial oxidative phosphorylation were highly enriched after exposure to cigarette smoke. Mitochondrial respiratory complexes I, II, III, and IV were highly expressed in the mitochondrial oxidative phosphorylation pathway (Fold change >2, Supplementary Figure 10).
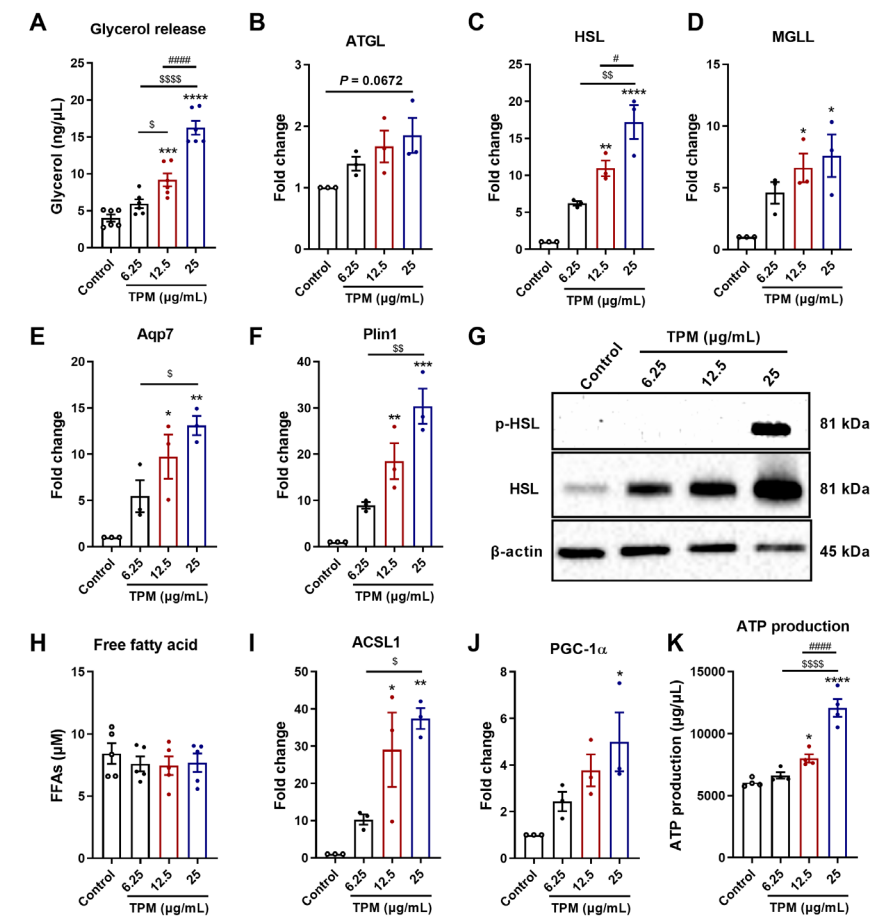

Figure 6. Lipolysis and fatty acid oxidation in 3T3-L1 adipocytes. Different TPM concentrations (6.25, 12.5 and 25 μg/mL) were added to the 3T3-L1 pre-adipocytes during the differentiation process of 8 days. Glycerol release (**A**) was determined in the supernatants (N = 6 replicates) and mRNA expression of ATGL (**B**), HSL (**C**), MGLL (**D**), Aqp7 (**E**), Plin1 (**F**), ACSL1 (**I**) and PGC-1α (**J**) were determined by qRT-PCR; the data were normalized to β-actin and were calculated relative to control (N = 3 replicates). FFAs (**H**) were determined in the supernatants (N = 5 replicates) and ATP production (**K**) was measured in the cell lysates (N = 4 replicates). Protein expression levels of HSL, phosphorylated HSL (phosphor-HSL) and β-actin (**G**) were analyzed by Western blot. Values are expressed as mean ± SEM, * $p < 0.05$, ** $p < 0.01$, *** $p < 0.001$ and **** $p < 0.0001$ compared with control group; \$ $p < 0.05$, \$\$ $p < 0.01$ and \$\$\$\$ p < 0.0001 compared with 6.25 μg/mL of TPM group; # $p < 0.05$ and #### $p < 0.0001$ compared with 12.5 μg/mL of TPM group.

Discussion

About 25% of patients with COPD will develop cachexia [17], which is associated with excessive mortality [21]. Cachexia is a syndrome characterized by an involuntary loss of body weight. Although muscle wasting is the main clinical manifestation observed in cachexia, recent studies show that fat loss occurs more rapidly and more precociously than the decrease in lean mass in cancer cachexia [11].

Information about the effect of cigarette smoke exposure on adipose tissue, as well as the important role of adipose tissue in the interrelationship with muscle maintenance is scarce. Therefore, in this study, a murine cigarette smoke-induced COPD model was used to investigate the effects of cigarette smoke exposure on body composition (body weight, fat mass, lean mass), adipose tissue morphology and inflammation, as well as on muscle function and muscle mitochondrial and protein turnover markers. In addition, 3T3-L1 pre-adipocytes were exposed to TPM from cigarette smoke to further understand the effect of cigarette smoke exposure on lipid metabolism (lipolysis).

In the *in vivo* study, COPD-like characteristics, including enlarged alveolar diameters and increased inflammatory cells in the lung [19], were observed, as well as a decreased body weight gain, which was detected after smoke exposure. It is recognized that weight and fat mass loss is common in many COPD patients, which is correlated with the extent of emphysema [5, 22], whereas COPD patients with a more chronic bronchitis phenotype are more likely to gain weight [23]. In this present study, a cigarette smoke-induced decrease in lean mass and fat mass was found. The drop in fat mass was relatively more obvious than the drop in lean mass. A decrease in food intake was also found in the cigarette smoke-exposed group. A possible explanation might be that nicotine is a strong signal that suppresses appetite and decreases food intake, leading to reduced body weight [24].

Adipose (fat) tissue is the main source for producing leptin, which is involved in energy homeostasis and controls body weight via the regulation of appetite and energy expenditure [25, 26]. Decreased serum leptin levels and decreased body weight are commonly found in many COPD patients [27]. Circulating leptin levels were found independent of the TNF-α system, and they were regulated physiologically even in the presence of cachexia in patients with COPD [28]. In this study, KC levels were negatively correlated with fat mass, indicating a link between systemic inflammation and fat mass loss. Leptin exerts multiple effects on the respiratory system, as this cytokine-like hormone plays important physiological roles. Leptin has the ability to modulate inflammation, which may integrate systemic inflammation [29]; therefore, the leptin-signaling pathway might be involved in this low systemic inflammatory response [30]. Nevertheless, the low inflammatory systemic response following cigarette smoke exposure may also be related to the "spill over" of the initial, localized pulmonary

inflammatory response [18, 31], as in the current murine model, exposure to cigarette smoke significantly enhanced the levels of CRP and KC in BAL fluid as well as in serum, and a significant positive correlation between the level of KC in BAL fluid and the amount of KC in serum was observed [18].

Adipose tissue wasting also occurred in cancer cachexia patients [11]. However, information about the changes in adipose tissue in cigarette smoke-induced COPD is scarce. Adipose tissue is currently viewed as a highly dynamic endocrine organ that is involved in a wide range of metabolic and inflammatory processes [32]. Visceral (para-ovary) adipose tissue is located around the vital organs and is commonly linked to metabolic disorders, while subcutaneous (inguinal) adipose tissue is located beneath the skin and is associated with beneficial metabolic effects [33]. In this *in vivo* study, the morphology of both para-ovary and inguinal adipose tissues showed a significant decrease in the size of adipocytes and increased the number of adipocytes (atrophy) after 10 weeks of cigarette smoke exposure. Within adipose tissue, adipocytes and macrophages are the major cell types that synthesize and release a large number of different proteins involved in inflammation, immunity, lipid metabolism and homeostasis, such as inflammatory cytokines and adipokines [32]. The number of macrophages were increased in both para-ovary and inguinal white adipose tissue in cigarette smoke-exposed mice. Inflammatory cytokines produced by adipose tissue contribute to adipose depletion [34], and we observed that IL-1β, IL-6 and TNF-α levels were increased in para-ovary and inguinal adipose tissue after cigarette smoke exposure. Interestingly, the increase in IL-1β, IL-6 and TNF-α levels induced by cigarette smoke exposure was more pronounced in para-ovary adipose tissue, which might be due to a difference in blood supply or susceptibility between these two different types of adipose tissue, as para-ovary adipose tissue is a perigonadal depot and inguinal tissue is a subcutaneous depot [33].

Until now, it has remained unclear whether abnormalities in adipose tissue and thereby enhanced systemic inflammation are a putative driver of skeletal muscle impairment. In this present murine model, cigarette smoke exposure decreased the maximum and average grip strength, indicating that muscle weakness was present. Skeletal muscle dysfunction is common in many COPD patients, which represents an important comorbidity that is associated with a poor health-related quality of life and reduced survival [35]. In addition, handgrip strength is associated with functional limitation and COPD-specific symptoms, as well as with higher exacerbation frequencies [36]. The observed muscle weakness could be related to the systemic release of the pro-inflammatory cytokines and adipokines produced in the adipose tissue [37], as higher levels of systemic inflammatory mediators are associated with lower muscle strength and skeletal muscle mass over time [13]. However, it cannot be excluded that systemic factors produced by other organs may also play a role in this process.

A previous study showed that cigarette smoke exposure enhances proteolysis and inhibits protein synthesis, resulting in a depletion of muscle mass [38]. Although muscle weights were not significantly reduced in the current study, protein synthesis signaling was affected in the muscle of cigarette smoke-exposed mice, whereas other markers of protein turnover were similar in both cigarette smoke- and air-exposed mice. In the cigarette smoke-exposed animals in the current study, muscle contractile force (fore-limbs grip strength) was reduced, in support of developing a loss of muscle mass. Other than a loss of muscle mass, a loss of muscle oxidative phenotype or mitochondrial dysregulations can also be important drivers of muscle weakness. In a cancer cachexia mouse model, it has been shown that mitochondrial degeneration precedes cachectic muscle wasting in tumor-bearing mice [16]. Furthermore, 16 weeks of cigarette smoke exposure in mice increased the expression of the inflammatory cytokine TNF-α, and thereby suppressed the mRNA expression of PGC-1α, which may affect muscle function [39]. In patients with cancer-associated cachexia, dysfunctional mitochondria are associated with lower muscle strength and muscle atrophy [40]. In the current study, no obvious changes in the expression of molecular markers involved in mitochondrial biogenesis and content were observed (except Nrf1) in the muscles of cigarette smoke-exposed mice when compared to control mice. It indicates that there might be an initial (premature) decrease in oxidative phenotype regulation in the muscle, based on the decrease in Nrf1 expression and the decreased PGC-1α trend, but there were no alterations in the downstream gene expression levels of TFAM and the oxidative phosphorylation complexes. The molecular signaling alterations in the muscle may depend on the duration of cigarette smoke exposure. In this study, 10 weeks of cigarette smoke exposure clearly affected adipose tissue, but the duration might not have been long enough to induce solid changes in the molecular markers of protein turnover or oxidative phenotype in skeletal muscle tissue, as seen after longer cigarette smoke exposure times [41-43]. In future experiments, an extended period of smoke exposure may, therefore, adequately elicit chronic effects of cigarette smoke exposure on skeletal muscle that clarify whether the systemic release of the pro-inflammatory cytokines and adipokines produced by the adipose tissue affect skeletal muscle.

In order to explore the potential mechanism for the fat mass loss and adipose atrophy in the cigarette smoke-induced COPD model, an in vitro model was used in which 3T3-L1 pre-adipocytes were exposed to TPM (from cigarettes smoke). Based on the Nile red staining, 12.5 µg/mL of TPM showed increased lipid droplets when compared to the 6.25 µg/mL of TPM. However, when the concentration of TPM reached 25 µg/mL, the lipid amount in the adipocytes decreased. Leptin levels corresponded with the amount of lipid droplets in the adipocytes. TPM affected lipid metabolism; however, contrasting results were obtained between 12.5 µg/mL and 25 µg/mL of TPM exposure, which might be related to changes in the balance between lipolysis (lipid consumption) and lipogenesis (lipid accumulation). It might be suggested that the lipolysis was enhanced after adding 25 µg/mL of TPM.

Changes in adipocytes size might be mainly dependent on cellular triglyceride content [44], and the loss of adipose tissue in cancer cachexia is partly the result of increased lipolysis [45]. In addition, increased lipolysis and fat oxidation, as well as impaired lipid deposition and adipogenesis, may underlie adipose atrophy in cancer cachexia [34]. All these findings indicate that lipolysis and fatty acid oxidation might play a pivotal role in fat loss and adipose atrophy. In this current study, glycerol, the end-product of lipolysis, was concentration dependently increased by TPM, which is indicative for an increased lipolysis. Adipose ATGL, HSL and MGLL are three major enzymes acting in sequence in the hydrolysis of TAG producing FFAs and glycerol. ATGL catalyzes the initial step of TAG hydrolysis, generating diacylglycerol (DAG) and one fatty acid. HSL is rate-limiting for the second step of TAG lipolysis converting DAG to one fatty acid and monoacylglycerol (MAG); this process involves the protein kinase A-dependent phosphorylation of HSL. MGLL is the key enzyme in the hydrolysis of the endocannabinoid 2-arachidonoylglycerol and converts MAG to a free fatty acid and glycerol. Plin 1 is known as a lipid droplet-associated protein and is also associated with the lipolysis process [46]. The mRNA expression levels of ATGL, HSL, MGLL and Plin 1 were all increased after TPM exposure in 3T3-L1 pre-adipocytes, and 25 µg/mL of TPM caused the most pronounced effect on lipolysis. In addition, HSL protein levels were also enhanced after TPM exposure, and 25 µg/mL of TPM induced an increase in the expression of phosphorylated HSL. Aqp7, a water selective membrane channel functioning as a glycerol transporter, was also highly enhanced by 25 µg/mL of TPM. Taken together, the results indicate that TPM in a concentration-dependent way promoted the lipolysis in 3T3-L1 pre-adipocytes.

The majority of studies have indicated elevated lipolysis as a reason for fat loss. Consequently, increasing fatty acid oxidation can be a tentative approach to utilize surplus FFAs. By increasing fatty acid oxidation within adipose tissue, FFAs are oxidized and cannot be re-esterified into TAG [47]. In this present study, there were no significant differences in FFAs levels in the supernatants of TPM-exposed and control 3T3-L1 pre-adipocytes. However, based on the increased glycerol and lipolysis-related mRNA expressions, the current hypothesis is that the produced FFAs from lipolysis are mainly used for fatty acid oxidation and energy production. ACSL1 has a specific function in directing the metabolic partitioning of fatty acids towards β-oxidation [48], and PGC-1α is also involved in mitochondrial fat oxidation [49]. The mRNA levels of ACSL1 and PGC-1α were measured in 3T3-L1 pre-adipocytes and were both up-regulated by TPM in a concentration-dependent manner. The excess of FFAs from enhanced lipolysis are oxidized by mitochondria to produce energy [34], which might contribute to adipocyte senescence and atrophy [50]. The production of ATP was measured, and 25 µg/mL of TPM particularly enhanced the ATP production in the 3T3-L1 pre-adipocytes. At a closer look of the Kyoto Encyclopedia of Genes and Genomes (KEGG) pathway analysis (Supplementary Figure 9), a significant enrichment of genes related to lipolysis was observed after 25 µg/mL of TPM exposure to the pre-adipocytes. This supports

the hypothesis postulated in this present manuscript and the obtained results indicating that TPM exposure to the 3T3-L1 pre-adipocytes enhanced lipolysis, thus, enhancing the fatty acid oxidation, which could be the reason for the fat mass loss and adipose atrophy in the cigarette smoke-exposed mice. This finding was further confirmed by the highly expressed genes involved in mitochondrial oxidative phosphorylation, including complexes I, II, III, and IV, as detected by RNA-sequence (Supplementary Figure 10). The postulated mechanism is described in Figure 7. However, it is difficult to adequately extrapolate the present in vitro findings to the *in vivo* situation as, for example, the duration of cigarette smoke/TPM exposures was not equal.

Importantly, in this current study it was demonstrated for the first time that a relatively short period of chronic cigarette smoke exposure (± 10 weeks) *in vivo* results in adipose tissue wasting and, to a lesser extent, skeletal muscle wasting. Although whole body lean mass was decreased and skeletal muscle function was deteriorated, no significant changes were observed in skeletal muscle weight and, apart from evidence for reduced protein synthesis signaling, no profound alterations in the expression of markers for muscle protein and mitochondrial turnover were present in the cigarette smoke-induced murine model for COPD. In the in vitro study, enhanced lipolysis and fatty acid oxidation was demonstrated, which might play a role in the fat mass loss and adipose atrophy. More research is needed to elucidate whether fat mass loss and adipose tissue atrophy precedes muscle wasting and to clearly understand the interaction between adipose and muscle tissue. The presented knowledge contributes to a better understanding of the important role of adipose tissue in COPD pathogenesis and progression.
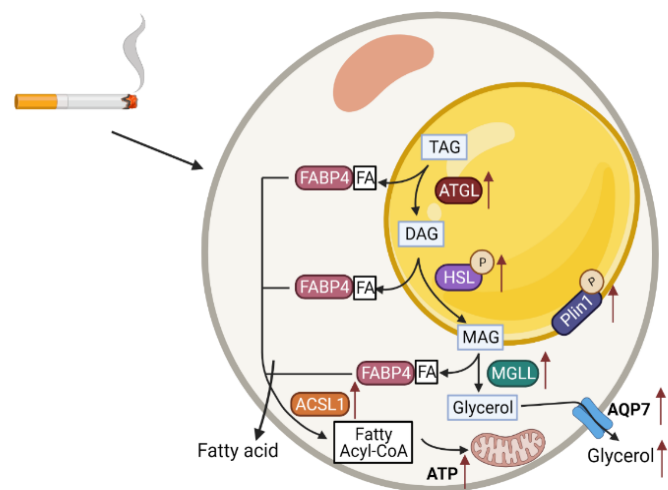

Figure 7. Molecular mechanisms of lipolysis in adipocytes and the effects of TPM exposure (red arrow). Lipolysis in adipocytes, the hydrolysis of triacylglycerol (TAG) to release fatty acids (FAs) and glycerol for use by other organs as energy substrates is a unique function of white adipose tissue. The

activation of lipases including ATGL, HSL and MGLL is crucial for the initiation of lipolysis, and Plin1 phosphorylation is a key event in the activation of TAG hydrolysis. HSL phosphorylation promotes the translocation of the enzyme from the cytosol to the surface of the lipid droplet. Docking of adipocyte FA-binding protein 4 (FABP4) to HSL facilitates outflow from the cell of non-esterified fatty acid (NEFAs) released by the hydrolysis of TAGs. AQP7 is the water-selective membrane channel responsible for glycerol efflux. Released FFAs requires the activation via ACSL1 that converts FFAs to Fatty acyl-CoA. Converted Fatty acyl-CoA can be transferred to mitochondrial matrix and oxidized in mitochondria to produce ATP as the central part of the human energy metabolism. The lipolysis was enhanced after TPM exposure, as observed by increased lipases, released glycerol, as well as augmented fatty acid oxidation by increased ATP production.

Materials and Methods

In Vivo Study
Animals
Specific-pathogen free female Balb/c mice, 11-13 weeks old (N = 15/16 per group) were obtained from Charles River Laboratories [51, 52]. The mice were housed in groups (3 or 4 animals/cage) in filter-topped Makrolon cages (22 cm×16 cm×14 cm, floor area 350 cm^2, Tecnilab-BMI, Someren, the Netherlands) with wood-chip bedding (Tecnilab-BMI, Someren, the Netherlands) and tissues (VWR, the Netherlands) available as cage enrichment. The mice were kept under standard conditions on a 12 h light/dark cycle (lights on from 7.00 am to 7.00 pm) at controlled relative humidity (relative humidity of 50—55%) and temperature (21 ± 2 °C) at the animal facility of Utrecht University. Food (AIN-93M, SNIFF) and water were available ad libitum. The *in vivo* study described in this article is part of a larger trial, including an air control group, smoke exposure group, and 6 other groups [18]. In accordance with the purpose of this study, investigating the effect of cigarette smoke exposure on both adipose and muscle tissue weight and function, the results of the analyses of the control and cigarette smoke exposure groups were investigated. All animal procedures described in this study were approved by the Ethics Committee of Animal Research of Utrecht University, Utrecht, the Netherlands (AVD1080020184785), and were conducted in accordance with the governmental guidelines.

Cigarette smoke exposure
The mice were exposed in whole-body chambers to mainstream cigarette smoke or air for 72 consecutive days by peristaltic pump (SCIQ 232, Watson-Marlow 323, USA). Research cigarettes (3R4F) were obtained from the Tobacco Research Institute (University of Kentucky, Lexington, Kentucky) and filters were removed before use. The smoke chamber was connected to a peristaltic pump and vacuum to control the air circulation. The mice were exposed to cigarette smoke once a day, 7 days a week for 72 consecutive days, except on day 42, 52 and 62 (on these days, the mice received saline via intra-tracheal instillation, as they served as controls in a larger trial) using 4 cigarettes on day 1; 6 cigarettes on day 2; 8 cigarettes on day 3; 10 cigarettes on day 4; 12 cigarettes on day 5; and 14 cigarettes from

day 6 to the end of the study. The speed of the peristaltic pump was kept at 35 rpm and the CO levels ranged between 200 and 400 ppm [52]. The mice were killed on day 73, as previously described [18].

Body composition

After the last smoke exposure, the body weight was determined using a weighing scale and fat and lean mass were measured by using the EchoMRI Scan (Houston, TX, USA).

Grip strength and muscle weight

After the last smoke exposure, grip strength was measured as forelimb grip strength by a calibrated grip strength tester (Panlab, Cornella, Spain); the absolute average strength and absolute maximum strength were recorded over five repetitions [53]. Tibialis, soleus, extensor digitorum longus (EDL) and gastrocnemius muscle tissues were harvested; muscle tissues were weighed and snap-frozen for the following measurements.

H&E staining of adipose tissue and determination of fat cell number and size

The inguinal and para-ovary white adipose tissues were harvested, and the left side tissues were fixed in 10% formalin. Tissues were embedded in paraffin (Tissue processor, Leica); 5 μm sections were cut using a microtome (Leica RM 2165) and mounted on glass slides (StarFrost adhesive slides, Knittelgläser, Germany). The slides were deparaffinized and used for hematoxylin and eosin (H&E) staining according to the standard protocols. Microscopic images were taken using an Olympus BX50 microscope (Olympus, Tokyo, Japan). The number and size of fat cells were analyzed by ImageJ.

Immunofluorescent staining adipose tissue

The tissues were placed on glass slides, deparaffinized and rehydrated in decreasing concentrations of ethanol and incubated with 0.3% H_2O_2/methanol for 30 min to quench endogenous peroxidase activity. Thereafter, the slides were incubated with rabbit-anti-CD 68 primary antibody (1:150; #97778S, Cell Signaling Technology, Leiden, the Netherlands) overnight at 4 °C after blocking with 5% goat serum in PBS containing 1% bovine serum albumin (BSA). After three-times washing steps with PBS containing 0.2% Tween 20 (PBST; pH 7.4), the slides were incubated with Alexa fluorescently conjugated goat anti-rabbit secondary antibody (1:200; Invitrogen, the Netherlands) for 2 h at room temperature. The nuclei were stained by Hoechst (1:2000; Invitrogen, USA) and the slides were rinsed after the Hoechst staining and mounted with FluorSave reagent (Merk Millipore, St. Louis, MO, USA). Rabbit IgG (1:150; #ab176094, Abcam, Cambridge, UK) was used as isotype control. Images were captured by the confocal microscope (TCS SP8 X, Leica, Germany).

Adipose tissue homogenates for cytokine measurement

The inguinal and para-ovary white adipose tissues were harvested, and the right-side tissues were homogenized with cold 1% Triton X-100 (Sigma-Aldrich)/PBS solution containing protease inhibitors (Complete Mini, EDTA-free Protease Inhibitor Cocktail, Sigma-Aldrich, the Netherlands) by Precellys 24 tissue homogenizer (Bertin Technologies, France) at 4 °C. Thereafter, homogenates were centrifuged (15,000 g, 10 min, 4 °C) and the supernatant was collected. The protein concentration of the samples was measured using the Pierce BCA protein assay kit (Thermo Fisher Scientific, Waltham, MA, USA) according to the manufacturer's instructions. The samples were diluted to 2 mg of protein/mL and stored at −20 °C until further analyses. IL-6, TNF-α and IL-1β were measured by ELISA (Mouse IL-6 (#88-7064-88), TNF-α (#88-7324-88) and IL-1β (#88-7013-88) ELISA kit; Thermo Fisher Scientific, Waltham, MA, USA) according to the manufacturer's instruction.

Leptin and KC levels in serum

Blood was obtained by heart puncture and collected in Mini collect tubes (Greiner Bio-One, Alphen aan den Rijn, the Netherlands) on day 72 ± 18 h after the last air or smoke exposure. Blood samples were centrifuged (14,000 g for 10 min) and serum was stored at −20 °C for future use. Leptin and KC levels were determined by a quantitative Milliplex Luminex assay kit (ProcartaPlex, Thermo Fisher Scientific, Austria) according to the manufacturer's instructions and using Luminex 200TM with Xponent software.

RNA isolation and quantitative Real-Time PCR (qRT-PCR) for skeletal muscle tissue

RNA preparation

Total RNA was isolated and extracted from muscle tissue using the RNeasy Mini Kit according to the manufacturer's protocol (Qiagen, Germany). RNA integrity and quantitation were assessed using the RNA Nano 6000 Assay Kit of the Bioanalyzer 2100 system (Agilent Technologies, CA, USA).

qRT-PCR

cDNA was synthesized by the Tetro cDNA Synthesis Kit (Meridian, Tennessee, USA) according to the manufacturer's protocol in the T100 thermal cycler (Bio-Rad Laboratories, USA). A mixture of specific forward and reverse primers, SYBR® Green Supermixes for Real-Time PCR (Bio-Rad Laboratories or Meridian USA) and samples were prepared. Amplifications were performed according to the manufacturer's instructions using LightCycler 480II (Roche, USA). Primers (Table S1) were commercially manufactured (Sigma-Aldrich, Missouri, USA). The mRNA quantity was calculated relative to the expression of the average value of GeNorm of Cyclo, RPLP0, HPRT, B2M, GUSB, YWHAZ.

Western blot for skeletal muscle tissue

Muscle tissue (soleus) from the mice was isolated. Proteins were isolated from the muscle tissue by homogenization in IP-buffer and subsequently heat denatured in Laemmli buffer

(Sigma-Aldrich, the Netherlands) for the separation by polyacrylamide gel electrophoresis, as previously described [54]. Blots were blocked with 5% milk powder in PBST (0.1% Tween 20 in PBS) at room temperature for 1 h and incubated with primary antibodies (p)-S6 Ribosomal protein, (p)-4EBP1, LC3B-I(II), 1:1000, Cell Signaling Technology, MA, USA) at 4 °C overnight, followed by washing blots in PBST. Goat Anti Rabbit IgG ((p)-S6, (p)-4EBP1, LC3B-I(I), 1:5000, Vector Laboratories, California, USA) were applied for 1h incubation at room temperature. Membranes were incubated with ECL Western blotting substrates (Bio-Rad Laboratories, Hercules, CA, USA) prior to obtaining the digital images. The digital images were acquired with the Molecular Imager Gel Doc XR system (Bio-Rad Laboratories, Hercules, CA, USA). Western blots were normalized by Ponceau-S staining.

In Vitro Study
T3-L1 preadipocyte cell culture
The 3T3-L1 cell line (ATCC) was maintained in high glucose (4.5 g/L) Dulbecco's modified Eagle's medium (DMEM, Thermo Fisher Scientific, the Netherlands) supplemented with 10% (V/V) fetal bovine serum (FBS, Thermo Fisher Scientific, Brazil), 100 U/mL of penicillin (Sigma-Aldrich, the Netherlands) and 100 μg/mL of streptomycin (Sigma-Aldrich, the Netherlands) at 5% CO_2 and 37 °C. Cells at passage 6—8 were used in this study. Cells were passaged at 80% confluence using a solution of 0.05% trypsin and 0.5 mM of EDTA.

TPM preparation
TPM was collected by pumping the mainstream cigarette smoke of 3R4F research cigarettes through a peristaltic pump (SCIQ 232, Watson-Marlow 323, USA). TPM was collected by the type A/E glass fiber filter (PALL Life Sciences, Mexico), and the obtained TPM was dissolved in dimethyl sulfoxide (DMSO, Sigma-Aldrich, Zwijndrecht, the Netherlands) to a yield stock concentration of 50 mg/mL. This stock concentration was diluted to different concentrations, including 1.5625, 3.125, 6.25, 12.5, 25 and 50 μg/mL for the following experiment.

Cell viability and cytotoxicity assay
3T3-L1 pre-adipocytes were seeded and grown on 96-well plates until visual confluency was reached by microscopic inspection. Cells were exposed to different TPM concentrations for 24 h. To quantify the cell viability, after removing supernatants and rinsing the cells with warm PBS, 200 μL of the 0.5 mg/mL MTT labelling reagent was added into each well and incubated at 37 °C and 5% CO_2 covered by aluminum foil for 2.5—3 h. A total of 100 μL of DMSO was added to each well after emptying the plate. When the crystals were solubilized entirely, the absorbance was measured using a microplate reader (Glomax discover, Promega) at 570 nm. To quantify the integrity of the cell membranes, the release of LDH into the growth media was measured after exposure to TPM. To this end, 50 μL of supernatant was incubated with a 50 μL well-mixed catalyst and dye substrate mixture

(46:1) for 30 min at room temperature. The assay was terminated by adding 25 μL of stop solution, and the absorbance was measured using the microplate reader (Glomax discover, Promega) at 490 nm [55].

Cell differentiation and TPM treatment
To induce the differentiation of preadipocytes to mature adipocytes, confluent 3T3-L1 pre-adipocytes cultured in phenol red-free DMEM (Thermo Fisher Scientific, the Netherlands) were treated with 0.5 mM of 3-sobutyl-1-methylxanthine (IBMX, Sigma-Aldrich, the Netherlands) that was dissolved in 1 mM of potassium hydroxide solution and 1 μg/mL of insulin (Sigma-Aldrich, the Netherlands) during day 0 until day 1, in order to induce cell differentiation (differentiation induction period). Maintenance medium (phenol-free DMEM supplemented with 1 μg/mL of insulin) was added and refreshed on day 2, 4 and day 7 (differentiation maintenance period) until day 8. During these 8 days, TPM, DMSO (for control group) or 100 mM of rosiglitazone (Sigma-Aldrich, the Netherlands) as a positive control was administrated to the cells simultaneously with the differentiation inducer (insulin or insulin with IBMX). TPM concentrations (6.25, 12.5 and 25 μg/mL) were selected based on the cell viability and cytotoxicity assays. TPM and rosiglitazone were dissolved in DMSO (0.1% V/V); therefore, this concentration of DMSO was added to the undifferentiated control (UDC) and differentiated control (DC) cells. After these 8 days of differentiation, supernatant or cells were collected for the Nile red staining, glycerol measurement, qPCR and Western blot analyses. See Supplementary Figure 1 for the detailed overview of the cell culture procedures.

Nile red staining
On day 8, after removing the supernatants, the cells were washed twice with PBS and fixed with 10% formalin at room temperature for 15 min. Deionized water was added for background measurement. Thereafter, the cells were incubated with the mixture of 0.1% Nile red (Sigma-Aldrich, the Netherlands), a fluorescent probe for the detection of the intracellular lipid content, and 0.05% Hoechst dye (Invitrogen, Carlsbad, CA, USA) for 20 min in the dark. The fluorescence intensity was measured by using a microplate reader (Glomax discover, Promega). The morphology images were captured by confocal microscope (Leica TCS SP8 X).

Free glycerol, FFAs and ATP Assays
Cell culture supernatants (25x dilution) were used to test the levels of free glycerol release and FFAs release from cells using the free glycerol assay kit (#ab65337, Abcam, the Netherlands) and FFAs assay kit (#ab65341, Abcam, the Netherlands). Cells lysates were used for ATP measurement by the ATP assay kit (#MAK190-1KT, Sigma-Aldrich, the Netherlands). All the assays were performed according to the manufacturer's instructions.

RNA isolation and quantitative Real-Time PCR (qRT-PCR)/gene sequence

RNA preparation

Total RNA was isolated and extracted from the cells using the RNeasy Mini Kit according to the manufacturer's protocol (Qiagen, Germany). RNA integrity and quantitation were assessed using the RNA Nano 6000 Assay Kit of the Bioanalyzer 2100 system (Agilent Technologies, Palo Alto, CA, USA). RNA degradation and contamination were monitored on 1% agarose gels (Supplementary Figure 2).

qRT-PCR

cDNA was synthesized by an iScript TM advanced kit (Bio-Rad, Hercules, CA, USA) (adipocytes) according to the manufacturer's protocol in the T100 thermal cycler (Bio-Rad Laboratories, Hercules, CA, USA). A mixture of specific forward and reverse primers, SYBR® Green Supermixes for Real-Time PCR (Bio-Rad Laboratories or Meridian USA) and samples were prepared, and amplifications were performed according to the manufacturer's instructions using the CFX96 Touch™ Real-Time PCR Detection System (Bio-Rad Laboratories, Hercules, CA, USA). Primers (Table S1) were commercially manufactured (Biolegio BV, Nijmegen, Netherlands). The specificity and efficiency of the primers were tested by a temperature gradient, the melting curve was evaluated, and the optimum annealing temperature was determined. The mRNA quantity was calculated relative to the expression of β-actin.

mRNA Non-Directional (polyA)

RNA samples were used for library preparation using NEB Next® Ultra RNA Library Prep Kit for Illumina ®. Indices were included to multiplex multiple samples. Briefly, mRNA was purified from total RNA using poly-T oligo-attached magnetic beads. After fragmentation, the first strand cDNA was synthesized using random hexamer primers, followed by the second strand cDNA synthesis. The library was ready after end repair, A-tailing, adapter ligation and size selection. After amplification and purification, the insert size of the library was validated on an Agilent 2100 and quantified using a q-PCR. Libraries were then sequenced on Illumina NovaSeq 6000 S4 FlowCell with PE150 according to results from library quality control and expected data volume. Library preparation, sequencing and analysis was performed by Novogene (Cambridge, UK) Company Limited.

Western blot

After the differentiation procedure, 3T3-L1 cell lysates were collected by adding RIPA cell lysis buffer (Thermo Fisher Scientific, Waltham, MA, USA) containing protease inhibitors (Roche Applied Science, Pennsburg, Germany). Total protein concentrations were determined using a Pierce BCA protein assay kit (Thermo Fisher Scientific, Waltham, MA, USA) according to the manufacturer's instructions. A total of 30 µg of protein sample was loaded onto polyacrylamide gels (4–20% Tris–HCl, Bio-Rad Laboratories, Hercules, CA,

USA) that were separated using electrophoresis, and electro transferred onto polyvinylidene difluoride membrane (Bio-Rad Laboratories, Hercules, CA, USA) using the Trans-Blot Turbo system (Bio-Rad Laboratories, Hercules, CA, USA). Blots were blocked with 5% milk powder in PBST (0.1% Tween 20 in PBS) at room temperature for 1 h and incubated with primary antibodies (p-)HSL, HSL, β-actin, (1:1000, Cell Signaling Technology, MA, USA) at 4 °C overnight, followed by washing the blots in PBST. Corresponding horseradish peroxidase-coupled secondary antibodies from Dako (for p-HSL, HSL, β-actin) (1:10000, Agilent Technologies, Santa Clara, CA, USA) were applied for 1h incubation at room temperature. Membranes were incubated with ECL Western blotting substrates (Bio-Rad Laboratories, Hercules, CA, USA) prior to obtaining the digital images. The digital images were acquired with the Molecular Imager Gel Doc XR system (Bio-Rad Laboratories, Hercules, CA, USA).

Statistical analysis

The results are presented as mean ± SEM. The student t-test and spearman tests (analyses of correlation) were conducted for *in vivo* results. The in vitro results from different groups were statistically determined by a one-way ANOVA, followed by Tukey's multiple comparison post hoc test. The difference was considered statistically significant at $p < 0.05$. All statistical analyses were conducted using GraphPad Prism (version 8.3). The required sample size was calculated with G*Power v 3.1.9 based on a power of 80% and α = 0.05 and a primary outcome parameter derived from previous observations.

References

1. Quaderi, S.A. and Hurst, J.R., *The unmet global burden of COPD*. Glob Health Epidemiol Genom, 2018. **3**: p. e4.

2. Houben-Wilke, S., Augustin, I.M., Vercoulen, J.H., van Ranst, D., Bij de Vaate, E., Wempe, J.B., Spruit, M.A., Wouters, E.F.M., and Franssen, F.M.E., *COPD stands for complex obstructive pulmonary disease*. Eur Respir Rev, 2018. **27**(148).

3. Evans, W.J., Morley, J.E., Argiles, J., Bales, C., Baracos, V., Guttridge, D., Jatoi, A., Kalantar-Zadeh, K., Lochs, H., Mantovani, G., et al., *Cachexia: a new definition*. Clin Nutr, 2008. **27**(6): p. 793-9.

4. Remels, A.H., Gosker, H.R., Langen, R.C., and Schols, A.M., *The mechanisms of cachexia underlying muscle dysfunction in COPD*. J Appl Physiol (1985), 2013. **114**(9): p. 1253-62.

5. Kurosaki, H., Ishii, T., Motohashi, N., Motegi, T., Yamada, K., Kudoh, S., Jones, R.C., and Kida, K., *Extent of emphysema on HRCT affects loss of fat-free mass and fat mass in COPD*. Intern Med, 2009. **48**(1): p. 41-8.

6. Arner, P., *Medicine. Lipases in cachexia*. Science, 2011. **333**(6039): p. 163-4.

7. Das, S.K. and Hoefler, G., *The role of triglyceride lipases in cancer associated cachexia*. Trends Mol Med, 2013. **19**(5): p. 292-301.

8. Edwards, M. and Mohiuddin, S.S., *Biochemistry, Lipolysis*, in *StatPearls*. 2021: Treasure Island (FL).

9. Richard, A.J., White, U., Elks, C.M., and Stephens, J.M., *Adipose Tissue: Physiology to Metabolic Dysfunction*, in *Endotext*, K.R. Feingold, et al., Editors. 2000: South Dartmouth (MA).

10. Plihalova, A., Bartakova, H., Vasakova, M., Gulati, S., deGlisezinski, I., Stich, V., and Polak, J., *The effect of hypoxia and re-oxygenation on adipose tissue lipolysis in COPD patients*. Eur Respir J, 2016. **48**(4): p. 1218-1220.

11. Batista, M.L., Jr., Henriques, F.S., Neves, R.X., Olivan, M.R., Matos-Neto, E.M., Alcantara, P.S., Maximiano, L.F., Otoch, J.P., Alves, M.J., and Seelaender, M., *Cachexia-associated adipose tissue morphological rearrangement in gastrointestinal cancer patients*. J Cachexia Sarcopenia Muscle, 2016. **7**(1): p. 37-47.

12. Lakhdar, R. and Rabinovich, R.A., *Can muscle protein metabolism be specifically targeted by nutritional support and exercise training in chronic obstructive pulmonary disease?* J Thorac Dis, 2018. **10**(Suppl 12): p. S1377-S1389.

13. Tuttle, C.S.L., Thang, L.A.N., and Maier, A.B., *Markers of inflammation and their association with muscle strength and mass: A systematic review and meta-analysis*. Ageing Res Rev, 2020. **64**: p. 101185.

14. Abdulai, R.M., Jensen, T.J., Patel, N.R., Polkey, M.I., Jansson, P., Celli, B.R., and Rennard, S.I., *Deterioration of Limb Muscle Function during Acute Exacerbation of Chronic Obstructive Pulmonary Disease*. Am J Respir Crit Care Med, 2018. **197**(4): p. 433-449.

15. Jagoe, R.T. and Engelen, M.P., *Muscle wasting and changes in muscle protein metabolism in chronic obstructive pulmonary disease*. Eur Respir J Suppl, 2003. **46**: p. 52s-63s.

16. Brown, J.L., Rosa-Caldwell, M.E., Lee, D.E., Blackwell, T.A., Brown, L.A., Perry, R.A., Haynie, W.S., Hardee, J.P., Carson, J.A., Wiggs, M.P., et al., *Mitochondrial degeneration precedes the development of muscle atrophy in progression of cancer cachexia in tumour-bearing mice*. J Cachexia Sarcopenia Muscle, 2017. **8**(6): p. 926-938.

17. Wagner, P.D., *Possible mechanisms underlying the development of cachexia in COPD*. Eur Respir J, 2008. **31**(3): p. 492-501.

18. Wang, L., Pelgrim, C.E., Peralta Marzal, L.N., Korver, S., van Ark, I., Leusink-Muis, T., van Helvoort, A., Keshavarian, A., Kraneveld, A.D., Garssen, J., et al., *Changes in intestinal homeostasis and immunity in a cigarette smoke- and LPS-induced murine model for COPD: the lung-gut axis*. Am J Physiol Lung Cell Mol Physiol, 2022. **323**(3): p. L266-L280.

19. Pelgrim, C.E., Wang, L., Peralta Marzal, L.N., Korver, S., van Ark, I., Leusink-Muis, T., Braber, S., Folkerts, G., Garssen, J., van Helvoort, A., et al., *Increased exploration and hyperlocomotion in a cigarette smoke and LPS induced murine model of COPD: linking pulmonary and systemic inflammation with the brain*. Am J Physiol Lung Cell Mol Physiol, 2022. **323**(3): p. L251-L265.

20. Shen, W.J., Patel, S., Miyoshi, H., Greenberg, A.S., and Kraemer, F.B., *Functional interaction of hormone-sensitive lipase and perilipin in lipolysis*. J Lipid Res, 2009. **50**(11): p. 2306-13.

21. McDonald, M.N., Wouters, E.F.M., Rutten, E., Casaburi, R., Rennard, S.I., Lomas, D.A., Bamman, M., Celli, B., Agusti, A., Tal-Singer, R., et al., *It's more than low BMI: prevalence of cachexia and associated mortality in COPD*. Respir Res, 2019. **20**(1): p. 100.

22. Rutten, E.P., Breyer, M.K., Spruit, M.A., Hofstra, T., van Melick, P.P., Schols, A.M., and Wouters, E.F., *Abdominal fat mass contributes to the systemic inflammation in chronic obstructive pulmonary disease*. Clin Nutr, 2010. **29**(6): p. 756-60.

23. Guerra, S., Sherrill, D.L., Bobadilla, A., Martinez, F.D., and Barbee, R.A., *The relation of body mass index to asthma, chronic bronchitis, and emphysema*. Chest, 2002. **122**(4): p. 1256-63.

24. Chen, H., Vlahos, R., Bozinovski, S., Jones, J., Anderson, G.P., and Morris, M.J., *Effect of short-term cigarette smoke exposure on body weight, appetite and brain neuropeptide Y in mice*. Neuropsychopharmacology, 2005. **30**(4): p. 713-9.

25. Klok, M.D., Jakobsdottir, S., and Drent, M.L., *The role of leptin and ghrelin in the regulation of food intake and body weight in humans: a review*. Obes Rev, 2007. **8**(1): p. 21-34.

26. Karakas, S., Karadag, F., Karul, A.B., Gurgey, O., Gurel, S., Guney, E., and Cildag, O., *Circulating leptin and body composition in chronic obstructive pulmonary disease*. Int J Clin Pract, 2005. **59**(10): p. 1167-70.

27. Calikoglu, M., Sahin, G., Unlu, A., Ozturk, C., Tamer, L., Ercan, B., Kanik, A., and Atik, U., *Leptin and TNF-alpha levels in patients with chronic obstructive pulmonary disease and their relationship to nutritional parameters*. Respiration, 2004. **71**(1): p. 45-50.

28. Takabatake, N., Nakamura, H., Abe, S., Hino, T., Saito, H., Yuki, H., Kato, S., and Tomoike, H., *Circulating leptin in patients with chronic obstructive pulmonary disease*. Am J Respir Crit Care Med, 1999. **159**(4 Pt 1): p. 1215-9.

29. Perez-Perez, A., Sanchez-Jimenez, F., Vilarino-Garcia, T., and Sanchez-Margalet, V., *Role of Leptin in Inflammation and Vice Versa*. Int J Mol Sci, 2020. **21**(16).

30. Jutant, E.M., Tu, L., Humbert, M., Guignabert, C., and Huertas, A., *The Thousand Faces of Leptin in the Lung*. Chest, 2021. **159**(1): p. 239-248.

31. Wouters, E.F., Reynaert, N.L., Dentener, M.A., and Vernooy, J.H., *Systemic and local inflammation in asthma and chronic obstructive pulmonary disease: is there a connection?* Proc Am Thorac Soc, 2009. **6**(8): p. 638-47.

32. Tkacova, R., *Systemic inflammation in chronic obstructive pulmonary disease: may adipose tissue play a role? Review of the literature and future perspectives*. Mediators Inflamm, 2010. **2010**: p. 585989.

33. Bagchi, D.P. and MacDougald, O.A., *Identification and Dissection of Diverse Mouse Adipose Depots*. J Vis Exp, 2019(149).

34. Ebadi, M. and Mazurak, V.C., *Evidence and mechanisms of fat depletion in cancer*. Nutrients, 2014. **6**(11): p. 5280-97.

35. Jaitovich, A. and Barreiro, E., *Skeletal Muscle Dysfunction in Chronic Obstructive Pulmonary Disease. What We Know and Can Do for Our Patients*. Am J Respir Crit Care Med, 2018. **198**(2): p. 175-186.

36. Martinez, C.H., Diaz, A.A., Meldrum, C.A., McDonald, M.N., Murray, S., Kinney, G.L., Hokanson, J.E., Curtis, J.L., Bowler, R.P., Han, M.K., et al., *Handgrip Strength in Chronic Obstructive Pulmonary Disease. Associations with Acute Exacerbations and Body Composition*. Ann Am Thorac Soc, 2017. **14**(11): p. 1638-1645.

37. Biltz, N.K., Collins, K.H., Shen, K.C., Schwartz, K., Harris, C.A., and Meyer, G.A., *Infiltration of intramuscular adipose tissue impairs skeletal muscle contraction*. J Physiol, 2020. **598**(13): p. 2669-2683.

38. Degens, H., Gayan-Ramirez, G., and van Hees, H.W., *Smoking-induced skeletal muscle dysfunction: from evidence to mechanisms*. Am J Respir Crit Care Med, 2015. **191**(6): p. 620-5.

39. Tang, K., Wagner, P.D., and Breen, E.C., *TNF-alpha-mediated reduction in PGC-1alpha may impair skeletal muscle function after cigarette smoke exposure*. J Cell Physiol, 2010. **222**(2): p. 320-7.

40. de Castro, G.S., Simoes, E., Lima, J., Ortiz-Silva, M., Festuccia, W.T., Tokeshi, F., Alcantara, P.S., Otoch, J.P., Coletti, D., and Seelaender, M., *Human Cachexia Induces Changes in Mitochondria, Autophagy and Apoptosis in the Skeletal Muscle*. Cancers (Basel), 2019. **11**(9).

41. Decker, S.T., Kwon, O.S., Zhao, J., Hoidal, J.R., Heuckstadt, T., Richardson, R.S., Sanders, K.A., and Layec, G., *Skeletal muscle mitochondrial adaptations induced by long-term cigarette smoke exposure*. Am J Physiol Endocrinol Metab, 2021. **321**(1): p. E80-E89.

42. Gosker, H.R., Langen, R.C., Bracke, K.R., Joos, G.F., Brusselle, G.G., Steele, C., Ward, K.A., Wouters, E.F., and Schols, A.M., *Extrapulmonary manifestations of chronic obstructive pulmonary disease in a mouse model of chronic cigarette smoke exposure*. Am J Respir Cell Mol Biol, 2009. **40**(6): p. 710-6.

43. Caron, M.A., Morissette, M.C., Theriault, M.E., Nikota, J.K., Stampfli, M.R., and Debigare, R., *Alterations in skeletal muscle cell homeostasis in a mouse model of cigarette smoke exposure*. PLoS One, 2013. **8**(6): p. e66433.

44. Stenkula, K.G. and Erlanson-Albertsson, C., *Adipose cell size: importance in health and disease*. Am J Physiol Regul Integr Comp Physiol, 2018. **315**(2): p. R284-R295.

45. Kliewer, K.L., Ke, J.Y., Tian, M., Cole, R.M., Andridge, R.R., and Belury, M.A., *Adipose tissue lipolysis and energy metabolism in early cancer cachexia in mice*. Cancer Biol Ther, 2015. **16**(6): p. 886-97.

46. Brejchova, K., Radner, F.P.W., Balas, L., Paluchova, V., Cajka, T., Chodounska, H., Kudova, E., Schratter, M., Schreiber, R., Durand, T., et al., *Distinct roles of adipose triglyceride lipase and hormone-sensitive lipase in the catabolism of triacylglycerol estolides*. Proc Natl Acad Sci U S A, 2021. **118**(2).

47. Zuijdgeest-van Leeuwen, S.D., van den Berg, J.W., Wattimena, J.L., van der Gaast, A., Swart, G.R., Wilson, J.H., and Dagnelie, P.C., *Lipolysis and lipid oxidation in weight-losing cancer patients and healthy subjects*. Metabolism, 2000. **49**(7): p. 931-6.

48. Ellis, J.M., Li, L.O., Wu, P.C., Koves, T.R., Ilkayeva, O., Stevens, R.D., Watkins, S.M., Muoio, D.M., and Coleman, R.A., *Adipose acyl-CoA synthetase-1 directs fatty acids toward beta-oxidation and is required for cold thermogenesis*. Cell Metab, 2010. **12**(1): p. 53-64.

49. Bing, C., Russell, S., Becket, E., Pope, M., Tisdale, M.J., Trayhurn, P., and Jenkins, J.R., *Adipose atrophy in cancer cachexia: morphologic and molecular analysis of adipose tissue in tumour-bearing mice*. Br J Cancer, 2006. **95**(8): p. 1028-37.

50. Pini, M., Czibik, G., Sawaki, D., Mezdari, Z., Braud, L., Delmont, T., Mercedes, R., Martel, C., Buron, N., Marcelin, G., et al., *Adipose tissue senescence is mediated by increased ATP content after a short-term high-fat diet exposure*. Aging Cell, 2021. **20**(8): p. e13421.

51. Roda, M.A., Xu, X., Abdalla, T.H., Sadik, M., Szul, T., Bratcher, P.E., Viera, L., Solomon, G.M., Wells, J.M., McNicholas, C.M., et al., *Proline-Glycine-Proline Peptides Are Critical in the Development of Smoke-induced Emphysema*. Am J Respir Cell Mol Biol, 2019. **61**(5): p. 560-566.

52. Wang, L., Pelgrim, C.E., Swart, D.H., Krenning, G., van der Graaf, A.C., Kraneveld, A.D., Leusink-Muis, T., van Ark, I., Garssen, J., Folkerts, G., et al., *SUL-151 Decreases Airway Neutrophilia as a Prophylactic and Therapeutic Treatment in Mice after Cigarette Smoke Exposure*. Int J Mol Sci, 2021. **22**(9).

53. van Dijk, M., Dijk, F.J., Hartog, A., van Norren, K., Verlaan, S., van Helvoort, A., Jaspers, R.T., and Luiking, Y., *Reduced dietary intake of micronutrients with antioxidant properties negatively impacts muscle health in aged mice*. J Cachexia Sarcopenia Muscle, 2018. **9**(1): p. 146-159.

54. Leermakers, P.A., Kneppers, A.E.M., Schols, A., Kelders, M., de Theije, C.C., Verdijk, L.B., van Loon, L.J.C., Langen, R.C.J., and Gosker, H.R., *Skeletal muscle unloading results in increased mitophagy and decreased mitochondrial biogenesis regulation*. Muscle Nerve, 2019. **60**(6): p. 769-778.

55. Cai, Y., Varasteh, S., van Putten, J.P.M., Folkerts, G., and Braber, S., *Mannheimia haemolytica and lipopolysaccharide induce airway epithelial inflammatory responses in an extensively developed ex vivo calf model*. Sci Rep, 2020. **10**(1): p. 13042.
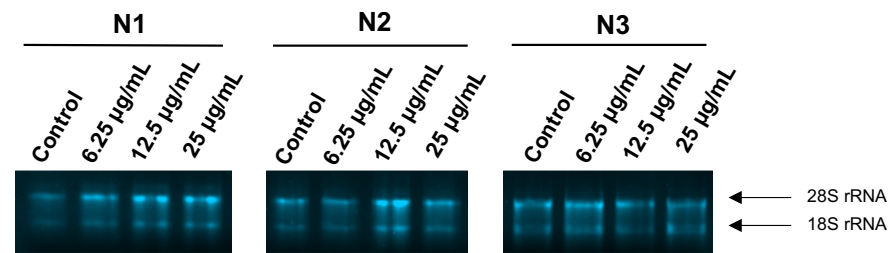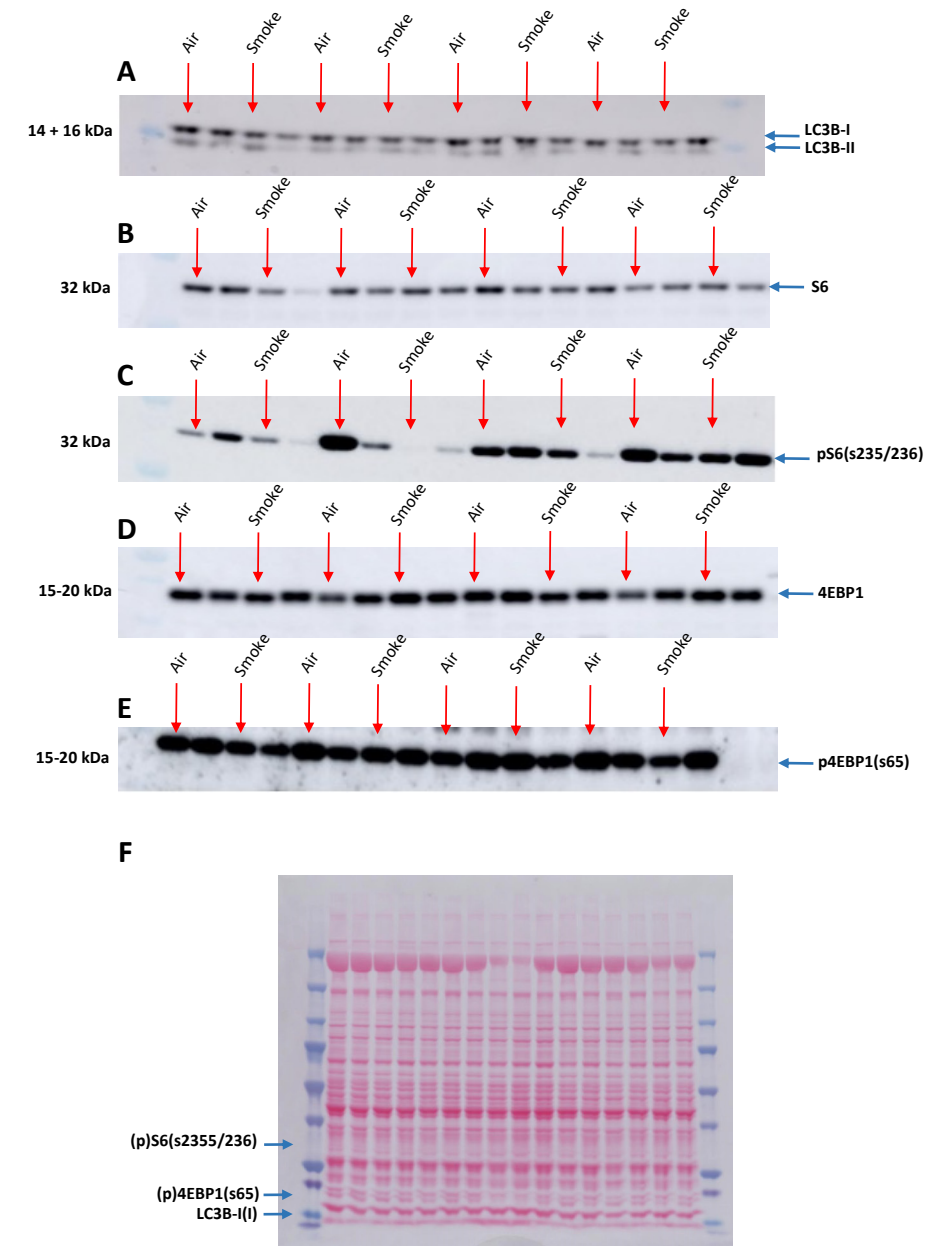
Supplementary data
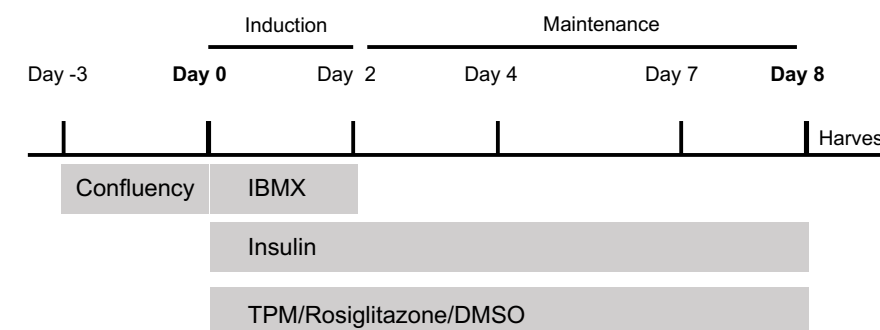
Supplementary Figure 1. Timeline of cell differentiation procedure. Proliferating preadipocytes were seeded in plates and cultured in phenol red-free medium until reaching confluence (day -3 till day 0). Thereafter, the differentiation medium (insulin with IBMX (day 0 till day 2) and insulin without IBMX (day 2 till day 8). Stimulants (different concentrations of TPM from cigarette smoke, rosiglitazone (positive control), or DMSO (solvent control)) were added from day 0 till day 8 and refreshed on day 2, 4 and 7.

**Supplementary Table 1. Sequences of the primers**

Gene name	Forward Sequence (5' →3')	Reverse Sequence (5' →3')
Primers for *in vitro*		
β-actin	TAA GGC CAA CCG TGA AAA G	ACC AGA GGC ATA CAG GGA CA
Leptin	CTG CCC CCC AGT TTG ATG	GCC AGG CTG CCA GAA TTG
ATGL	TTA GGA GGA ATG CCC TGC TG	AGC ATG TTG GAA AGG GTG GT
HSL	TCC TGG AAC TAA GTG GAC GCA AG	CAG ACA CAC TCC TGC GCA TAG AC
MGLL	CGG AAC AAG TCG GAG GTT GAC	CAT TGC TCG CTC CAC TCT TG
Plin1	CTG TGT GCA ATG CCT ATG AGA	CTG GAG GGT ATT GAA GAG CCG
Aqp7	CTG GAT GAG GCA TTC GTG ACT	TGA TGG CGA AGA GAC ACA GC
ACSL1	AAA GAT GGC TGG TTA CAC ACG	CGA TAA TCT TCA AGG TGC CAT T
PGC-1α	TGA TGT GAA TGA CTT GGA TAC A	GCT CAT TGT TGT ACT GGT TGG A
Primers for *in vivo*		
Mstn	AAC CTT CCC AGG ACC AGG AGA A	TGT CTG TTA CCT TGA CCT CTA AAA ACG G
Atrogin-1	GAA GAA ACT CTG CCA GTA CCA CTT C	CCC TTT GTC TGA CAG AAT TAA TCG
SMART	AAT TAA TCT GAA AGG CAC TGT GTC	TGA AGA CAG AAT GTC ACA AAC TG
MuRF-1	GCG AGG TGG CCC CAT T	GAT GGT CTG CAC ACG GTC ATT
FoXO-1	CCT GGA CAT GCT CAG CAG ACA TC	TTG GGT CAG GCG GTT CAT ACC
REDD1	CTG ACC CTC GTG CTG CGC CTG	GGA AGC CAG TGC TCA GCG TCA G
NEDD4	TCA CTG GCA CAT CTC GGG TG	TCA TAA GGT GGC AAG TCC AGG C
PGC-1α	CAA CAA TGA GCC TGC GAA CA	CTT CAT CCA CGG GGA GAC TG
Tfam	CCG GCA GAG ACG GTT AAA AA	TCA TCC TTT GCC TCC TGG AA
Nrf1	AGC CAC ATT GGC TGA TGC TT	GGT CAT TTC ACC GCC CTG TA
(Complex II)	AAT TTG CCA TTT ACC GAT GGG A	AGC ATC AAA CAC CAT AGG TCC
(Complex III)	GCA TTC GGA GGG GTT TCC AG	CCG CAT GAA CAT CTC CCC A
(Complex IV)	CCA TCC CAG GCC GAC TAA	ATT TCA GAG CAT TGG CCA TAG AA

Supplementary Figure 2. The total RNA degradation and contamination were monitored on 1% agarose gels. Non-denaturing agarose gel (1%) of total RNA from 3T3-L1 pre-adipocytes after exposure to TPM, N=3.

Supplementary Figure 3. Original blots. Mice were exposed to air or cigarette smoke for 72 days. Protein expression levels of protein turnover markers, LC3B-I(II) (A), S6 (B), pS6(s235/236) (C), 4EBP1 (D and, p4EBP1(s65) (E), were determined in soleus muscle via Western Blot analysis and original blots are depicted, and protein targets were quantified with Ponceau-S (F). N=8 mice/group.

5

5
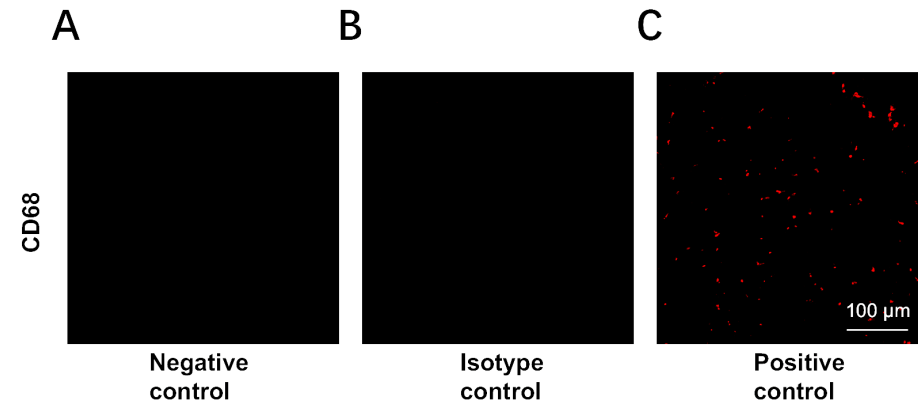
Supplementary Figure 4. Representative pictures of the negative control, isotype control and positive control related to the immunofluorescent staining for CD68 in white adipose tissue. Mice were exposed to air or cigarette smoke for 72 days. The presence of macrophages in white adipose tissue was investigated by immunofluorescence microscopy using anti-CD68 antibodies, while the negative control by omission of the primary antibodies (A) and rabbit IgG polyclonal isotype control (Abcam, UK) (B) showed no staining and positive control (C) (scale bar = 100 μm).
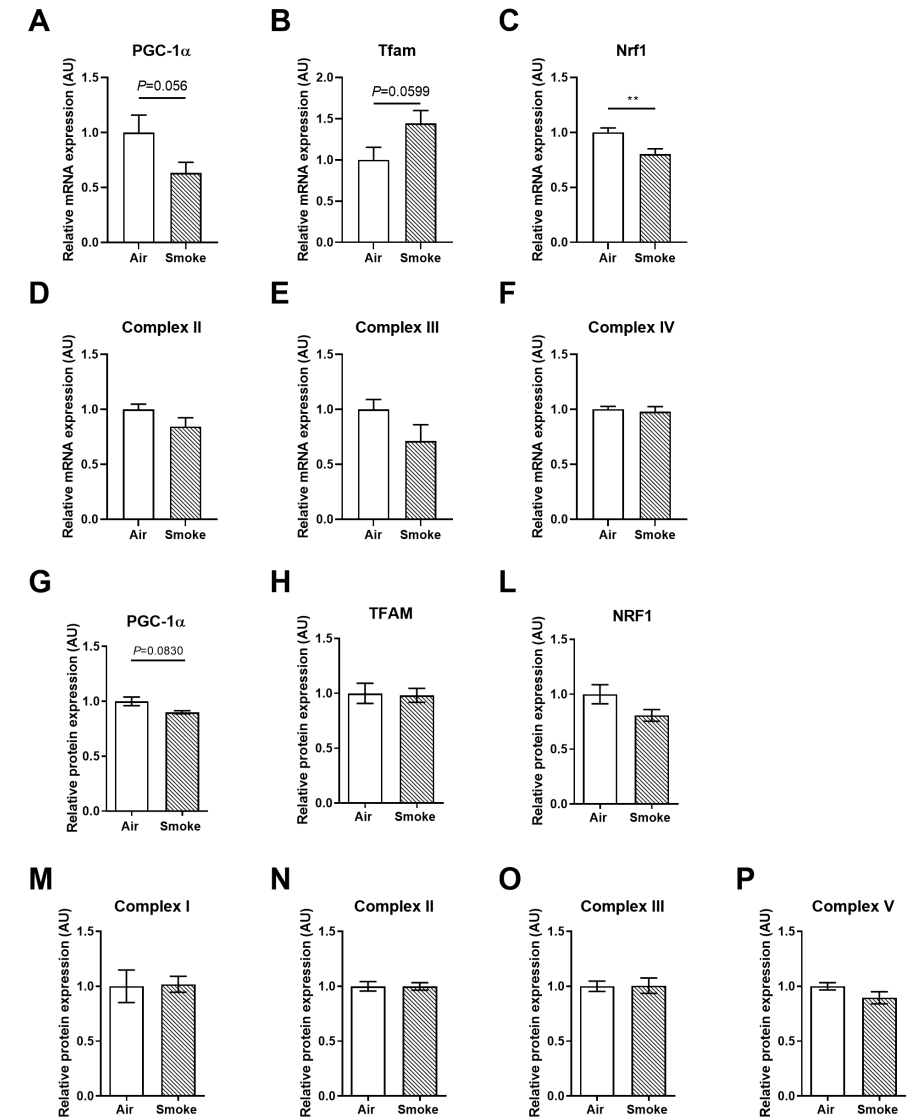
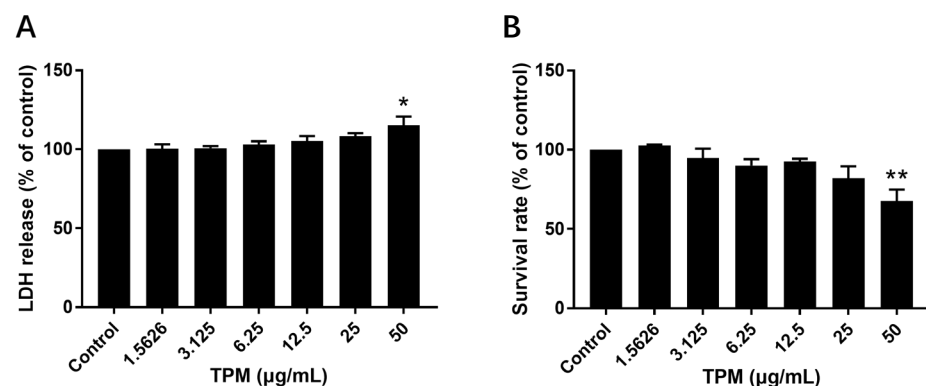**Supplementary Figure 5. The effect of cigarette smoke exposure on molecular markers of mitochondrial biogenesis and mitochondrial content.** Mice were exposed to air or cigarette smoke for 72 days. Gene expression levels of molecular markers for mitochondrial biogenesis PGC-1α (A), Tfam (B), Nrf1 (C), complex II (D), complex III (E) and complex IV (F) were determined in soleus muscle by qRT-PCR. Data was normalized to GeNorm and expressed as fold change compared to control. Protein expression levels of molecular markers for mitochondrial biogenesis PGC-1α (G), TFAM (H), NRF1 (L), complex I (M), complex II (N), complex III (O) and complex IV (P) were determined in soleus muscle by Western blot, and protein targets were quantified with Ponceau-S. Values are represented as mean ± SEM. N=8 mice/group.

Supplementary Figure 6. The effect of TPM on the viability of 3T3-L1 pre-adipocytes. The effect of TPM on cell viability of 3T3-L1 pre-adipocytes was evaluated by LDH (A) and MTT (B) assay after exposing 3T3-L1 pre-adipocytes to different concentrations of TPM (1.5626, 3.125, 6.25, 12.5, 25, 50 µg/mL) for 24h. Values are analyzed by one-way ANOVA, Tukey post hoc, and expressed as mean±SEM, *$p < 0.05$ compared with the control group. N=3.
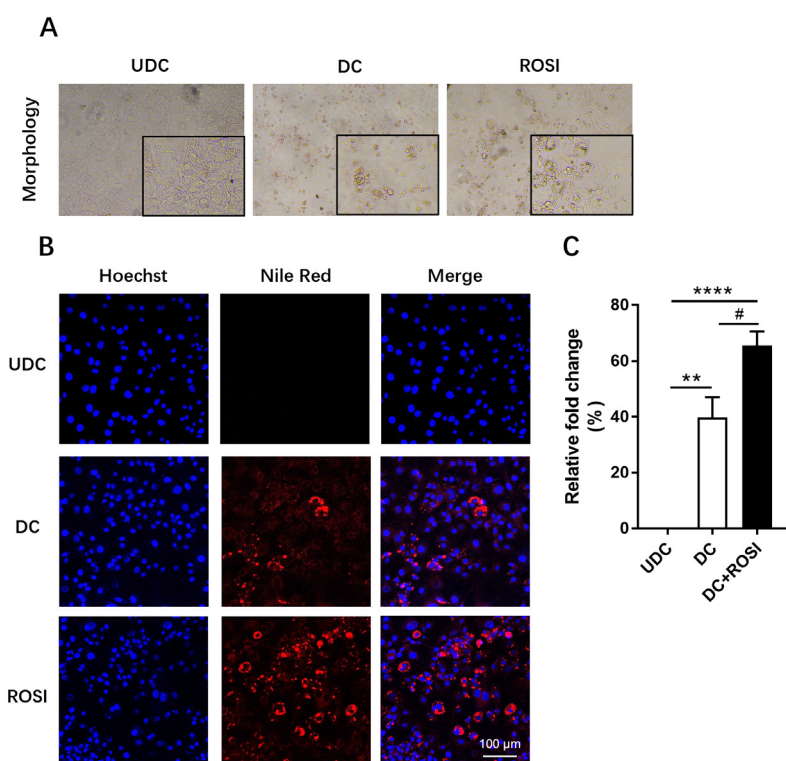
Supplementary Figure 7. Optimization of the 3T3-L1 pre-adipocyte differentiation model. 3T3-L1 cells, cultured from pre-adipocytes were differentiated with insulin and IBMX to achieve the mature adipocyte phenotype following an 8-day differentiation protocol (2 days induction of differentiation and 5 days maintenance of differentiation). Rosiglitazone (ROSI) was added as the positive control. The cell morphology was imaged on day 8 (A). In the undifferentiated control (UDC) group, the cells displayed

a fibroblast phenotype, whereas the cells in the differentiated control (DC) group were more rounded and compact. These rounded and compact cells were even more obvious in the positive control group incubated with rosiglitazone. Nuclei and lipid droplets were stained with a Hoechst (blue color) and Nile red (red color) dye, respectively (B). The Nile red fluorescent intensity was read and quantified via a fluorescent reader (C). The expression of the lipid droplets was around 40% and 60% higher in the DC group and positive control group, respectively as compared to the UDC group. Values are analyzed by one-way ANOVA, Tukey post hoc and expressed as mean±SEM, N=4. **$p < 0.01$, ****$p < 0.001$, compared with UDC; #$p < 0.05$, compared with DC.
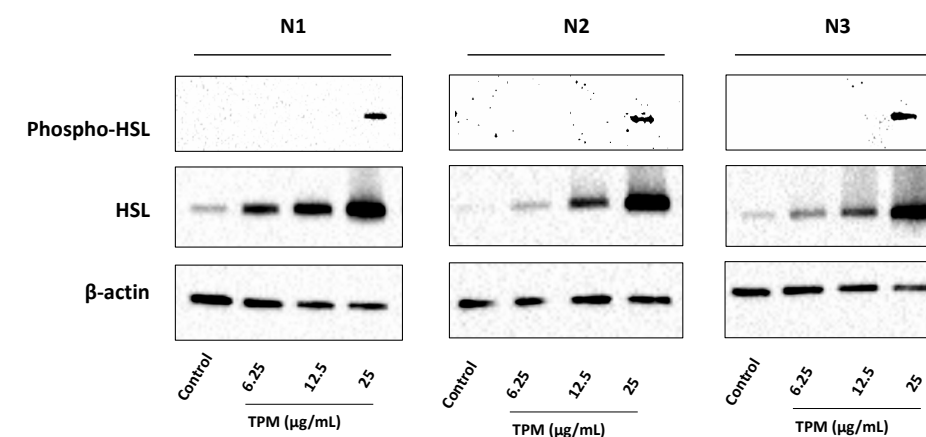
Supplementary Figure 8. Original blots of adipocytes N=3 replicates. Protein expression levels of Phospho-HSL, HSL, and β-actin were determined in adipocytes after exposure to TPM.
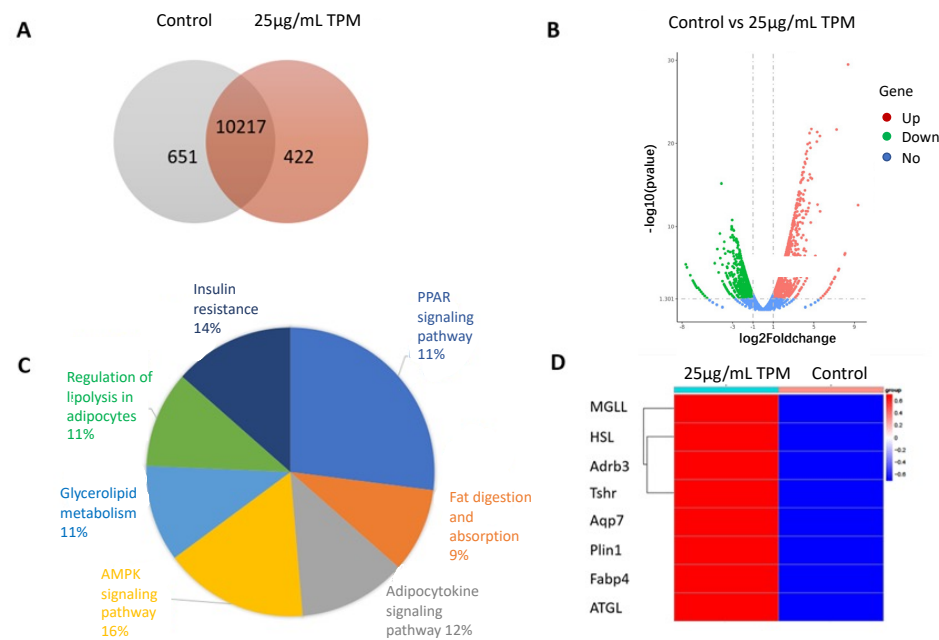
Supplementary Figure 9. Transcriptome sequencing of 3T3-L1 pre-adipocytes exposed to control medium or 25 µg/ml TPM. Control medium and 25 µg/ml TPM were added to the 3T3-L1 pre-adipocytes during the differentiation procedure of 8 days. RNA was isolated and transcriptome sequencing was performed. Venn chart of genes with significantly altered mRNA expression (A) | log2 FoldChange |>2; Volcanic chart of genes with significantly altered mRNA expression (B)| log2 FoldChange |>2; KEGG pathway enrichment analysis of genes with significantly altered mRNA expression (C)| log2 FoldChange |>5; Heatmap of genes involved in lipolysis (D) (N=1). Adrb3: Adrenoceptor beta 3; Tshr: Thyroid stimulating hormone receptor; Fabp4: Fatty Acid Binding Protein 4.
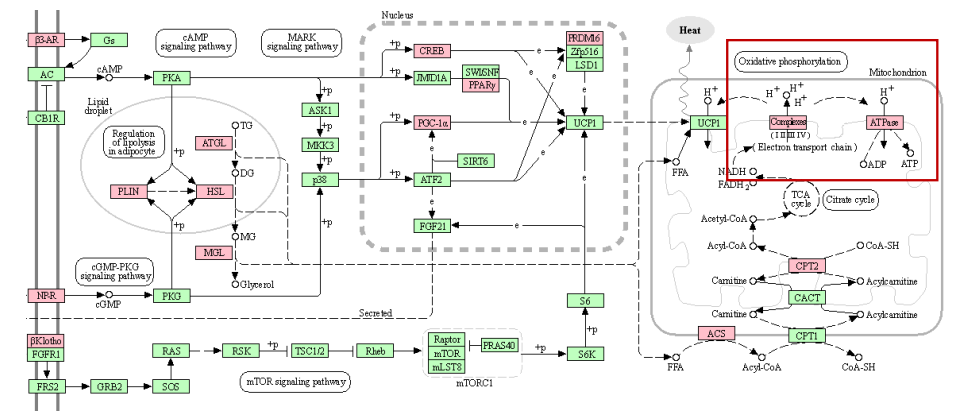
Supplementary Figure 10. KEGG pathway for mitochondrial oxidative phosphorylation of 3T3-L1 pre-adipocytes exposed to control medium or 25 µg/ml TPM. Control medium and 25 µg/ml TPM were added to the 3T3-L1 pre-adipocytes during the differentiation procedure of 8 days. RNA was isolated and transcriptome sequencing was performed. KEGG pathway enrichment analysis of genes involved in mitochondrial oxidative phosphorylation (Genes labeled in pink were significantly altered, Fold change >2).

Chapter 6

SUL-151 Decreases Airway Neutrophilia as a Prophylactic and Therapeutic Treatment in Mice after Cigarette Smoke Exposure

Lei Wang[1], Charlotte E. Pelgrim[1], Daniël H. Swart[3], Guido Krenning[2,3], Adrianus C. van der Graaf[3], Aletta D. Kraneveld[1], Thea Leusink-Muis[1], Ingrid van Ark[1], Johan Garssen[1,4], Gert Folkerts[1] and Saskia Braber[1*]

[1] Division of Pharmacology, Utrecht Institute for Pharmaceutical Sciences, Faculty of Science, Utrecht University, 3584 CG, Utrecht, The Netherlands.
[2] Cardiovascular Regenerative Medicine, Dept. Pathology and Medical Biology, University of Groningen, University Medical Center Groningen, Groningen, The Netherlands.
[3] Sulfateq B.V., Groningen, The Netherlands.
[4] Nutricia Research, Department of Immunology, Utrecht, The Netherlands.

Abstract

Chronic obstructive pulmonary disease (COPD) caused by cigarette smoke is featured by oxidative stress and chronic inflammation. Due to the poor efficacy of standard glucocorticoid therapy, new treatments are required. Here, we investigated whether the novel compound SUL-151 with mitoprotective properties can be used as a prophylactic and therapeutic treatment in a murine cigarette smoke-induced inflammation model. SUL-151 (4 mg/kg), budesonide (500 µg/kg), or vehicle were administered via oropharyngeal instillation in this prophylactic and therapeutic treatment setting. The number of immune cells was determined in the bronchoalveolar lavage (BAL) fluid. Oxidative stress response, mitochondrial adenosine triphosphate (ATP) production, and mitophagy-related proteins were measured in lung homogenates. SUL-151 significantly decreased more than 70% and 50% of cigarette smoke-induced neutrophils in BAL fluid after prophylactic and therapeutic administration, while budesonide showed no significant reduction in neutrophils. Moreover, SUL-151 prevented the cigarette smoke-induced decrease in ATP and mitochondrial mtDNA and an increase in putative protein kinase 1 expression in the lung homogenates. The concentration of SUL-151 was significantly correlated with malondialdehyde level and radical scavenging activity in the lungs. SUL-151 inhibited the increased pulmonary inflammation and mitochondrial dysfunction in this cigarette smoke-induced inflammation model, which implied that SUL-151 might be a promising candidate for COPD treatment.

Keywords
COPD; inflammation; oxidative stress; budesonide; neutrophils; SUL compound; mitochondria; PINK1; chromanol

Introduction

Chronic obstructive pulmonary disease (COPD) is a lung disease primarily characterized by the presence of airflow limitation and inflammation, due to elevated inflammatory cells, especially neutrophils, in the lungs [1]. Cigarette smoke is one of the major causes of COPD, which is responsible for chronic inflammation and mitochondria dysfunction in the lungs [2, 3]. It is well known that mitochondria are an important source of reactive oxygen species (ROS) [4]. Decreased adenosine triphosphate (ATP) and increased ROS production in dysfunctional mitochondria cause an imbalance in intracellular homeostasis [5]. Recent studies identify changes in lung cell mitochondria, including a reduction in mitochondrial biogenesis, changes in mitochondrial DNA (mtDNA), selective degradation of mitochondria, and substantial morphological defects, as contributors to COPD pathogenesis [6-11].

Glucocorticoids, β_2-adrenoceptor agonists, and muscarinic receptor antagonists are the major current therapy for COPD, which can reduce symptoms and/or exacerbations, but do not specifically target oxidative stress, nor do they diminish chronic respiratory inflammation and COPD progression or mortality in all patients [12, 13]. A large case-control study indicated that treatment of COPD with a long-acting β_2-agonist or a long-acting muscarinic antagonist was associated with a 50% higher risk of serious cardiovascular complications, including patients that had no cardiovascular disease history [14]. In addition, a large group of COPD patients have a poor response to glucocorticoids or are completely resistant [15]. Oxidative stress causes a reduction in histone deacetylase-2 (HDAC-2) activity and has been implicated as an important cause of steroid resistance in COPD [16, 17]. Therefore, there is an urgent need for the development of novel therapies that effectively suppresses chronic inflammation in COPD patients.

Recently, a novel class of pharmacological compounds, 6-hydroxychromanols, were developed, which are also called SUL compounds. SULs are water-soluble Trolox-derivatives and accumulate in the mitochondria, displaying antioxidant and mitoprotective properties by alleviating ROS production and preserving ATP production [18]. Interestingly, SUL-121 (6-hydroxy-2,5,7,8-tetramethylchroman-2-yl (piperazin-1-yl) methanone), a racemic mix of SUL compounds dose-dependently reduced LPS-induced airway neutrophilia and airway hyperresponsiveness in guinea pigs. Furthermore, it also inhibited the cigarette smoke-induced interleukin 8 (IL-8) release accompanied by a decreased cellular ROS production in human airway smooth muscle cells [19].

In this study, the efficacy of SUL-151 (Figure 1), the s-enantiomer of SUL-121, was examined in a prophylactic and therapeutic setting in mice triggered by cigarette smoke to provoke oxidative stress and neutrophilic inflammation. Budesonide was used as a standard therapy to compare with the effectiveness of SUL-151 under the same conditions. Moreover, the

mode of action of SUL-151 was explored. SUL-151 suppressed the cigarette smoke-induced lung inflammation and mitochondrial dysfunction in this study, which appears as a promising candidate for the treatment of COPD to be assessed in future (pre) clinical trials.
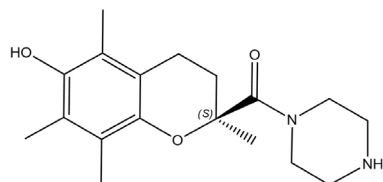

Figure 1. Chemical structure of SUL-151.

Results

Prophylactic treatment of SUL-151 prevents pulmonary inflammation in a cigarette smoke-exposure model

SUL-151 concentrations in the lungs after 5 days of oropharyngeal administration to the lungs were on average 768.3 ± 101.2 pg/mg (ranged between 125 and 2264 pg/mg protein). The levels of SUL-151 in the serum were below the lower limit of detection (i.e., <5 pg/mL, data not shown).

Cigarette smoke exposure for 5 consecutive days significantly increased the number of total bronchoalveolar lavage (BAL) fluid cells (Figure 2A), macrophages (Figure 2B), neutrophils (Figure 2C), and BAL fluid TNF-α level (Figure 2E), when compared to the air control group. SUL-151 administration for 5 days to the air-exposed animals did not significantly affect the number of neutrophils, lymphocytes, or TNF-α levels in BAL fluid; however, it doubled the number of total cells in BAL fluid, represented by an increase in macrophages (Supplementary Figure 1).

SUL-151 prophylaxis decreased the cigarette smoke-induced increase in total cells in BAL fluid (Figure 2A), wherein specifically neutrophilic infiltration was blunted (Figure 2C). Budesonide did not significantly affect the cigarette smoke-induced increase of BAL fluid total cells and neutrophils (Figure 2A, C). SUL-151 and budesonide did not affect the cigarette smoke-induced increase in the numbers of macrophages and lymphocytes in BAL fluid (Figure 2B, D); however, both compounds did reduce the TNF-α levels in BAL fluid (Figure 2E).
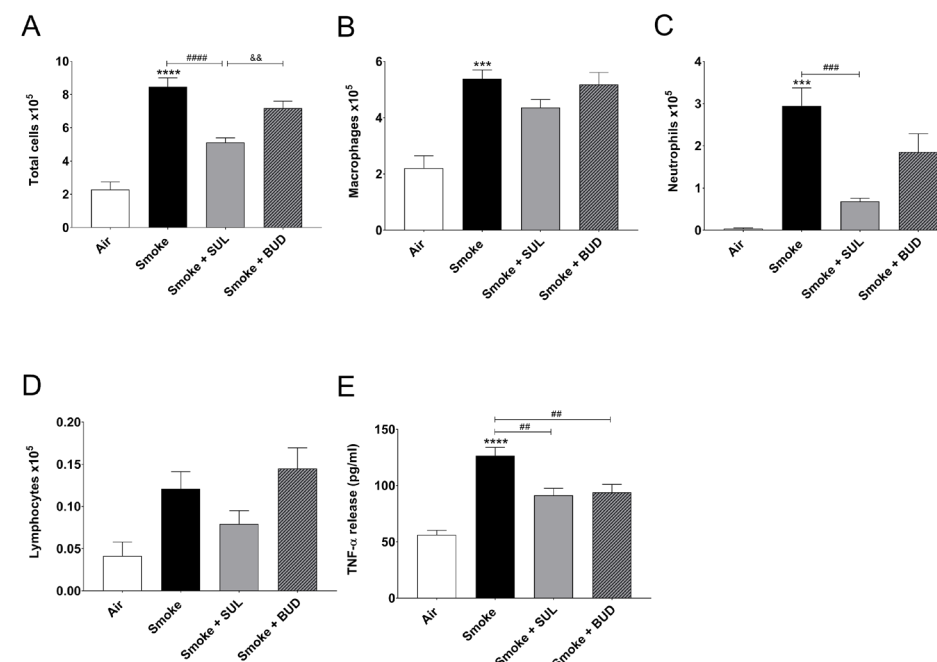
Figure 2. Prophylactic SUL-151 administration prevents pulmonary inflammation in a cigarette smoke exposure model. Mice were exposed to cigarette smoke for 5 days (twice/day) and received SUL-151 or budesonide via oropharyngeal administration (once/day) 30 min before the first-time smoke exposure during these 5 days. On day 6, lungs were lavaged, and BAL fluid was collected for total (**A**) and differential BAL fluid cell counts, including macrophages (**B**), neutrophils (**C**), and lymphocytes (**D**), and TNF-α levels (**E**) were measured in BAL fluid. Values are expressed as mean ± SEM. ***$p < 0.001$, ****$p < 0.0001$, smoke group compared to air group; ##$p < 0.01$, ###$p < 0.001$, ####$p < 0.0001$, smoke + SUL group or smoke + budesonide (BUD) group compared to smoke group; &&$p < 0.01$, smoke + BUD group compared to smoke + SUL group. $n = 4–8$ mice/group.

Prophylactic treatment of SUL-151 prevents oxidative stress in the lungs of cigarette smoke-exposed mice

Cigarette smoke exposure for 5 consecutive days decreased the radical scavenging activity (Figure 3A) and increased the MDA levels (Figure 3B). In addition, a decrease in mtDNA (Figure 3C) and ATP (Figure 3D) was observed in the lung homogenates after cigarette smoke exposure when compared to air-exposed mice. SUL-151 tended to increase the cigarette smoke-induced decrease in radical scavenging capacity ($p = 0.0771$), but budesonide did not affect the cigarette smoke-induced decrease in radical scavenging capacity ($p = 0.2819$) (Figure 3A), while both reduced the cigarette smoke-induced increase in MDA in lung tissue (Figure 3B). SUL-151, but not budesonide, attenuated the loss of mitochondria by restoring the copy numbers of mtDNA (Figure 3C) and restored ATP production in lung tissue of cigarette smoke-exposed mice (Figure 3D).
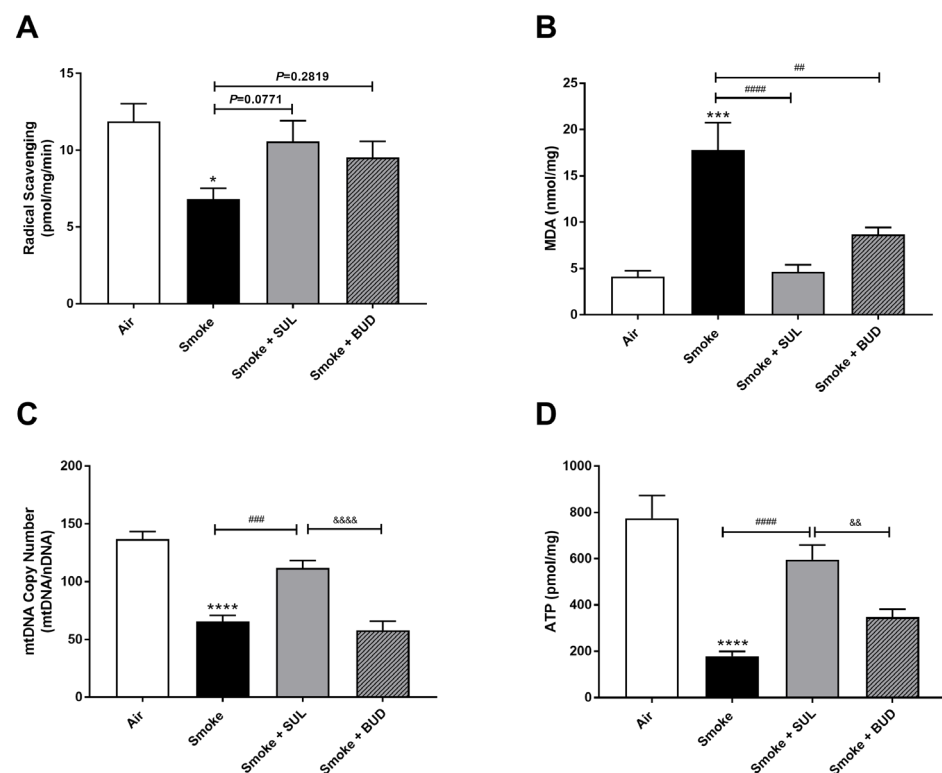
Figure 3. Prophylactic SUL-151 administration prevents oxidative stress in the lungs of a cigarette smoke exposure model. Mice were exposed to cigarette smoke for 5 days (twice/day) and received SUL-151 or budesonide via oropharyngeal administration 30 min before the first-time smoke exposure during these 5 days. On day 6, lung tissue was collected, and the radical scavenging activity (**A**), MDA concentration (**B**), mtDNA copy numbers (**C**), and ATP levels (**D**) were measured. Values are expressed as mean ± SEM. *$p < 0.05$, ***$p < 0.001$, ****$p < 0.0001$, smoke group compared to air group; ##$p < 0.01$, ###$p < 0.001$, ####$p < 0.0001$, smoke + SUL group or smoke + budesonide (BUD) group compared to smoke group; &&$p < 0.01$, &&&&$p < 0.0001$, smoke + BUD group compared to the smoke + SUL group. n = 4–8 mice/group.

SUL-151 reduces the influx of neutrophils in the BAL fluid after the development of cigarette smoke-induced pulmonary inflammation

Based on the promising effects of SUL-151 prophylaxis in the cigarette smoke exposure model, the effect of SUL-151 was further explored in a therapeutic setting. Mice were first exposed to cigarette smoke for 5 days without therapy, followed by 5 days of cigarette smoke exposure with the same therapies as described for the prophylactic approach. The number of total BAL fluid cells (Figure 4A), macrophages (Figure 4B), and neutrophils (Figure 4C) were significantly increased after 10 days of cigarette smoke exposure, compared to the air-exposed group, while a slight effect of cigarette smoke exposure was observed on the number of lymphocytes in BAL fluid.

Both the treatment with SUL-151 and budesonide did not significantly affect the cigarette smoke-induced increase in the number of total cells, macrophages, and lymphocytes in the BAL fluid (Figure 4 A,B,D). No differences were observed in TNF-α levels in BAL fluid (data not shown). SUL-151, but not budesonide, was able to significantly reduce the cigarette smoke-induced influx of neutrophils in the second set of 5 days cigarette smoke exposure (day 10, Figure 4C) to a similar degree as in the prophylactic setting (Figure 2C).

Figure 4. SUL-151 reduces the influx of neutrophils in the BAL fluid after the development of cigarette smoke-induced pulmonary inflammation. Mice were exposed to cigarette smoke for 10 days (twice/day) and received SUL-151 or budesonide via oropharyngeal administration (once/day) 30 min before the first-time smoke exposure during the last 5 days of the cigarette smoke exposure period. On day 11, lungs were lavaged, and BAL fluid was collected for total (**A**) and differential BAL cell counts, including macrophages (**B**), neutrophils (**C**), and lymphocytes (**D**). Values are expressed as mean ± SEM. **$p < 0.01$, ***$p < 0.001$, ****$p < 0.0001$, smoke group compared to air group; #$p < 0.05$, smoke + SUL group or smoke + budesonide (BUD) group compared to smoke group. n = 6–7 mice/group.

SUL-151 reduces the oxidative stress in the lungs after the development of cigarette smoke-induced pulmonary inflammation

The radical scavenging activity was decreased (Figure 5A), and MDA levels were increased (Figure 5C) in the lungs after cigarette smoke exposure. Moreover, the mtDNA copy numbers (Figure 5E) and the ATP levels (Figure 5F) were decreased in the lung homogenates 10 days after cigarette smoke exposure. As observed in the prophylactic setting, SUL-151 tended to restore the cigarette smoke-induced changes in the radical scavenging ability (p = 0.0513, Figure 5A), and both SUL-151 and budesonide decreased MDA levels in the lungs obtained from the mice of the therapeutic approach (Figure 5C). The increase in scavenging activity and the reduction of lipid peroxidation products observed in individual mice correlated to the concentration of SUL-151 in the lung homogenates (Figure 5B and 5D, respectively). Interestingly, SUL-151, significantly restored mtDNA copy numbers and ATP levels in the cigarette smoke-exposed mice, while budesonide was not effective at restoring mtDNA or ATP levels (Figure 5E, F).

0.001, ****p < 0.0001, smoke group compared to air group; ###p < 0.001, ####p < 0.0001, smoke + SUL group or smoke + budesonide (BUD) group compared to smoke group; &p < 0.05, smoke + BUD group compared to smoke + SUL group. n = 6–7 mice/group.

SUL-151 inhibits the increase in PINK1-expression in the lungs after the development of cigarette smoke-induced pulmonary inflammation

Parkin, a ubiquitin–protein ligase, and PTEN-induced putative kinase 1 (PINK1), a mitochondrial serine–threonine kinase, both exhibit protection against oxidative stress and act in a common mitophagy pathway [20,21]. The expression of PINK1 was significantly increased after 10 days of cigarette smoke exposure. SUL-151, but not budesonide, significantly inhibited the cigarette smoke-induced increase in PINK1 protein expression (Figure 6A, B). Cigarette smoke did not significantly change the Parkin protein expression in lung tissue (Figure 6A, C), while budesonide, but not SUL-151, further decreased the Parkin protein expression compared with the cigarette smoke-exposed group.
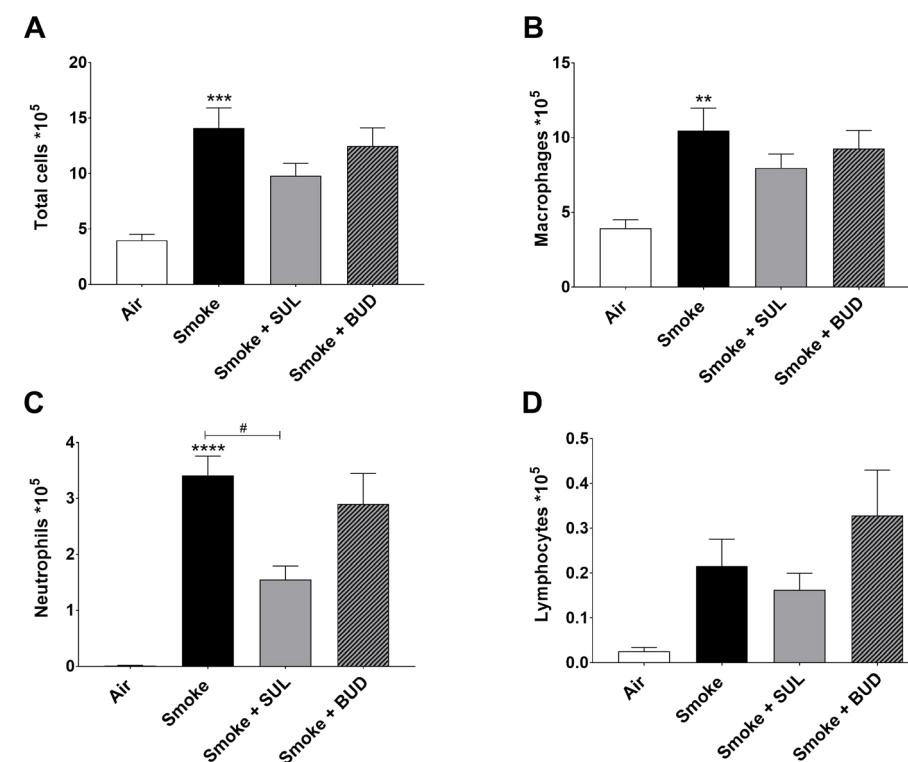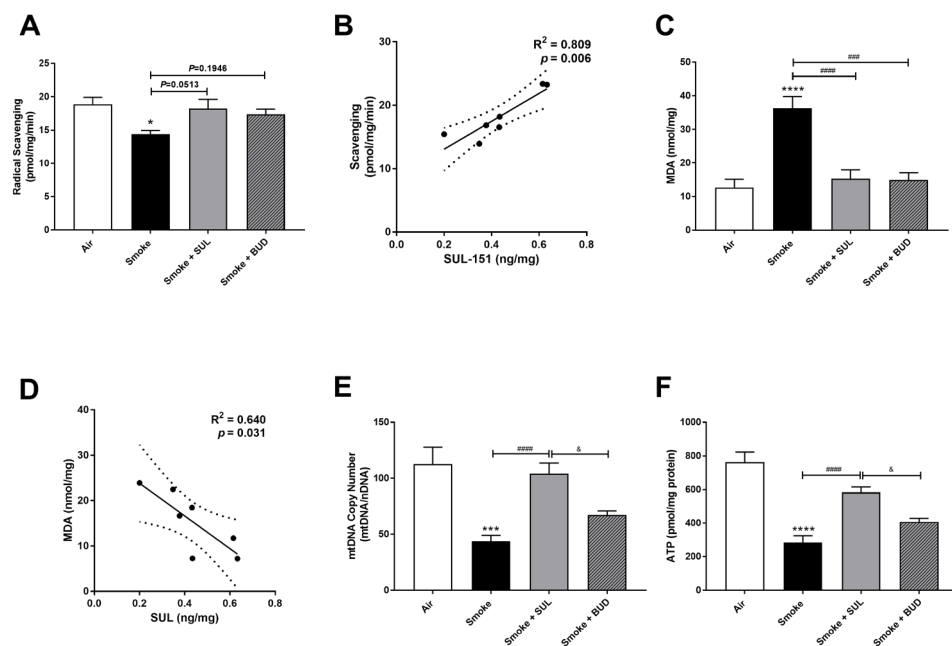

Figure 5. SUL-151 reduces the oxidative stress in the lungs after the development of cigarette smoke-induced pulmonary inflammation. Mice were exposed to cigarette smoke for 10 days (twice/day) and received SUL-151 or budesonide via oropharyngeal administration (once/day) 30 min before the first smoke exposure during the last 5 days of the cigarette smoke exposure period. On day 11, lung tissue was collected, and the radical scavenging activity (A), MDA concentration (C), mtDNA copy numbers (E), and ATP levels (F) were measured. Correlation of radical scavenging activity and SUL-151 concentration in lung tissue (B) and the correlation of MDA and SUL-151 concentration in lung tissue (D) analyzed using Pearson r correlation test. Values are expressed as mean ± SEM. *p < 0.05, ***p <

Figure 6. SUL-151 inhibited the increase in PINK1-expression in the lungs after the development of cigarette smoke-induced pulmonary inflammation. Mice were exposed to cigarette smoke for 10 days (twice/day) and received SUL-151 or budesonide via oropharyngeal administration (once/day) 30 min before the first smoke exposure during the last 5 days of the cigarette smoke period. Western blot analysis for protein levels of PINK1, Parkin, and α-tubulin (A) was measured in the lung homogenates, and relative densities of the PINK1/α-tubulin (B) and Parkin /α-tubulin (C) were calculated. Values are expressed as mean ± SEM. ***p < 0.001, smoke group compared to air group; #p < 0.05, smoke + SUL group or smoke + budesonide (BUD) group compared to smoke group; &p < 0.05, smoke + BUD group compared to smoke +SUL group. n = 6–7 mice/group.

SUL-151 hardly affects KC levels in lung homogenates but concentration-dependently inhibits IL8-production in human bronchial epithelial cells

To find a link between the reduced oxidative stress and decrease in BAL fluid neutrophil numbers, KC levels were measured in lung homogenates. Indeed, cigarette smoke induced an increase in KC levels in the lungs. However, this cigarette smoke-induced increase in KC levels was hardly affected by SUL-151 or budesonide as a prophylactic or therapeutic treatment (Figure 7A, B).

To further explore the effect of SUL-151 on IL-8 production, human bronchial epithelial (16HBE) cells were stimulated with cigarette smoke extract (CSE). IL-8 production was significantly enhanced after CSE exposure for 24 h. Surprisingly, SUL-151 concentration-dependently decreased the CSE-induced IL-8 production (Figure 7C).
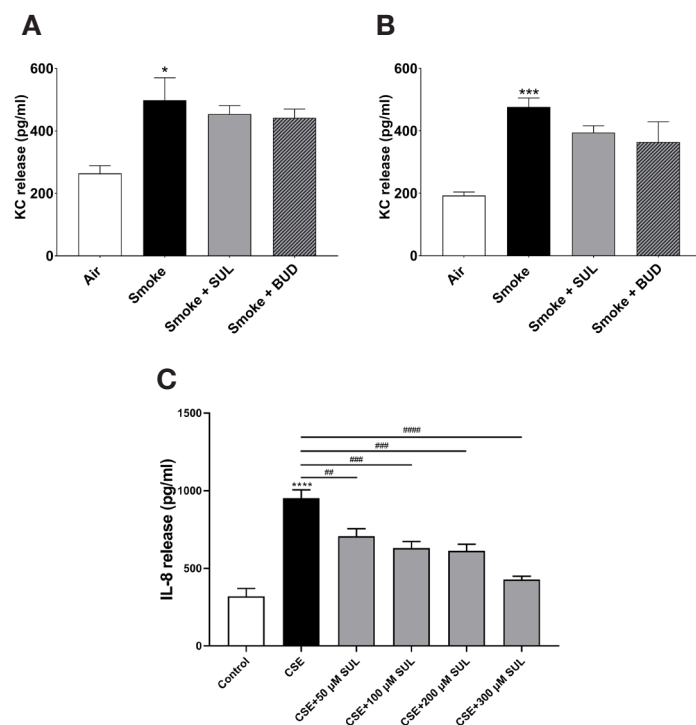
Figure 7. SUL-151 hardly affects KC levels in lung homogenates but concentration-dependently inhibits IL-8 production in human bronchial epithelial cells. Mice were exposed to cigarette smoke for 5 days (twice/day) and received SUL-151 or budesonide via oropharyngeal administration 30 min before the first-time smoke exposure during these 5 days (**A**) or mice were exposed to cigarette smoke for 10 days (twice/day) and received SUL-151 or budesonide via oropharyngeal administration (once/day) 30 min before the first smoke exposure during the last 5 days of the cigarette smoke period (**B**). KC levels were measured in the lung homogenates via ELISA measurement. Human bronchial epithelial cells (16HBE cells), grown on 96-well plates, were preincubated with different concentrations of SUL-

151 (50, 100, 200, and 300 µM) (24h) prior to CSE exposure for 24 h. Thereafter, IL-8 secretion was measured in the supernatants (**C**). Values are expressed as mean ± SEM. *$p < 0.05$, ***$p < 0.001$, ****$p < 0.0001$, smoke/CSE group compared to air/control group; ##$p < 0.01$, ###$p < 0.001$, ####$p < 0.0001$, CSE group compared to the CSE + SUL group. $n = 4$–8 mice/group in vivo, $n = 5$, in vitro.

Discussion

COPD is one of the most common lung diseases worldwide, characterized by an accelerated loss of lung function [1]. Neutrophilic inflammation, a central feature of COPD, is closely associated with the severity of peripheral airway dysfunction in COPD [22]. Long-acting antimuscarinics or long-acting β_2-adrenoceptor agonists, with or without inhaled glucocorticoids, are suggested by the COPD guidelines [23]. Clinical studies indicate that inhaled budesonide can be a good alternative for patients with acute exacerbation of chronic obstructive pulmonary disease [24]. These strategies reduce respiratory symptoms and exacerbations but do not affect the disease progression or suppress the sustained inflammation. In addition, most COPD patients respond poorly to high doses of inhaled or oral glucocorticoids. PDE4 inhibitors are new therapeutic options for COPD and a few new candidates, such as the dual PDE3/PDE4 inhibitor Ensifentrine, entered a phase 3 clinical trial, but none has yet reached the market. Therefore, there is an urgent need for the development of safe and effective new drugs for patients with COPD.

Recently, a novel class of pharmacological compounds was developed of which SUL-121 was one of the lead structures exhibiting promising mitoprotective effects due to the antioxidative capacities [25]. Our colleagues of the University of Groningen examined the pharmacological potential of SUL-121 in in vivo experimental airway inflammation models and showed that SUL-121 could prevent airway neutrophilia in BAL fluid, airway hyperresponsiveness, and oxidative stress in the airways caused by LPS in a guinea pig model. SUL-121 also exhibited the capacity to inhibit the cigarette smoke-induced IL-8 release in cultured human airway smooth muscle cells, which was associated with an inhibition of cellular ROS generation and a decrease in nuclear translocation of Nrf2 [19]. Based on these findings, we now explored the efficacy of the s-enantiomer of SUL-121, SUL-151, in a murine model of cigarette smoke-induced lung inflammation. SUL-151 was administered into the airways for 5 days during cigarette smoke exposure and the therapeutic possibilities were investigated by first exposing the mice to cigarette smoke for 5 days without treatment followed by 5 days cigarette smoke exposure with SUL-151 treatment. The efficacy was compared with the standard COPD treatment: the glucocorticoid budesonide.

SUL-151 was administrated oropharyngeally to the lungs and was detected in the lung, which indicated that oropharyngeal administration is an effective route to target the lung in this model. The concentration of SUL-151 in the serum was lower than the detection limit,

which might indicate that the compound remained and functioned in the lungs without leakage into the systemic compartment and was completely metabolized in the lungs with no parent molecule present in the serum or was cleared at the endpoint of the study.

Neutrophilic inflammation is an important hallmark for COPD [22], which has been extensively associated with disease pathogenesis and progression [26]. As expected on the basis of earlier results with SUL-121 [19], SUL-151 significantly decreased the number of neutrophils in the BAL fluid by more than 70% when used prophylactically and by ~50% when used therapeutically. In contrast, budesonide did not significantly decrease the number of neutrophils in the BAL fluid, although the efficacy of this dose of budesonide (500 μg/kg) was confirmed in a murine asthma model [27] and in an LPS-induced acute lung injury model [28]. This dose seems rather ineffective in the cigarette smoke-induced inflammation model and glucocorticoid insensitivity might be developed, as observed in the neutrophil influx.

Due to the activation of inflammatory cells, during the inflammatory process in the lungs of COPD patients, oxidative stress is induced, which causes an oxidant/antioxidant imbalance [29]. Oxidative stress, including elevated ROS levels, is a major mechanism driving airway inflammation and airway damage in the pathophysiology of COPD [30,31]. A possible mechanism by which oxidants can cause lung injury is via lipid peroxidation [32]. MDA, a lipid peroxidation product, which is linked to the severity of COPD [33,34], was significantly increased after 5 and 10 days of cigarette smoke exposure. Exhaled ethane, a marker for lipid peroxidation, is also elevated in COPD patients and correlates with FEV_1 [35]. Moreover, serum MDA concentration correlates with FEV_1 and disease severity in patients with COPD [36]. In our study, budesonide significantly decreased the cigarette smoke-induced MDA increase in the lungs, which is in an agreement with the study of Zhang et al. [37], who showed that budesonide decreases MDA levels by scavenging free radicals and ROS in a bronchitis model with rats [37]. Compared to budesonide, SUL-151 inhibited the cigarette smoke-induced MDA levels in the lungs and prevented the cigarette smoke-induced decrease in ATP and mtDNA copy numbers, emphasizing that SUL-151 may influence the mitophagy pathway.

The observed decrease in ATP after cigarette smoke exposure can be caused by damage to mitochondria, which is associated with lipid peroxidation, mitochondrial swelling, and disrupted mitochondrial respiratory chain [38,39]. The cigarette smoke-induced decrease in ATP production and mtDNA copy numbers in the lungs was consistent with previous research findings [40,41]. mtDNA, as a specific genome of mitochondria, can present thousands of copies and form parts of the respiratory chain complex but are vulnerable due to the lack of protective histones and the capacity of DNA repairment [42]. Cigarette smoke is one of the main factors for oxidative stress in COPD, which can lead to mtDNA damage, mutation, and

mitochondrial dysfunction in the lung [43]. We show here that, compared to budesonide, SUL-151 protects mitochondria in the lungs from cigarette smoke-induced damages, as observed in the maintenance of both mtDNA copy numbers and ATP production.

The damaged mitochondria and mitochondrial dysfunction caused by cigarette smoke might be related to mitophagy. Mitophagy is considered as a mechanism of selectively delivering the damaged mitochondria for lysosomal degradation, which is regulated by the PINK1-Parkin pathway. The PINK1–Parkin-dependent mitophagy might be involved in the pathogenesis of COPD [3,21]. In unhealthy mitochondria, the inner mitochondrial membrane becomes depolarized, which causes PINK1 to accumulate in the outer mitochondrial membrane. Increased mitophagy is related to the Parkin translocation to the damaged mitochondria, accompanied by PINK1 accumulation [11,44]. In our experiment, PINK1 accumulation was found after cigarette smoke exposure, which was reduced by SUL-151 but not budesonide. Moreover, although Parkin levels were not significantly affected by cigarette smoke exposure, budesonide, but not SUL-151, further decreased the level of Parkin. The decreased Parkin might indicate less effective mitophagy, thus leading to more damaged mitochondria accumulated in the lung.

To link the reduction in oxidative stress with the decreased number of neutrophils in the BAL fluid, KC levels were measured in lung homogenates. Unfortunately, SUL-151 did not significantly reduce the cigarette smoke-induced increase in KC levels. In contrast, the *in vitro* data on human bronchial epithelial cells showed that SUL-151 concentration-dependently inhibits IL-8 levels after CSE stimulation. Similar results were obtained with airway smooth muscle cells [19]. However, it has to be stressed that *in vivo*, the mice were exposed to cigarette smoke twice a day and SUL-151 was only administered once, 30 min before the first cigarette smoke exposure. It cannot be excluded that SUL-151 was more effective during the first cigarette smoke challenge and inhibited KC production and hence the influx of neutrophils, while during the second cigarette smoke exposure, SUL-151 was less effective since SUL-151 concentration dropped over time, leading to KC production and corresponding neutrophil influx.

This is supported by the fact that the influx of neutrophils was partly reduced by SUL-151 (50–70%). In our *in vitro* experiments, it was clearly demonstrated that SUL-151 almost completely decreased the CSE-induced IL-8 production in human bronchial epithelial cells. Based on these results, it is tempting to speculate that the effectiveness of SUL-151 might be further increased when administered twice daily.

As mentioned before, oxidative stress is proposed as the basis for the development of COPD following exposure to cigarette smoke [45]. Cigarette smoke increases the burden of oxidants in the respiratory tract, either directly included in cigarette smoke [46] or generated

by inflammatory cells, depleting antioxidant defenses and injuring lung cells and beyond [11]. Although promising results of antioxidants have been highlighted by Fisher et al. (2015), this group of medicines in the treatment of COPD has not reached the market yet. SUL-151, however, as mentioned above, specifically prevents ROS production in the mitochondria, which may maintain the mitochondrial function and dampen subsequent inflammatory processes. Targeting oxidative stress in mitochondria might offer opportunities as a future therapy, especially since the consequent specific neutrophilic inflammation was tremendously suppressed. Such a pronounced reduction in an ongoing airway inflammation has not been demonstrated before with regular interventions, such as antioxidant treatments. Glucocorticoids are the most effective anti-inflammatory therapy, yet are relatively ineffective in COPD patients [47]. Various molecular mechanisms of glucocorticoid resistance have been characterized, which are associated with post-translational modifications of the glucocorticoid receptor. Due to the oxidative/nitrative stress, the activity and expression of HDAC-2 are noticeably inhibited, leading to a relative resistance to the anti-inflammatory actions of glucocorticoids [48]. Therefore, it would be interesting to further investigate whether an SUL-151 treatment or pretreatment with SUL-151 before glucocorticoid administration can treat COPD and prevent the development of glucocorticoid insensitivity, respectively. Due to the fact that the mode of action of SUL-151 is different from that of phosphodiesterase-4 inhibitors, combination therapies with this group of medicines may also be interesting [49].

This study supports the hypothesis that SUL-151, a mitoprotective compound with modest antioxidant capacity, exerts anti-inflammatory effects by normalizing oxidative stress (Figure 8 depicts a schematic overview of the postulated mechanism of SUL-151), and it might be a promising therapeutic option in the treatment of COPD.
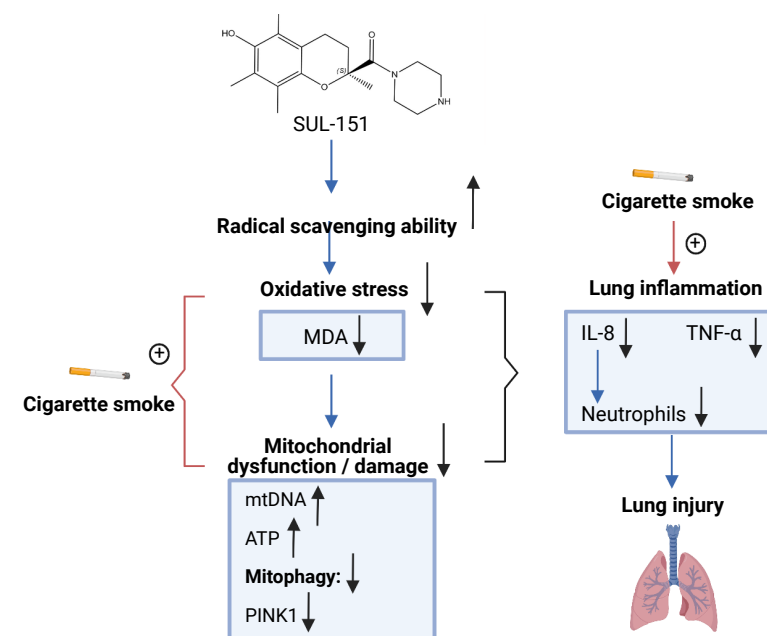
Figure 8. Schematic overview of the postulated mechanism of SUL-151 on cigarette smoke-induced lung inflammation. SUL-151 has the ability to increase radical scavenging in the airways, possibly leading to a decrease in the cigarette smoke-induced oxidative stress as measured by inhibition in MDA levels in lung homogenates. The decrease in oxidative stress might lead to a decrease in mitochondrial dysfunction/damage, as observed by the increase in mtDNA, the capacity to produce more ATP in the lungs, and the mitoprotective properties measured by a decrease in PINK1 expression. In this regard, the cigarette smoke-induced oxidative stress and mitochondrial dysfunction can be inhibited by SUL-151, in turn leading to a decrease in cigarette smoke-induced lung inflammation.

Materials and Methods

Animals

Specific-pathogen-free female Balb/c mice, 8–10 weeks old, were obtained from Charles River Laboratories and housed under standard conditions on a 12 h light/dark cycle in filter-topped Makrolon cages at the animal facility of the Utrecht University. Food and water were provided ad libitum and mice were randomly divided into experimental groups (n = 4–8 mice/group for the prophylactic approach and n = 6–7 mice/group for the therapeutic approach). All animal procedures described in this study were approved by the independent ethics committee for animal experimentation (the Ethical Committee of Animal Research of Utrecht University, Utrecht, the Netherlands) (DEC number: AVD243002016408) on 14th of March 2016 and were conducted in accordance with the governmental guidelines.

Experimental in vivo procedures

In this study, two cigarette smoke exposure experiments were conducted: 1) the prophylactic approach, in which SUL-151 (4 mg/kg), budesonide (500 µg/kg) [27], or vehicle (saline) was administered via the oropharyngeal route 30 min before the first cigarette smoke exposure daily for 5 consecutive days to investigate the anti-inflammatory and antioxidative effects of SUL-151 (SUL-151 administration during the induction of the disease, Figure 9A) and 2) the therapeutic approach, in which mice were first exposed to cigarette smoke for 5 days without treatment, followed by 5 days of cigarette smoke exposure with the different therapies (once daily, 30 min before the first cigarette smoke exposure) and a possible anti-inflammatory and antioxidative therapeutic approach of SUL-151 and associating potential mechanism were investigated (SUL-151 after induction of the disease, Figure 9B).

Mice were exposed in whole-body chambers to air or to mainstream cigarette smoke for 5 or 10 consecutive days (twice a day) using a peristaltic pump (SCIQ 232, Watson-Marlow 323, USA) at speed 35 rpm [50]. Research cigarettes (3R4F) were obtained from the Tobacco Research Institute (University of Kentucky, Lexington, Kentucky), and filters were removed before use. Mice were exposed to either cigarette smoke or to ambient air twice daily with a minimum interval of 5 h using 4–6 cigarettes on day 1, 8–10 cigarettes on day 2, 12–14 cigarettes on day 3, and 14 cigarettes till the end of the smoke exposure period (two cigarettes/round). Cigarette smoke exposures were analyzed periodically for carbon monoxide (CO), ranging between 200 and 400 ppm. The mass concentration of cigarette smoke total particulate matter (TPM) was determined by gravimetric analysis of type A/E glass fiber filter (PALL life sciences, Mexico) [51]. The TPM concentration in the smoke exposure box generated by 14 cigarettes reached approximately 828 µg/L (828 ± 4.5 µg/L).

Mice were killed by an intraperitoneal overdose of pentobarbital approximately 18 h hours after the last air or smoke exposure. Blood was obtained by heart puncture and collected in Mini collect tubes (Greiner Bio-One, Alphen aan den Rijn, the Netherlands). Blood samples were centrifuged (14000 rpm for 10 min) and serum was stored at –20°C. Lungs were collected, snap-frozen in liquid nitrogen, and kept at –80 °C until further analyses.
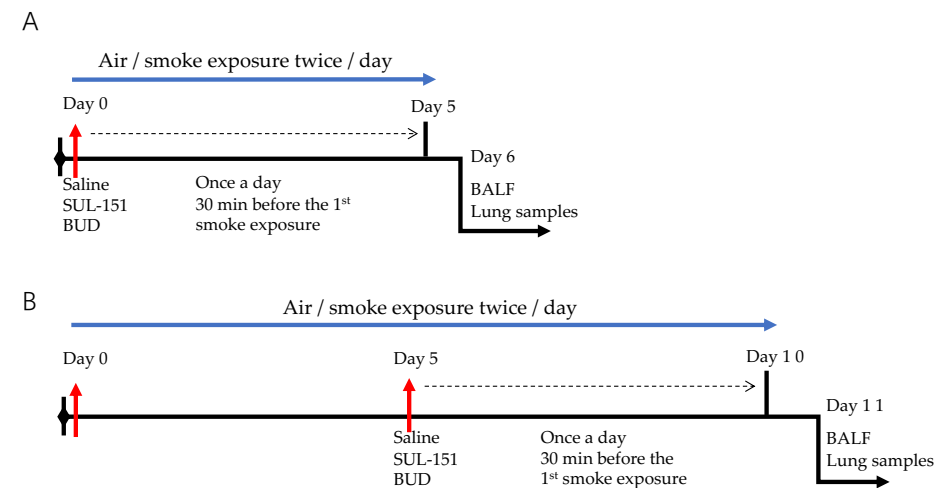
Figure 9. Schematic overview of the experimental design for the prophylactic treatment (A) and therapeutic treatment (B) of vehicle (saline), SUL-151, and budesonide (BUD) in the cigarette smoke exposure model. The blue line represents the smoke exposure procedure (twice a day); the dotted line represents the saline, SUL-151, and BUD treatment (once a day, 30 min before the first round of smoke exposure).

Bronchoalveolar lavage fluid

Directly after blood sample collection, the trachea was exposed, and a cannula was inserted in the trachea after making a small incision. BAL fluid was collected by lung lavage with 1 mL pyrogen-free saline (0.9% NaCl, 37°C), supplemented with protease inhibitors (Complete Mini, EDTA-free Protease Inhibitor Cocktail, Sigma-Aldrich, Zwijndrecht, the Netherlands). This step was repeated three times with 1 mL pyrogen-free saline. The BAL fluid was centrifuged (400 × g, 4°C, 5 min) and the supernatant of the first mL was stored at –20°C for ELISA measurement, and the pellets of the four lavages were pooled. Total numbers of BAL fluid cells were counted using a Bürker-Türk chamber and differential BAL fluid cell counts of macrophages, neutrophils, lymphocytes, and eosinophils were determined on cytospin preparations stained by Diff-Quik (Merz & Dade A.G., Düdingen, Switzerland). Differential cell counts were performed with at least 200 cells [52]. The first 1ml BAL fluid was used for TNF-α measurements by ELISA (Mouse TNF-α ELISA kit, Thermo Fisher Scientific, Waltham, MA, USA) according to the manufacturer's instructions.

Radical scavenging activity, lipid peroxidation product malondialdehyde (MDA), and ATP measurements

Lung samples were homogenized in ddH$_2$O using a TissueRuptor II (Qiagen, Hilden, Germany), followed by sonication at 20 kHz for 3 times 1 min (Sonopuls 2000, Bandelin, Berlin, Germany) and centrifugation at 14000 g to pellet insoluble proteins. The supernatant

was used to assess radical scavenging activity by ABTS radical decolorization [53], and lipid peroxidation by assessing the reactivity to thiobarbituric acid [19]. ATP content was determined using the ATP Determination Kit (Thermo Fisher Scientific, Waltham, MA, USA) according to manufacturer's instructions. The total protein content of the supernatants was determined by DC Protein Assay (Bio-Rad, Hercules, CA, USA) and used for data normalization.

mtDNA copy number

Lung samples were homogenized in DNA isolation buffer (100 mM NaCl, 10 mM EDTA, 0.5% SDS in 20 mM Tris-HCl, pH 7.4) containing 50 U·mL^{-1} RNase I and 100 U·mL^{-1} proteinase K (both Fermentas, Waltham, MA, USA). After overnight incubation at 55°C, total DNA was precipitated using 2-propanol. Aliquots of 10 ng DNA were amplified on a ViiA7 Real-time PCR system (Thermo Fisher Scientific, Waltham, MA, USA) using iTaq Universal SYBR Green Supermix (Bio-Rad, Hercules, CA, USA) and primers specific for mitochondrial DNA (MT-ND1; sense 5'-CGCCATAGCCTTCCTAACAT-3', antisense 5'-ATGCCGTATGGACCAACAAT-3') or nuclear DNA (NDUFA1; sense 5'-CCCCATGCTCTATCCATGTT-3', antisense 5'-GCCATTTCTCTGCCTCTCAC-3'). Amplification was performed for 40 cycles of 15 s at 95°C for denaturation, and 1 min at 60°C for annealing and elongation. MtDNA copy number was calculated as mtDNA = $2 \times 2^{(Cq(NDUFA1)-Cq(MT-ND1))}$

Immunoblotting

Lung samples were homogenized in Radioimmunoprecipitation Assay (RIPA) buffer containing 0.5% proteinase inhibitor cocktail (Sigma-Aldrich, St. Louis, MO, USA) and 0.5% Halt™ phosphatase inhibitor (Thermo Fisher Scientific, Waltham, MA, USA) using a TissueRuptor II (Qiagen, Hilden, Germany), followed by sonication at 20 kHz for 3 × 30 s (Sonopuls 2000, Bandelin, Berlin, Germany) and centrifugation at 14000 g to pellet insoluble proteins. The total protein content of the supernatants was determined by DC Protein Assay (Bio-Rad, Hercules, CA, USA). 10 µg of total protein per sample were loaded on mini-PROTEAN precast gradient gels (4–15% denaturing SDS–polyacrylamide gel; Bio-Rad, Hercules, CA, USA), separated by gel electrophoresis and blotted onto nitrocellulose membrane using the Trans-Blot Turbo System (Bio-Rad, Hercules, CA, USA) according to standard protocols. Blots were blocked with 5% bovine serum albumin in 20 mM Tris-HCl (pH 7.4) at room temperature for 30 min and incubated at 4 °C overnight with primary antibodies to PINK1 (BC100-494, Bio-Techne, Abingdon, UK), PARKIN (Santa Cruz Biotechnology, Dallas, TX, USA) or Tubulin (Sigma-Aldrich, St. Louis, MO, USA), all at a dilution of 1:500. Alkaline phosphatase-conjugated secondary antibodies and NBT/BCIP (Bio-Rad, VA, USA) were used for detection. Densitometric analysis was performed using Totallab 120 (Nonlinear Dynamics, Newcastle upon Tyne, England) [54].

Assessment of SUL-151 levels in serum and lung

Measurement of SUL-151 levels in the serum and in lung tissue homogenates was performed by chromatography and mass spectrometry. Serum or lung tissue homogenates were supplemented with acetonitrile and sonicated, followed by centrifugation at 14000 g to liberate SUL-151 from the samples and pellet protein precipitates. Tissue samples were subjected to additional solid-phase extraction using an SPE Strata C-18 cartridge (100 mg, 55 µm, 70Å, Phenomenex, Torrance, CA, USA), prepared with 1 mL methanol, followed by 1 mL water. Analytes were eluted in acetonitrile:methanol (3:7 v/v). Analyte recovery was >70%. Liquid chromatography of the samples was performed on a 1260 Infinity HPLC device (Agilent Tech., Santa Clara, CA, USA) using a ZORBAX Eclipse AAA column (3.0x150 mm, particle size 3.5 µm) in a reversed-phase setup and a flow rate of 0.5 mL·min^{-1}. Solvents consisted of methanol (6%): acetonitrile (4%) acetate and methanol (54%): acetonitrile (36%) in water with 0.1% ammonium for solvent A and B, respectively. MS/MS detection was performed on a QQQ 6460 mass spectrometer (Agilent Tech., Santa Clara, CA, USA). Detection was set for a quantifier ion (205.1, CE 25V) and a qualifier ion (190.1, CE 40V). Gas temperature for MS was set to 300°C and flow was set to 6 L·min^{-1}. Quantification of the samples was performed using an external standard for calibration. Limit of detection (LoD) and limit of quantitation (LoQ) were 5 pg·mL^{-1} and 17 pg·mL^{-1}, respectively.

KC measurement in the lung homogenates

The lungs were homogenized in cold 1% Triton X-100 (Sigma-Aldrich)/PBS solution containing protease inhibitors (Complete Mini, EDTA-free Protease Inhibitor Cocktail, Sigma-Aldrich, Zwijndrecht, the Netherlands) using the Precellys 24 tissue homogenizer (Bertin Technologies, France). Thereafter, lung homogenates were centrifuged (15000 rpm, 10 min, 4°C) and the supernatant was collected. The protein concentration of the samples was measured by the Pierce BCA protein assay kit (Thermo Fisher Scientific, Waltham, MA, USA) according to the manufacturer's instructions. Samples were diluted to 2 mg protein/mL and stored at –20°C until further analyses. The KC levels were measured by ELISA (Mouse KC DuoSet ELISA kit, R&D system, Oxon, UK) according to the manufacturer's instructions.

CSE preparation and IL-8 measurement in the human bronchial epithelial cells

CSE was freshly prepared just before each experiment by bubbling the CS of two 3R4F research cigarettes through 10 mL PBS without using the cigarette filters. Thereafter, the pH was adjusted to 7.4. The CSE preparation was standardized by measuring the optical density (OD) at 320 nm after filtering through a 0.22 µm filter using the spectrophotometer (UV mini-1240, SHIMADZU). The 100% CSE (OD ~ 8) was diluted to a working concentration of 5% CSE and used in this experiment.

A SV40-transformed and immortalized human bronchial airway epithelial cell line, 16HBE14o- (16HBE), was kindly provided by the University Medical Center Utrecht (Utrecht,

The Netherlands). The cells were maintained and passaged in Minimum Essential Medium (MEM, Thermo Fisher Scientific) containing 10% inactivated fetal bovine serum (v/v) (Gibco, Brazil), 100 U/mL penicillin (Sigma-Aldrich, Zwijndrecht, the Netherlands), and 100 μg/mL streptomycin (Sigma-Aldrich, Zwijndrecht, the Netherlands). Cells (1x10^4 cells /well) were seeded in 96-well plates till reaching 80–90% confluence and were pretreated with 50, 100, 200, 300 μM SUL-151 for 24 h before exposure to CSE for another 24 h at 37°C in humidified atmosphere comprised of 95% air and 5% of CO_2. The supernatant was collected, and IL-8 was measured by ELISA (Human IL-8 ELISA kit, R&D system, Oxon, UK) according to the manufacturer's instruction.

Statistical analysis

All results are presented as mean ± SEM. Differences between groups were statistically determined by one-way ANOVA, followed by Tukey's multiple comparison post hoc test. The difference was considered statistically significant at $p < 0.05$. Pearson's correlation test was conducted for analyses of correlation. All statistical analyses were conducted using GraphPad Prism (version 8.0).

Funding

Patents

Sulfateq B.V. holds preexisting intellectual property rights related to the work reported in this manuscript, especially PCT/EP2015/063579. No additional intellectual property claims resulted from the reported work.

References

1. Eapen, M.S., et al., *Airway inflammation in chronic obstructive pulmonary disease (COPD): a true paradox.* Expert Rev Respir Med, 2017. **11**(10): p. 827-839.
2. Lundback, B., et al., *Not 15 but 50% of smokers develop COPD?--Report from the Obstructive Lung Disease in Northern Sweden Studies.* Respir Med, 2003. **97**(2): p. 115-22.
3. Tsubouchi, K., J. Araya, and K. Kuwano, *PINK1-PARK2-mediated mitophagy in COPD and IPF pathogeneses.* Inflamm Regen, 2018. **38**: p. 18.
4. Dan Dunn, J., et al., *Reactive oxygen species and mitochondria: A nexus of cellular homeostasis.* Redox Biol, 2015. **6**: p. 472-485.
5. Hara, H., K. Kuwano, and J. Araya, *Mitochondrial Quality Control in COPD and IPF.* Cells, 2018. **7**(8).
6. Zhang, L., et al., *Epithelial Mitochondrial Dysfunction in Lung Disease.* Adv Exp Med Biol, 2017. **1038**: p. 201-217.
7. Jiang, Y., X. Wang, and D. Hu, *Mitochondrial alterations during oxidative stress in chronic obstructive pulmonary disease.* Int J Chron Obstruct Pulmon Dis, 2017. **12**: p. 1153-1162.
8. Hoffmann, R.F., et al., *Prolonged cigarette smoke exposure alters mitochondrial structure and function in airway epithelial cells.* Respir Res, 2013. **14**: p. 97.
9. Yue, L. and H. Yao, *Mitochondrial dysfunction in inflammatory responses and cellular senescence: pathogenesis and pharmacological targets for chronic lung diseases.* Br J Pharmacol, 2016. **173**(15): p. 2305-18.
10. Liu, S.F., et al., *Leukocyte Mitochondrial DNA Copy Number Is Associated with Chronic Obstructive Pulmonary Disease.* PLoS One, 2015. **10**(9): p. e0138716.
11. Ahmad, T., et al., *Impaired mitophagy leads to cigarette smoke stress-induced cellular senescence: implications for chronic obstructive pulmonary disease.* FASEB J, 2015. **29**(7): p. 2912-29.
12. Ernst, P., N. Saad, and S. Suissa, *Inhaled corticosteroids in COPD: the clinical evidence.* Eur Respir J, 2015. **45**(2): p. 525-37.
13. Barnes, P.J., *COPD 2020: new directions needed.* Am J Physiol Lung Cell Mol Physiol, 2020. **319**(5): p. L884-L886.
14. Wang, M.T., et al., *Association of Cardiovascular Risk With Inhaled Long-Acting Bronchodilators in Patients With Chronic Obstructive Pulmonary Disease: A Nested Case-Control Study.* JAMA Intern Med, 2018. **178**(2): p. 229-238.
15. Jiang, Z. and L. Zhu, *Update on molecular mechanisms of corticosteroid resistance in chronic obstructive pulmonary disease.* Pulm Pharmacol Ther, 2016. **37**: p. 1-8.
16. Barnes, P.J. and I.M. Adcock, *Glucocorticoid resistance in inflammatory diseases.* Lancet, 2009. **373**(9678): p. 1905-17.
17. Marwick, J.A., et al., *Oxidative stress and steroid resistance in asthma and COPD: pharmacological manipulation of HDAC-2 as a therapeutic strategy.* Expert Opin Ther Targets, 2007. **11**(6): p. 745-55.
18. Hajmousa, G., et al., *The 6-chromanol derivate SUL-109 enables prolonged hypothermic storage of adipose tissue-derived stem cells.* Biomaterials, 2017. **119**: p. 43-52.
19. Han, B., et al., *The novel compound Sul-121 inhibits airway inflammation and hyperresponsiveness in experimental models of chronic obstructive pulmonary disease.* Sci Rep, 2016. **6**: p. 26928.
20. Poole, A.C., et al., *The PINK1/Parkin pathway regulates mitochondrial morphology.* Proc Natl Acad Sci U S A, 2008. **105**(5): p. 1638-43.
21. Ashrafi, G. and T.L. Schwarz, *The pathways of mitophagy for quality control and clearance of mitochondria.* Cell Death Differ, 2013. **20**(1): p. 31-42.
22. O'Donnell, R.A., et al., *Relationship between peripheral airway dysfunction, airway obstruction, and neutrophilic inflammation in COPD.* Thorax, 2004. **59**(10): p. 837-42.
23. Hanania, N.A., S.C. Lareau, and B.P. Yawn, *Safety of inhaled long-acting anti-muscarinic agents in COPD.* Postgrad Med, 2017. **129**(5): p. 500-512.
24. Zhang, R., et al., *Optimization of Nebulized Budesonide in the Treatment of Acute Exacerbation of Chronic Obstructive Pulmonary Disease.* Int J Chron Obstruct Pulmon Dis, 2020. **15**: p. 409-415.
25. Lambooy, S.P.H., et al., *The Novel Compound Sul-121 Preserves Endothelial Function and Inhibits Progression of Kidney Damage in Type 2 Diabetes Mellitus in Mice.* Sci Rep, 2017. **7**(1): p. 11165.
26. Butler, A., G.M. Walton, and E. Sapey, *Neutrophilic Inflammation in the Pathogenesis of Chronic Obstructive Pulmonary Disease.* COPD, 2018. **15**(4): p. 392-404.
27. Verheijden, K.A., et al., *Dietary galacto-oligosaccharides prevent airway eosinophilia and hyperresponsiveness in a murine house dust mite-induced asthma model.* Respir Res, 2015. **16**: p. 17.
28. Dong, L., et al., *Intranasal Application of Budesonide Attenuates Lipopolysaccharide-Induced Acute Lung Injury by Suppressing Nucleotide-Binding Oligomerization Domain-Like Receptor Family, Pyrin Domain-Containing 3 Inflammasome Activation in Mice.* J Immunol Res, 2019. **2019**: p. 7264383.
29. van Eeden, S.F. and D.D. Sin, *Oxidative stress in chronic obstructive pulmonary disease: a lung and systemic process.* Can Respir J, 2013. **20**(1): p. 27-9.
30. Kirkham, P.A. and P.J. Barnes, *Oxidative stress in COPD.* Chest, 2013. **144**(1): p. 266-273.

31. Ceylan, E., et al., *Increased DNA damage in patients with chronic obstructive pulmonary disease who had once smoked or been exposed to biomass.* Respir Med, 2006. **100**(7): p. 1270-6.

32. Ciencewicki, J., S. Trivedi, and S.R. Kleeberger, *Oxidants and the pathogenesis of lung diseases.* J Allergy Clin Immunol, 2008. **122**(3): p. 456-68; quiz 469-70.

33. Kluchova, Z., et al., *The association between oxidative stress and obstructive lung impairment in patients with COPD.* Physiol Res, 2007. **56**(1): p. 51-6.

34. Montano, M., et al., *Malondialdehyde and superoxide dismutase correlate with FEV(1) in patients with COPD associated with wood smoke exposure and tobacco smoking.* Inhal Toxicol, 2010. **22**(10): p. 868-74.

35. Paredi, P., et al., *Exhaled ethane, a marker of lipid peroxidation, is elevated in chronic obstructive pulmonary disease.* Am J Respir Crit Care Med, 2000. **162**(2 Pt 1): p. 369-73.

36. Bajpai, J., et al., *Study of oxidative stress biomarkers in chronic obstructive pulmonary disease and their correlation with disease severity in north Indian population cohort.* Lung India, 2017. **34**(4): p. 324-329.

37. Zhang, Z., et al., *Protective Effects of Astragaloside IV Combined with Budesonide in Bronchitis in Rats by Regulation of Nrf2/Keap1 Pathway.* Med Sci Monit, 2018. **24**: p. 8481-8488.

38. van der Toorn, M., et al., *Cigarette smoke-induced blockade of the mitochondrial respiratory chain switches lung epithelial cell apoptosis into necrosis.* Am J Physiol Lung Cell Mol Physiol, 2007. **292**(5): p. L1211-8.

39. Yang, Z., et al., *The role of tobacco smoke induced mitochondrial damage in vascular dysfunction and atherosclerosis.* Mutat Res, 2007. **621**(1-2): p. 61-74.

40. Wu, K., et al., *Cigarette smoke extract increases mitochondrial membrane permeability through activation of adenine nucleotide translocator (ANT) in lung epithelial cells.* Biochem Biophys Res Commun, 2020. **525**(3): p. 733-739.

41. Szczesny, B., et al., *Mitochondrial DNA damage and subsequent activation of Z-DNA binding protein 1 links oxidative stress to inflammation in epithelial cells.* Sci Rep, 2018. **8**(1): p. 914.

42. Hahn, A. and S. Zuryn, *Mitochondrial Genome (mtDNA) Mutations that Generate Reactive Oxygen Species.* Antioxidants (Basel), 2019. **8**(9).

43. Nam, H.S., et al., *Mitochondria in chronic obstructive pulmonary disease and lung cancer: where are we now?* Biomark Med, 2017. **11**(6): p. 475-489.

44. Mizumura, K., et al., *Mitophagy-dependent necroptosis contributes to the pathogenesis of COPD.* J Clin Invest, 2014. **124**(9): p. 3987-4003.

45. Lee, W. and P.S. Thomas, *Oxidative stress in COPD and its measurement through exhaled breath condensate.* Clin Transl Sci, 2009. **2**(2): p. 150-5.

46. Fischer, B.M., J.A. Voynow, and A.J. Ghio, *COPD: balancing oxidants and antioxidants.* Int J Chron Obstruct Pulmon Dis, 2015. **10**: p. 261-76.

47. Barnes, P.J., *Glucocorticosteroids: current and future directions.* Br J Pharmacol, 2011. **163**(1): p. 29-43.

48. Barnes, P.J., *Mechanisms and resistance in glucocorticoid control of inflammation.* J Steroid Biochem Mol Biol, 2010. **120**(2-3): p. 76-85.

49. Cazzola, M., et al., *Pharmacological treatment and current controversies in COPD.* F1000Res, 2019. **8**.

50. Kumawat, K., et al., *LAIR-1 Limits Neutrophilic Airway Inflammation.* Front Immunol, 2019. **10**: p. 842.

51. Braber, S., et al., *Cigarette smoke-induced lung emphysema in mice is associated with prolyl endopeptidase, an enzyme involved in collagen breakdown.* Am J Physiol Lung Cell Mol Physiol, 2011. **300**(2): p. L255-65.

52. Verheijden, K.A.T., et al., *The Combination Therapy of Dietary Galacto-Oligosaccharides With Budesonide Reduces Pulmonary Th2 Driving Mediators and Mast Cell Degranulation in a Murine Model of House Dust Mite Induced Asthma.* Front Immunol, 2018. **9**: p. 2419.

53. Ilyasov, I.R., et al., *ABTS/PP Decolorization Assay of Antioxidant Capacity Reaction Pathways.* Int J Mol Sci, 2020. **21**(3).

54. Vogelaar, P.C., et al., *The 6-hydroxychromanol derivative SUL-109 ameliorates renal injury after deep hypothermia and rewarming in rats.* Nephrol Dial Transplant, 2018. **33**(12): p. 2128-2138.

Supplementary data
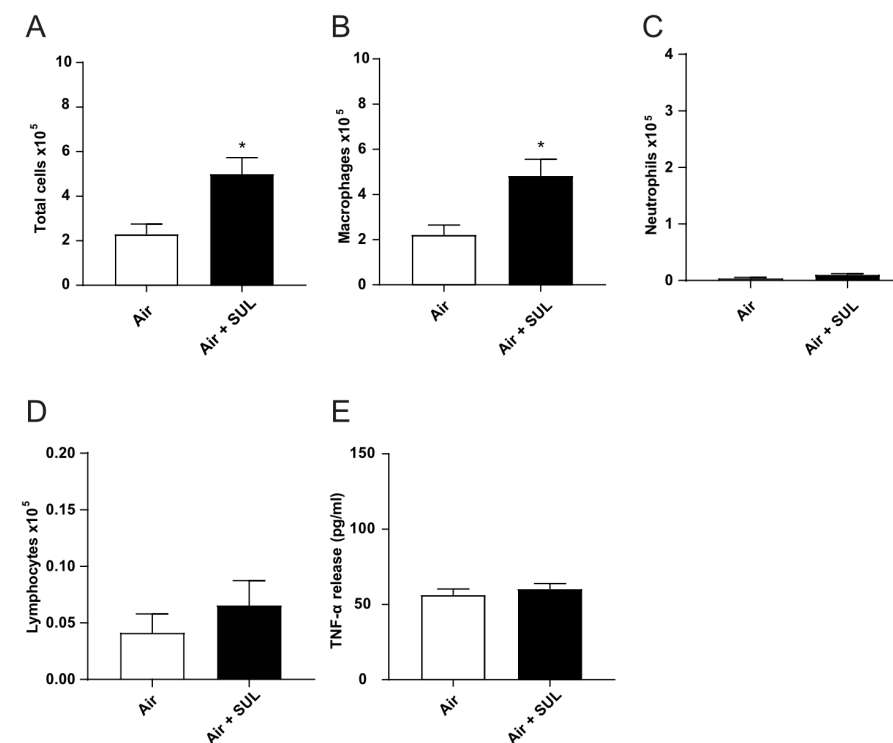
Supplementary Figure 1. The effects of SUL-151 on pulmonary inflammation in an air control group. Mice were exposed to ambient air for 5 days and received SUL-151 via oropharyngeal administration (once/day) during these 5 days. Lungs were lavaged and BAL fluid was collected for total (A) and differential BAL fluid cell counts, including macrophages (B), neutrophils (C) lymphocytes (D) and TNF-α (E) measurement. Values are expressed as mean (x105)/mean ±SEM. *P<0.05; compared to air control group, n=4-8 mice/group.

Chapter 7

General Discussion and
Future Perspectives

COPD

Chronic obstructive pulmonary disease (COPD) reduces quality of life and causes millions of deaths worldwide [1]. In addition, it is a costly disease that drains healthcare resources [2]. COPD is a progressive lung disease, which is characterized by persistent respiratory symptoms and airflow limitation due to airway and/or alveolar abnormalities [3]. The main symptoms of COPD include coughing, mucus production, and shortness of breath.

 COPD has two phenotypes: chronic bronchitis and emphysema [4]. Chronic bronchitis is accompanied by hypersecretion of mucus and the severity of symptoms varies from patient to patient. Chronic bronchitis increases the exacerbation rate, accelerates the decline in lung function, and worsens the health-related quality of life [4]. In emphysema, major pathological changes occur in the distal air spaces, such as the destruction of the alveolar walls and enlargement of the alveoli [5].

Risk factors and pathogenesis

COPD is mainly caused by cigarette smoking, but also other factors, such as exposure to indoor and outdoor pollution, occupational hazards and infections as well as advanced age, genetic predisposition, and malnutrition play an important role in generating COPD [1, 6]. Cigarette smoking affects the body in multiple ways, for example, by stimulating the immune system, causing oxidative stress, and altering the microbiota composition of the lungs and intestine.

Firstly, chronic inflammatory and immune responses play key roles in the development and progression of COPD. Exposure to cigarette smoke leads to chronic inflammation via activation of structural and immune cells, like airway epithelial cells and alveolar macrophages. In turn, these cells release pro-inflammatory cytokines and chemokines, resulting in the recruitment of additional inflammatory cells, such as neutrophils, monocytes, and lymphocytes and contributing to a state of chronic inflammation, ultimately resulting in airway remodeling and obstruction [7].

Secondly, cigarette smoking is associated with increased oxidative stress, possibly attributed to the high concentration of reactive oxygen species (ROS) in cigarette smoke [8]. Cigarette smoking can stimulate the ROS production of neutrophils and macrophages, which further promotes inflammatory responses [9, 10]. Long-term cigarette smoke exposure will eventually cause lung damage due to the systemic oxidants-antioxidants imbalance as reflected by increased products of lipid peroxidation and depleted levels of antioxidants [11]. Short-term cigarette smoke exposure does not cause emphysema, but can induce

oxidative stress and inflammation [12]. The assertion that short-term cigarette smoke exposure promotes oxidative stress and inflammatory responses was shown in Chapter 5. After 5 and 10 days of cigarette smoke exposure, radical scavenging capacity decreased, while levels of the lipid peroxidation product MDA increased in the lungs. In addition, the number of inflammatory cells, including macrophages and neutrophils, increased in the bronchoalveolar lavage (BAL) fluid.

Thirdly, cigarette smoking might influence lung health by causing an imbalance of the airway microbial composition. It has been described that the airway and bronchial tree are not sterile but harbor a complex microbial ecosystem, even in healthy individuals [13]. The airway microbiome is a collection of viable and nonviable microbiota (bacteria, viruses, and fungi) residing in the bronchial tree and parenchymal tissues and can build a protective environment associated with colonization resistance to pathogens, preserved epithelial integrity, and immune regulation [14, 15]. Dysbiosis of the lung microbiota could play an important role in COPD development and progression, leading to exacerbations and mortality [16]. In addition, cigarette smoke exposure might affect airway microbial composition by promoting the formation of bacterial biofilms [17, 18].

COPD exacerbations

An exacerbation of COPD, is a sustained worsening of the patient's condition, from a stable state and beyond day-to-day variation, which is acute in onset leading to a change in additional medical treatment, hospitalization and to substantial morbidity and mortality [19, 20]. Bacterial or viral infection can precede an exacerbation in a significant proportion of patients but the actual prevalence is uncertain [21]. Over the past two decades, clinicians and researchers have broadened their treatment goals for COPD beyond improving lung function and respiratory symptoms and have started to focus on the importance of preventing and reducing exacerbations. However, the current state of the art with respect to the definition and treatment of COPD exacerbations still faces many challenges and there are opportunities for improvement [22]. Therefore, in **Chapter 3** a cigarette smoke and lipopolysaccharide (LPS)-induced murine COPD model was used to mimic COPD exacerbations and to increase our knowledge regarding this topic.

COPD as a systemic disease

COPD is a complex lung disease involving more than inflammation and airflow obstruction. COPD is associated with significant systemic abnormalities, such as cardiovascular disease, cognitive dysfunction, skeletal muscle wasting, and cachexia, as well as gastrointestinal

disorders [16]. The systemic abnormalities have, among others, been attributed to systemic inflammation. The "spill-over" of inflammatory mediators into the circulation may result in systemic manifestations of diseases [23]. However, this "spill-over" might not be the only cause of the systemic effects of COPD. The role of hypoxia induced by the impaired gas exchange, repair failures, genetic and epigenetic factors, immunological disorders and infections are also potential causes of the systemic manifestations of COPD [24].

The gut-lung axis in COPD

Intestinal symptoms are highly prevalent among COPD patients, and the severity of these intestinal symptoms coincides with the severity of the respiratory symptoms [25]. Patients with COPD appear to be at higher risk for inflammatory bowel disease (IBD), and other gastrointestinal disorders, such as gastroesophageal reflux disease, irritable bowel syndrome, and functional dyspepsia [26]. Although the gut and lungs are separate organs with different functions and environments, they have anatomical similarities and can interact with each other in health and disease (**Chapters 2, 3, and 4**). In **Chapter 2,** we summarized the evidence of clinical trials, animal models, and *in vitro* studies to describe the possible mechanisms that drive the interaction between the gut-lung axis in COPD.

The gut-lung axis: systemic inflammation
Immune dysfunction, including systemic inflammation, probably precedes the symptoms of intestinal disorders. Circulating immune cells and corresponding cytokines may play an essential role in gut-lung crosstalk. Elevated circulating levels of interleukin 6 (IL-6) and C-reactive protein (CRP) are associated with an increased risk of Crohn's disease (CD) and Ulcerative colitis (UC) before diagnosis [27]. Moreover, increased plasma levels of CRP and IL-6 are also present in COPD patients [28]. In **Chapter 3**, increased CRP and KC levels in the BAL fluid and serum were detected in cigarette smoke-exposed mice. Furthermore, it has been described that IL-6 and TGF-β may drive cross-organ Th-17-induced inflammation, and IL-13 may drive aberrant natural killer T-cells and macrophages responses across organs [29]. In **Chapter 4**, the cytokine-cytokine interaction pathway was found to be the most highly enriched pathway in the murine lung and intestine (proximal and distal small intestines) after cigarette smoke exposure. Interestingly, gene *Il21r* from the cytokine-cytokine interaction pathway was the only significantly up-regulated in the lung, as well as in the proximal and distal small intestine in cigarette smoke-exposed mice. *Il21* produced by CD4^{+} T cells could promote Th1- and Tc1-responses, leading to systemic inflammation in emphysema [30]. The amount of *Il21* was also increased in peripheral blood and intestinal tissue of patients with CD or UC, suggesting that *Il21/Il21r* signaling may be involved in the pathogenesis of IBD [31]. Therefore, *Il21/Il21r* signaling might be a potential target for future research on the gut-lung axis.

The gut-lung axis: systemic hypoxia
Besides systemic inflammation, systemic hypoxia may play a crucial role in the gut-lung crosstalk. Hypoxia in COPD patients during daily activities increases intestinal permeability and causes enterocyte damage [32]. Impaired gas exchange in COPD patients is associated with systemic hypoxia, which can drive damage to the integrity of intestinal epithelial barrier [33]. This impaired gas exchange after chronic cigarette smoke exposure was also observed in a murine model, leading to systemic and intestinal hypoxia, driving angiogenesis and intestinal epithelial barrier dysfunction, resulting in increased risk and severity of CD [33].

The gut-lung axis: gut microbiota
COPD patients have an altered gut microbiota compared with healthy individuals and cigarette smoking is associated with intestinal microbiota dysbiosis. A systemic review demonstrated that *Prevotella* spp. are significantly increased in smokers and former smokers but not in electronic cigarette users, while *Proteobacteria* showed a progressive increase in *Desulfovibrio* with the number of pack-years of cigarette smoking and an increase in *Alpha-proteobacteria* in current versus never smokers [34]. Active cigarette smoke exposure reduces the abundance of *Clostridium, Turicibacter* and increases the abundance of *Desulfovibrio, Bilophila* in a rat model [35]. We also observed an imbalanced microbiota in our murine model of cigarette smoke-induced COPD [43] (Figure 1). At the family level, *Eubacteriaceae* were enriched, and *Ruminococcaceae*, *Desulfovibrionaceae*, and *Rikenellacease* were depleted in the fecal samples of the 10 weeks cigarette smoke-exposed mice (see Figure 1).

In agreement with our findings, COPD patients have been shown to have an increased abundance of *Eubacteriaceae* at the family level, and less abundance of the family levels of *Ruminococcaceae, Desulfovibrionaceae*, and genus level of *Rikenellaceae* in the intestine [36, 37]. *Eubacterium rectale* can contribute to colorectal cancer initiation via promoting colitis [38]. *Ruminococcaceae*, producers of butyrate and acetate, were drastically reduced in IBD patients [39]. The *Ruminococcaceae* represent the first step of microbiome-linked carbohydrate metabolism, as they degrade several types of polysaccharides (starch, cellulose, and xylan) in the lower gastrointestinal tract [40]. The *Desulfovibrionaceae* family was depleted in COPD patients, however, the data was highly variable among individuals [36], while the abundance of *Desulfovibrionaceae* was increased in UC patients [41]. The *Rikenellaceae* genus was less prevalent in COPD patients than in healthy controls [36]. However, *Rikenellaceae* was more abundant in irritable bowel syndrome (IBS) than IBD, and was underrepresented in IBD [42]. All these findings show that there are some similarities in gut microbiota dysbiosis in both COPD and IBD patients. Interestingly, mice receiving fecal transplantation from COPD patients developed lung inflammation and cigarette smoking aggravated the deterioration of lung function [44]. This strengthens the hypothesis that the gut microbiota can modulate lung function and lung immunity.
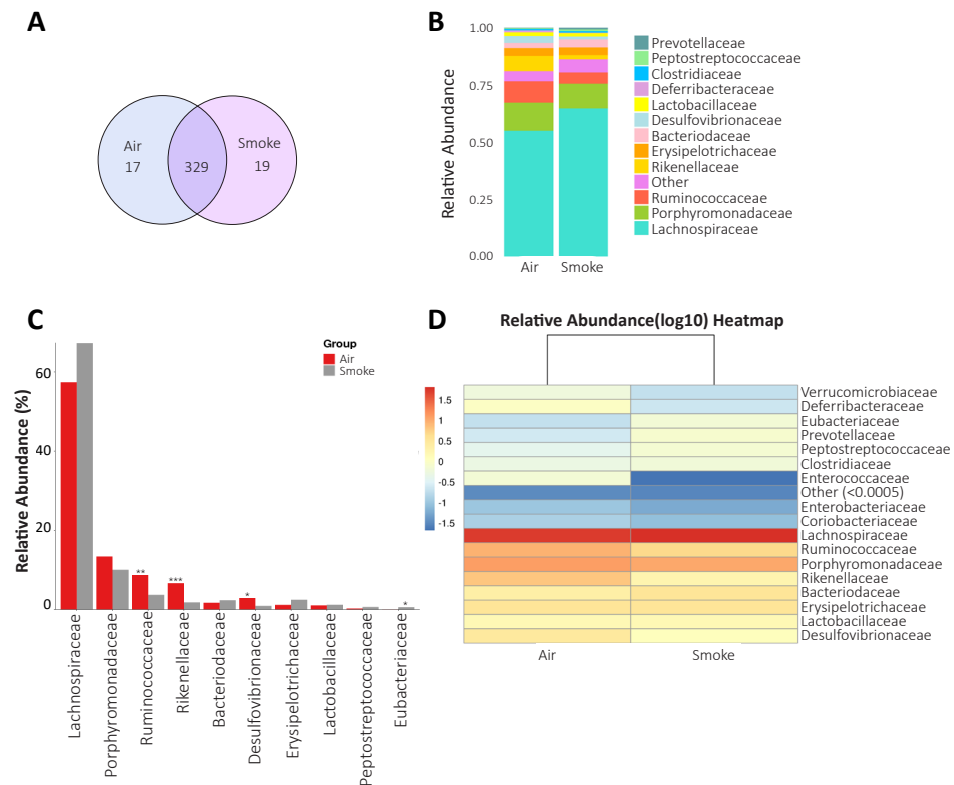
7

A

B

C

D

Relative Abundance(log10) Heatmap

Figure 1. Fecal microbial composition (at the family level) in cigarette smoke-exposed mice. Mice were exposed to cigarette smoke for about 10 weeks and fecal samples were used to measure the microbial composition. Operational taxonomic unit (OTU) Venn diagrams of shared and unique OTUs in the feces of cigarette smoke- and air- exposed mice (A). Stacked column plots of the most abundant bacterial populations in the feces of cigarette smoke- and air-exposed mice (B). The top 10 families are chosen to show the average relative abundance of smoke and air exposure groups. Significance of the test are marked with "*" at the top of the histogram, *p <0.05, **p <0.01, ***p <0.001 (C). The horizontal clusters for indicating the similarity of certain families among different groups were presented in the heatmap (D). N=11 samples/group.

The gut-lung axis: short-chain fatty acids

Short-chain fatty acids (SCFAs), such as acetate, propionate, and butyrate, are fatty acids derived from intestinal microbial fermentation of indigestible foods. COPD patients as well as patients with active IBD have lower levels of fecal SCFAs compared to healthy individuals [44, 45]. No obvious changes in cecal SCFA production were observed after cigarette smoke or LPS only exposure in **Chapter 3** of this thesis, however, total iso-SCFAs, valeric acid and iso-valeric acid levels were significantly decreased in mice after cigarette smoke exposure plus LPS treatment compared to the LPS treatment only group. Cecal levels of valeric acid might be associated with a decreased population of *Bifidobacterium* as described in

cigarette smoke-exposed rats [46]. However, the decreased population of *Bifidobacterium* was not found in our mice model. Accumulating evidence suggests that SCFAs, as the most prominent immunomodulatory metabolites, have been shown to exert their functions along the gut-lung axis. SCFAs disseminate from the gut into the bloodstream reaching the bone marrow to promote bone marrow hematopoiesis leading to the resolution of airway inflammation and maintenance of a healthy homeostasis in the lung [47]. Moreover, as SCFAs produced in the gut can pass into the circulation, these metabolites may have direct effects on the lungs, or may even be produced by the lung microbiota [48]. SCFAs are known to strengthen the gut barrier function and to regulate inflammation and oxidative stress via SCFA signaling mechanism, like promotion of histone acetylation and activation of G-protein-coupled receptors [47]. This indicated that SCFAs may exert a promising therapeutic potential for the treatment or prevention of COPD.

The role of adipose tissue in COPD pathogenesis

Besides the higher prevalence of intestinal disorders observed in COPD patients, COPD patients also often suffer from other concomitant disorders, such as metabolic disorders that influence the disease prognosis [49]. The disturbances of the complex network of interorgan-connected responses can modulate the disease progression. Adipose tissue is a less obvious but very important responding element of this network in systemic disease development. Not only because adipose tissue is a key source of signaling molecules, such as adipokines, but also a vital source of stem cells that may be involved in tissue repair [50]. Systemic inflammation is considered as a hallmark of COPD, which is potentially associated with the increased incidence of metabolic abnormalities such as cachexia [51].

Adipokines are primarily expressed in adipose tissue, but can also be detected in the lungs [52]. Leptin exerts multiple effects in the respiratory system as this cytokine-like hormone plays important physiological roles. The leptin-signaling pathway is involved in immune modulation and cell proliferation, and its dysregulation can lead to the onset of lung diseases [53]. Leptin also contributes to pulmonary defense by regulating the innate and adaptive immune responses in the lung. It exerts protective anti-inflammatory effects in models of acute inflammation and during activation of innate immune responses [54]. Mice lacking leptin or its functional receptor have multiple defects in cell-mediated and humoral immunity [53]. Clinical studies have produced inconsistent results, indicating a complex role for leptin in immune-mediated inflammatory conditions in humans [54]. For example, congenital leptin-deficient patients exhibit defects in immunity and an increased incidence of death due to infections. Importantly, leptin therapy reverses these defects [55]. In **Chapter 5**, the leptin level was decreased in serum of cigarette smoke-exposed mice, which was positively correlated with the fat mass. In addition, morphological changes and pro-inflammatory

responses were observed in white adipose tissue of cigarette smoke-exposed mice, including increased numbers of macrophages and corresponding elevated cytokine levels of IL-6, IL-1β and TNF-α. This indicates that the adipokines and/or adipose tissue might need more attention in future lung research and could be a promising therapeutic target in lung inflammation and injury related to COPD.

Skeletal muscle in COPD cachexia

Skeletal muscle dysfunction often occurs in patients with COPD and represents very important comorbidity that is associated with a poor quality of life and high mortality [56]. Skeletal muscle dysfunction includes a complex combination of functional, metabolic, and anatomical alterations, which worsen during COPD exacerbations [57]. Muscle wasting is more prevalent in patients with emphysema than in patients with bronchitis [58]. COPD is often associated with muscle wasting and a change from slow-to-fast (type I- to type II) composition in the fiber type, resulting in muscle weakness and an earlier onset of muscle fatigue [59]. Type I fibers have a predominantly oxidative metabolism and are more fatigue resistant than type II fibers, which depend more on anaerobic metabolism [60]. Importantly, impaired muscle function and muscle mass loss negatively impact the prognosis and survival of COPD patients [61]. In **Chapter 5** of this thesis**,** decreased muscle function and whole-body lean mass were observed in mice after 10 weeks of cigarette smoke exposure. However, skeletal muscle weight and mitochondrial turnover makers were not significantly altered. More research is needed to elucidate whether the muscle function preceding the muscle mass loss, as well as the relation with mitochondrial biogenesis in the longer term of smoking (or more intense smoking) model.

COPD treatment

Current treatment for COPD mainly controls the symptoms and exacerbations but does not influence disease progression. For example, glucocorticoids, β2-adrenoceptor agonists, and muscarinic receptor antagonists are the major current therapies for COPD, which can reduce symptoms and/or exacerbations, but do not specifically target oxidative stress, nor do they diminish chronic respiratory inflammation and COPD progression or mortality in these patients [62, 63]. In addition, a large group of COPD patients respond poorly or are completely resistant to glucocorticoids [64]. Therefore, multiple approaches such as smoking cessation, counseling, and pharmaceutical therapies targeting inflammation and oxidative stress are recommended for COPD treatment. In **Chapter 6**, a novel pharmacological compound (also called SUL compound), significantly decreased more than 70% and 50% of the cigarette smoke-induced neutrophil influx in BAL fluid after prophylactic and therapeutic

administration, respectively, while budesonide showed no significant reduction in neutrophil numbers. Moreover, SUL-151 prevented the cigarette smoke-induced decrease in ATP and mitochondrial mtDNA and increase in putative protein kinase 1 expression in the lung homogenates. This implied that targeting the mitochondria and oxidative stress would be a promising therapy for reducing lung inflammation and COPD development.

Limitations

It should be noted that there are some limitations in the described studies which might be useful to consider in future research. Firstly, the duration of the smoke exposure can be extended to better understand whether the duration of smoke exposure affects the severity of intestinal changes, such as the pathophysiology and the small fluctuations in cecal SCFA levels as observed in **Chapter 3**. Besides extending the duration, different time points of smoke exposure should be considered to explore the systemic effects at different stages of cigarette smoke exposure in **Chapters 3, 4, and 5**. In **Chapter 4,** measurements at different time points can contribute to further understanding whether loss of fat mass and atrophy of adipose tissue precedes muscle wasting. In addition, the inter-tissue crosstalk between adipose tissue and skeletal muscle in relation to metabolic processes in COPD development could be further clarified.

Secondly, in **Chapter 3,** cigarette smoke exposure combined with LPS treatment was used to mimic COPD exacerbations, however, LPS was not able to induce additional effects in the lung (Lm, total BAL fluid cells, neutrophils, and mucus production,) as well as in the intestine (morphology of the small intestines, IgA level). This might be due to the frequency, interval and dosage of LPS. In future studies, other bacterial triggers (or real-life bacterial pathogens) may be considered for inducing exacerbations.

On the other hand, it could be possible that LPS-induced immune responses might exert protective effects on cigarette smoke-induced symptoms as observed by an increased number of macrophages and a decreased number of neutrophils in the BAL fluid after additional LPS treatment (see **Chapter 3**).

The reported efficacy of long-term antibiotic treatment with macrolides in reducing exacerbation frequency in COPD patients may suggest that bacteria are relevant for the induction of exacerbations, although this is a matter of debate. Viral infections contribute as well to the exacerbations of COPD [65]. Viral triggers, such as polyinosinic:polycytidylic acid (poly I:C), or the original viral pathogens detected in COPD patients with exacerbations, such as picornaviruses, influenza A, respiratory syncytial virus, and parainfluenza, may be considered to be used in COPD exacerbation models.

Last but not least, although the cigarette smoke-induced murine COPD model has been considered as a suitable model to investigate the airway responses and systemic effects in COPD, it cannot fully mimic the real situation due to the considerable human-to-human variation in the pattern of COPD, as well as the differences between animal and human in lung anatomy, development and maturation and susceptibility to injurious agents [66].

Future perspectives

The intestine might be a promising target for influencing lung health and minimizing COPD exacerbations through the bi-directional gut and lung crosstalk. Diets as an integral part of COPD management, from prevention to treatment, attracts more and more attention. Especially those nutraceuticals endowed with antioxidant and anti-inflammatory properties and when consumed in combinations in the form of balanced dietary patterns, are associated with better pulmonary function, less lung function decline, and reduced risk of COPD [67]. For example, SCFAs, the byproducts of intestinal microbial fermentation of indigestible foods, are potent anti-inflammatory molecules for lung health through systemic effects in circulation. In addition, a mixture of non-digestible oligosaccharides decreases lung inflammation and prevent the development of lung emphysema [68], which indicates that shaping the gut microbiota composition with dietary supplementation might be a potential treatment for COPD.

Adipose tissue is not an inert organ but rather a systemic modulator of the response to environmental exposures [69]. Adipokines, such as leptin, exert multiple effects in the respiratory system, as this cytokine-like hormone plays important physiological roles by regulating the innate and adaptive immune responses in the lung. Interference with adipokines and/or adipose tissue might have a protective effect on lung inflammation and injury in COPD. Future COPD research should not only focus on the lung as the target organ, but also consider a broader perspective in relation to other organs. Future therapeutical strategies for COPD should not only target the lung, but also the complicated signal interactions between the lung and other tissues, such as the intestine and adipose tissue to reduce systemic disease progression and related co-morbidities.

There is also an urgent need for developing safer and more effective anti-inflammatory therapies to reduce disease progression, exacerbations, and comorbidities of COPD. Promising new approaches include novel antioxidants, multi-kinase inhibitors as well as drugs that target cellular senescence. Drugs that hold the potential of repairing the damaged tissue or reverse corticosteroid resistance are also urgently needed.

A multi-organ targeted approach may be beneficial for the treatment of COPD but also for the concomitant co-morbidities (Figure 2).
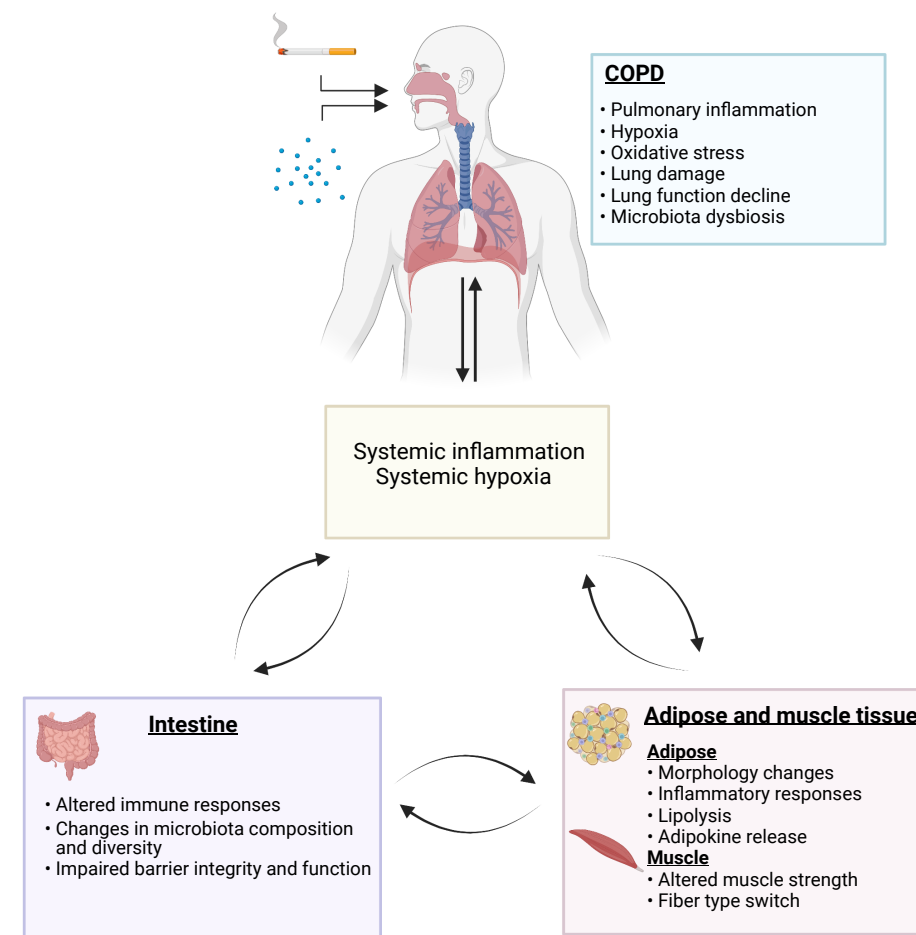

Figure 2. The proposed systemic multi-organ axis involved in chronic obstructive pulmonary diseases (COPD). COPD is a chronic lung disease characterized by a range of pathological changes in the respiratory system, including persistent respiratory symptoms and airflow limitation, structural changes of the small airways, damaged alveolar walls, as well as inflammation, oxidative stress, hypoxia, and microbiota dysbiosis in the lung (green box). COPD is also a systemic disease and it has significant systemic consequences. Many comorbidities in COPD are associated with multi-organ-associated systemic inflammation and systemic hypoxia (yellow box). The extrapulmonary manifestations and comorbidities worsen COPD progression and quality of life. Intestinal disorders are prevalent comorbidity of COPD as observed by disturbed (intestinal) immune responses, altered microbiota composition, and diversity, as well as impaired barrier integrity and function (purple box). In turn, abnormal intestinal responses can also cause further lung damage. Another prevalent comorbidity in COPD are metabolic disorders. Many patients demonstrate a gradual and significant weight loss that exacerbates the course and prognosis of the disease. The weight loss is often accompanied by skeletal muscle dysfunction and weakness, which markedly contribute to exercise limitation and impaired quality of life. Weight loss has been postulated to be the result of a high metabolic rate that is not compensated by increased dietary intake. This can be due to enhanced lipolysis, morphological changes, and inflammatory responses observed in adipose tissue (pink box).

In addition, adipokines can play an important role in this multi-organ-associated systemic interaction. Moreover, the gut microbiota is also involved in the regulation of multiple host metabolic pathways, giving rise to interactive host-microbiota metabolic, signaling, and immune-inflammatory axes that physiologically connect the gut, lung, adipose and muscle tissue. These gut microbes influence energy metabolism by regulating glucose metabolism, appetite, and fat storage. In this figure, a few examples of these multi-organ changes involved in COPD are described, and more detailed information can be found in the corresponding chapters of this thesis.

References

1. Mannino, D.M. and A.S. Buist, *Global burden of COPD: risk factors, prevalence, and future trends.* Lancet, 2007. **370**(9589): p. 765-73.
2. McLean, S. and A. Sheikh, *Does telehealthcare offer a patient-centred way forward for the community-based management of long-term respiratory disease?* Prim Care Respir J, 2009. **18**(3): p. 125-6.
3. Mirza, S., et al., *COPD Guidelines: A Review of the 2018 GOLD Report.* Mayo Clin Proc, 2018. **93**(10): p. 1488-1502.
4. Kim, V. and G.J. Criner, *Chronic bronchitis and chronic obstructive pulmonary disease.* Am J Respir Crit Care Med, 2013. **187**(3): p. 228-37.
5. Tsutsumi, A., et al., *Characteristics of chronic obstructive pulmonary disease patients with robust progression of emphysematous change.* Sci Rep, 2021. **11**(1): p. 9548.
6. Berry, C.E. and R.A. Wise, *Mortality in COPD: causes, risk factors, and prevention.* COPD, 2010. **7**(5): p. 375-82.
7. Strzelak, A., et al., *Tobacco Smoke Induces and Alters Immune Responses in the Lung Triggering Inflammation, Allergy, Asthma and Other Lung Diseases: A Mechanistic Review.* Int J Environ Res Public Health, 2018. **15**(5).
8. Churg, A., M. Cosio, and J.L. Wright, *Mechanisms of cigarette smoke-induced COPD: insights from animal models.* Am J Physiol Lung Cell Mol Physiol, 2008. **294**(4): p. L612-31.
9. Bowler, R.P., P.J. Barnes, and J.D. Crapo, *The role of oxidative stress in chronic obstructive pulmonary disease.* COPD, 2004. **1**(2): p. 255-77.
10. MacNee, W., *Oxidants and COPD.* Curr Drug Targets Inflamm Allergy, 2005. **4**(6): p. 627-41.
11. Yanbaeva, D.G., et al., *Systemic effects of smoking.* Chest, 2007. **131**(5): p. 1557-66.
12. Kennedy-Feitosa, E., et al., *Eucalyptol attenuates cigarette smoke-induced acute lung inflammation and oxidative stress in the mouse.* Pulm Pharmacol Ther, 2016. **41**: p. 11-18.
13. Huang, Y.J., et al., *The role of the lung microbiome in health and disease. A National Heart, Lung, and Blood Institute workshop report.* Am J Respir Crit Care Med, 2013. **187**(12): p. 1382-7.
14. Russo, C., et al., *Impact of Lung Microbiota on COPD.* Biomedicines, 2022. **10**(6).
15. Wang, L., et al., *Role of the Lung Microbiome in the Pathogenesis of Chronic Obstructive Pulmonary Disease.* Chin Med J (Engl), 2017. **130**(17): p. 2107-2111.
16. Barnes, P.J. and B.R. Celli, *Systemic manifestations and comorbidities of COPD.* Eur Respir J, 2009. **33**(5): p. 1165-85.
17. Kulkarni, R., et al., *Cigarette smoke increases Staphylococcus aureus biofilm formation via oxidative stress.* Infect Immun, 2012. **80**(11): p. 3804-11.
18. Turek, E.M., et al., *Airway microbial communities,*

19. smoking and asthma in a general population sample.* EBioMedicine, 2021. **71**: p. 103538.
19. Burge, S. and J.A. Wedzicha, *COPD exacerbations: definitions and classifications.* Eur Respir J Suppl, 2003. **41**: p. 46s-53s.
20. Beghe, B., et al., *Exacerbation of respiratory symptoms in COPD patients may not be exacerbations of COPD.* Eur Respir J, 2013. **41**(4): p. 993-5.
21. Ritchie, A.I. and J.A. Wedzicha, *Definition, Causes, Pathogenesis, and Consequences of Chronic Obstructive Pulmonary Disease Exacerbations.* Clin Chest Med, 2020. **41**(3): p. 421-438.
22. Kim, V. and S.D. Aaron, *What is a COPD exacerbation? Current definitions, pitfalls, challenges and opportunities for improvement.* Eur Respir J, 2018. **52**(5).
23. Sinden, N.J. and R.A. Stockley, *Systemic inflammation and comorbidity in COPD: a result of 'overspill' of inflammatory mediators from the lungs? Review of the evidence.* Thorax, 2010. **65**(10): p. 930-6.
24. Huertas, A. and P. Palange, *COPD: a multifactorial systemic disease.* Ther Adv Respir Dis, 2011. **5**(3): p. 217-24.
25. Ojha, U.C., et al., *Correlation of Severity of Functional Gastrointestinal Disease Symptoms with that of Asthma and Chronic Obstructive Pulmonary Disease: A Multicenter Study.* Int J Appl Basic Med Res, 2018. **8**(2): p. 83-88.
26. Chiu, Y.C., et al., *Chronic obstructive pulmonary disease is associated with a higher risk of functional gastrointestinal disorders.* Respir Med, 2022. **197**: p. 106833.
27. Lochhead, P., et al., *Association Between Circulating Levels of C-Reactive Protein and Interleukin-6 and Risk of Inflammatory Bowel Disease.* Clin Gastroenterol Hepatol, 2016. **14**(6): p. 818-824 e6.
28. Yanbaeva, D.G., et al., *IL6 and CRP haplotypes are associated with COPD risk and systemic inflammation: a case-control study.* BMC Med Genet, 2009. **10**: p. 23.
29. Labarca, G., et al., *Association between inflammatory bowel disease and chronic obstructive pulmonary disease: a systematic review and meta-analysis.* BMC Pulm Med, 2019. **19**(1): p. 186.
30. Duan, M., et al., *IL-21 is increased in peripheral blood of emphysema mice and promotes Th1/Tc1 cell generation in vitro.* Inflammation, 2014. **37**(3): p. 745-55.
31. Wang, Y., et al., *IL-21/IL-21R signaling suppresses intestinal inflammation induced by DSS through regulation of Th responses in lamina propria in mice.* Sci Rep, 2016. **6**: p. 31881.
32. Rutten, E.P.A., et al., *Disturbed intestinal integrity in patients with COPD: effects of activities of daily living.* Chest, 2014. **145**(2): p. 245-252.

33. Fricker, M., et al., *Chronic cigarette smoke exposure induces systemic hypoxia that drives intestinal dysfunction.* JCI Insight, 2018. **3**(3).

34. Antinozzi, M., et al., *Cigarette Smoking and Human Gut Microbiota in Healthy Adults: A Systematic Review.* Biomedicines, 2022. **10**(2).

35. Wang, X., et al., *Active Smoking Induces Aberrations in Digestive Tract Microbiota of Rats.* Front Cell Infect Microbiol, 2021. **11**: p. 737204.

36. Bowerman, K.L., et al., *Disease-associated gut microbiome and metabolome changes in patients with chronic obstructive pulmonary disease.* Nat Commun, 2020. **11**(1): p. 5886.

37. Chiu, Y.C., et al., Comprehensive profiling of the gut microbiota in patients with chronic obstructive pulmonary disease of varying severity. PLoS One, 2021. 16(4): p. e0249944.

38. Wang, Y., et al., Eubacterium rectale contributes to colorectal cancer initiation via promoting colitis. Gut Pathog, 2021. 13(1): p. 2.

39. Wang, L., et al., *An engineered probiotic secreting Sj16 ameliorates colitis via Ruminococcaceae/ butyrate/retinoic acid axis.* Bioeng Transl Med, 2021. **6**(3): p. e10219.

40. Morgan, X.C., et al., *Dysfunction of the intestinal microbiome in inflammatory bowel disease and treatment.* Genome Biol, 2012. **13**(9): p. R79.

41. Rowan, F., et al., Desulfovibrio bacterial species are increased in ulcerative colitis. Dis Colon Rectum, 2010. 53(11): p. 1530-6.

42. Lo Presti, A., et al., *Fecal and Mucosal Microbiota Profiling in Irritable Bowel Syndrome and Inflammatory Bowel Disease.* Front Microbiol, 2019. **10**: p. 1655.

43. Wang, L., et al., *Changes in intestinal homeostasis and immunity in a cigarette smoke- and LPS-induced murine model for COPD: the lung-gut axis.* Am J Physiol Lung Cell Mol Physiol, 2022. **323**(3): p. L266-L280.

44. Li, N., et al., *Gut microbiota dysbiosis contributes to the development of chronic obstructive pulmonary disease.* Respir Res, 2021. **22**(1): p. 274.

45. Machado, M.G., V. Sencio, and F. Trottein, *Short-Chain Fatty Acids as a Potential Treatment for Infections: a Closer Look at the Lungs.* Infect Immun, 2021. 89(9): p. e0018821.

46. Tomoda, K., et al., *Cigarette smoke decreases organic acids levels and population of bifidobacterium in the caecum of rats.* J Toxicol Sci, 2011. 36(3): p. 261-6.

47. Dang, A.T. and B.J. Marsland, *Microbes, metabolites, and the gut-lung axis.* Mucosal Immunol, 2019. 12(4): p. 843-850.

48. Parada Venegas, D., et al., *Short Chain Fatty Acids (SCFAs)-Mediated Gut Epithelial and Immune Regulation and Its Relevance for Inflammatory Bowel Diseases.* Front Immunol, 2019. 10: p. 277.

49. Putcha, N., et al., *Comorbidities and Chronic Obstructive Pulmonary Disease: Prevalence, Influence on Outcomes, and Management.* Semin

50. Agusti, A., et al., *Lungs, bone marrow, and adipose tissue. A network approach to the pathobiology of chronic obstructive pulmonary disease.* Am J Respir Crit Care Med, 2013. 188(12): p. 1396-406.

51. Tkacova, R., *Systemic inflammation in chronic obstructive pulmonary disease: may adipose tissue play a role? Review of the literature and future perspectives.* Mediators Inflamm, 2010. 2010: p. 585989.

52. Malli, F., et al., *The role of leptin in the respiratory system: an overview.* Respir Res, 2010. 11: p. 152.

53. Jutant, E.M., et al., *The Thousand Faces of Leptin in the Lung.* Chest, 2021. **159**(1): p. 239-248.

54. Bernotiene, E., G. Palmer, and C. Gabay, *The role of leptin in innate and adaptive immune responses.* Arthritis Res Ther, 2006. **8**(5): p. 217.

55. Farooqi, I.S., et al., *Beneficial effects of leptin on obesity, T cell hyporesponsiveness, and neuroendocrine/metabolic dysfunction of human congenital leptin deficiency.* J Clin Invest, 2002. **110**(8): p. 1093-103.

56. Mador, M.J. and E. Bozkanat, *Skeletal muscle dysfunction in chronic obstructive pulmonary disease.* Respir Res, 2001. **2**(4): p. 216-24.

57. Jaitovich, A. and E. Barreiro, *Skeletal Muscle Dysfunction in Chronic Obstructive Pulmonary Disease. What We Know and Can Do for Our Patients.* Am J Respir Crit Care Med, 2018. **198**(2): p. 175-186.

58. Vanfleteren, L.E., et al., *Clusters of comorbidities based on validated objective measurements and systemic inflammation in patients with chronic obstructive pulmonary disease.* Am J Respir Crit Care Med, 2013. **187**(7): p. 728-35.

59. Wust, R.C. and H. Degens, *Factors contributing to muscle wasting and dysfunction in COPD patients.* Int J Chron Obstruct Pulmon Dis, 2007. **2**(3): p. 289-300.

60. Schiaffino, S. and C. Reggiani, *Fiber types in mammalian skeletal muscles.* Physiol Rev, 2011. **91**(4): p. 1447-531.

61. Barreiro, E. and A. Jaitovich, *Muscle atrophy in chronic obstructive pulmonary disease: molecular basis and potential therapeutic targets.* J Thorac Dis, 2018. **10**(Suppl 12): p. S1415-S1424.

62. Ernst, P., N. Saad, and S. Suissa, *Inhaled corticosteroids in COPD: the clinical evidence.* Eur Respir J, 2015. **45**(2): p. 525-37.

63. Barnes, P.J., *COPD 2020: new directions needed.* Am J Physiol Lung Cell Mol Physiol, 2020. **319**(5): p. L884-L886.

64. Jiang, Z. and L. Zhu, *Update on molecular mechanisms of corticosteroid resistance in chronic obstructive pulmonary disease.* Pulm Pharmacol Ther, 2016. **37**: p. 1-8.

65. Viniol, C. and C.F. Vogelmeier, *Exacerbations of COPD.* Eur Respir Rev, 2018. **27**(147).

66. Wright, J.L., M. Cosio, and A. Churg, *Animal

Respir Crit Care Med, 2015. 36(4): p. 575-91.

models of chronic obstructive pulmonary disease.* Am J Physiol Lung Cell Mol Physiol, 2008. **295**(1): p. L1-15.

67. Scoditti, E., et al., *Role of Diet in Chronic Obstructive Pulmonary Disease Prevention and Treatment.* Nutrients, 2019. **11**(6).

68. Janbazacyabar, H., et al., *Non-digestible oligosaccharides partially prevent the development of LPS-induced lung emphysema in mice.* PharmaNutrition, 2019. **10**: p. 100163.

69. Divo, M.J., *The adipose tissue and lung health: like many things in life, the extremes are not good.* Eur Respir J, 2020. **55**(4).

Appendices

English summary

The studies described in this thesis were conducted to gain more insight into the multi-organ dysfunction in chronic obstructive pulmonary disease (COPD), with a special focus on intestinal and metabolic (adipose and muscle tissue) responses. In addition, the therapeutical potential of a novel compound "SUL-151" was investigated in a murine cigarette smoke-induced inflammation model.

The Gut-lung axis in COPD

COPD patients often have a high prevalence and incidence of intestinal manifestations such as inflammatory cell infiltration, increased intestinal permeability, and absorptive impairment. The crosstalk between the gut and lung can be noticed by intestinal disease manifestations during respiratory diseases and vice versa.

The gut-lung axis has been investigated in **Chapters 2, 3, and 4**. **In Chapter 2**, we summarized clinical trials, animal models, and *in vitro* studies that describe the possible mechanisms that drive the interactions between the gut and lungs in COPD. The main interaction between the lungs and the gut can occur through circulating cigarette smoke particles, inflammatory mediators and cells. In addition, gut microbiota dysbiosis observed in both COPD and intestinal disorders can lead to an altered mucosal environment, including the intestinal barrier and immune system, and hence, may negatively affect both the gut and the lungs. Last but not least, systemic hypoxia and oxidative stress that occurs in COPD, may also be involved in intestinal injury and play a role in the gut-lung axis.

Cigarette smoking, one of the major causes of COPD, can impact the gastrointestinal system and promotes intestinal diseases. In **Chapter 3**, a murine model of long-term cigarette smoke exposure with or without LPS co-stimulation was used to investigate the effects of pulmonary inflammation and emphysema on systemic inflammation and intestinal homeostasis and immunity. Cigarette smoke with or without LPS affected intestinal health as observed by changes in intestinal histomorphology and the immune network for IgA production. Elevated systemic mediators might play a role in the lung-gut crosstalk. These findings contribute to a better understanding of intestinal disorders related to COPD.

To gain more insight into the lung-gut axis in COPD, the molecular changes in the lung and ileum (distal small intestine) of cigarette smoke-exposed mice were analyzed by RNA sequencing followed by KEGG pathway analysis (**Chapter 4)**. Altered gene expression in the murine lung tissue was detected after cigarette smoke exposure, and some of these genes were also affected in COPD patients, which confirms COPD-like changes in this murine model. Cigarette smoke exposure highly altered the expression of genes in the murine ileum, however, these changes were less comparable to the altered genes observed in the ileum of Crohn's disease patients. The cytokine-cytokine receptor interaction pathways and pathways related to cell adhesion molecules were the most enriched pathways observed in the lungs as well as in the ileum. This transcriptome dataset of the lung and ileum of smoke-exposed mice would be a valuable tool for future directions of research and new therapeutical approaches in COPD and related gastrointestinal comorbidities.

Metabolic responses in COPD

COPD is a chronic and complex systemic disease that can lead to systemic manifestations beyond the lungs, including metabolic comorbidities involving alterations in adipose and skeletal muscle tissues. The extent of emphysema in COPD patients is correlated with weight loss and fat loss. Adipose tissue is an important systemic organ in modulating a range of local and systemic metabolic and inflammatory pathways by releasing different bioactive factors, including cytokines, adipokines, and hormones, which may contribute to respiratory disease progression. Skeletal muscle wasting is one of the core symptoms in COPD patients, however, it is suggested that adipose tissue wasting probably occurs before the appearance of the reduction in lean mass. The spill-over of systemic inflammation by the adipose tissue may be one of the underlying mechanisms involved in the depletion of skeletal muscle mass. **Chapter 5** investigated the adaptive and pathological alterations in adipose and skeletal muscle following cigarette smoke exposure using *in vivo* and *in vitro* models. Cigarette smoke exposure induced loss of whole-body fat mass and adipose tissue wasting, and to a lesser extent skeletal muscle wasting. In the *in vitro* studies, enhanced lipolysis and fatty acid oxidation were demonstrated, which might play a role in fat mass loss and adipose atrophy. It remains to be elucidated whether adipose tissue loss and parallel deterioration of skeletal muscle function might precede muscle wasting. The presented knowledge contributes to a better understanding of the important role of adipose tissue in COPD pathogenesis.

Novel compound for COPD treatment

COPD has been associated with oxidative stress. Glucocorticoids, β_2-adrenoceptor agonists, and muscarinic receptor antagonists are the major current treatments for COPD, which can reduce symptoms and/or exacerbations. However, they do not specifically target oxidative stress, nor do they diminish chronic respiratory inflammation and COPD progression or mortality in all patients. In addition, a large group of COPD patients have a poor response to glucocorticoids or are completely resistant. Therefore, in **Chapter 6**, the effects of a novel pharmacological compound with mito-protective properties and modest antioxidant capacity (called SUL-151) was investigated prophylactically and therapeutically in a murine cigarette-smoke-induced inflammation model. SUL-151 significantly decreased more than 70% and 50% of the cigarette smoke-induced neutrophil influx in the broncho-alveolar lavage fluid after prophylactic and therapeutic administration, respectively. Moreover, SUL-151 prevented the cigarette smoke-induced decrease in ATP and mitochondrial mtDNA and

an increase in putative protein kinase 1 expression in the lung homogenates. This implied that targeting mitochondria and oxidative stress would be a promising therapy for reducing lung inflammation and associated COPD development.

The end...

Finally, in **Chapter 7** the main findings of this thesis and the overall conclusions have been discussed. Briefly, in a murine cigarette smoke-induced COPD model systemic manifestations, including intestinal and metabolic disorders, have been investigated. Cigarette smoke exposure caused alterations in intestinal and metabolic (adipose and muscle tissue) responses. This indicates that future COPD research should not only focus on the lung as the target organ, but also consider a broader perspective related to other organs. For instance, therapeutic strategies for COPD should also target the complicated signal interactions between the lungs and the intestine/adipose tissue to reduce systemic disease progression and related co-morbidities. This multi-organ targeted approach might be beneficial for the treatment of COPD, but also for the concomitant co-morbidities. Moreover, targeting mitochondria and oxidative stress by, e.g., the novel mito-protective and anti-inflammatory compound SUL-151, would be a promising approach to combat COPD.

Nederlandse samenvatting

De studies beschreven in dit proefschrift zijn uitgevoerd om meer inzicht te krijgen in de multi-orgaandisfunctie bij de chronische obstructieve longziekte COPD, met speciale aandacht voor veranderingen in de darmen en het vet- en spierweefsel. Bovendien werd de effectiviteit van een nieuwe farmaceutische verbinding, genaamd SUL-151, onderzocht in een door sigarettenrook-geïnduceerd ontstekingsmodel bij muizen.

De connectie tussen de darm en de longen bij COPD

COPD-patiënten hebben vaak een hoge prevalentie en incidentie van darmproblemen, zoals darmontstekingen, verhoogde darmpermeabiliteit, en een verstoorde opname van voedingsstoffen. De connectie tussen darm en longen is merkbaar aan darmziektes die tot uiting komen tijdens longziektes (COPD) en ook omgekeerd.

De connectie tussen de darm en de longen wordt beschreven in **Hoofdstuk 2**. Hier zijn de gegevens van klinische studies, diermodellen en *in vitro* studies samengevat die de interacties tussen de darm en de longen bij COPD beschrijven. De belangrijkste interactie tussen de longen en de darmen kan plaatsvinden via circulerende sigarettenrookdeeltjes, ontstekingscellen en allerlei verschillende mediatoren. Bovendien kan zowel bij COPD als bij darmaandoeningen, de microbiota van de darm uit balans raken. Dit kan leiden tot een verminderde darmbarrière en een verzwakt immuunsysteem en kan dus zowel het functioneren van de darm als van de longen negatief beïnvloeden. Tevens kunnen systemische hypoxie (zuurstoftekort) en oxidatieve stress die optreden bij COPD, ook betrokken zijn bij darmschade en een rol spelen in de connectie tussen de darm en de longen.

Roken, één van de belangrijkste oorzaken van COPD, kan het maagdarmstelsel aantasten en bijdragen aan het ontstaan van darmziekten. In **Hoofdstuk 3** werden muizen langdurig blootgesteld aan sigarettenrook met of zonder een bacteriële trigger (LPS) om de effecten van ontstekingen in de longen en emfyseem op de systemische ontsteking en de homeostase en immuniteit in de darm te bestuderen. Sigarettenrook met of zonder LPS, induceerde veranderingen in de darmmorfologie en het immuunnetwerk voor de productie van IgA-antistoffen in de darm. De verhoging van mediatoren in het hele lichaam zou een rol kunnen spelen in de connectie tussen longen en darmen. De bevindingen van deze studie dragen bij tot een beter begrip van het ontstaan van darmaandoeningen gerelateerd aan COPD.

Om meer inzicht te krijgen in de connectie tussen de longen en de darm in COPD, werden ook de moleculaire veranderingen in de longen en het ileum (distale dunne darm) van aan sigarettenrook blootgestelde muizen geanalyseerd met behulp van RNA sequencing (in kaart brengen van algehele genexpressie en transcriptionele activiteit; **Hoofdstuk 4**).

Gewijzigde genexpressie in het longweefsel van de muis werd vastgesteld na blootstelling aan sigarettenrook. De expressie van sommige van deze genen was ook gewijzigd bij COPD-patiënten, wat bevestigt dat het gebruikte muismodel COPD-achtige veranderingen laat zien. Blootstelling aan sigarettenrook veranderde ook de expressie van genen in het ileum van de muis, maar deze veranderingen waren minder vergelijkbaar met de veranderde genexpressie waargenomen in het ileum van patiënten met de ziekte van Crohn. Genen gerelateerd aan de interacties tussen cytokine en cytokine receptoren en genen met betrekking tot adhesiemoleculen lieten de grootste veranderingen zien in de longen en het ileum. Deze genexpressieprofielen van de longen en het ileum van aan rook blootgestelde muizen zouden een waardevol middel kunnen zijn voor toekomstige onderzoeksrichtingen en therapeutische mogelijkheden bij COPD en daarmee samenhangende darmproblemen.

Metabole veranderingen bij COPD

COPD is een chronische en complexe ziekte die kan leiden tot systemische aandoeningen, waaronder veranderingen in de stofwisseling van vet- en (skelet)spierweefsel. Vetweefsel is een belangrijk systemisch orgaan dat een reeks lokale en systemische metabole en ontstekingsroutes moduleert door verschillende bioactieve factoren af te geven, waaronder cytokines, adipokines en hormonen, die mogelijk kunnen bijdragen tot de progressie van longziekten. Spierafbraak is één van de belangrijkste symptomen bij COPD-patiënten, maar er wordt gesuggereerd dat vetweefselafbraak waarschijnlijk optreedt vóór de vermindering van de spiermassa. De systemische ontsteking veroorzaakt door onder andere het vetweefsel kan een van de onderliggende mechanismen zijn die betrokken is bij de afname van skeletspiermassa. **Hoofdstuk 5** onderzocht de veranderingen in vetweefsel en skeletspieren na blootstelling aan sigarettenrook met behulp van *in vivo* en *in vitro* modellen. Blootstelling van muizen aan sigarettenrook leidde tot het verlies van vetmassa, afbraak van vetweefsel en in mindere mate tot afbraak van skeletspieren. In de *in vitro* studie werd een verhoogde lipolyse en vetzuuroxidatie aangetoond, die beiden een rol zouden kunnen spelen in het verlies van vetmassa en vetweefselatrofie. Het moet nog worden opgehelderd of verlies van vetweefsel en parallelle verslechtering van de skeletspierfunctie voorafgaan aan de spierafbraak. De gepresenteerde kennis draagt bij tot een beter begrip van de rol van vetweefsel in de pathogenese en progressie van COPD.

Nieuw potentieel geneesmiddel voor de behandeling van COPD

Glucocorticoïden, β2-adrenoceptor agonisten en muscarine receptor antagonisten zijn op dit moment de belangrijkste geneesmiddelen voor de behandeling van COPD. Deze geneesmiddelen kunnen de symptomen en/of exacerbaties verminderen, maar zijn niet specifiek gericht op oxidatieve stress en verminderen niet de progressie of mortaliteit bij alle COPD-patiënten. Bovendien reageert een groot aantal COPD-patiënten slecht of helemaal niet op glucocorticoïden. Het is bekend dat oxidatieve stress een sleutelrol speelt bij de pathogenese van COPD. Daarom werden in **Hoofdstuk 6** de effecten van een

nieuwe farmacologische verbinding met antioxiderende capaciteit (SUL-151), profylactisch en therapeutisch onderzocht in een door sigarettenrook-geïnduceerd ontstekingsmodel bij muizen. SUL-151 verminderde meer dan 70% en 50% van de door sigarettenrook veroorzaakte toename van neutrofielen in de longvloeistof na respectievelijk profylactische en therapeutische toediening. Bovendien kon de SUL-151, de door sigarettenrook veroorzaakte afname van ATP (universele drager van chemische energie) en mitochondriaal DNA *voorkómen* en toename van de expressie van een mitochondriale eiwitkinase in de longen tegengaan. Dit impliceert dat het beïnvloeden van mitochondriën en oxidatieve stress een veelbelovende therapie zou zijn voor het verminderen van ontstekingen in de longen gerelateerd aan COPD.

Tot slot

Tot slot zijn in **Hoofdstuk 7** de belangrijkste bevindingen en de algemene conclusies van dit proefschrift beschreven. In een door sigarettenrook geïnduceerd COPD-model bij muizen zijn systemische effecten onderzocht en werd aangetoond dat sigarettenrook veranderingen in de darm en vet- en spierweefsels veroorzaakt. Dit suggereert dat toekomstig COPD-onderzoek zich niet alleen moet richten op de longen als doelorgaan, maar een breder perspectief met betrekking tot andere organen aan te bevelen is. Toekomstige therapeutische strategieën voor COPD zouden dus niet alleen gericht moeten zijn op de long, maar ook op andere weefsels, zoals de darm en het vetweefsel om de systemische ziekteprogressie en de daarmee samenhangende co-morbiditeiten te verminderen. Deze op meerdere organen gerichte aanpak zou gunstig kunnen zijn voor de behandeling van COPD, maar ook voor de bijkomende co-morbiditeiten. Bovendien zou het beïnvloeden van mitochondriën en oxidatieve stress door bijvoorbeeld de nieuwe ontstekingsremmende verbinding SUL-151, een veelbelovende aanpak zijn voor de behandeling van COPD.

中文总结

本论文旨在更深入地阐释慢性阻塞性肺疾病（简称慢阻肺）中多器官功能障碍的发生和发展机制，特别关注肠道和代谢（脂肪和肌肉组织）反应。此外，还研究了新型化合物SUL-151在小鼠香烟烟雾诱导的炎症模型中的治疗潜力，为慢阻肺的发病机制及临床治疗方案的选择提供新思路和研究方向。

慢阻肺中的肺-肠轴

虽然慢阻肺主要被认为是一种呼吸道疾病，但慢性肠道疾病通常在慢阻肺中有较高的发病率，表现为炎症细胞浸润、肠道通透性增加和营养吸收障碍等。肺部疾病的发展与肠道功能的变化相互影响（即肺-肠轴），但其具体机制尚不清楚。

在本论文的第 2、3 和 4 章对慢阻肺中的肺-肠轴进行了深入探讨。在第 2 章中，通过总结临床试验、动物模型和体外研究的证据，描述了在慢阻肺中肺-肠相互作用的可能机制。肺和肠道之间的相互作用可直接由进入体循环的香烟烟雾颗粒、炎症细胞和介质介导。此外，肠道微生物群失调导致黏膜环境改变，进而影响肠道屏障和免疫系统，可能对肠道和肺部产生负面作用。最后，慢阻肺中发生的全身性缺氧和氧化应激也可能与肠道损伤有关，并通过肺-肠轴扩大影响。

吸烟或长期烟雾暴露是慢阻肺最重要的环境致病因素，显著影响胃肠系统并增加患病风险。在第 3 章中，我们使用仅香烟烟雾长期暴露以及合并LPS 共同刺激的小鼠模型来研究肺部炎症和肺气肿对全身炎症、肠道稳态以及免疫系统的影响。肠道组织形态学变化和IgA相关免疫应答的波动是香烟烟雾以及合并LPS 刺激对机体影响的具体表现，揭示了全身系统性炎症在肺肠轴中可能发挥重要作用。以上发现进一步加深了对慢阻肺诱发的肠道应答的作用机制的理解。

为了深入研究慢阻肺中的肺-肠轴，第 4 章中通过转录组学（RNA-sequencing）和差异表达分析（Differential Expression），基于现有数据库（KEGG, Kyoto Encyclopedia of Genes and Genomes），从分子层面揭示暴露于香烟烟雾的小鼠中肺和回肠（远端小肠）的变化。香烟烟雾暴露后，小鼠肺组织基因表达显著变化，其中高表达基因在慢阻肺患者样本中呈现相同趋势，此结果证实香烟烟雾诱导的小鼠模型可导致慢阻肺样病变。同时，小鼠回肠中基因表达也变化明显，但并不与其在肠炎患者回肠中的表达模式相似。通路富集分析显示，细胞因子-细胞因子受体相互作用与细胞粘附分子相关的通路与肺-（回）肠联系紧密，基因表达显著升高。此外，该数据库作为研究慢阻肺和相关胃肠道合并症的宝贵工具，在机制研究和临床应用中的价值不容忽视。

慢阻肺的代谢障碍

慢阻肺患者通常合并代谢综合征和骨骼肌功能障碍，患者的肺气肿程度与体重减轻和脂肪减少有关。脂肪是重要的系统性器官，通过释放不同的生物活性因子（细胞因子、脂肪因子和激素）调节一系列局部及全身的代谢和炎症反应，且与呼

吸系统疾病的加重有关。骨骼肌萎缩是慢阻肺患者的核心症状之一，然而，肌肉重量下降和脂肪组织萎缩的发生的时空顺序尚不清楚。脂肪组织参与的系统性炎症可能是导致骨骼肌功能减弱的潜在机制之一。

第 5 章中，通过香烟烟雾刺激建立体内体外模型，研究脂肪和骨骼肌的适应性和病理性变化。体内研究发现，香烟烟雾暴露主要导致了全身脂肪量减少和脂肪组织萎缩，但对于骨骼肌萎缩程度的影响较轻。体外研究通过全程烟雾刺激并诱导分化3T3L-L1脂肪细胞，进一步阐述脂肪细胞通过增强脂质分解和脂肪酸氧化，在脂肪重量减少和脂肪萎缩中发挥重要作用。脂肪组织流失和骨骼肌功能损伤是否先于肌肉萎缩发生仍有待阐明。本章节的研究成果对理解脂肪组织在慢阻肺发病机制和进展中的角色有重要意义。

治疗慢阻肺的新型化合物

糖皮质激素以及支气管扩张剂，包括ß2-肾上腺素受体激动剂和毒蕈碱受体拮抗剂单独及联合使用是慢阻肺的基础一线治疗药物，可减轻症状，降低急性加重风险。在临床应用发现，慢阻肺对糖皮质激素治疗的反应存在异质性（反应不佳或完全耐药），而其他一线药物无法靶向氧化应激，亦不能减轻慢性呼吸道炎症或降低病死率。因此，第6章中研究了新型化合物（也称为 SUL-151 化合物）在香烟烟雾暴露的小鼠炎症模型中的预防和治疗作用。SUL-151化合物在前给药和后给药的模型中，分别减少了超过 70% 和 50% 的支气管肺泡灌洗液中的中性粒细胞数量。此外，SUL-151 化合物可防止香烟烟雾引起肺匀浆中的 ATP 和线粒体 DNA 减少以及PINK1 表达增加。该结果证明靶向线粒体和氧化应激有可能成为减轻肺部炎症和减缓慢阻肺发展的潜在疗法。

最后，第7章，包含本文的主要发现以及总体结论概括。简而言之，本文主要研究了在小鼠香烟烟雾诱导的慢阻肺模型中的系统性并发症，特别关注肠道和代谢紊乱。结果表明香烟烟雾诱导可以导致肠道和代谢（脂肪和肌肉组织）表观改变及功能失调。通过结合（转录）组学、炎症免疫调控相关机制、肺与全身器官的交互作用等角度，进一步加深对慢阻肺发生、发展规律的理解。同时，多器官靶向研究和治疗可能对慢阻肺的临床研究及治疗提供新的思考和展望。此外，针对性作用于线粒体保护和氧化应激的新型化合物，例如本文研究的化合物 SUL-151，是对抗慢阻肺有力的潜在治疗方案，为优化防治策略提供依据。

Acknowledgments

It is a genuine pleasure to express my deep thanks and gratitude to the people who helped and supported me during my PhD journey! Their kind help and support have made my work and life in the Netherlands a wonderful time.

I would like to acknowledge and give my warmest thanks to my supervisors and daily supervisors who made this work possible.

Dear **Gert**, thank you so much for providing me with the great opportunity to do my PhD in your group. You are such a kind and friendly person, we always had relaxed conversations and you always made me laugh with your jokes. You are so supportive, and your continuous support made a lot of things possible, for example, you gave me the possibility to explore all my ideas regarding my research project, and support me to join several interesting conferences. You are also the person who always tries to look for solutions to specific problems, instead of focusing on problems during my PhD project. I would like to give you my sincere gratitude for all your support.

Dear **Johan**, your immense knowledge and plentiful experience have encouraged me during my academic career and daily life. I am very impressed by your great work as the head of our division. I still remember every time we met, you always told me that you always have time for me, no matter how busy you are. Your support gave me a lot of power during my PhD study.

Dear **Saskia**, I feel so lucky to have you as my daily supervisor. You are so kind and friendly. Your support and encouragement helped me a lot through my whole PhD period. You are not only a supervisor for me but also a friend. We discussed a lot about research together, but also shared a lot of happiness and sadness with each other. Thank you for your invaluable advice and patience, which carried me through all the stages of writing my papers and thesis. I have learned a lot from you, and I super appreciated your help and support!

Dear **Paul**, thank you for being a co-promoter for me, you are always very supportive. I really enjoyed the moments when you passed by when I was working behind my computer. Then we updated each other about the progress of the project and had a good conversation. You also have very sharp eyes, you always found the smallest mistakes in my writing. I felt very comfortable when you double-checked my paperwork. Thank you very much for all your help!

I would like to thank the committee members: **prof. dr. G.M.H. Engels**, **prof. dr. H.I. Heijink**, **prof. dr. J.M. Argilés**, **prof. dr. R.F. Witkamp**, **prof. dr. H. Wichers**. Thank you for your valuable time to assess my thesis.

I would like to thank all the people who were involved in this project:
Dear **Aletta**, I would like to thank you for your help and input related to this project. Your comments and suggestions for my manuscripts were always helpful. Your ambition and critical thinking really inspired me.

Dear **Charlotte**, I still remember the first day when I started at our department and I was introduced to you as we were working on the same project. You were very friendly, helpful and showed me around, it was a good start! Although the process was not easy, and there were many challenges during our project, we had many nice experiences together. Eventually, we published two great papers together.

I would like to thank the people from other institutes, especially **Guido and Kees** from Sulfateq, **Ardy** from Danone Nutricia Research, as well as **Lieke**, **Harry**, **Ramon**, and **Annemie** from Maastricht University Medical Centre for their valuable scientific support.
I also would like to thank **Pim** from Tytgat Institute for Liver and Intestinal Research, Amsterdam University Medical Centers, you are very kind and professional. I can always learn something from you during our meetings and conversations. Wish you all the best for your future career!

I would like to express my sincere thanks to **Ingrid**, **Thea**, **Suzan**, **Mara**, **Bart**, and **Koen** for all the technical support during my PhD. I have learned a lot from **Ingrid** and **Thea** about animal experiments, including different techniques and laboratory skills. Without your help, the long sectioning days would not go that smoothly. I would also like to thank **Gemma** for all the arrangements in the lab. You are such a well-organized and responsible person, we always get quick responses from you when we need your help. Thank you for your great work at our department. **Suzan**, you are a very sincere person, and a highly-skilled technician. It always felt comfortable to work with you. Your smile and kindness really gave me power. **Mara**, you are a very happy and sweet person, you are always willing to help people when they need your help. Thank you for organizing those group activities, canoeing, pancake diners, and laser games, I really enjoyed this. **Bart**, you are a very professional and experienced technician. I have always been impressed by your pretty experimental design and results. You are also a funny person, you like to make jokes with people. Every time I go to your lab, the atmosphere is "gezellig". I would also like to thank **Koen** for your instructions with confocal.

I would also like to thank all the students who participated in my research projects, **Jingyi**, **Floortje**, **Dagmar**, **Ayla**, **Lucía,** and **Shiyu**. I really enjoyed the time working with you and I very much appreciated your input in our projects. Supervising you really made me an academic researcher. Special thanks to **Jingyi** for your support during lock down.

To my dear friends and colleagues:

Very special thanks to my paranymphs. Dear **Sabbir,** you are such a sincere, kind, generous and responsible person. I feel so lucky to have you as a friend. I can share almost everything with you, and I know you are always there to help and support me. I like all the nice food you have cooked for us and I really enjoyed all the activities that we have done together. There are not enough words to express my gratitude to you. Dear **Lily,** thank you for your company over the last couple of years, we have had so many nice experiences together. I really enjoyed the period being your neighbor, I can easily be lazy and come to you for dinner. Together with our "Panda group" with **Xiaoyi**, **Jan**, **Thomas**, and **Boaz**, we celebrated a lot of important moments together. Dear **Sabbir** and **Lily**, I am so glad that you will stand by me and support me during my defense.

Dear **Yang** and **Jing,** you both started your PhD earlier than me. I really appreciated your help and accompany when you were in the Netherlands. It was my great pleasure to be your paranymph. I wish you all the best in your life in China. I would also like to thank the other Chinese friends from our department, **Puqiao, Yuanpeng, Deguang, Zhenguo, Shiyi**, **Yi, Yulong.** It was nice to have you around, it gave me the feeling that I was back in China when we were making dumplings and eating hotpot together.

Dear **Ali**, it has been a good experience for me to join and help with your PhD project at the end of my PhD. I am very happy to see, the more you learn, the more confident and motivated you became. I also learned a lot from this experience. You are a very positive and hard-working person, I believe you will make a great PhD achievement. **Arezoo**, you are a very warm and caring person, I really enjoyed the time worked together with you. I hope you will enjoy your new job. Also thank you **Jeroen**, I learn a lot from you during working on this project.

Dear **Laura,** it was a great pleasure to sit next to you for the last two years of my PhD. We always went for a drink in the morning and had very funny conversations together. We both like plants and flowers, and the city tour and flower market we went together are great memories for me. I also really liked the Italian food you made for me.

Dear **Negisa** and **Veronica,** you are both very kind and sweet people, I very much appreciated all the experiences that you shared with me and the support that you gave me when I just started my PhD. **Negisa**, we have a lot of things in common, so we really understand each other and shared a lot. We always have a lot to talk about. **Veronica**, you are a very warm person, and you are always willing to help people. Thank you very much for sharing your experience and information for preparing my defense.

Dear **João**, thank you for being so nice, you like to organize pleasant dinners and drinks to bring people together. We have joined the Dutch course and BioBusiness Summer School together, it was a nice experience together, and also so nice to share and talk with you there.

Dear **Soheil**, I felt so lucky to have my desk next to you for the first two years of my PhD, you are so kind, wise, and calm. You gave me a lot of nice suggestions and support when I just started my PhD. Thank you for helping and staying with me till late during the animal experiment. I wish you all the best with your career!

Dear **Adel**, you are such a strong person and a kind friend. I really like to talk with you. Your confidence and positive thinking always helped me to stay positive. It is so impressive that you are so busy with arranging your pharmacy in Iran and still managed to do your PhD. Thank you and your wife for the delicious Iranian food!

Dear **Karin**, thank you very much for your arrangements and quick answers whenever we need your help. You make our Pharmacology family very lovely. I would also like to thank **Brenda and Lidija** for their help and arrangements during these years.

I would like to thank other nice colleagues from our department. **Thom**, you are such a nice person and kind to everyone, it is also very comfortable to talk with you. Wish you all the best for your project. **Mehrdad**, you are a very funny person, you can easily make people happy and laugh. It is very enjoyable to talk with you. **Mirelle**, you are a girl full of positive energy, your smile can always cheer people up. **Hamed**, thank you for your help when I just started my PhD, you gave me many nice suggestions and technical support. **Roos V.**, I really enjoyed the time together during the Dutch Lung Congress. We had a nice time together as teammates for the Pub quiz, also thank you for your power bank. I would like to extend my gratitude to **Roos M.**, **Frank**, **Betty**, **Linette**, **Astrid**, **Pieter**, **José**, **Silvia**, **Marit**, **Sandra**, **Robine**, **Bart H.**, **Anne Metje**, **Elena**, **Marta**, **Paula**, **Irene**, **Paniz**, **Anastasia**, **Quentin**, **Paul J.**, **Lucía**, **Elise**, **Alejandro**, **Lousanne**, **Naika**, **Devon,** **Joshua**, **Amir,** **Suzanne**, **Kirsten**, **Atanaska**, and **Marlotte**. Thank you for being so kind and creating a nice working environment, you made our department more colorful and energetic!

I am also very grateful to my badminton friends, **Lesly**, **Wenxin**, and **Calvin** for the nice time we had at Olympus. Also, thanks to **Mark**, **He**, **Lu**, and **Hong** for the badminton time during the weekends. I also enjoyed a lot of the drinks and talks after playing. I would like to give special thanks to the people from the DVS club at Utrecht, they are always so friendly and kind, and the atmosphere there always cheers me up!

在此，特别感谢在荷兰的中国朋友们，　园姐，我们来荷兰的第一年我们就一见如故，你就像大姐姐一样照顾我。　你总能给我一些很好的建议和启发。我们一起去探索新的城市和美食，谢谢你的陪伴，希望你的事业蒸蒸日上。晓白，君豪，博宁，庆午，亚龙，爽，建男，雪峰，当汉，很感谢可以在国外工作学习的这几年有你们的陪伴，支持和帮助，希望你们接下来毕业，工作以及再深造一切顺利。西西，丁云，谢谢你们在我刚来荷兰时合租时的照顾，以及那段时间我们一起经历留下的美好回忆。同时，我也要谢谢佳佳和璠璠姐。璠姐，你是一个特别独立，能干的榜样，虽然你当时在德国读博，我们仍然可以计划去其他地方一起旅行。在你身上我总能学到很多。希望你的博后生涯一切顺利。佳佳，虽然你在德国，但是我们总能随时聊天分享感受，经历，美食，帮彼此排忧解难，也希望你博士顺利完成，继续追求你向往的生活。除此之外，我还要感谢我在国内的好朋友们，艳艳，小平平，宇婷，丹宇，郭英，强仔，宝哥，盖盖，培峰，老肖和老杨。虽然在过去的几年我们见面的次数有限，但是我们的革命友谊丝毫不会受到影响。谢谢你们在我成长的路上一路的陪伴和见证，也谢谢你们一直以来无条件的支持和鼓励，给我很多力量，我也很珍惜我们的友情。愿你们都可以开开心心的过自己想要的生活。

I am particularly grateful to **Boaz**, thank you for all your support during this special period. We have experienced a lot together, you brought me a lot of happiness and your accompany and encouragement are always the best gifts for me. Also thanks to **Esther** and **Hans** for all your love and care for me. The other family members, **David**, **Joshua**, **Wendy**, **Gijs**, and **Joel**, as well as **Jos** and **Evert**, thank you for the nice time we spent together, you made me feel at home.

最后，我要感谢祖国对我的培养，感谢基金委的支持。我更要感谢我的家人，特别幸运我生活在一个非常开明且有爱的家庭。在此，我要谢谢小姨，小姨父，大姨，大姨夫，奶奶，欢欢妹妹以及佳信叔一直以来对我的关心。你们时刻关心着我在国外的生活和工作，也一直让我知道你们永远都在默默的支持我。我要向我的爸爸妈妈表达我最真挚的感谢，谢谢你们永远无条件的爱，包容，理解和支持。你们永远是我最坚实的后盾，在我迷茫困惑地时候，你们总能帮我指明方向。谢谢你们在我成长路上的辛苦付出。我想要在这里对你们说：我爱你们!

Curriculum vitae

Lei Wang was born on October 09, 1992 in Heilongjiang province, China. She started her bachelor's degree in 2009 at the Pharmaceutical Science department of the Qiqihar Medical University. In 2014, she received her bachelor's degree and continued with a master's degree program in Pharmacology at Jilin University. During her master's degree, she focused on the cardiovascular system and investigated the potential therapeutic effects of different pharmaceutical components against myocardial ischemia-reperfusion injury in rats, under the supervision of Prof. dr. Dayun Sui and Xiaofeng Yu. In 2017, she finished her master's degree and started her PhD project at the Pharmacology division of the Utrecht Institute for Pharmaceutical Sciences at Utrecht University. Here, she investigated multi-organ dysfunction in COPD using a murine model, with a special focus on the gut-lung axis and metabolic disorders. Furthermore, a potential therapeutic strategy to decrease cigarette smoke-induced airway inflammation was explored. She was supervised by Prof. Dr. Gert Folkerts, Prof. Dr. Johan Garssen, Dr. Saskia Braber, and Dr. Paul A.J. Henricks. In addition to this COPD project, she also participated in a project to improve the altered functioning of the immune system of offspring caused by maternal exposure to air pollution through the administration of a dietary intervention with synbiotics in collaboration with Danone Nutricia Research.

List of publications

Lei Wang, Charlotte Pelgrim, Daniël Swart, Guido Krenning, Adrianus C. van der Graaf, Aletta D. Kraneveld, Thea Leusink-Muis, Ingrid van Ark, Johan Garssen, Gert Folkerts and Saskia Braber. SUL-151 decreases airway neutrophilia as a prophylactic and therapeutic treatment in mice after cigarette smoke exposure. *International Journal of Molecular Sciences.* 22 (9): 4991 (2021).

Lei Wang, Charlotte E. Pelgrim, Lucía N. Peralta Marzal, Stephanie Korver, Ingrid van Ark, Thea Leusink-Muis, Ardy van Helvoort, Ali Keshavarzian, Aletta D. Kraneveld, Johan Garssen, Paul A.J. Henricks, Gert Folkerts, Saskia Braber. Changes in intestinal homeostasis and immunity in a cigarette smoke- and LPS-induced murine model for COPD: the lung-gut axis. *American Journal of Physiology-Lung Cellular and Molecular Physiology*. 323 (3): L266-L280 (2022).

Charlotte E. Pelgrim, **Lei Wang**, Lucía N. Peralta Marzal, Stephanie Korver, Ingrid van Ark, Thea Leusink-Muis, Saskia Braber, Gert Folkerts, Johan Garssen, Ardy van Helvoort, Aletta D. Kraneveld. Increased exploration and hyperlocomotion in a cigarette smoke and LPS induced murine model of COPD: linking pulmonary and systemic inflammation with the brain. *American Journal of Physiology-Lung Cellular and Molecular Physiology*. 323 (3): L251-265 (2022).

Lei Wang, Lieke E.J. van Iersel, Charlotte E. Pelgrim, Jingyi Lu, Ingrid van Ark, Thea Leusink-Muis, Harry R. Gosker, Ramon C.J. Langen, Annemie M.W.J. Schols, Josep Argilés, Ardy van Helvoort, Aletta D. Kraneveld, Johan Garssen, Paul. A.J. Henricks, Gert Folkerts, Saskia Braber. Effects of cigarette smoke on adipose and skeletal muscle tissue: *in vivo* and *in vitro* studies. *Cells* 11 (18): 2893 (2022).

Lei Wang, Yang Cai, Johan Garssen, Paul. A.J. Henricks, Gert Folkerts, Saskia Braber. The Gut-lung axis in COPD (Under the major revision of the *American Journal of Respiratory and Critical Care Medicine*).

Lei Wang, Pim J. Koelink, Johan Garssen, Paul .A.J. Henricks, Gert Folkerts, Saskia Braber. The overlap transcriptomic insight of lung and intestinal tissues of smoke-exposed mice with human COPD and IBD (Ready for submission).

Zongbao Zhou, Zixuan Dong, **Lei Wang**, Rijian Song, Naibin Mei, Tao Chen, Lei Luo, Qiang Ding, Xiaoying Wang, Shunqing Tang. Cellulose membrane modified with LED209 as an antibacterial and anti-adhesion material. *Carbohydrate polymers*. 252: p. 117138 (2021).

Yaozhen Wang, Xiaofeng Yu, Ping Zhang, Yinglin Ma, **Lei Wang**, Huali Xu, Dayun Sui. Neuroprotective effects of pramipexole transdermal patch in the MPTP-induced mouse model of Parkinson's disease. *Journal of Pharmacological Sciences.* 138 (1): 31-37 (2018).